CHEMICAL ISOLATION AND ELECTRO-CHEMICAL CHARACTERIZATION OF ANTIDIABETIC COMPOUNDS FROM SELECTED SOUTH AFRICAN LAMIACEAE PLANTS SPECIES

By

NINON GEORNEST EUDES RONAULD ETSASSALA

BSc Honours Chemistry, MSc Chemistry (University of the Western Cape)

A thesis submitted in fulfilment of the requirements for the degree of

UNIVERSITY of the
WESTERN CAPE

DOCTOR OF PHILOSOPHY

Department of Chemistry
Faculty of Science
University of the Western Cape, South Africa

Supervisor: **Prof. Emmanuel Iwuoha**
Co-supervisors: **Prof. Ahmed Mohammed**
Prof. Christopher N. Cupido

December 2019

https://etd.uwc.ac.za/

ABST RACT

Diabetes mellitus (DM), being one of the most common metabolic disorders with an elevated morbidity and mortality rate around the world. It is characterised by deficiency in insulin secretion or degradation of secreted insulin. Many internal and external factors such as oxidative stress, obesity and sedentary lifestyle among others have been suggested as the major causes of these cell alterations. Diabetes I and II are the most common types of diabetes.

Treatment of type I requires insulin injection, while type II can be managed using different synthetic antidiabetic agents. However, their effectiveness is limited as a result of low bioavailability, high cost of drug production, and unfavourable side effects. There is a great need to develop alternative and more active antidiabetic drugs from natural sources. Natural products are a well-known source for the discovery of new scaffold for drugs discovery, and South Africa is one of the most important megaflora with high percentage of endemism.

Lamiaceae is an important family in South Africa megaflora with ±308 species assigned to 41 genera and contains many important plants (~23%) traditionally used in the treatment of different human diseases. The phytochemical profile of Lamiaceae is very rich in terpenoids in general and more specifically abietane diterpene, which is an interesting class of compounds with a broad spectrum of promising biological activities including diabetes.

The phytochemical investigation of methanolic extracts of *Salvia africana-lutea*, *S. aurita* and *Plectranthus ecklonii* resulted in the isolation and identification of seventeen terpenoids (**1-14**, **16-18**) and one flavonoid (**15**). Among the isolated terpenoids, four new compounds were described for the first time from natural source; 19-acetox y-12-methoxy carnosic acid (**1**), 3β-acetoxy-7α-methoxyrosmanol (**2**), 19-acetoxy-7α-methoxyrosmanol (**3**), 19-acetoxy-

UNIVERSITY of the WESTERN CAPE
https://etd.uwc.ac.za/

12-methoxy carnosol (**4**). The structural elucidation of the newly isolated compounds was determined on the basis of 1 and 2D NMR, HRMS, UV, IR, Raman spectroscopy.

The in vitro bio-evaluation against alpha-glucosidase showed strong inhibitory activities for **13**, **8**, **12** and **10** with IC_{50} values of 4.2 ± 0.7; 11.3 ± 1.0, 16.4 ±. 1.1 and 22.9 ± 2.0 µg/mL respectively while **7**, **14** and **11** demonstrated the strongest in vitro alpha-amylase inhibitory activities among the tested compounds with IC_{50} of 12.5 ± 0.7; 16.2 ± 0.3 and 19.8 ± 1.4 µg/mL. Additionally, excellent total antioxidant capacities were demonstrated by **12**, **18** as ORAC (25789.9 ± 10.5; 25726.1 ± 8.1) µM TE/g; **11** and **12** as FRAP (3917.8 ± 2.1; 1522.3 ± 0.9) µM AAE/g; **18**, **15** and **12** as TEAC (3526.1 ± 0.6; 3190.4 ± 2.8; 2055.0 ± 2.6) µM TE/g respectively.

Cyclic voltammetry (CV) shows that all the abietane diterpenes are electro-active with well-defined oxidation-reduction peaks. Compound **12**, when compared to others, exhibits the lowest oxidation potential value (E_{pa} = 120 mV), indicating that it has the highest antioxidant power, which is in good agreement with ORAC and TEAC. Additionally, compounds with catechol moiety in the C ring demonstrated the lowest oxidation potential compared to others, and their mechanism of reaction involve two electrons two protons reversible reaction and formation of an o-quinone. This is the first scientific report to be carried out on the phytochemical and biological profiles of *S. aurita* as well as the isolation and characterization of compounds (**1-10**) and **18** from *S. africana lutea* and *P. ecklonii*, respectively. The results suggest that these compounds might become natural candidates to inhibit alpha-glucosidase and alpha-amylase as well as oxidative stress related to diabetes with the prospect to be used in the formulation of diabetes products/drugs upon further biological studies.

https://etd.uwc.ac.za/

KEYWORDS

Alpha-glucosidase

Alpha-amylase

Cape Floristic Region

Diabetes mellitus

Lamiaceae

Oxidative stress

Plectranthus ecklonii

Salvia africana-lutea

Salvia aurita

Secondary metabolites

Terpenoids

UNIVERSITY of the
WESTERN CAPE

https://etd.uwc.ac.za/

ABBREVIATIONS

AAE/g	Ascorbic acid per gram
AAPH	2,2- Azibis (2-methylpropionamidine) dihydrochloride, perchloric acid
ABTS	2, 2- Azino-bis (3-ethylbenzo thiazoline-6-sulfonic acid) diammoniun salt
Br.d	Broad doublet
BHT	Butylated hydroxytoluene
$CDCl_3$	Deuterated chloroform
COSY	Correlation spectroscopy
d	Doublet
dd	Doublet doublet
ddd	Doublet doublet doublet
DIW	De-ionized water
DMSO	Dimethyl sulfoxide
DNA	Deoxyribonucleic acid
DNS	Di-nitro salicylic acid
ECM	Extra cellular matrix
EDTA	Ethylenediaminetetraacetic acid
EGCG	Epigallocatechin gallate
EtOAc	Ethyl acetate
DPPH	2,2-diphenyl-1-picrylhydrazyl
Fig	Figure
FRAP	Ferric-ion reducing antioxidant power
g	Gram
HMBC	Heteronuclear multiple bond correlation

UNIVERSITY of the WESTERN CAPE
https://etd.uwc.ac.za/

HMQC	Heteronuclear multiple quantum coherence
HPLC	High performance liquid chromatography
H_2SO_4	Sulphuric acid
IC_{50}	Half maximal inhibitory concentration
KCl	Potassium chloride
L	Liter
mg	Milligram
mL	Milliliter
min	Minute
mM	Millimolar
M	Molar
MeOH	Methanol
NMR	Nuclear magnetic resonance
nm	Nanometer
ORAC	Oxygen radicals absorbance capacity
pNPG	Para-nitro-phenyl-α-D-glucopyranoside
ROS	Reactive oxygen specie
t	Triplet
TEAC	Trolox equivalent absorbance capacity
TE/g	Trolox equilalent per gram
TCA	Trichloroacetic acid
TLC	Thin layer chromatography
TPTZ	(2,4,6-tri[2-pyridyl]-s-triazine, Iron (III) chloride hexahydrate
Trolox	6-Hydroxyl-2,5,7,8-tetramethylchroman-2-carboxylic acid

UNIVERSITY of the
WESTERN CAPE

https://etd.uwc.ac.za/

μL	Microliter
U	Unit
UV	Ultraviolet
s	Singlet
sept	Septuplet
V	Volume
^{1}H-NMR	Proton nuclear magnetic resonance
1D-NMR	One-dimensional nuclear magnetic resonance
2D NMR	Two-dimensional nuclear magnetic resonance

UNIVERSITY of the
WESTERN CAPE

https://etd.uwc.ac.za/

DECLARATION

I declare that Chemical isolation and electro-chemical characterization of antidiabetic compounds from selected South African Lamiaceae plant species is my own work and it has not been submitted before for any degree or examination in any other university, and that all the sources I have used or quoted have been indicated and acknowledged as complete references.

Signature ----------

05/12/2019

Ninon G.E.R Etsassala

Day Month Year

UNIVERSITY of the
WESTERN CAPE

https://etd.uwc.ac.za/

DEDICATION

I would like to dedicate this dissertation to my family, especially my father **Georges Etsassala** and my mother **Ernestine Gayaba**, who gave me their unwavering support throughout my life. Also to my wife **Grace Murti Milounguidi**, my son **Ninon Ephraim Etsassala**, my sisters **Georgea** and **Horcia Etsassala**, friends and to the Congolese communities.

UNIVERSITY of the
WESTERN CAPE

https://etd.uwc.ac.za/

ACKNOWLEDGEMENTS

I would like to thank my wonderful Supervisor **Professor Emmanuel Iwuoha** for introducing me into **Electrochemistry**. Again I am very thankful for his motivation, inspiration, and financial support and finally for giving me the opportunity to travel to France for PhD research purposes.

I would like to thank my amiable Supervisor **Professor Ahmed Mohammed** for his wonderful encouragement, motivation during the period of this work. I am extremely delighted to him for introducing me into **Organic Chemistry/Medicinal Chemistry**.

I would like to thank my amiable Supervisor **Prof. Christopher Cupido**, for his full assistance in collection and identification of the plant species used for this research work.

Special thanks to the HOD of Chemistry department, **Prof. Mabusela** for his academic support; special thanks to **Prof. Priscilla Baker** for her wonderful encouragement, suggestion and motivations. To **Dr. Tesfaye waryo** for his assistance and motivation during the course work and to **Prof. Fanelwa Ajayi, Dr Chinwe Ikpo** and the Secretary, **Ms Wilma Jackson**. I also extend thanks to **Sensorlab** colleagues, **Miranda Mengwi Ndipingwi**, **Penny Mathumba**.

Special thanks to **Dr. Olugbenga Popoola, Dr. Badmus Jelili, Dr Adewale O. Adeloye, Dr Anne Djouemessi, Maelsand Aliwa Awongo, Luveni Sonka, Abobaker Ibrakaw, Wakwanyembo Eloge Lwamba, Abdulrahman Elbagory**, **Selena Eunice Orango Adewinogo**, **Akeem Omolaja Akinfenwa, Umar Mohummad Badeggi**, **Masande Yalo**, **Mthandazo Rondo**, **Ndikho Nako**. Above all, I give all the glory to **God** for the provision of strength, wisdom towards successful completion of this work.

https://etd.uwc.ac.za/

LIST OF PUBLICATIONS

1. Ninon G.E.R. Etsassala., **Tesfaye Waryo.**, **Olugbenga K. Popoola.**, **Adewale O. Adeloye., Emmanuel I. Iwuoha and Ahmed A. Hussein**. (2019). Electrochemical Screening and Evaluation of Lamiaceae Plant Species from South Africa with Potential Tyrosinase Activity. *Sensors*, *19*(5), 1035. https://doi.org/10.3390/s19051035.

2. Ninon G.E.R. Etsassala., **Adewale O. Adeloye.**, **Ali El-Halawany.**, **Ahmed A. Hussein*** and **Emmanuel I. Iwuoha**. **(2019)**. Investigation of In-Vitro Antioxidant and Electrochemical Activities of Isolated Compounds from *Salvia chamelaeagnea* P.J.Bergius Extract. *Antioxidants*, *8*(4), 98. https://doi.org/10.3390/antiox8040098.

3. Ninon G.E.R. Etsassala., Badmus J.A., Tesfaye T. Waryo., Jeanine L. Marnewick., Christopher N Cupido., Ahmed A. Hussein* and Emmanuel I. Iwuoha 1. (2019). Alpha-Glucosidase and Alpha-Amylase Inhibitory Activities of Novel Abietane Diterpenes from Salvia Africana-lutea. Antioxidants, 8(10), 421. https://doi.org/10.3390/antiox8100421

4. Ninon G.E.R. Etsassala., Christopher N. Cupido., Emmanuel I. Iwuoha and Ahmed A. Hussein*. (2019). **Review:** Abietane Diterpenes as Potential Candidates for the Management of type 2 Diabetes. *Current Pharmaceutical Design*. **Accepted**.

5. Ninon G.E.R. Etsassala., Kadidiatou O. Ndjoubi., Thilly J. Mbira., Brendon Pearce., Keenau Pearce., Emmanuel I. Iwuoha., Mongi Benjeddou* and Ahmed A. Hussein. (2019). Glucose Uptake Activity and Cytotoxicity of Abietane Diterpenes and Triterpenes Isolated from Lamiaceae Plant Species. *Molecules*. **Submitted**

https://etd.uwc.ac.za/

LIST OF ISOLATED COMPOUNDS

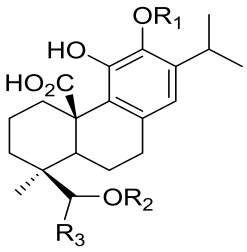

1 $R_1 = CH_3$, R_2 = Ac, R_3 = H

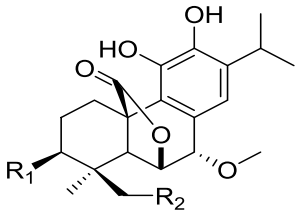

2 R_1 = OAc R_2 = H,
3 R_1 = H, R_2 = OAc

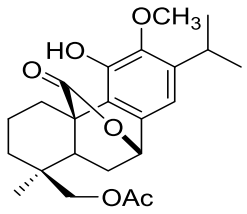

4

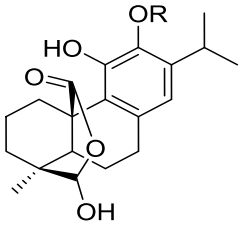

5 R = H
6 R = CH3

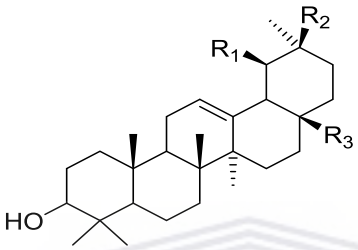

7 R_1 = H, $R_2 = CH_3$, R_3 =COOH
8 $R_1 = CH_3$, R_2 = H, R_3 =COOH
10 $R_1 = R_3$ = H, $R_2 = CH_3$

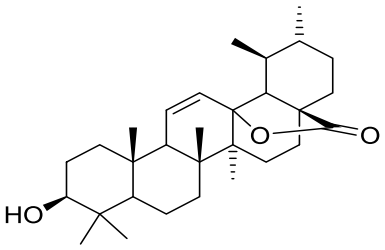

9

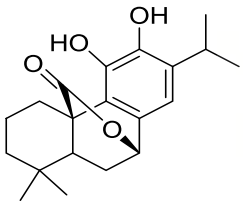

11

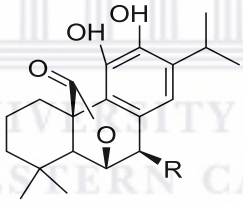

12 R: OH
13 R: OCH3

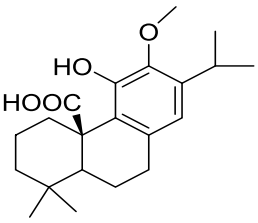

14

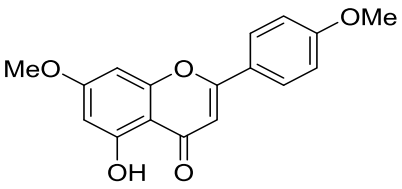

15

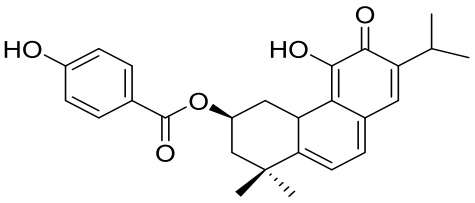

16

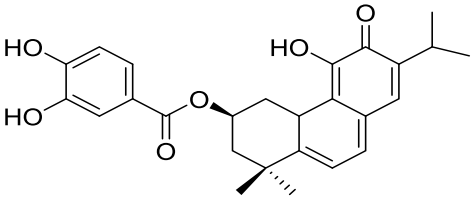

17

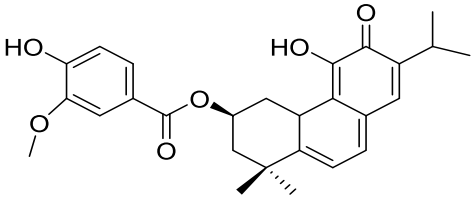

18

https://etd.uwc.ac.za/

TABLE OF CONTENT

ABSTRACT i
KEYWORDS iii
ABBREVIATIONS iv
DECLARATION vii
DEDICATION viii
ACKNOWLEDGEMENTS ix
LIST OF PUBLICATIONS x
LIST OF ISOLATED COMPOUNDS xi
TABLE OF CONTENT xii
LIST OF FIGURES xviii
LIST OF TABLES xxvii
LIST OF SCHEMES xxx
CHAPTER ONE 1
INTRODUCTION 1
1.1 General overview of the use of medicinal plants as source of medicines 1
1.2 General overview of Diabetes 1
1.2.1 Type 1 diabetes mellitus 2
1.2.2 Type 2 diabetes mellitus 4
1.2.3 Diabetes complications 5
1.3 Diabetes mellitus in Africa 5
1.4 Drugs used in the treatment of diabetes 6
1.4.1 Insulin secretagogues: Sulfonylureas 6
1.4.2 Insulin secretagogues: Meglitinides 7
1.4.3 Biguanides 7
1.4.4 Thiazolidinediones 7
1.4.5 Alpha-glucosidase inhibitors 8
1.4.6 Alpha-amylase inhibitors 8
1.5 Oxidative stress and diabetes complications 9
1.6 Rationale 10
1.7 Aim of this study 11
1.8 Objectives 11

https://etd.uwc.ac.za/

1.9 Scope of the study 11
References 12
CHAPTER TWO: SECTION A 18
POTENTIAL APPLICATION OF LAMIACEAE PLANT SPECIES IN THE MANAGEMENT OF DIABETES 18
2.1 Aim of this chapter 18
2.2 Lamiaceae family 18
2.2.1 Plant Morphology: Description and distribution 19
2.3 Medicinal plants used in the treatment of diabetes 20
2.4 Lamiaceae plants species used for diabetes 21
2.4.1 *Calamintha officinalis* Moench 21
2.4.2 *Coleus forskohlii* 22
2.4.3 *Leonotis leonurus* L. 24
2.4.4 *Rosmarinus officinalis* L. 26
2.4.5 *Salvia lavandulifolia* Valh 27
2.4.6 *Salvia officinalis* 28
2.4.7 *Teucrium polium* L. 30
2.4.8 *Leonotis nepetaefolia*, R.Br 31
2.4.9 *Teucrium cubense* 33
2.4.10 *Ocimum sanctum* 34
2.4.10.2 Phytochemical constituents 34
2.4.11 *Hyptis suaveolens* 35
2.4.12 *Ocimum gratissium* 37
2.5 Antidiabetic activity of some notable chemical constituents isolated from Lamiaceae plants species 38
2.6 Conclusion 41
References 41
CHAPTER TWO: SECTION B 47
REVIEW: ABIETANE DITERPENES AS POTENTIAL CANDIDATES FOR THE MANAGEMENT OF TYPE 2 DIABETES 47
2.7 Abstract 47
2.8 Introduction 48
2.9 *In vitro* models 51
2.10 *In vivo* models/animal models 57

UNIVERSITY of the WESTERN CAPE
https://etd.uwc.ac.za/

2.11. Conclusion....60
References....61
CHAPTER THREE....65
PHYTOCHEMICAL ISOLATION AND BIOLOGICAL INVESTIGATION OF *SALVIA AFRICANA -LUTEA*....65
3.1 Abstract....65
3.2 Background information....66
CHEMICAL CHARACTERIZATION OF *SALVIA AFRICANA-LUTEA* CONSTITUENTS....67
3.3 General experiment procedure....67
3.3.1 Reagents and solvents....67
3.3.2 Chromatography....67
3.3.3 Spectroscopy....68
3.4 Collection and identification of plant material....69
3.5 Extraction and Fractionation of the total extract....70
3.6 Isolation of pure compounds....73
3.6.1 Isolation of compound **1**....73
3.6.2 Isolation of compound **2**....76
3.6.3 Isolation of compound **3** and **10**....77
3.6.4 Isolation of compound **4**....79
3.6.5 Isolation of compound **5**....80
3.6.6 Isolation of compound **6**....81
3.6.7 Isolation of compound **7**....82
3.6.8 Isolation of compound **8**....83
3.6.9 Isolation of compound **9**....84
BIOLOGICAL CHARACTERIZATION OF SALVIA AFRICANA CONSTITUENTS....87
3.7 General experimental procedure for biological assays....87
3.7.1 Reagents....87
3.7.2 Alpha-glucosidase inhibitory activity....87
3.7.3 Alpha-amylase inhibitory activity....88
3.7.4 Antioxidant Assays....88
3.8 Statistical Analysis....90
3.9 Chemical characterization: Results and discussion....90
3.9.1 Structure elucidation of 19-acetoxy-12-methoxy carnosic acid (**1**)....91

UNIVERSITY of the WESTERN CAPE
https://etd.uwc.ac.za/

3.9.2 Structure elucidation of 3β-acetoxy-7-methoxy rosmanol (**2**) 99
3.9.3 Structure elucidation of 19-acetoxy-7α-methoxyrosmanol (**3**) 107
3.9.4 Structure elucidation of 19-acetoxy-12-methoxy carnosol (**4**) 113
3.9.5 Structure elucidation of clinopodiolide A (**5**) 120
3.9.6 Structure elucidation of clinopodiolide B (**6**) 128
3.9.7 Structure elucidation of oleanolic acid (**7**) 135
3.9.8 Structure elucidation of ursolic acid (**8**) 139
3.9.9 Structure elucidation of 11,12-dehydroursolic acid lactone (**9**) 143
3.9.10: Structure elucidation of β-amyrin (**10**) 143
3.10 Biological evaluation: Results and discussion 144
3.10.1 Alpha-glucosidase and alpha-amylase activities 144
3.10.2 Antioxidant activity 146
3.11 Conclusion 149
References 150
CHAPTER FOUR 155
PHYTOCHEMICAL AND BIOLOGICAL INVESTIGATION OF SALVIA AURITA 155
4.1 Abstract 155
4.2 Background information on *Salvia aurita* 156
CHEMICAL CHARACTERIZATION OF *SALVIA AURITA* CONSTITUENTS 157
4.3 General experiment procedure 157
4.3.1 Reagents and solvents 157
4.3.2 Thin layer chromatography (TLC) 157
4.3.3 Spectroscopy 158
4.4 Plant material 158
4.5 Extraction and purification of chemical constituents 158
4.6 Isolation of pure compounds 162
4.6.1 Isolation of compound **11** 162
4.6.2 Isolation of compound **12** 164
4.6.3 Isolation of compound **13** and **15** 165
4.6.5 Isolation of compound **14** 168
BIOLOGICAL CHARACTERIZATION OF ISOLATED COMPOUNDS 171
4.7.1 General experimental procedure for biological assays 171
4.7.1.1 Reagents 171

UNIVERSITY of the WESTERN CAPE
https://etd.uwc.ac.za/

4.7.2 Alpha-glucosidase inhibitory activity 171
4.7.3 Alpha-amylase inhibitory activity 171
4.7.4 Total Antioxidant capacities assays 171
4.8 Statistical analysis 171
4.9 Chemical characterization: Results and discussion 171
4.9.1 Structure elucidation of carnosol (**11**) 172
4.9.2 Structure elucidation of rosmanol (**12**) 176
4.9.3 Structure elucidation of 7-methoxyrosmanol (**13**) 181
4.9.4 Structure elucidation of 12-methoxycarnosic acid (**14**) 185
4.9.5 Structure elucidation of 4,7-dimethylapigenin ether (**15**) 189
4.10 Biological evaluation: Results and discussion 191
4.10.1 Alpha-glucosidase and alpha-amylase activities 191
4.10.2 Antioxidant activity 193
4.11 Conclusion 196
References 196
CHAPTER FIVE 202
PHYTOCHEMICAL ISOLATION AND BIOLOGICAL INVESTIGATION OF *PLECTRANTHUS ECKLONII* 202
5.1 Abstract 202
5.2 Background information 202
CHEMICAL CHARACTERIZATION OF *P. ECKLONII* CONSTITUENTS 204
5.3 General experiment procedure 204
5.3.1 Reagents and solvents 204
5.3.2 Chromatography 204
5.3.3 Spectroscopy 204
5.4 Plant material 205
5.5 Extraction and purification of different chemical constituents from *P. ecklonii* 205
5.6 Isolation of pure compounds 208
5.6.1 Isolation of compound **16** and **17** 208
5.6.2 Isolation of compound **18** 209
BIOLOGICAL CHARACTERIZATION OF ISOLATED COMPOUNDS 212
5.7 General experimental procedure for biological assays 212
5.7.1 Reagents 212
5.7.2 Alpha-glucosidase inhibitory activity 212

UNIVERSITY of the WESTERN CAPE
https://etd.uwc.ac.za/

5.7.3 Alpha-amylase inhibitory activity 212
5.7.4 Total Antioxidant capacities assays 212
5.8 Statistical analysis 212
5.9 Chemical characterization: Results and discussion 212
5.9.1 Structure elucidation of parvifloron D (**16**) 213
5.9.2 Structure elucidation of parviflorone F (**17**) 217
5.9.3 Structure elucidation of parviflorone G (**18**) 220
5.10 Biological evaluation: Results and discussion 225
5.10.1 Alpha-glucosidase and alpha-amylase activities 225
5.10.2 Antioxidant activity 225
5.11 Conclusion 226
References 227
CHAPTER SIX 229
ELECTROCHEMICAL CHARACTERIZATION OF ISOLATED COMPOUNDS 229
6.1 Abstract 229
6.2 Aim of this chapter 229
ELECTROCHEMICAL ANALYSIS 230
6.3 General experiment procedure 230
6.3.1 Reagents and solvents 230
6.3.2 Procedure for voltammetry analysis 230
6.3.3 Electrochemical characterization: Results and discussion 231
6.4 Correlation between cyclic voltammetry and antioxidant capacity 245
6.5 Conclusion 247
References 248
CHAPTER SEVEN 250
CONCLUSION AND RECOMMENDATIONS 250
ANNEXURE 255

UNIVERSITY of the
WESTERN CAPE

https://etd.uwc.ac.za/

LIST OF FIGURES

Figure 1.1	Type 1 diabetes	3
Figure 1.2	Type 2 diabetes	4
Figure 2.1	Morphology of *Calamintha officinalis* Moench	21
Figure 2.2	Morphology of *Coleus forskohlii*	22
Figure 2.3	Morphology of *Leonotis leonurus*	24
Figure 2.4	Morphology of *Rosmarinus officinalis*	26
Figure 2.5	Morphology of *Salvia lavandulifolia*	27
Figure 2.6	Morphology of *Salvia officinalis*	28
Figure 2.7	Morphology of *Teucrium polium*	30
Figure 2.8	Morphology of *Leonotis nepetaefolia*	31
Figure 2.9	Morphology of *Teucrium cubense*	33
Figure 2.10	Morphology of *Ocimum sanctum*	34
Figure 2.11	Morphology of *Hyptis suaveolens*	35
Figure 2.12	Morphology of *Ocimum gratissium*	37
Figure 2.13	Biosynthesis of abietane diterpenes	50
Figure 3.1A	*Salvia africana lutea* description	66
Figure 3.1B	Distribution along South African coastal	66
Figure 3.2	TLC plate (silica gel) of combined fractions under UV (254 nm; A&C), and after spraying with H_2SO_4/vanillin and then heated (B&D). TLC was developed using solvent system C	72
Figure 3.3	TLC plate of collected fractions of SAL-XVII	74
Figure 3.4	TLC plate of of SAL-XVII-3-3-2	75
Figure 3.5A	TLC plate of SAL-XI-5-5	77

UNIVERSITY of the WESTERN CAPE
https://etd.uwc.ac.za/

Figure 3.5B	HPLC of sub fraction XI-5	77
Figure 3.6	TLC plate of combined fractions of SAL-XIII	78
Figure 3.7A	TLC plate of SAL-XIII-3-7	79
Figure 3.7B	HPLC chromatogram of sub fraction XIII-3	79
Figure 3.8A	TLC plate of SAL-XIII-2-10	80
Figure 3.8B	HPLC chromatogram of sub fraction XIII-2	80
Figure 3.9A	TLC plate of SAL-XIII-4-5	81
Figure 3.9B	HPLC chromatogram of XIII-4	81
Figure 3.10A	TLC plate of SAL-XIII-5-5	82
Figure 3.10B	HPLC chromatogram of XIII-5	82
Figure 3.11	TLC plate of SAL-X	83
Figure 3.12	TLC plate of SAL-XI-4-5	84
Figure 3.13	HPLC chromatogram of sub fraction XI-4	85
Figure 3.14	Chemical structures of the isolated compounds (**1-10**) from *S. africana-lutea*	91
Figure 3.15	Chemical structure of **1**	92
Figure 3.16	Key $^{1}H-^{1}H$ COSY, HMBC and NOESY correlations of **1**	92
Figure 3.17	^{1}H-NMR (400 MHz, CDCl3) spectrum of **1**	94
Figure 3.18	^{13}C-NMR (400 MHz, CDCl3) spectrum of **1**	94
Figure 3.19	DEPT-NMR (400 MHz, CDCl3) spectrum of **1**	95
Figure 3.20	COSY (400 MHz, CDCl3) spectrum of **1**	95
Figure 3.21	HSQC (400 MHz, CDCl3) spectrum of **1**	96
Figure 3.22	HMBC (400 MHz, CDCl3) spectrum of **1**	96
Figure 3.23	NOESY (400 MHz, CDCl3) spectrum of **1**	97

UNIVERSITY of the WESTERN CAPE

https://etd.uwc.ac.za/

Figure 3.24	HR-MS spectrum of **1**	97
Figure 3.25	UV spectrum of **1**	98
Figure 3.26	FTIR spectrum of **1**	98
Figure 3.27	Chemical structure of **2**	100
Figure 3.28	Key $^{1}H-^{1}H$ COSY, HMBC, and NOESY correlations of **2**	100
Figure 3.29	^{1}H-NMR (400 MHz, CDCl3) spectrum of **2**	102
Figure 3.30	^{13}C-NMR (400 MHz, CDCl3) spectrum of **2**	102
Figure 3.31	DEPT-NMR (400 MHz, CDCl3) spectrum of **2**	103
Figure 3.32	COSY (400 MHz, CDCl3) spectrum of **2**	103
Figure 3.33	HSQC (400 MHz, CDCl3) spectrum of **2**	104
Figure 3.34	HMBC (400 MHz, CDCl3) spectrum of **2**	104
Figure 3.35	NOESY (400 MHz, CDCl3) spectrum of **2**	105
Figure 3.36	HR-MS spectrum of **2**	105
Figure 3.37	UV spectrum of **2**	106
Figure 3.38	FTIR spectrum of **2**	106
Figure 3.39	Raman spectrum of **2**	107
Figure 3.40	Chemical structure of the **3**	108
Figure 3.41	^{1}H-NMR (400 MHz, CDCl3) spectrum of **3**	109
Figure 3.42	^{13}C-NMR (400 MHz, CDCl3) spectrum of **3**	109
Figure 3.43	DEPT-NMR (400 MHz, CDCl3) spectrum of **3**	110
Figure 3.44	HSQC (400 MHz, CDCl3) spectrum of **3**	110
Figure 3.45	HMBC (400 MHz, CDCl3) spectrum of **3**	111
Figure 3.46	HR-MS spectrum of **3**	111
Figure 3.47	UV spectrum of **3**	112

UNIVERSITY of the WESTERN CAPE

https://etd.uwc.ac.za/

Figure 3.48	FTIR spectrum of **3**	112
Figure 3.49	Chemical structure of **4**	113
Figure 3.50	^{1}H-NMR (400 MHz, CDCl3) spectrum of **4**	115
Figure 3.51	^{13}C-NMR (400 MHz, CDCl3) spectrum of **4**	115
Figure 3.52	DEPT-NMR (400 MHz, CDCl3) spectrum of **4**	116
Figure 3.53	COSY (400 MHz, CDCl3) spectrum of **4**	116
Figure 3.54	HSQC (400 MHz, CDCl3) spectrum of **4**	117
Figure 3.55	HMBC (400 MHz, CDCl3) spectrum of **4**	117
Figure 3.56	HR-MS spectrum of **4**	118
Figure 3.57	UV spectrum of **4**	118
Figure 3.58	FTIR spectrum of **4**	119
Figure 3.59	Raman spectrum of **4**	119
Figure 3.60	Chemical structure of **5**	121
Figure 3.61	^{1}H-NMR (400 MHz, CDCl3) spectrum of **5**	122
Figure 3.62	^{13}C-NMR (400 MHz, CDCl3) spectrum of **5**	122
Figure 3.63	DEPT-NMR (400 MHz, CDCl3) spectrum of **5**	123
Figure 3.64	COSY (400 MHz, CDCl3) spectrum of **5**	123
Figure 3.65	HSQC (400 MHz, CDCl3) spectrum of **5**	124
Figure 3.66	HMBC (400 MHz, CDCl3) spectrum of **5**	124
Figure 3.67	NOESY (400 MHz, CDCl3) spectrum of **5**	125
Figure 3.68	HR-MS spectrum of **5**	125
Figure 3.69	UV spectrum of **5**	126
Figure 3.70	FTIR spectrum of **5**	126
Figure 3.71	Raman spectrum of **5**	127

UNIVERSITY of the WESTERN CAPE

https://etd.uwc.ac.za/

Figure 3.72	Chemical structure of **6**	128
Figure 3.73	^{1}H-NMR (400 MHz, CDCl3) spectrum of **6**	130
Figure 3.74	^{13}C-NMR (400 MHz, CDCl3) spectrum of **6**	130
Figure 3.75	COSY (400 MHz, CDCl3) spectrum of **6**	131
Figure 3.76	HSQC (400 MHz, CDCl3) spectrum of **6**	131
Figure 3.77	HMBC (400 MHz, CDCl3) spectrum of **6**	132
Figure 3.78	HR-MS spectrum of **6**	132
Figure 3.79	UV spectrum of **6**	133
Figure 3.80	FTIR spectrum of **6**	133
Figure 3.81	Raman spectrum of **6**	134
Figure 3.82	Chemical structure of **7**	135
Figure 3.83	^{1}H-NMR (400 MHz, CDCl3) spectrum of **7**	136
Figure 3.84	^{13}C-NMR (400 MHz, CDCl3) spectrum of **7**	136
Figure 3.85	DEPT-NMR (400 MHz, CDCl3) spectrum of **7**	137
Figure 3.86	HR-MS spectrum of **7**	137
Figure 3.87	FTIR spectrum of **7**	138
Figure 3.88	Raman spectrum of **7**	138
Figure 3.89	Chemical structure of **8**	140
Figure 3.90	^{1}H-NMR (400 MHz, CDCl3) spectrum of **8**	140
Figure 3.91	^{13}C-NMR (400 MHz, CDCl3) spectrum of **8**	141
Figure 3.92	DEPT-NMR (400 MHz, CDCl3) spectrum of **8**	141
Figure 3.93	HR-MS spectrum of **8**	142
Figure 3.94	FTIR spectrum of **8**	142
Figure 3.95	Chemical structure of **9**	143

UNIVERSITY of the WESTERN CAPE

https://etd.uwc.ac.za/

Figure 3.96	Chemical structure of **10**	144
Figure 4.1A	*Salvia aurita* description	156
Figure 4.1B	Distribution along South African coastal	156
Figure 4.2A	TLC plate (silica gel) of combined fractions under UV (254 nm)	161
Figure 4.2B	TLC plate (silica gel) of combined fractions after spraying with H_2SO_4/vanillin and then heated	161
Figure 4.3	TLC plate of combined fractions of SA-XIII	163
Figure 4.4A	TLC plate of SA-XIII-5-2	164
Figure 4.4B	HPLC chromatogram of sub fraction XIII-5	164
Figure 4.5A	TLC plate of SA-XIII-4-6	165
Figure 4.5B	HPLC chromatogram of sub fraction XIII-4	165
Figure 4.6	TLC plate of combined fractions of SA-XIV	166
Figure 4.7A	TLC plate of SA-XIV-2-4 and SA-XIV-2-6	167
Figure 4.7B	HPLC chromatogram of XIV-2	167
Figure 4.8	TLC plate of combined fractions of SA-XI-4	168
Figure 4.9	Chemical structures of the isolated compounds (**11-15**) from *S. aurita*	171
Figure 4.10	Chemical structure of **11**	173
Figure 4.11	^{1}H-NMR (400 MHz, CDCl3) spectrum of **11**	174
Figure 4.12	^{13}C-NMR (400 MHz, CDCl3) spectrum of **11**	174
Figure 4.13	DEPT-NMR (400 MHz, CDCl3) spectrum of **11**	175
Figure 4.14	FTIR spectrum of **11**	175
Figure 4.15	Raman spectrum of **11**	176

UNIVERSITY of the WESTERN CAPE

https://etd.uwc.ac.za/

Figure 4.16	Chemical structure of 1**2**	177
Figure 4.17	^{1}H-NMR (400 MHz, CDCl3) spectrum of **12**	179
Figure 4.18	^{13}C-NMR (400 MHz, CDCl3) spectrum of **12**	179
Figure 4.19	DEPT-NMR (400 MHz, CDCl3) spectrum of **12**	180
Figure 4.20	FTIR spectrum of **12**	180
Figure 4.21	Raman spectrum of **12**	181
Figure 4.22	Chemical structure of 1**3**	182
Figure 4.23	^{1}H-NMR (400 MHz, CDCl3) spectrum of **13**	183
Figure 4.24	^{13}C-NMR (400 MHz, CDCl3) spectrum of **13**	183
Figure 4.25	DEPT-NMR (400 MHz, CDCl3) spectrum of **13**	184
Figure 4.26	FTIR spectrum of **13**	184
Figure 4.27	Raman spectrum of **13**	185
Figure 4.28	Chemical structure of **14**	186
Figure 4.29	^{1}H-NMR (400 MHz, CDCl3) spectrum of **14**	187
Figure 4.30	^{13}C-NMR (400 MHz, CDCl3) spectrum of **14**	187
Figure 4.31	DEPT-NMR (400 MHz, CDCl3) spectrum of **14**	188
Figure 4.32	FTIR Spectrum of **14**	188
Figure 4.33	Chemical structure of the compound **15**	189
Figure 4.34	^{1}H-NMR (400 MHz, CDCl3) spectrum of **15**	189
Figure 4.35	^{13}C-NMR (400 MHz, CDCl3) spectrum of **15**	190
Figure 4.36	DEPT-NMR (400 MHz, CDCl3) spectrum of **15**	190
Figure 4.37	FTIR Spectrum of **15**	191
Figure 5.1	*P. ecklonii* description	203
Figure 5.2A	TLC plate (silica gel) of combined fractions under UV (254 nm	207

UNIVERSITY of the WESTERN CAPE

https://etd.uwc.ac.za/

Figure 5.2B	TLC plate (silica gel) of combined fractions after spraying with H_2SO_4/vanillin and then heated	207
Figure 5.3	TLC plate of collected fractions	208
Figure 5.4A	TLC plate of **16**	209
Figure 5.4B	TLC plate of **17**	209
Figure 5.5A	TLC plate of PE- III-2-1	210
Figure 5.5B	HPLC chromatogram of **18**	210
Figure 5.6	Chemical structures of the isolated compounds	213
Figure 5.7	Chemical structure of **16**	214
Figure 5.8	^{1}H-NMR (400 MHz, CDCl3) spectrum of **16**	214
Figure 5.9	^{13}C-NMR (400 MHz, CDCl3) spectrum of **16**	215
Figure 5.10	DEPT-NMR (400 MHz, CDCl3) spectrum of **16**	215
Figure 5.11	FTIR spectrum of **16**	216
Figure 5.12	Raman spectrum of **16**	216
Figure 5.13	Chemical structure of **17**	217
Figure 5.14	^{1}H-NMR (400 MHz, CDCl3) spectrum of **2**	218
Figure 5.15	^{13}C-NMR (400 MHz, CDCl3) spectrum of **2**	218
Figure 5.16	DEPT-NMR (400 MHz, CDCl3) spectrum of **17**	219
Figure 5.17	FTIR spectrum of **17**	219
Figure 5.18	Raman spectrum of **17**	220
Figure 5.19	Chemical structure of **18**	221
Figure 5.20	^{1}H-NMR (400 MHz, CDCl3) spectrum of **18**	221
Figure 5.21	^{13}C-NMR (400 MHz, CDCl3) spectrum of **18**	222
Figure 5.22	DEPT-NMR (400 MHz, CDCl3) spectrum of **18**	222

UNIVERSITY of the WESTERN CAPE

https://etd.uwc.ac.za/

Figure 5.23	COSY (400 MHz, CDCl3) spectrum of **18**	223
Figure 5.24	HSQC (400 MHz, CDCl3) spectrum of **18**	223
Figure 5.25	HMBC (400 MHz, CDCl3) spectrum of **18**	224
Figure 5.26	FTIR spectrum of **18**	224
Figure 6.1	Cyclic voltammogram of 19β-acetoxy-12-methoxy carnosic (**1**)	231
Figure 6.2	Cyclic voltammogram of 3β-acetoxy-7-methoxy rosmanol (**2**)	232
Figure 6.3	Cyclic voltammogram of 19-acetoxy-12-methoxy carnosol (**3**)	233
Figure 6.4	Cyclic voltammogram of clinopodiolide A (**5**)	234
Figure 6.5	Cyclic voltammogram of clinopodiolide B (**6**)	235
Figure 6.6	Cyclic voltammogram of carnosol (**11**)	236
Figure 6.7	Cyclic voltammogram of rosmanol (**12**)	237
Figure 6.8	Cyclic voltammogram of 12-methoxycarnosic acid (**14**)	237
Figure 6.9	Cyclic voltammogram of parvifloron D (**16**)	238
Figure 6.10	Cyclic voltammogram of parvifloron F (**17**)	239

UNIVERSITY of the
WESTERN CAPE

https://etd.uwc.ac.za/

LIST OF TABLES

Table 1.1	Top 10 countries by Diabetes cases in Africa	6
Table 2.1	Antidiabetic activity of different constituents of Lamiaceae plant species	38
Table 2.2	In vitro antidiabetic activity of some abietane diterpenes	53
Table 2.3	In vivo antidiabetic activity of some abietane diterpenes	59
Table 3.1	TLC solvent systems	68
Table 3.2	Fractionation of the extract of *S. africana lutea*	70
Table 3.3	Fractions obtained upon fractionation of total extract of *S. africana lutea*	71
Table 3.4	Fractions grouped from the column	73
Table 3.5	Fractions grouped from the column	76
Table 3.6	Fractions grouped from the column	78
Table 3.7	^{1}H and ^{13}C NMR spectroscopic data assignments (400 MHz) for compound **1** (δ in ppm, m, J in Hz) in $CDCl_3$	93
Table 3.8	^{1}H and ^{13}C NMR spectroscopic data assignments (400 MHz) for compound **2** (δ in ppm, m, J in Hz) in $CDCl_3$	101
Table 3.9	^{1}H and ^{13}C NMR spectroscopic data assignments (400 MHz) for compounds **3** (δ in ppm, m, J in Hz) in $CDCl_3$	108
Table 3.10	^{1}H and ^{13}C NMR spectroscopic data assignments (400 MHz) for compound **4** (δ in ppm, m, J in Hz) in $CDCl_3$	114
Table 3.11	^{1}H and ^{13}C NMR spectroscopic data assignments (400 MHz) for compound **5** (δ in ppm, m, J in Hz) in $CDCl_3$	121

UNIVERSITY of the WESTERN CAPE
https://etd.uwc.ac.za/

Table 3.12	^{1}H and ^{13}C NMR spectroscopic data assignments (400 MHz) for compound **6** (δ in ppm, m, J in Hz) in $CDCl_3$	129
Table 3.13	Inhibitory activities of the isolated compounds on alpha-glucosidase and alpha-amylase	146
Table 3.14	Antioxidant activities of the isolated compounds	148
Table 4.1	TLC solvent systems	157
Table 4.2	Fractionation of the extract of *S. aurita*	159
Table 4.3	Fractions obtained upon fractionation of total extract of *S. aurita*	160
Table 4.4	Fractions grouped from the column	162
Table 4.5	Fractions grouped from the column	166
Table 4.6	Fractions grouped from the column	168
Table 4.7	^{1}H and ^{13}C NMR spectroscopic data assignments (400 MHz) for compound **11** (δ in ppm, m, J in Hz) in $CDCl_3$	173
Table 4.8	^{1}H and ^{13}C NMR spectroscopic data assignments (400 MHz) for compounds **12** (δ in ppm, m, J in Hz) in $CDCl_3$	178
Table 4.9	^{1}H and ^{13}C NMR spectroscopic data assignments (400 MHz) for compounds **13** (δ in ppm, m, J in Hz) in $CDCl_3$	182
Table 4.10	^{1}H and ^{13}C NMR spectroscopic data assignments (400 MHz) for compound **14** (δ in ppm, m, J in Hz) in $CDCl_3$	186
Table 4.11	Inhibitory activities of *S. aurita* constituents on alpha-glucosidase and alpha-amylase	192
Table 4.12	Total antioxidant capacity of *S. aurita* constituents	195
Table 5.1	TLC solvent systems	204
Table 5.2	Fractionation of the extract of *P. ecklonii*	206

UNIVERSITY of the WESTERN CAPE

https://etd.uwc.ac.za/

Table 5.3	Fractions obtained upon fractionation of total extract of *P. ecklonii*	207
Table 5.4	Fractions grouped from the column	208
Table 5.5	Alpha glucosidase and alpha amylase inhibitory activities of the isolated compounds.	225
Table 5.6	Antioxidant activities of the isolated compounds	226
Table 6.1	Electrochemical characterization of some isolated compounds	240
Table 6.2	Anodic peak properties of tested samples	247
Table 7.1	Summarized the extensive phytochemical analyses of the isolated compounds	251

UNIVERSITY of the
WESTERN CAPE

https://etd.uwc.ac.za/

LIST OF SCHEMES

Scheme 3.1	A flow diagram of experimental procedure for the isolation of compounds from *S. africana lutea*	86
Scheme 4.1	A flow diagram of experimental procedure for the isolation of compounds from *S. aurita*	170
Scheme 5.1	A flow diagram of experimental procedure for the isolation of compounds from *P.ecklonii*	211
Scheme 6.1	Oxidation of catechol moiety of 3β-acetoxy-7-methoxy rosmanol to o-quinone	232
Scheme 6.2	Oxidation of catechol moiety of parvifloron F to o-quinone	239

UNIVERSITY of the
WESTERN CAPE

https://etd.uwc.ac.za/

CHAPTER ONE

INTRODUCTION

1.1 General overview of the use of medicinal plants as source of medicines

Medicinal plants have been utilised as a source of medicine since time immemorial for curing numerous human afflictions (Sofowora, et al., 2013). The practice of medicnal plant was initially considered either an option for the less privileged or low-income jobholders (Ekor, 2014). The use of herbal remedies in developing countries is a common practice and up to 80% of the population living in Africa uses traditional medicine to treat various types of diseases in their respective locality in the mode of decoction and infusion (Mahomoodally, 2013). Herbal remedies play an essential role in South Africa, where it constitutes the backbone of rural communities with approximately 60% of the population consulting an estimation of 200000 traditional healers (Semenya, et al., 2013). This huge turnout was ascribed to affordability, accessibility and most importantly, freedom of expression of personal health status unlike orthodox medicines. In South Africa, only 10% of 30000 species of higher plants have been found useful in traditional medicine around the country to treat different types of diseases such as cough, diarrhoea, headaches, heart related problems, inflammation, prevention of miscarriage, diabetes (Street & Prinsloo, 2012). From the aforementioned, the usage of herbal medicine is gaining valuable global recognition compared to synthetic drugs due to side effects free of the former (Pan, et al., 2013).

1.2 General overview of Diabetes

Diabetes mellitus (DM) is one of the most common metabolic disorders with significant morbidity and mortality rate around the world. It is caused either by deficiency in insulin secretion or degradation of secreted insulin (Cao, et al., 2012), which is the result of cell alterations caused by many internal and external factors such as oxidative stress, obesity and

https://etd.uwc.ac.za/

sedentary lifestyle among others (Mamun-or-Rashid, et al., 2014; Ullah, et al., 2016). In order to understand diabetes, it is essential to know the normal physiological process that occurs during and after a meal. The food proceeds through the digestive system, where nutrients such as proteins, fat and carbohydrates are absorbed into the bloodstream. The presence of sugar and carbohydrate generate/activate signals to the endocrine pancreas to secrete insulin, which is responsible for the uptake and storage of sugar for almost all types of tissues in the body, mainly the liver as well as musculature and fat tissues (Coelho, et al., 2013; Sears & Perry, 2015). There is currently no cure available for diabetes, but it can be managed by controlling blood sugar levels through a healthy diet, exercise and medication. This can decrease the risk of long-term complications associated with diabetes (Asif, 2014).

The prevalence of diabetes reported by the International Diabetes Federation (IFD) indicated that the number of adult diabetic patients globally was 366 million in November 2011, and it is projected to increase to 552 million by the year 2030, which accounts for approximately 70% increase in developing countries and 20% in developed countries (Mohiuddin, et al., 2016).

UNIVERSITY of the
WESTERN CAPE

Diabetes mellitus is broadly classified into two categories, namely, type 1 DM commonly referred to as insulin-dependent diabetes mellitus (IDDM) and type 2 DM commonly referred to as non-insulin-dependent diabetes mellitus (NIDDM) in which about 90-95% of diabetic patients suffer from type 2 DM (Mohammed, et al., 2015).

1.2.1 Type 1 diabetes mellitus

Type 1 DM is caused by the inability of pancreas to produce insulin (Mohiuddin, et al., 2016). It is a catabolic disorder characterised by the absence of insulin's circulation, the increase of plasma glucagon level and the lack of response by the pancreatic B cells to all insulinogenic stimuli as shown in Figure 1.1 (Röder, et al., 2016).

https://etd.uwc.ac.za/

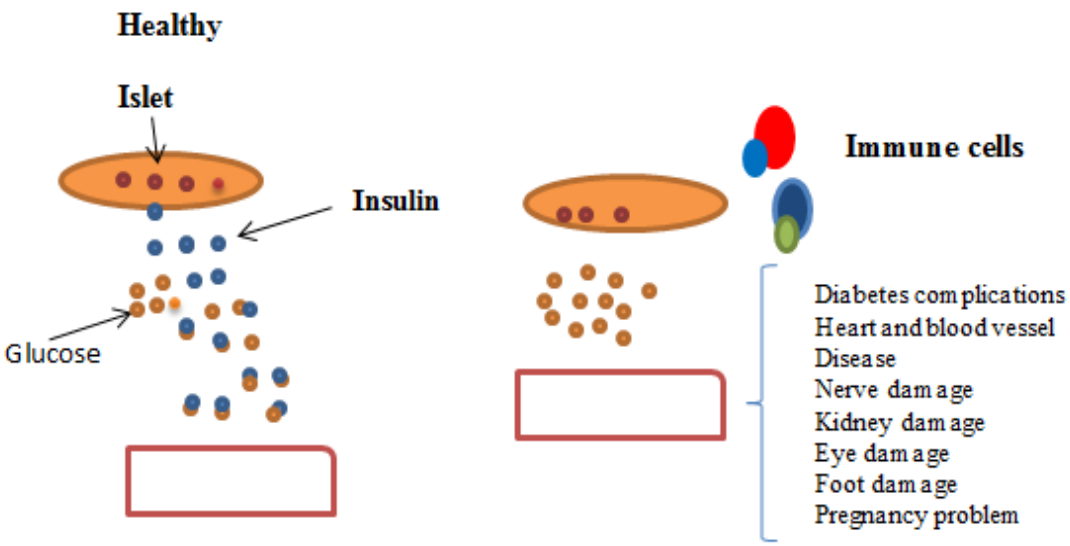

Figure 1.1: Type 1 diabetes

Type I diabetes is believed to result from an infectious or toxic environmental juncture in people whose immune systems are genetically predisposed to evolve a robust autoimmune response against pancreatic B cell antigens. There are various factors that can affect pancreatic B cell functioning such as damage caused by viruses, chemical agents, destructive cytotoxins and antibodies released from sensitized immunocytes (Rekittke, et al., 2016). A basal genetic defect in connection to pancreatic B cell replication or function might predispose a person to evolve pancreatic B cell failure after viral infections. Additionally, specific human leukocytes antigen (HLA genes) might be responsible for increasing the sensitivity to a diabetogenic virus or might be linked to precise immune response genes that predispose patients to auto-aggression, which means a destructive autoimmune response against their own islet cells (Graham, et al., 2012). The pancreatic B cell damage appears to be minimised when immunosuppressive drugs such as cyclosporine or azathioprine are prescribed at the initial stage of type 1 diabetes to support the value of auto-aggression by the immune system as a major factor in the pathogenesis of this disease. Therefore, patients with type 1 DM need regular insulin injection (Li, et al., 2014).

UNIVERSITY of the WESTERN CAPE
https://etd.uwc.ac.za/

1.2.2 Type 2 diabetes mellitus

Type 2 DM is mainly caused by degradation of secreted insulin. It can be managed by diet control and consumption of synthetic anti-diabetic drugs (Mohiuddin, et al., 2016). Type 2 diabetes affects more people compared to all other forms of diabetes, and patients with NIDDM do not depend on exogenous insulin for the prevention of ketonuria as well as ketosis (Preeti & Sushil, 2016). The pathogenesis in type 2 diabetes is characterized by the fact that the pancreas produces insulin, which is not utilized correctly by the body (Wu, et al., 2014). This is primarily due to peripheral tissue insulin resistance where insulin-receptors or other intermediates in the insulin signalling pathways inside the cells are insensitive to insulin. It results in the inability of glucose to enter the tissue, leading to hyperglycaemia or elevated level of glucose concentrations in blood as shown in Figure 1.2 (Wilcox, 2005). Obesity is one of the major risk factors of type 2 diabetes, which generally results in impaired insulin action and most patients in this case are obese (Wu, et al., 2014). However, the use of multiple anti-diabetic agents is required to maintain glycaemic control (Krentz & Bailey, 2005).

UNIVERSITY of the
WESTERN CAPE

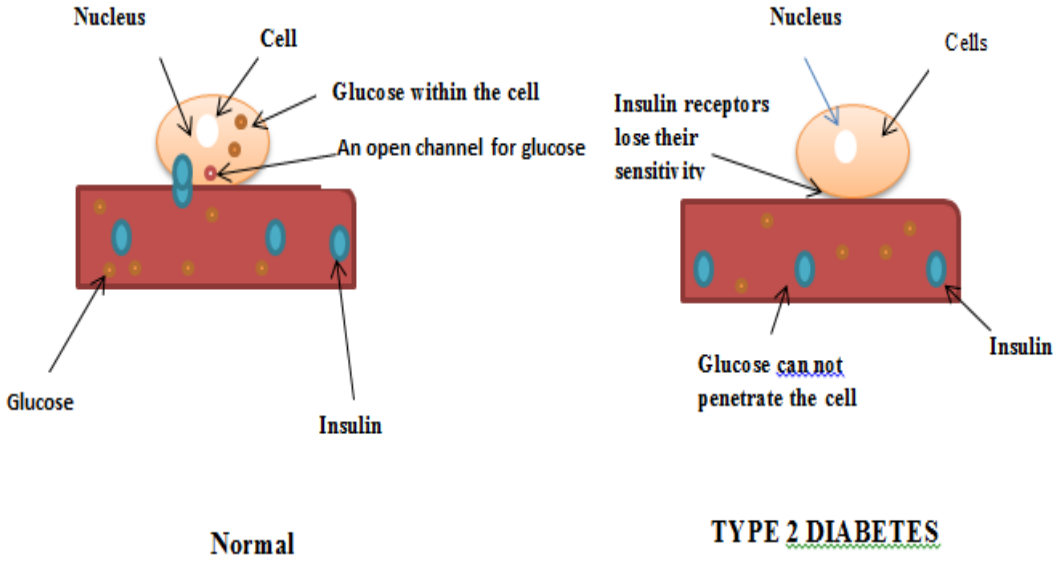

Figure 1.2: Type 2 diabetes

https://etd.uwc.ac.za/

1.2.3 Diabetes complications

Diabetes complications result in long-term damage, dysfunction, and failure of some organs, mostly the eyes (diabetic retinopathy), kidneys (diabetic nephropathy), nerves (diabetic neuropathy), heart (myocardial infarction), and blood vessels (atherosclerosis), which are related to uncontrolled hyperglycemia (Cade, 2008). Additionally, some other symptoms related to hyperglycemia encompass polyuria, polydipsia and weight loss. Impairment of growth and sensitivity to some infections migh also accompany chronic hyperglycemia. Acute, life-threatening outcome of uncontrolled diabetes result to hyperglycemia with ketoacidosis or the nonketotic hyperosmolar syndrome (Shaaban, et al., 2016). Long-term complications associated with diabetes include nephropathy, can lead to renal failure, peripheral neuropathy with high risk of foot ulcers, amputations and autonomic neuropathy, causing gastrointestinal, genitourinary, cardiovascular symptoms and sexual dysfunction. Diabetes patients have an increased incidence of atherosclerotic cardiovascular, peripheral arterial and cerebrovascular disease (Rekha, et al., 2017). Hypertension and abnormalities of lipoprotein metabolism are mostly present in people with diabetes (Ozder, 2014).

UNIVERSITY of the
WESTERN CAPE

1.3 Diabetes mellitus in Africa

African societies are experiencing a huge incease in nutritional deficiencies, which appear to be associated to poverty, socio-economic deprivation, malnutrition and war. Rural areas are exposed to rural migration, which is one the main factor that contributes to the unavailability of food. These lifestyle changes evolved against a background of increasing prevalence of diabetes mellitus and diabetic complications in Africa, especially in countries that have a low daily *per capita* dietary energy supply and poor quality of food (Azevedo & Alla, 2008). In Africa, more than 14 million people have diabetes accounting for about 4.3% of adults as shown in Table 1.1 and it caused about 401276 deaths in 2012 (Mohammed et al., 2014). In South Africa, there is an estimation of 6.5 million known diabetic patients and probably an

https://etd.uwc.ac.za/

approximation of an equal number that are currently undiagnosed. Additionally, the prevalence of diabetes in South Africa is very considerable, and it is estimated to be 14% in the Coloured, 13% in the Indian, 6% in the African and 6% in the European communities (Peer, et al., 2014).

Table 1.1: Top 10 countries by Diabetes cases in Africa

Country	**Cases**	**Population** (million)
Nigeria	3.2 million	168.8
South Africa	2.0 million	52.27
Ethiopia	1.4 million	91.73
Democratic Republic of Congo	737.000	65.71
Kenya	720.730	43.18
Zimbabwe	568.679	13.72
Cameroon	517.860	21.7
Tanzania	492.948	47.78
Madagascar	477.469	22.29
Cote d Ivoire	421.023	19.84

1.4 Drugs used in the treatment of diabetes

There are four (4) different categories of oral antidiabetic agents readily available in the market namely insulin secretagogues, biguanides, thiazolidinediones, and alpha-glucosidase inhibitors (Nolte & Karam, 2001).

UNIVERSITY of the
WESTERN CAPE

1.4.1 Insulin secretagogues: Sulfonylureas

Seven sulfonylurea drugs are available in the United States of America and are conventionally divided into first- and second-generation agents, which differ primarily in their potency. The first-generation comprises tolbutamide, tolazamide, acetohexamide and chlorpropamide while the second generation comprises glyburide, glipizide and glimepiride (Aquilante, 2010). After a prolonged sulfonylurea therapy, serum insulin levels no longer increase but may even decrease. It was also established that chronic administration of sulfonylureas to type 2 diabetic patients reduced serum glucagon levels but increased the binding of insulin to the tissue receptors (Nolte & Karam, 2001).

https://etd.uwc.ac.za/

1.4.2 Insulin secretagogues: Meglitinides

Meglitinides are new classes of insulin secretagogues, where repaglinide is the first member of the group. It was approved for clinical use by Food and Drug Administration (FDA) in 1998 (Beariz, et al., 2001). These drugs modulate Beta cell insulin release by controlling potassium efflux through the potassium channels. Meglitinides and sulfonylureas overlap in their molecular binding sites since meglitinides possess two binding sites in common with sulfonylureas and one unique binding site (Wet & Proks, 2015). However, meglitinides have no direct effect on insulin exocytosis as does sulfonylureas (Nolte & Karam, 2001).

1.4.3 Biguanides

There are three types of biguanides used in the treatment of diabetes namely phenformin, buformin and metformin. The use of the first two was discontinued in the United States of America due to its association with lactic acidosis (Nolte & Karam, 2001). Biguanides have been the most prescribed drugs for patients with refractory obesity, in which insulin resistance has been the main cause of hyperglycaemia. Metformin is an insulin-sparing agent and does not increase weight or evoke hypoglycaemia; it has the advantage over sulfonylureas in treating hyperglycemia. The most common toxic effect evolving on the usage of metformin is gastrointestinal and there is a risk of lactic acidosis (DeFronzo, et al., 2016).

1.4.4 Thiazolidinediones

There are two types of thiazolidinediones which are commercially available namely rosiglitazone and pioglitazone (Raptis & Dimitriadis, 2001). Troglitazone was the first thiazolidinedione drug to be approved but withdrawn due to its association with significant rate of idiosyncratic liver damages (Suchard & Faaem, 2001). Rosiglitazone and pioglitazone demonstrated efficacy similar to troglitazone but with no evidence of hepatocytotoxicity (Nolte & Karam, 2001).

https://etd.uwc.ac.za/

1.4.5 Alpha-glucosidase inhibitors

Alpha-glucosidase is an enzyme found in the brush border of the small intestine epithelium. It catalyses the breaking down of the reaction of disaccharides and starch to glucose (Bajpai & Kang, 2015). It also hydrolyses complex polysaccharides to produce oligosaccharides and disaccharides, which are then hydrolysed by alpha-glucosidase to monosaccharide, then absorbed in the small intestines into the hepatic portal vein and increase postprandial glucose levels (Uddin, et al., 2014).

Alpha-glucosidase inhibitors are classes of oral anti-diabetic drugs used for type 2 diabetes in the inhibition process of the pancreatic alpha-glucosidase enzyme (Derosa & Maffioli, 2012). They delay the rate of complex carbohydrates (starches, oligosaccharides and disaccharides) digestion and reduce the rate of glucose absorption (Lovegrove, et al., 2017).

Acarbose and miglitol are the main two agents available in this class. They are both competitive inhibitors of alpha-glucosidase and modulate the postprandial digestion and absorption of starch and disaccharides (Thilagam, et al., 2013). Acarbose and Miglitol have different chemical structures and acarbose is six time less active than miglitol in inhibiting sucrose (Gao, et al., 2016). The binding affinity of the two compounds are totally different towards the alpha-glucosidase enzymes such as sucrase, maltase, glucoamylase, dextranase, but miglitol target isomaltase and beta-glucosidase only while acarbose target alpha-amylase (Yilmazer-Musa, et al., 2012).

1.4.6 Alpha-amylase inhibitors

Alpha-amylase is an enzyme, which is directly involved in the breakdown of starch to simpler sugars (Nickavar, et al., 2008). Alpha amylase inhibitors play a crucial role in the management of post-prandial hyperglycaemia. It inhibits the action of alpha-amylase enzyme, leading to a reduction in starch hydrolysis to maltose and consequentially reduces post-prandial hyperglycaemia (Gautam, et al., 2013).

https://etd.uwc.ac.za/

1.5 Oxidative stress and diabetes complications

Diabetes mellitus is considered as a group of metabolic disorders characterized by hyperglycaemia, which is directly related to oxidative stress, a phenomenon caused by an imbalance between the production of free radicals [(reactive oxygen species (ROS)] and their accumulation in cells and tissues and the capacity of a biological system to detoxify these reactive products (Liguori, et al., 2018). Free radicals are well known to play a double role as both deleterious and beneficial species. At low level, free radicals play beneficial effects such as defence against patogens, induction of a mitogenic response and the maturation process of cellular structures, while in high level they result in deleterious processes that can damage cell structures (Pham-Huy, et al., 2008). However, oxidative stress occurs when the production of free radicals overwhelms the detoxification capacity of cellular antioxidant system resulting in biological damages. Its plays a vital role in the development of diabetes complications such as microvascular and cardiovascular. The metabolic abnormalities of diabetes result to mitochondrial superoxide overproduction, which is the principal mediator of diabetes tissue damage, insulin resistance, β-cell dysfunction and impaired glucose tolerance (Giacco & Brownlee, 2010). Additionally, the excess nourishment combined with a sedentary lifestyle result in excess of glucose and fatty acid accumulation inside the muscle, adipose tissue and pancreatic cells, which lead to the production of excess reactive oxygen species (ROS), mainly superoxide anion, through the mitochondrial electron-transport chain (Wright, et al., 2006). The principal sources of oxidative stress in diabetes include auto-oxidation of glucose, shifts in redox balances, decreased tissue concentrations of low molecular weight antioxidants, such as reduced glutathione (GSH) and vitamin E, and impaired activities of antioxidant defence enzymes such as superoxide dismutase (SOD) and catalase (CAT) (Matough, et al., 2012).

UNIVERSITY of the
WESTERN CAPE
https://etd.uwc.ac.za/

1.6 Rationale

The world is experiencing an increase in nutritional deficiencies due to poverty, socio-economic deprivation, malnutrition, war and consumption of fast food, which are the major factors for the development of various types of diseases including diabetes.

Diabetes mellitus (DM) is one of the most common endocrine ailments that affect approximately 6% of the worldwide population. It is projected to affect five times more people in the next ten (10) years (World Health Organization and American Diabetes Association).

Numerous synthetic anti-diabetic agents such as acarbose, miglitol, sulfonylurea, metformin, thiazolidinedione are readily available in the market, but the usage of these products is limited as a result of low bioavailability, high cost and high adverse side effects such as hypoglycaemia, damage to liver, flatulence, diarrhoea, abdominal pain, dropsy, drug-resistance, weight gain and heart failure.

UNIVERSITY of the
WESTERN CAPE

Three species from Lamiaceae were selected for this study based on their phytochemical profile and their availability in the Cape Floristic Region. Phenolic compounds especially abietane diterpenoids are the main constituents of this family, and they have been reported to play a vital role in the inhibition process of some enzymes implicated in diabetes such as alpha-glucosidase and alpha-amylase.

Therefore, it is of great need to evaluate Lamiaceae species for the discovery of new bioactive compounds for their potential application in the prevention and management of diabetic complications with proposition of replacing unsafe products readily available in the market.

https://etd.uwc.ac.za/

1.7 Aim of this study

The aim of this research project is directed towards the phytochemical study of three (3) South African Lamiaceae plant species namely *Salvia africana lutea*, *Salvia aurita* and *Plectranthus ecklonii* as well as the in-vitro bio-evaluation of the isolated compounds against alpha-glucosidase, alpha-amylase enzymes and their antioxidant properties. The electrochemical behaviour and the structure-activity relationship to be established for possible explanation of the mechanism of reaction demonstrated by each isolated compound.

1.8 Objectives

The main objectives of the study are:

- Collection, documentation and identification of Lamiaceae species.
- Extraction of each plant materials with methanol.
- Perform chromatographic isolation of different constituents present in the three-plant extracts using different chromatographic techniques including semi-prep HPLC.
- Structural elucidation of the isolated compounds using different spectroscopic techniques such as 1 and 2 D NMR, HRMS, IR, RAMAN and UV.
- In-vitro bio-evaluation of the isolated compounds against alpha-glucosidase and alpha-amylase enzymes
- Determination of the antioxidant properties of the isolated compounds.
- Electrochemical characterization of the isolated compounds and the relationship between oxidation potential and antioxidant activity using cyclic voltammetry.

1.9 Scope of the study

The scope of this thesis is general introduction in Chapter 1, followed by literature review of medicinal plant and abietane diterpenes used for the management of diabetes in Chapter 2 (A&B). Chapter 3, 4 and 5 deal with the phytochemical and biological investigation of *Salvia*

UNIVERSITY of the WESTERN CAPE
https://etd.uwc.ac.za/

africana lutea, *S. aurita and Plectranthus ecklonii* respectively, while Chapter 6 focuses on the electrochemical characterization of the isolated compounds as well as the prediction of their antioxidant activity based on their oxidation potential and finally, correlate the conventional antioxidant capacity assay and the oxidation potential. Chapter 7 deals with conclusions and recommendations.

References

Aquilante, L. (2010). Sulfonylurea pharmacogenomics in Type 2 diabetes: The influence of drug target and diabetes risk polymorphisms. *Expert Review of Cardiovascular Therapy*, 8(3), 359-72.

Asif, M. (2014). The prevention and control the type-2 diabetes by changing lifestyle and dietary pattern. *Journal of Educcation and Health Promotion*, 3(1).

Azevedo, M and Alla, S. (2008). Diabetes in Sub-Saharan Africa: Kenya, Mali, Mozambique, Nigeria, South Africa and Zambia. *International Journal of Diabetes in Developing Countries*, 28(4), 101-108.

Bajpai, V.K and Kang, S.C. (2015). Tyrosinase and alpha-glucosidase inhibitory effects of an abietane type diterpenoid taxodone from *Metasequoia glyptostroboides*. *National Academy Science Letters*, 38(5), 399–402

Beariz, L., Pharm, D., Mark, N and Feinglos, M.D. (2001). Oral agents in the management of type 2 diabetes mellitus. *American Family Physician*, 63(9), 1747-1756.

Cade, W. (2008). Diabetes-related microvascular and nacrovascular diseases in the physical therapy setting. *Physical Therapy*, 88(11), 1322–1335.

UNIVERSITY of the WESTERN CAPE
https://etd.uwc.ac.za/

Cao, A., Tang, Y and Liu, Y. (2012). Novel fluorescent biosensor for alpha-glucosidase inhibitor screening based on cationic conjugated polymers. *ACS Applied Materials and Interfaces*, 4(8), 3773-8.

Coelho, M., Oliveira, T and Fernandes, R. (2013). Biochemistry of adipose tissue: An endocrine organ. *Archice of Medical Sciences*, 9(2), 191–200.

DeFronzo, R., Fleming, G.A., Chen, K and Bicsak, T.A. (2016). Metformin-associated lactic acidosis: Current perspectives on causes and risk. *Metabolism*, 65(2):20-9.

Derosa, G. M. (2012). Alpha-glucosidase inhibitors and their use in clinical practice. *Archive of Medical Science*, 8(5), 899-906.

Ekor, M. (2014). The growing use of herbal medicines: Issues relating to adverse reactions and challenges in monitoring safety. *Frontiers in Pharmacology, 4*, 177-187.

Gao, K., Zheng, C., Wang, T., Zhao, H., Wang, J., Wang, Z., Zhai, X., Jia, Z., Chen, J., Zhou, Y and Wang, W. (2016). 1-Deoxynojirimycin: Occurrence, extraction, chemistry, oral pharmacokinetics, biological activities and in silico target fishing. *Molecules*, 21(11), 1600.

Gautam, K., Kumar, P and Jain, C. (2013). Comparative study of alpha amylase inhibitory activity of flavonoids of *Vitex negundo* Linn. and *Andrographis paniculata* Nees. *International Journal of Green Pharmacy*, 7, 25-8.

Giacco, F and Brownlee, M. (2010). Oxidative stress and diabetic complications. *Circulation Research*, 107(9), 1058-70.

Graham, K.L., Sutherland, R.M., Mannering, S.I., Zhao, Y., Chee, J., Krishnamurthy, B., Thomas, H.E., Lew, A.M and Kay, W.T.H. (2012). Pathogenic mechanisms in Type 1

https://etd.uwc.ac.za/

diabetes: The islet is both target and driver of disease. *Review of Diabetes Studies*, 9(4), 148-168.

Krentz, A.J and Bailey, C.J. (2005). Oral antidiabetic agents: Current role in type 2 diabetes mellitus. *Drugs*, 65(3), 385-411.

Li, M., Song, L.J and Qin, X.Y. (2014). Advances in the cellular immunological pathogenesis of type 1 diabetes. *Journal of Cellular and Molecular Medicine*, 18(5), 749-758.

Liguori, I., Russo, G., Curcio, F., Bulli, G., Aran, L., Della-Morte, D., Gargiulo, G., Testa, G., Cacciatore, F., Bonaduce, D and Abete, P. (2018). Oxidative stress, aging, and diseases. *Clinical Interventions in Aging*, 13: 757-772.

Lovegrove, A. E. (2017). Role of polysaccharides in food, digestion, and health. *Critical Reviews in Food Science and Nutrition*, 57(2), 237-253.

Mahomoodally, M. (2013). Traditional medicines in Africa: An appraisal of ten potent African medicinal plants. *Evidence-Based Complementary and Alternative Medicine*, 1-14.

Mamun-or-Rashid, A., Hossain, M., Hassan, N., Dash, B., Sapon, M and Kumer Sen, M. (2014). A review on medicinal plants with antidiabetic activity. *Journal of Pharmacognosy and Phytochemistry*, *3*(4). 149-159.

Mohammed, A., Ibrahim, M.A and Islam, M.S. (2014). African medicinal plants with antidiabetic potentials: A review. *Planta Medica,* 80(5), 354-77.

Mohammed, A., Kumar, D and Rizvi, S.I. (2015). Antidiabetic potential of some less commonly used plants in traditional medicinal systems of India and Nigeria. *Journal of Intercultural Ethnopharmacology,* 4(1), 78–85.

https://etd.uwc.ac.za/

Mohiuddin, M., Arbain, D., Shafiqul Islam, A.K.M., Ahmad, M.S and Ahmad, M.N. (2016). Alpha-glucosidase enzyme biosensor for the electrochemical measurement of antidiabetic potential of medicinal plants. *Nanoscale Research Letters*, 11(1), 95.

Nickavar, B., Abolhasani, L and Izadpanah, H. (2008). Alpha-amylase inhibitory activities of six *Salvia* species. *Iranian Journal of Pharmaceutical Research*, 7, 297-303.

Nolte, M.S and Karam, J.H. (2001). Pancreatic hormones and anti-diabetic drugs. *Basic and Clinical Pharmacology*, 13.

Ozder, A. (2014). Lipid profile abnormalities seen in T2DM patients in primary healthcare in Turkey: A cross-sectional study. *Lipids Health Diseases*, 13, 183.

Pan, S.Y., Shu-Feng, Z., Si-Hua, G., Zhi-Ling, Y., Shuo-Feng, Z., Min-Ke, T., Jian-Ning, S., Dik-Lung, M., Yi-Fan, H., Wang-Fun, F and Kam-Ming, K. (2013). New perspectives on how to discover drugs from herbal medicines: CAM's outstanding contribution to modern therapeutics. *Evidence Based Complementary and Alternative Medicine*, 627375.

Peer, N., Kengne, A.P and Motala, A.A. (2014). Diabetes in the Africa region: An update. *Diabetes Research and Clinical Practice*, 197-205.

Pham-Huy, L.A., He, H and Pham-Huy, C. (2008). Free radicals, antioxidants in disease and health. *International Journal of Biomedical Science*, 4(2), 89-96.

Preeti, K.M and Sushil, K.J. (2016). Hyperketonemia and ketosis increase the risk of complications in type 1 diabetes. *Free Radical Biology and Medicine*, 95, 268–277.

Raptis, S.A and Dimitriadis, G.D. (2001). Oral hypoglycemic agents: Insulin secretagogues, alpha-glucosidase inhibitors and insulin sensitizers. *Experimental amd clinical Endocrinoly and Diabetes*, *109*.

UNIVERSITY of the WESTERN CAPE
https://etd.uwc.ac.za/

Rekha, K.D., Farid, B.M and Balu, M.K. (2017). Human cartilage glycoprotein 39 (YKL-40): A view in type 2 diabetes mellitus. *International Journal of Pharmaceutical Sciences and Research*, 37, 4852-56.

Rekittke, N.E., Ang, M., Rawat, D., Khatri, R and Linn, T. (2016). Regenerative therapy of type 1 diabetes mellitus: From pancreatic islet transplantation to mesenchymal stem cells. *Stem Cells International*, 3764681.

Röder, P.V., Wu, B., Liu, Y and Han, W. (2016). Pancreatic regulation of glucose homeostasis. *Experimental and Molecular Medicine*, 48(3), 219.

Sears, B and Perry, M. (2015). The role of fatty acids in insulin resistance. *Lipids Health Diseases*, 14, 121.

Semenya, S., Maroyi, A., Potgieter, M.J and Erasmus, L.J.C. (2013). Herbal medicines used by Bapedi traditional healers to treat reproductive ailments in the Limpopo province, South African. *African Journal of Traditional and Complementary Alternative Medicine*, 10(2), 331-339.

Shaaban, M.A., Dawod, A.E.A and Nasr, M.A. (2016). Role of iron in diabetes mellitus and its complications. *Menoufia Medical Journal*, 29(1),11-16.

Sofowora, A., Ogunbodede, E and Onayade, A. (2013). The role and place of medicinal plants in the strategies for disease prevention. *African Journal of Traditional and Complementary Alternative Medicine*, 10(5), 210–229.

Street, R.A and Prinsloo, G. (2012). Commercially important medicinal plants of South Africa: A review. *Journal of Chemistry*, 1-16.

UNIVERSITY of the
WESTERN CAPE

https://etd.uwc.ac.za/

Suchard, J and Faaem, M.D (2001). Review: Wherefore withdrawal? The science behind recent drug withdrawals and war. *Journal of Medical Toxicology, 4*(2), 15.

Thilagam, E., Parimaladevi, B., Kumarappan, C and Mandal, S.C. (2013). Alpha-glucosidase and alpha-amylase inhibitory activity of *Senna surattensis. Journal of Acupuncture and Meridian Studies*, 6(1), 24-30.

Uddin, N.M. (2014). In vitro alpha-amylase inhibitory activity and in vivo hypoglycemic effect of methanol extract of *Citrus macroptera* Montr. fruit. *Asian Pacific Journal of Tropical Biomedicine*, 4(6), 473-479.

Ullah, A., Khan, A and Khan, I. (2016). Diabetes mellitus and oxidative stress—A concise review. *Saudi Pharmaceutical Journal, 24*(5), 547-553.

Wet, H and Proks, P. (2015). Molecular action of sulphonylureas on KATP channels: A real partnership between drugs and nucleotides. *Biochemical Society Transactions*, 43(5), 901-907.

Wilcox, G. (2005). Insulin and insulin resistance. *Clinical Biochemist Reviews*, 26(2), 19-39.

Wright, E.J., Scism-Bacon, J.L and Glass, L.C. (2006). Oxidative stress in type 2 diabetes: The role of fasting and postprandial glycaemia. *International Journal of Clinical Practice*, 60(3), 308-314.

Wu, Y., Ding, Y., Tanaka, Y and Zhang, W. (2014). Risk factors contributing to type 2 diabetes and recent advances in the treatment and prevention. *International Journal of Medical Science*, 11, 1185–1200.

Yilmazer-Musa, M., Griffith, A.M., Michels, A.J., Schneider, E and Frei, B eed extracts and their constituent catechins. *Journal of Agriculture and Food Chemistry*, 60(36), 8924–8929.

UNIVERSITY of the WESTERN CAPE
https://etd.uwc.ac.za/

CHAPTER TWO: SECTION A

POTENTIAL APPLICATION OF LAMIACEAE PLANT SPECIES IN THE MANAGEMENT OF DIABETES

2.1 Aim of this chapter

Medicinal plants and natural products have been used since ancient time in traditional medicine for diverse applications including diabetes related complications, which is one of the most common metabolic disorders with significant morbidity and mortality rate around the world. A huge number of internal and external factors such as oxidative stress, obesity, sedentary lifestyle factors including poverty, poor eating habit, and hormonal imbalance are responsible for the occurrence of this disease. Nowadays, diabetes is one of a major health challenge in Africa and its prevalence continues to increase exponentially as time going. Various treatments, particularly the usage of herbs has been effective for the management of diabetes because they are widely accepted, affordable, and have no adverse side effects. Hence, this chapter summarizes the existing information from SciFinder on the traditional uses, phytochemical constituents, and antidiabetic activities of twelve (12) Lamiaceae species used traditionally in some geographic locations as briefly described for the treatment of diabetes. The biological importance of some notable chemical constituents as applicable to this study is also described.

2.2 Lamiaceae family

Lamiaceae (formerly Labiateae), commonly known as the mint family, is a cosmopolitan flowering plant family with approximately 7136 species assigned to 236 genera. Most of the species are shrubby or herbaceous and trees are extremely rare (Hussein, 2018). The biggest genera are *Salvia* (900), *Scutellaria* (360), *Stachys* (300), *Plectranthus* (300), *Hyptis* (280), *Teucrium* (250), *Vitex* (250), *Thymus* (220) and *Nepeta* (200). *Clerodendrum* (150). The

https://etd.uwc.ac.za/

family possess a great economic value, as it contains some horticultural species, most of which are used as culinary herbs like salvia, rosemary, ocimum, and leonotis. They are well reputed to contain aromatic compounds within their leaves or flowers such as essential oils, and pharmacologically active terpenoids with a wide spectrum of applications, which are expected to play crucial roles in the process of drug discovery in cosmetic, food, and pharmaceutical industries (Uritu, et al., 2018). Many species are cultivated for their medicinal values as antiseptic, antispasmodic, calmative, antimicrobials. Additionally, it is also utilized for culinary, fragrance, flavour and aromatherapy (Raja, 2012).

In Southern Africa, Lamiaceae comprises approximately 980 species assigned to 60 genera, which are predominately found and display wide morphological diversities (Klopper, et al., 2006). South Africa is home to ± 308 species assigned to 41 genera, which is widely distributed in the country (Lee, et al., 2011).

2.2.1 Plant Morphology: Description and distribution

The leaves of Lamiaceae plant species are opposite or whorled, decussate and gland-dotted; the flowers are bisexual, rarely unisexual, arranged in compact auxiliary cymes. Zygomorphic flowers are the principal characteristic of this family with calyxes commonly persistent with 5 lobes. However, the occurrence of actinomorphic (regular) with 4 or 5 lobed flowers are also found in some genera (Raja, 2012). The corolla is tubular and 2-lipped with 2 lobed upper lips and 3 lobed lips, variously coloured and are hairy most of the time. The species are predominantly found in summer than winter in rainforest areas. The common habitats for the plants are rocky, woodland or grassland, but also along forest margins and in fynbos (Strelitzia, 2013)

.

UNIVERSITY of the WESTERN CAPE
https://etd.uwc.ac.za/

2.3 Medicinal plants used in the treatment of diabetes

Medicinal plants have been used as antidiabetic agents since time immemorial for their therapeutic potentials within the traditional healthcare system of divergent regions, communities and tribes in the African sub-region (Balogun, et al., 2016).

Lamiaceae plants species such as *Hyptis suaveolens*, *Leonotus leonorus*, *Ocimum gratissimum*, *Ocimum basillicum*, *Calamintha officinalis* Moench, *Coleus forskohlii*, *Leonotis leonurus*, *Leonotis nepetifolia*, *T. polium*, and *Salvia officinalis* have been used traditionally for diabetes related complications (Mazimba, 2015; Odeyemi & Bradley, 2018). Additionally, they have been reported to improve insulin response, lower blood glucose, inhibit alpha glucosidase, alpha amylase and other enzymes involved in diabetes complications (Wang, et al., 2010).

UNIVERSITY of the
WESTERN CAPE

https://etd.uwc.ac.za/

2.4 Lamiaceae plants species used for diabetes

2.4.1 *Calamintha officinalis* Moench

Retrieved from: http://www.phytonpathos.net/plante/detail/427

Figure 2.1: Morphology of *Calamintha officinalis* Moench

2.4.1.1 Traditional uses

Calamintha officinalis (Lamiaceae) is native to northern part of Iran (Moattar, et al., 2015), it is a perennial herb widely distributed in dry and sandy lands of Central and Southern Europe, North Africa, and Western Asia (Monforte, et al., 2011).

Different parts of *C. officinalis* (Stem, leaves and seeds) are used for the treatment of various kinds of diseases including lowering blood glucose (Khera & Bhatia, 2014). The plant is also used to treat cold, fever, parasitic infestations, inflammation, headaches and constipation. In addition, the infusion of the leaves of *C. officinalis* is traditionally utilised to treat neurovegetative distony, epilepsy, respiratory and gastrointestinal diseases (Monforte, et al., 2012).

UNIVERSITY of the WESTERN CAPE
https://etd.uwc.ac.za/

2.4.1.2 Phytochemical constituents

The phytochemical studies of the aerial part of *C. officinalis* revealed the presence of polyphenolic compounds such as caffeic, chlorogenic, hydroxycinnamic acids and rosmarinic acids (Singh, et al., 2017).

2.4.1.3 Antidiabetic activity

The bio-evaluation of *C. officinalis* extract shows a significant hypoglycaemic activity in normal and streptozotocin-induced diabetic rats without modifying the concentrations of basal plasma insulin (Lemhadri, et al., 2004). Additionally, the aqueous *C. officinalis* extract demonstrated a remarkable hypoglycaemic activity in normal and STZ diabetic rats without influencing basal plasma insulin concentrations (Singh, et al., 2017). The antidiabetic and antioxidant activities of the crude extract and its isolates (rosmarinic acid and caffeic acid) from the aerial parts of *C. officinalis* revealed that both rosamarinic acid and caffeic acid as shown in Table 2.1 are prominent natural agents for controlling diabetes (Singh, et al., 2017).

2.4.2 *Coleus forskohlii*

Retrieved from: https://www.indiamart.com/proddetail/coleus-forskohlii-tablets-10885766933.html

Figure 2.2: Morphology of *Coleus forskohlii*

https://etd.uwc.ac.za/

2.4.2.1 Traditional uses

Coleus forskohlii auct (Lamiaceae) is native to India, it is widely distributed in sandy-loam or loamy soil in the subtropical temperate climates of India, Nepal, Thailand and Sri Lanka (Loftus, et al., 2015).

Coleus is used throughout West Africa and India for the treatment of diabet*es* (Ríos-Silva, et al., 2014). It is also reputed to be used for the treatment of various kinds of diseases such as cardiovascular, respiratory, gastrointestinal, and central nervous systems (Henderson, et al., 2005). Historically, it has been used in the treamant of hypertension, eczema, congestive heart failure, colic, respiratory problems, painful urination, sleeplessness, and convulsions (Patel, 2010; Khan, et al., 2012).

2.4.2.2 Phytochemical constituents

The phytochemistry of *Coleus* is mainly composed of diterpenes (Khan, et al., 2012). Approximately 20 constituents have been found in different part of the plant, forskolin and coleonols are the most predominant phytochemicals of the root (Patel, 2010). Other minor diterpenes such as 9-deoxyforskolin, deactylforskolin, 9-dideoxy-7-deacetylforskolin have been isolated from the root extract of *C. forskohlii* (Bhowal & Mehta, 2017). Diterpenes quinines such as coleon S and coleon have been also isolated from the leaves of *Coleus* (Khan, et al., 2012). Forskolin is a first labdane diterpene isolated from the root of *coleus* in 1974 (Loftus, et al., 2015). Additionally, forskolin derivatives such as forskolin E, F G, and H have also been isolated from the same source (Bhowal & Mehta, 2017).

2.4.2.3 Antidiabetic activity

The Leaves of *Coleus* have been reported to possess a wide range of pharmaceutical applications including diabetes and weight-loss (Patel, 2010). The extract of *Coleus* has been reported to attenuate the hypoglycemic action of tolbutamide via a hepatic CYP2C-mediated mechanism (Yokotani, et al., 2014). Forskolin, the main predominant constituent of *C.*

https://etd.uwc.ac.za/

forskohlii, has been reported to stimulate glucose-induced insulin secretion *in vitro* (Khatun, et al., 2011; Bhowal & Mehta, 2017).

2.4.3 *Leonotis leonurus* L.

Retrieved from: http://pza.sanbi.org/leonotis-leonurus

Figure 2.3: Morphology of *Leonotis leonurus*

2.4.3.1 Traditional uses

Leonotis leonurus L. (Lamiaceae) is native to Southern Africa, it is widely distributed in the provinces of Eastern and Western Cape, Kwazulu-Natal and Mpumalanga (Afolayan & Sunmonu, 2010).

L. leonurus (leaves and stems) is traditionally used in South Africa to treat diabetes, cough, cold, influenza, chest infections, hypertension, eczema, epilepsy, menstruation delayed, intestinal worms, constipation, (Afolayan & Sunmonu, 2010; El-Ansari, et al., 2009). The infusions prepared from the seeds flowers and leaves are commonly used as tonics for tuberculosis, jaundice, muscular cramps, high blood pressure, diabetes, viral hepatitis, dysentery, and diarrhoea. The tea prepared from the whole plant is utilized for arthritis, piles, bladder and kidney diseases, obesity, cancer and rheumatism (Mazimba, 2015).

UNIVERSITY of the WESTERN CAPE
https://etd.uwc.ac.za/

2.4.3.2 Phytochemical constituents

The phytochemical investigation of *L. leonurus* showed the presence of sterols, diterpenes, tetracyclic triterpenoid, carbohydrates, tannins, flavonoids, alkaloids, quinines. Flavonoids were isolated from *L. leonurus* including apigenin 6-*C*-arabinoside-8-*C*-glucoside, apigenin 8-*C*-glucoside, apigenin 7-*O*-glucoside, luteolin 7-*O*-glucoside, luteolin 7-*O*-glucoside-3-methyl ether, apigenin 7-*O*-(6-*O*-p-coumaroyl)-glucoside, 6-methoxyluteolin-4-methyl ether, Luteolin 3-methyl ether, luteolin, apigenin (El-Ansari, et al., 2009). The diterpenoids such as marrubin, leoleorin K, leoleorin L, leoleorin M and leoleorin N have been reported from the leaves of *L. leonurus* (Mazimba, 2015).

2.4.3.3 Antidiabetic activity

The antidiabetic activity of *L. leonorus* has been reported to lower down the blood glucose level in streptozotocin-induced diabetic rats. The aqueous leaf extract of *L. leonorus* has also been reported to cause significant hypoglycaemic effect in rats, which was ascribed to different flavonoids, diterpenoids, polyphenolics and other phytochemical constituents of the plant extract (Odeyemi & Bradley, 2018).

UNIVERSITY of the
WESTERN CAPE

https://etd.uwc.ac.za/

2.4.4 *Rosmarinus officinalis* L.

Retrieved from: **http://florawww.eeb.uconn.edu/198501280.html**

Figure 2.4: Morphology of *Rosmarinus officinalis*

2.4.4.1 Traditional uses

Rosmarinus officinalis L. (Lamiaceae) is native to the Mediterranean region, it is one of the most popular evergreen culinary herbs cultivated worldwide including South America (de Oliveira, et al., 2019).

UNIVERSITY of the
WESTERN CAPE

Rosemary has been used traditionally since ancient time to alleviate renal colic, analgesic, rheumatic, carminative, diuretic, expectorant, anti-epileptic and dysmenorrhea, respiratory disorders (Sancheti & Goyal, 2007). Nowadays, rosemary extract is used in aromatherapy for treatment of anxiety-related conditions and increase awareness (Naimi, et al., 2017).

2.4.4.2 Phytochemical constituents

Rosemary has been reported to contain various classes of polyphenols such as phenolic acids, flavonoids and phenolic terpenes (Naimi, et al., 2017). Carnosol Carnosic and rosmarinic acid have been reported to be the most abundant constituents of rosemary (Naimi, et al., 2017; Sancheti & Goyal, 2007).

https://etd.uwc.ac.za/

2.4.4.3 Antidiabetic activity

Rosemary extract and its polyphenols (carnosic acid and rosmarinic acid) have been reported to exert significant anti-diabetic effects in different in-vivo models of type 2 diabetes and insulin-like effects in insulin target cells in-vitro models. The polyphenolic constituents of rosemary have been reported to have antioxidant, and anti-hyperglycemic properties. (Afolayan & Sunmonu, 2010).

2.4.5 *Salvia lavandulifolia* Valh

Retrieved from: http://www.floracatalana.net/salvia-officinalis-l-subsp-lavandulifolia-vahl-gams

Figure 2.5: Morphology of *Salvia lavandulifolia*

UNIVERSITY of the
WESTERN CAPE

2.4.5.1 Traditional uses

Salvia lavandulifolia Valh (Lamiaceae) is native to Iberian Peninsula, it is widely distributed in the Mediterranean area, mainly from East of Spain to western Mediterranean, South East France, North West Africa (Morocco and Algeria) (Porres-Martínez, et al., 2015)

S. lavandulifolia is used traditionally for its therapeutic properties as spasmolytic, antiseptic, analgesic, sedative, anti-inflammatory and locally anesthetic remedies. The plant has been employed for their psychoactive and psychotropic properties (Porres-Martínez, et al., 2013). The aerial parts of *S. lavandulifolia* are traditionally used as a choleretic, astringent, cicatrizing and antiseptic drug and antiperspirant effect for menopause symptoms. In addition, the leaves of Spanish sage are used traditionally for mouth ulcers and sore throat,

https://etd.uwc.ac.za/

colds, period pains and for treating of some menopause related symptoms such as flushing and sweating. The aqueous extract present hypoglycemic activity and is used as folk remedies to treat diabetic hyperglycemia (Usano-Alemany, et al., 2014).

2.4.5.2 Phytochemical constituents

The main constituents of *S. lavandulifolia* are flavonoids and terpenoids. Flavonoids, triterpenoids and monoterpenes are the most predominant components of the aerial parts (flowers and leaves), while diterpenoids are the main compounds found in the roots. The herb presents phenolic monoterpenoids, flavones and rosmarinic acid. *Salvia* is also a rich source of polyphenols (Porres-Martínez, et al., 2013).

2.4.5.3 Antidiabetic activity

The bio-evaluation of the hypoglycemic activity of *S. lavandulifolia* demonstrated that this plant significantly decreases blood glucose levels in alloxan-diabetic rabbits (Jimenez, et al., 1986).

2.4.6 *Salvia officinalis*

Retrived from: **https://www.amazon.com/Salvia-officinalis-evergreen-flowers-resistant/dp/B07N2GJXJN**

Figure 2.6: Morphology of *Salvia officinalis*

https://etd.uwc.ac.za/

2.4.6.1 Traditional uses

Salvia officinalis L. (Lamiaceae) is native to Southern Europe and Mediterranean areas, it is a perennial round shrub widely naturalized throughout the world (Craft, et al., 2017).

In folk medicine of Asia and Latin America, *S. officinalis* is used in the treatment of different kind of diseases such as seizure, ulcers, gout, rheumatism, inflammation, dizziness, tremor, paralysis, diarrhoea, obesity and diabetes. In traditional medicine of Europe, *S. officinalis* has been used for the treatment of mild dyspepsia, exude sweating, age-related cognitive problems, and some inflammations in the throat and skin. German Commission E has accepted the use of *S. officinalis* for a number of medical applications including inflammation and dyspepsia. (Eidi & Eidi, 2009)

2.4.6.2 Phytochemical constituents

The major phytochemicals found in flowers, leaves and stem of *S. officinalis* are carbohydrates, fatty acids, glycosidic derivatives (e.g., cardiac glycosides, flavonoid glycosides), phenolic compounds (e.g., coumarins, flavonoids, tannins), polyacetylenes, steroids, terpenes/terpenoids (e.g., monoterpenoids, diterpenoids, triterpenoids, sesquiterpenoids), and waxes (Hamidpour, et al., 2014). Further, the phenolic acids such as caffeic and 3-caffeoylquinic acid have been found in methanolic extract of *S. officinalis*. Several flavonoids like chlorogenic and ellagic acid, epicatechin, epigallocatechin gallate, quercetin, rutin, and luteolin-7-glucoside and rosmarinic acid are the most predominant flavonoids in *S. officinalis* extract in addition to rutin, and quercetin (Ahmad & Mahdi, 2017).

2.4.6.3 Antidiabetic activity

S. officinalis has been reported to possess a wide range of pharmaceutical applications including hypoglycemic and hypolipidemic effects. In addition, *S. officinalis* has been reported to possess hypoglycaemic effect on diabetic animals as well as to be beneficial for

https://etd.uwc.ac.za/

type 2 diabetic patients due to its capability to reduce liver glucose production (Behradmanesh, et al., 2013; Hamidpour, et al., 2014).

2.4.7 *Teucrium polium L.*

Retried from: https://esacademic.com/dic.nsf/eswiki/1140943

Figure 2.7: Morphology of *Teucrium polium*

2.4.7.1 Traditional uses

T. polium (Lamiaceae) is native to Southwest Asia and Mediterranean region. It is a perennial shrub widely distributed in the dry and stony areas of the hills and deserts of nearly all Mediterranean countries such as South-Western Asia, Europe and North Africa (Bahramikia & Yazdanparast, 2012).

T. polium has been used traditionally for the treatment of different kind of pathological conditions such as gastrointestinal disorders, inflammations, diabetes and rheumatism (Bahramikia & Yazdanparast, 2011). It has also been useful for Iranians for its diuretic, antipyretic, diaphoretic, antispasmodic, tonic, anti-inflammatory, antihypertensive analgesic, antibacterial, and antidiabetic effects (Movahedi, et al., 2014). In addition, the tea of *T. polium* is used to treat wide range of diseases including abdominal pain, indigestion, and cold. In Southern Iran, many type 2 diabetic patients used the aqueous extract (dried aerial parts) of *T. polium* as an antidiabetic drug (Bahramikia & Yazdanparast, 2012).

https://etd.uwc.ac.za/

2.4.7.2 Phytochemical constituents

The phytochemical investigations of *T. polium* have revealed that various classes of compounds such as flavonoids, iridoids, sterols, and terpenoids are present in its aerial part and root. Several authors have reported on the presence of various flavonoids such as apigenin, luteolin, rutin, cirsiliol, cirsimaritin, salvigenin and eupatorin in the roots, and aerial parts. Also, two iridoid glycosides teucardoside and teuhircoside from the hydrophilic fraction of *T. polium* have been isolated, whereas iridoid glycoside teucardoside was isolated for the first time (Bahramikia & Yazdanparast, 2012). Several steroidal compounds such as b-sitosterol, stigmasterol, campesterol, brassicasterol and clerosterol have also been isolated from the same source (Kawashty, et al., 1999).

2.4.7.3 Antidiabetic activity

T. polium and its isolates have been reported to have a broad spectrum of pharmacological applications including hypoglycaemic and hypolipidemic effects (Bahramikia & Yazdanparast, 2012). *T. polium* extract has been reported to reverse symptoms of streptozotocin-induced diabetes in rats by adjusting the pancreatic transcription factor pancreas/duodenum homeobox gene-1 (Pdx1) and forkhead transcription factor (FoxO1) expressions (Tabatabaie & Yazdanparast, 2017).

2.4.8 Leonotis nepetaefolia, R.Br

Retrieved from: http://www.africanplants.senckenberg.de/root/index.php?page_id=78&id=989

Figure 2.8: Morphology of *Leonotis nepetaefolia*

https://etd.uwc.ac.za/

2.4.8.1 Traditional uses

Leonotis nepetifolia (L.) R. Br (Lamiaceae) is native to tropical and subtropical Africa, it has been naturalized worldwide (Reshmi, et al., 2012).

L. nepetifolia is used traditionally to treat kidney diseases, rheumatism, dysmenorrhea, bronchial asthma, diarrhoea, fever, influenza, cold and cough (Choudhary, et al., 2015). In India, the plant is used for skin problems, malaria and rheumatism. The plant is also used in cases of asthma and for epilepsy in S. Africa (Dhawan, et al., 2013).

2.4.8.2 Phytochemical constituents

The phytochemical investigtion of the whole plant of *L. nepetifolia* have been reported to contain 8β,17:9,13-diepoxylabdane-16,15:19,6β-dilactone, 4,6,7-trimethoxy-5methylchromen-2-one, nepetaefolinol and leonotinin. The leaves contain labdane diterpenes such as nepetaefolin, and methoxynepetaefolin, *bis*-spirolabdane, leonepetaefolins A-E, 15-epi-leonepetaefolins A-E, flavonoids (apigenin and cirsiliol) (Li, et al., 2012; Okach, et al., 2013).

UNIVERSITY of the
WESTERN CAPE

2.4.8.3 Antidiabetic activity

Research conducted on the ethanolic extract of the whole plant of *L. nepetifolia* have reported the presence of antidiabetic activity in alloxan induced diabetic rats (Jayasree, et al., 2013)

https://etd.uwc.ac.za/

2.4.9 *Teucrium cubense*

Retrieved from: https://www.flickr.com/photos/lp_bob/7391934446/

Figure 2.9: Morphology of *Teucrium cubense*

2.4.9.1 Traditional uses

Teucrium cubense (Lamiaceae) is native to northern and tropical Africa, it is widely distributed in Coastal Germander, sandy clay, Padre and Matagorda Islands (Alonso-Castro, et al., 2010). *T. cubense* is considerably employed in the Mexican folklore for the treatment of type 2 diabetes (Alonso-Castro, et al., 2010). Teucrium species (*T. cubense*) are used as oral hypoglycemic agents in North Africa and Saudi Arabia.

2.4.9.2 Phytochemical constituents

Several furanoid diterpenes with the neo-clerodane skeleton, rearranged neo-clerodane and abietane diterpenes, sesquiterpenes, triterpenes and flavonoids have been isolated from *T. cubense* (Alonso-Castro, et al., 2010).

2.4.9.3 Antidiabetic activity

The aqueous extract of *T. cubense* has been reported to decrease plasma glucose levels in healthy rabbits. In addition, *T. cubense* activates glucose uptake in insulin-sensitive and insulin-resistant murine as well as human adipocytes (Alonso-Castro, et al., 2010).

https://etd.uwc.ac.za/

2.4.10 *Ocimum sanctum*

Retrieved from: https://www.indiamart.com/proddetail/organic-ocimum-sanctum-tulsi-6339091662.html

Figure 2.10: Morphology of *Ocimum sanctum*

2.4.10.1 Traditional uses

Ocimum sanctum L. (Lamiaceae) is native to India and is widely distributed to Malaysia, Australia, West Africa and some of the Arab countries (Mondal, et al., 2009). *O. sanctum* is used worldwide to reduce various risk factors associated with several diseases including hypoglycaemia (Jayant & Srivastava, 2016).

2.4.10.2 Phytochemical constituents

The following compounds rosmarinic acid, propanoic acid, apigenin, cirsimaritin, isothymusin, orientin, vicenin and isothymonin have been found from the leaves of *O. sanctum* (Pattanayak, et al., 2010).

2.4.10.3 Antidiabetic activity

The aqueous suspension of *O. sanctum* considerably decreases the level of blood glucose and oxidative stress with a significant increase in glycogen and protein in diabetic rats (Jayant & Srivastava, 2016). In addition, its high therapeutic potential as antidiabetic agent can be ascribed to eugenol, which is its main active constituent that can reduce/elevate serum sugar,

UNIVERSITY of the WESTERN CAPE
https://etd.uwc.ac.za/

cholesterol triglyceride levels and lactate dehydrogenase, alanine transaminase, aspartate transaminase and alkaline phosphatase (Singab, et al., 2014).

2.4.11 *Hyptis suaveolens*

Retrieved from: http://www.africanplants.senckenberg.de/root/index.php?page_id=78&id=854

Figure 2.11: Morphology of *Hyptis suaveolens*

2.4.11.1 Traditional uses

Hyptis suaveolens (L.) Poit. (Lamiaceae) is native to tropical America, it is an annual herb which is widely distributed in the northern territory and Queensland of Australia, China, Indonesia, Sovereign state, French Polynesia, Federated States of Micronesia, Niue Islands, and Guam and the Hawaiian Islands in the USA, West and Central Africa (Sharma, et al., 2013).

The leaves of *Hyptis* are traditionally used in India to treat swellings, abscesses and haemorrhoids, while the infusion is prepared for the uterus infections, colic and stomach ache. In Indonesia, the plant infusion is used to treat catarrhal (inflammation of mucous membranes, especially of the nose and throat) conditions, affections of the uterus, parasitic

UNIVERSITY of the WESTERN CAPE
https://etd.uwc.ac.za/

cutaneous diseases while the leaves are used as stomachic. In Philippines, the leaves are used for the antispasmodic, anti-rheumatic and antisoporific (Jayakumar & Ganesh, 2012).

The strong aromatic (mint/thyme) smell makes the plant to be used as an insectifuge. *H. suaveolens* serves also as a suitable substitute in infusion for tea. It is also used to treat flatulence, sweating problems and parasitic infections (Sharma, et al., 2013).

2.4.11.2 Phytochemical constituents

Diterpenes such as suaveolic acid, suaveolol, methyl suaveolate were isolated from *H. suaveolens* as well as rosamarinic acid and methyl rosmarinate, oleanolic and ursolic acid, (Sharma, et al., 2013).

2.4.11.3 Antidiabetic activity

H. suaveolens has been reported to possess significant antihyperglycemic activity in streptozotocin induced diabetic rats (Mishra, et al., 2011).

UNIVERSITY of the
WESTERN CAPE

https://etd.uwc.ac.za/

2.4.12 *Ocimum gratissium*

Retrieved from: https://www.ebay.com/c/869955936

Figure 2.12: Morphology of *Ocimum gratissimum*

2.4.12.1 Traditional uses

Ocimum gratissimum L (Lamiaceae) is native to Asia and South Africa (Silva, et al., 2016).

O. gratissimum is used traditionally throughout Western Africa and Nigeria as febrifuge, antimalarial, anticonvulsant, antimicrobial and antioxidant agents as well as in the treatment of epilepsy, high fever, diarrhoea, and mental illness. In addition, the plant is used in Africa to treat bacterial and fungal infections, fever, cold, stomach upset, haemorrhoids, catarrh, and diabetes (Omodamiro & Jimoh, 2015; Prabhu, et al., 2009). People of Kenyan and sub Saharan African communities use *O. gratissimum* for various purposes like abdominal pains, sore eyes, ear infections, coughs, barrenness, fever, convulsions, tooth gargle, regulation of menstruation and as a cure for prolapse of the rectum. In India, the whole plant has been used to treat sunstroke, headache, influenza (Pandey, 2017). The plant is frequently employed in folk medicine to treat different type of diseases such as upper respiratory tract infections, diarrhoea, headache, diseases of the eye, skin diseases, pneumonia, cough, fever and conjunctivitis (Obho, 2006).

UNIVERSITY of the WESTERN CAPE
https://etd.uwc.ac.za/

2.4.12.2 Phytochemical constituents

Numerous classes of compounds such as flavonoids, polyphenols, quinones, coumarins, and catechins were also found in the aqueous extract of *O. gratissimum* (Omodamiro & Jimoh, 2015; Venuprasad, et al., 2014).

2.4.12.3 Antidiabetic activity

The leaves extract of *O. gratissimum* was reported to possess antidiabetic activity in streptozocin-induced in diabetic rats (Prabhu, et al., 2009).

2.5 Antidiabetic activity of some notable chemical constituents isolated from Lamiaceae plants species

Numerous classes of compounds have been reported to be the bioactive constituents of numerous plant species of Lamiaceae family used in folk medicine for their potential applications in the management of diabetes related complications. Among these bioactive compounds, flavonoids demonstrated significant antidiabetic activity due to the hydroxyl group allocated at C-3 on the A-ring and additional hydroxyl groups attached to the C-ring which play an important role in the inhibition process of alpha-glucosidase and-amylase enzymes as well as hypoglycaemia, insulin activation, glucose uptake activation (Wang, et al., 2010). Hence, the mode of action of such compounds is illustrated in Table 2.1.

Table 2.1: Antidiabetic activity of different constituents of Lamiaceae plant species

Compounds	Plant source	Biological activity/mode of action	References
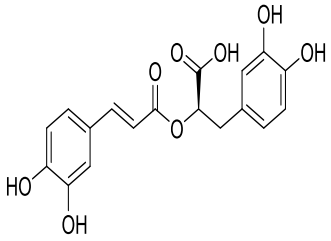 Rosmarinic acid	*C. officinalis* *Rosemary* *S. lavandulifolia* *O. canum*	Hypoglycaemic effect Significant anti-diabetic effects in different in-vivo models of type 2 diabetes and insulin-like effects in insulin target cells in-vitro models	(Singh, et al., 2017) (Afolayan & Sunmonu, 2010).

https://etd.uwc.ac.za/

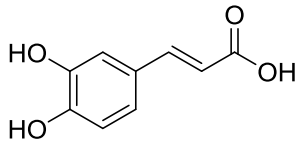 Caffeic acid	*C. officinalis* *S. officinalis*	Hypoglycaemic effect	(Singh, et al., 2017).
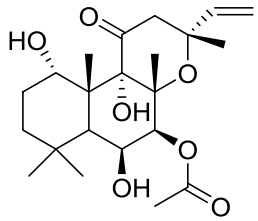 Forskolin	*C. forskohlii*	Glucose-induced insulin secretion Decreased fasting blood glucose levels	(Khatun, et al., 2011; Bhowal & Mehta, 2017)
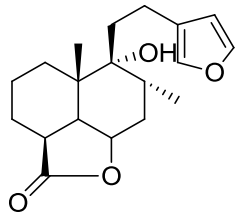 Marrubiin	*L. leonurus*	Increases the level of insulin and glucose transporter-2 gene expressions in INS-1 cells	(Firdous, 2014)
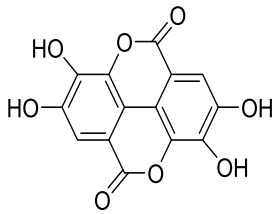 Ellagic acid	*S. officinalis*	Stimulates insulin secretion and decreases glucose intolerance	(Fatima, et al., 2017)
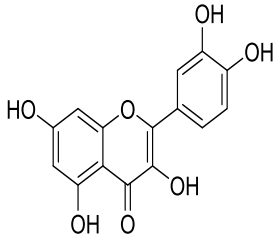 Quercetin	*S. officinalis*	Stimulate β-cells to release more insulin	(Jadhav & Puchchakayala, 2012)

https://etd.uwc.ac.za/

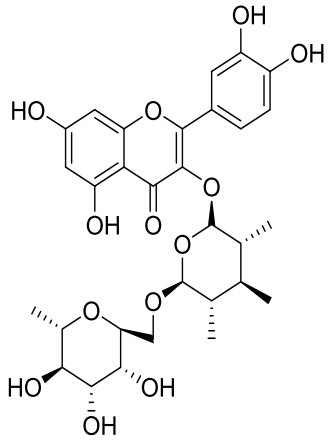 Rutin	*S. officinalis*	Stimulates β-cells to produce more insulin	(Jadhav & Puchchakayala, 2012)
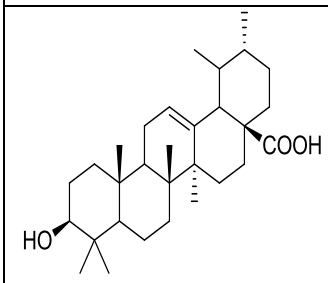 Ursolic acid	*S. officinalis*	Hypoglycemic, glucose-lowering effect and stimulate glucose uptake	(Wu, et al., 2014) (Guzmán-Ávila, et al., 2018)
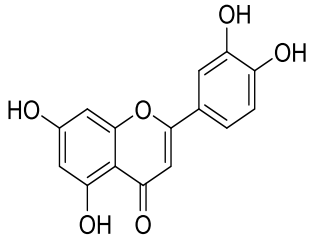 Luteolin	*T. polium*	Anti-diabetic effects and hypoglycemic effect	(Zang, et al., 2016)
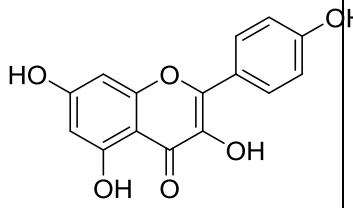 Apigenin	*T. polium*	Reduces blood glucose antidiabetic activity	(Osigwe, et al., 2017)
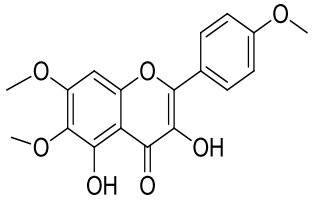 Salvigenin	*T. polium*	Improves diabetes through decreasing blood glucose, lipid profile, HbA1c. Increased insulin secretion	(Sadeghi, et al., 2016)

UNIVERSITY of the WESTERN CAPE

https://etd.uwc.ac.za/

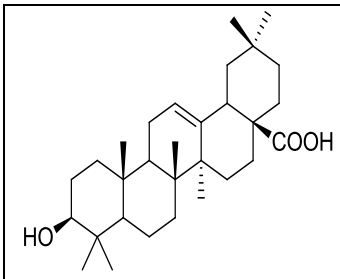 Oleanolic acid	*H. suaveolens*	Improves insulin response Significant blood glucose-lowering and weight-losing effect	(Castellano, et al., 2013) (Wang, et al., 2011)

2.6 Conclusion

This review decribes the traditional uses, phytochemical constituents, and antidiabetic activities of twelve (12) Lamiaceae plant species used traditionally in some geographic locations for the treatment of diabetes. Additioanally, it highlighted the biological importance of some notable chemical constituents isolated from Lamiaceae family for their potential application in the prevention and management of type 2 diabetes complications using different mechanism of action.

References

Afolayan, A.J and Sunmonu, T.O. (2010). In vivo studies on antidiabetic plants used in South African herbal medicine. *Journal of Clinical Biochemistry and Nutrition*, 47(2), 98-106.

Ahmad, G and Mahdi, E. (2017). Pharmacological properties of *Salvia officinalis* and its components. *Journal of Traditional and Complementary Medicine*, 7(4), 433–440.

Alonso-Castro, A., Zapata-Bustos, R., Romo-Yañez, J., Camarillo-Ledesma, P., Gómez-Sánchez, M and Salazar-Olivo, L. (2010). The antidiabetic plants *Tecomastans* (L.) Juss. ex Kunth (Bignoniaceae) and *Teucrium cubense* Jacq (Lamiaceae) induce the incorporation of glucose in insulin-sensitive and insulin-resistant murine and human adipocytes. *Journal of Ethnopharmacology*, 127(1), 1-6.

Bahramikia, S and Yazdanparast, R. (2012). Phytochemistry and medicinal properties of *Teucrium polium* L. (Lamiaceae). *Phytotherapy Research*, 26(11), 1581-93.

Balogun, F.O., Tshabalala, N.T and Ashafa, A.O.T. (2016). Antidiabetic medicinal plants used by the Basotho Tribe of Eastern Free State: A review. *Journal of Diabetes Research*, 2-13.

Behradmanesh, S., Derees, F and Rafieian-kopaei, M. (2013). Effect of *Salvia officinalis* on diabetic patients. *Journal of Renal Injury Prevention*, 2(2), 51–54.

https://etd.uwc.ac.za/

Bhowal, M and Mehta, D.M. (2017). *Coleus forskholii*: Phytochemical and pharmacological profile. *International Journal of Pharmaceutical Sciences and Research*, 1, 3599-3618.

Choudhary, M., Kumar, V and Malhotra, H. (2015). Medicinal plants with potential antiarthritic activity. *Journal of Intercultural Ethnopharmacology*, 4(2), 147-170.

Craft, J.D., Satyal, P and Setzer, W.N. (2017). The chemotaxonomy of common Sage (*Salvia officinalis*) based on the volatile constituents. *Medicines*, 4, 47.

De Oliveira, J.R., Camargo, S.E.A and de Oliveira, L.D. (2019). *Rosmarinus officinalis* L. (rosemary) as therapeutic and prophylactic agent. *Journal of Biomedical Science*, 26, 5.

Dhawan, N.G., Khan, A.S and Srivastava, P. (2013). A general appraisal of *Leonotis nepetifolia* (L) R. Br: An essential medicinal plant. *Bulletin of Environment, Pharmacology and Life Sciences*, 2(8), 118-121.

Eidi, A and Eidi, M. (2009). Antidiabetic effects of *sage* (*Salvia officinalis* L.) leaves in normal and streptozotocin-induced diabetic rats. *Diabetes and Metabolic Syndrome Clinical Research and Reviews*, 3(1), 40-44.

El-Ansari, M.A., Aboutabl, E.A., Farrag, A.R.H., Sharaf, M., Hawas, U.W., Soliman, G.M and El-Seed, G.S. (2009). Phytochemical and pharmacological studies on *Leonotis leonurus*. *Pharmaceutical Biology*, 47(9), 894–902.

Fatima, N., Hafizur, R.M., Hameed, A., Ahmed, S., Nisar, M and Kabir, N. (2017). Ellagic acid in *Emblica officinalis* exerts anti-diabetic activity through the action on β-cells of pancreas. *European Journal of Nutrition*, 56(2), 591-60.

Firdous, S. (2014). Phytochemicals for treatment of diabetes. *Excli Journal*, 451-453.

Habtemariam, S. (2016). The therapeutic potential of *Rosemary* (*Rosmarinus officinalis*) diterpenes for alzheimer's disease. *Evidence Based Complementary and Alternaternative Medicine*, 2680409.

Hamidpour, M., Hamidpour, R., Hamidpour, S and Shahlari, M. (2014). Chemistry, pharmacology, and medicinal property of *Sage* (*Salvia*) to prevent and cure illnesses such as obesity, diabetes, depression, dementia, lupus, autism, heart disease, and cancer. *Journal of Traditional and Complementary Medicine*, 4(2), 82–88.

Hussein, A.A. (2018). Chemistry of South African Lamiaceae: Structures and biological *activity of terpenoids.* Open access peer-reviewed chapter.

Jadhav, R and Puchchakayala, G. (2012). Hypoglycemic and antidiabetic activity of flavonoid: Boswellic acid, ellagic acid, quercetin, rutin on streptozotocin-nicotinamide induced type 2 diabetic rats. *International Journal of Pharmacy and Pharmaceutica*, 4(2).

Jayakumar, S.V and Ganesh, S.M.K. (2012). New enolic type bioactive constituents from *Hyptis suaveolens* (L.) Poit. *Asian Journal of Plant Science and Research*, 2(4), 403-408.

UNIVERSITY of the WESTERN CAPE

https://etd.uwc.ac.za/

Jayant, S.K and Srivastava, N. (2016). Effect of *Ocimum sanctum* against alloxan induced diabetes. *Integrative Obesity and Diabetes*, 2(5), 1-4.

Jayasree, G., Sunanda, S., Krishna, C.B., Alekhya, R and Ramesh, C. (2013). Antidiabetic activity of *Leonotis neptefolia* linn in alloxan induced diabetic rats. *International Journal of Preclinical and Pharmaceutical Research*, 4(1), 5-9.

Jimenez, J., Risco, S., Ruiz, T and Zarzuelo, A. (1986). Hypoglycemic activity of *Salvia lavandulifolia*. *Planta Medica*, 52(4), 260-2.

Kawashty, S.A., Gamal El-Din, E.M and Saleh, N.A.M. (1999). The flavonoid chemosystematics of two *Teucrium* species from Southern Sinai, Egypt. *Biochemical Systematics and Ecology*, 27(6), 657-660.

Khan, B.A., Akhtar, N., Anwar, M., Mahmood, T., Khan, H., Hussain, I and Khan, K.A (2012). Botanical description of *Coleus forskohlii*: A review. *Journal of Medicinal Plants Research*, 6(34), 4832-4835.

Khatun, S., Chatterjee, N.C and Cakilcioglu, U. (2011). Antioxidant activity of the medicinal plant *Coleus forskohlii*. *African Journal of Biotechnology*, 10(13), 2530-2535.

Khera, N and Bhatia, A. (2014). Medicinal plants as natural anti-diabetic agents. *International Journal Of Pharmaceutical Sciences and Research*, 5(3), 713-29.

Klopper, R.R., Chatelain, C., Banninger, V., Habashi, C., Steyn, H.M., De Wet, B.C., Arnold, T.H., Gautier, L., Smith, G.F and Spichiger, R. (2006). Checklist of the flowering plants of Sub-Saharan Africa. An index of accepted names and synonyms. *Southern African Botanical Diversity Network*.

Lee, C.J., Chen, L.G., Chang, T.L., Ke, W.M., Lo, Y.F and Wang, C.C. (2011). The correlation between skin-care effects and phytochemical contents in Lamiaceae plants. *Food Chemistry, 124*, 833-841.

Lemhadri, A., Zeggwagh, N.A., Maghrani, M., Jouad, H., Michel, J.B and Eddouks, M. (2004). Hypoglycaemic effect of *Calamintha officinalis* Moench. in normal and streptozotocin-induced diabetic rats. *Journal of Pharmacy and Pharmacology*, 56(6), 795-9.

Li, J., Fronczek, F.R., Ferreira, D., Burandt, C.L.J., Setola, V., Roth, B.L and Zjawiony, J.K. (2012). Bis-spirolabdane diterpenoids from *Leonotis nepetaefolia*. *Journal of Natural Products*, 5(4), 728-34.

Loftus, H.L., Astell, K.J., Mathai, M.L and Su, X.Q. (2015). *Coleus forskohlii* extract supplementation in conjunction with a hypocaloric diet reduces the risk factors of metabolic syndrome in overweight and obese subjects: A randomized controlled trial. *Nutrients*, 7(11), 9508-9522.

Mazimba, O. (2015). *Leonotis leonurus*: A herbal medicine review. *Journal of Pharmacognosy and Phytochemistry*, 3(6), 74-82.

UNIVERSITY of the WESTERN CAPE

https://etd.uwc.ac.za/

Mishra, S.B., Verma, A., Mukerjee, A and Vijayakumar, M. (2011). Anti-hyperglycemic activity of leaves extract of *Hyptis suaveolens* L. Poit in streptozotocin induced diabetic rats. *Asian Pacific Journal of Tropical Medicine*, 5(9), 689-693

Moattar, F.S., Sariri, R., Giahi, M., Yaghmaee, P., Ghafoori, H and Jamalzadeh, L (2015). Antioxidant and anti-proliferative activity of *Calamintha officinalis* extract on breast cancer Cell Line MCF-7. *Journal of Biological Sciences*, 15 (4), 194-198.

Mondal, S., Mirdha, B and Mahapatra, B. (2009). The science behind sacredness of tulsi (*Ocimum sanctum*). *Indian Journal of Physiology and Pharmacology*, 53(4), 291–306.

Monforte, M.T., Lanuzza, F., Pergolizzi, S., Mondello, F., Tzakou, O and Galati, M. (2012). Protective effect of *Calamintha officinalis* Moench leaves against alcohol-induced gastric mucosa injury in rats. Macroscopic, histologicand phytochemical analysis. *Phytotheurapy Research*, 26, 839-844.

Monforte, M.T., Zakou, O; Nostro, A., Zimbalatti, V and Galati, E.M. (2011). Chemical composition and biological activities of *Calamintha officinalis* Moench essential oil. *Journal of Medicinal Food*, 14, 3.

Movahedi, A., Basir, R., Rahmat, A., Charaffedine, M and Othman, F. (2014). Remarkable anticancer activity of *Teucrium polium* on hepatocellular carcinogenic rats. *Evidence Based Complementary and Alternative Medicine*, 726724.

Naimi, M., Vlavcheski, F., Shamshoum, H and Tsiani, E. (2017). *Rosemary* extract as a potential anti-hyperglycemic agent: Current evidence and future perspectives. *Nutrients*, 9, 968.

Obho, G. (2006). Antioxidant and antimicrobial properties of ethanolic extract of *Ocimum gratissimum* leaves. *Journal of Pharmacology and Toxicology*, 1(1), 47-53.

Odeyemi, S and Bradley, G. (2018). Medicinal plants used for the traditional management of diabetes in the Eastern Cape, South Africa: Pharmacology and toxicology. *Molecules*, 23, 2759.

Okach, D.O., Nyunja, A.R.O and Opande, G. (2013). Phytochemical screening of some wild plants from Lamiaceae and their role in traditional medicine in Uriri District Kenya. *International Journal of Herbal Medicine*, 1(5), 135-143.

Omodamiro, O.D and Jimoh, M.A. (2015). Antioxidant and antibacterial activities of *Ocimum gratissimum*. *Original article*, 2748.

Pandey, S. (2017). Phytochemical constituents, pharmacological and traditional uses of *Ocimum gratissimum* in tropics. *Indo American Journal of Pharmaceutical Sciences*, 4(11), 4234-4242.

Patel, M. (2010). Forskolin: A successful therapeutic phytomolecule. *East and Central African Journal of Pharmaceutical Sciences*, 13, 25- 32.

UNIVERSITY of the WESTERN CAPE

https://etd.uwc.ac.za/

Pattanayak, P., Behera, P., Das, D and Panda, S.K. (2010). *Ocimum sanctum* Linn. A reservoir plant for therapeutic applications: An overview. *Pharmacognosy Reviews*, 4(7), 95-105.

Porres-Martínez, M., Carretero Accame, M and Gómez-Serranillos, M.P. (2013). Pharmacological activity of *Salvia lavandulifolia* and chemical components of its essential oil. A review. *Lazaroa*, 34, 237-254.

Porres-Martínez, M., González-Burgos, E., Carretero, E.M.M and Gómez-Serranillos, M.P. (2015). Protective properties of *Salvia lavandulifolia* Vahl. essential oil against oxidative stress-induced neuronal injury. *Food and chemical toxicology*, 80, 154-162.

Raja, R. (2012). Medicinally potential plants of Lamiaceae family: An overview. *Research Journal of Medicinal Plants, 6*, 203-213.

Reshmi, P., Nishteswar, K and Kumari, H. (2012). Ethno medicinal claims of *Leonotis nepetifolia* (L.) R. BR: A review. *International Journal of Research in Ayurveda and Pharmacy*, 3(6), 783-785.

Ríos-Silva, M., Trujillo, X., Trujillo-Hernández, B., Sánchez-Pastor, E., Urzúa, Z., Mancilla, E and Huerta, M. (2014). Effect of chronic administration of forskolin on glycemia and oxidative stress in rats with and without experimental diabetes. *International Journal of Medical Science*, 11(5), 448–452.

Sancheti, G and Goyal, P.K. (2007). Role of Rosemary leaf extract against various doses of gamma radiation. *Trees for Life Journal*, 2, 2.

Sharma, P., Roy, R., Chaudhary, A., Gupta, D and Vipin, K. (2013). *Hyptis suaveolens* (L.) poit: A phyto-pharmacological review. *International Journal of Chemical and Pharmaceutical Sciences*, 4(1).

Silva, M.K.N., Carvalho, V.R.A and Matias, E.F.F. (2016). Chemical profile of essential oil of *Ocimum gratissimum* L. and evaluation of antibacterial and drug resistance-modifying activity by gaseous contact method. *journal in the field of Pharmacognosy Journal*, 8(11).

Singh, P.P., Jha, S., Irchhaiya, R., Fatima, A and Agarwal, P. (2017). A Review on phytochemical and pharmacological potential of *Calamintha officinalis* moench. *International Journal of Pharmaceutical Sciences and Research*, 3, 4.

Strelitzia. (2013). Plants of The Greater Cape Floristic Region. Pretoria: SANBI.

Tabatabaie, P.S and Yazdanparast, R. (2017). *Teucrium polium* extract reverses symptoms of streptozotocin-induced diabetes in rats via rebalancing the Pdx1 and FoxO1 expressions. *Biomedicine and Pharmacotherapy*, 93, 1033-1039

Uritu, C.M., Mihai, C.T., Stanciu, G.D., Dodi, G., Alexa-Stratulat, T., Luca, A., Leon-Constantin, M.M., Stefanescu, R., Bild, V., Melnic, S and Tam, B.I. (2018). Medicinal plants of the family Lamiaceae in pain therapy: A review. *Pain Research and Management*, 2-44.

https://etd.uwc.ac.za/

Usano-Alemany, J., Pala-Raul, J and Herraiz-Penalver, D. (2014). Comprehensive phenological description of essential-oil chemotypes of *Salvia lavandulifolia* Vahl grown under the same environmental conditions. *Chemistry & Biodiversity*, 11.

Venuprasad, M.P., Kandikattu, H.K., Razack, S and Khanum, F. (2014). Phytochemical analysis of *Ocimum gratissimum* by LC-ESI–MS/MS and its antioxidant and anxiolytic effects. *South African Journal of Botany*, 92,151-158.

Wang, H., Du, Y and Song, H. (2010). Alpha-glucosidase and alpha-amylase inhibitory activities of *guava* leaves. *Food Chemistry*, 123(1), 6-13.

Wu, P.Z. (2014). In vitro and in vivo evaluation of the antidiabetic activity of ursolic acid derivatives. *European Journal of Medicinal Chemistry*, 80, 502-508.

Yokotani, K., Chiba, T., Sato, Y and Umegaki, K. (2014). *Coleus forskohlii* extract attenuates the hypoglycemic effect of tolbutamide in vivo via a hepatic cytochrome P450-mediated mechanism. *Shokuhin Eiseigaku Zasshi*, 55(2), 73-8.

UNIVERSITY of the
WESTERN CAPE

https://etd.uwc.ac.za/

CHAPTER TWO: SECTION B

REVIEW: ABIETANE DITERPENES AS POTENTIAL CANDIDATES FOR THE MANAGEMENT OF TYPE 2 DIABETES

2.7 Abstract

Diabetes mellitus (DM), being one of the most common metabolic disorders with an elevated morbidity and mortality rate. It is characterised by deficiency in insulin secretion or degradation of secreted insulin. Many internal and external factors such as oxidative stress, obesity and sedentary lifestyle among others have been suggested as the major causes of these cell alterations. Diabetes I and II are the most common types of diabetes. Treatment of type I requires insulin injection, while type II can be managed using different synthetic antidiabetic agents. However, their effectiveness is limited as a result of low bioavailability, high cost of drug production, and unfavourable side effects. There is a great need to develop alternative and more active antidiabetic drugs from natural sources. Different forms of natural products have been used since time immemorial as a source of medicine for the purpose of curing numerous human diseases including diabetes. Secondary metabolites such as polyphenols, flavonoids, terpenoids, alkaloids and several other constituents have direct and indirect roles in controlling such diseases, among them, abietane diterpenes have been reported to display a broad spectrum of interesting biological activities including diabetes. This review aimed to summarize existing data from SciFinder (2005-2018) on the biological importance of abietane diterpenes in the prevention and management of type 2 diabetes and closely related diseases.

Keywords: Diabetes mellitus; oxidative stress; secondary metabolites.

https://etd.uwc.ac.za/

2.8 Introduction

Diabetes mellitus (DM), being one of the most common metabolic disorders with an elevated morbidity and mortality rate, which accounted for about 425 million diabetes patients worldwide in 2017. This number is expected to gradually increase to 629 million by 2045 (Tripathy, 2018). It is characterised by deficiency in insulin secretion or degradation of secreted insulin (Cao, et al., 2012), which is the result of cells alterations caused by many internal and external factors such as oxidative stress, obesity and sedentary lifestyle among others (Mamun-or-Rashid, et al., 2014; Ullah, et al., 2016). In Africa, an estimation of 14 million people accounting for approximately 4.3 % of adults have diabetes, which caused an estimated number of 401276 deaths in 2012 (Mohammed, et al., 2014). A huge number of synthetic antidiabetic agents such as acarbose, miglitol, sulfonylurea, metformin and thiozolidinedione are readily available in the market. However, their effectiveness is limited as a result of low bioavailability, high cost of drug production, and unfavourable side effects such as hypoglycaemia, damage to liver, flatulence, diarrhoea, abdominal pain, dropsy, drug-resistance, weight gain and heart failure (Lorenzati, et al., 2010; Marín-Peñalver, et al., 2016). Therefore, there is a great need of developing potent natural antidiabetic products of high safety margin. Natural products have been used since time immemorial as a source of medicine curing numerous human afflictions owing to their antidiabetic, antioxidant and they are the main sources of health-promoting substances that comprise secondary metabolites such as polyphenols, flavonoids, and several other constituents (Sofowora, et al., 2013). Among them, abietane diterpenes have been reported to display a broad spectrum of promising biological activities including diabetes.

Abietanes belong to the fanily of diterpenoids that have been reported from varieties of terrestrial plant sources of different family such as Araucariaceae, Cupressaceae, Phyllocladaceae, Pinaceae, Podocarpaceae, Asteraceae, Celastraceae, Hydrocharitaceae and

https://etd.uwc.ac.za/

Lamiaceae (Fan, et al., 2017). They are mainly characterised by a core skeleton of 20 carbons with different degree of oxygenation at several positions of B and C ring. The biosynthesis of abietane diterpenes occurs by two different pathways: The mevalonic acid pathway and the deoxyxylulose phosphate pathway, which involves a consecutive cyclisation reactions and/or rearrangement reactions of geranylgeranyldiphosphate as shown in Figure 2.13 (Gonzalez, 2015). Abietane diterpenes can be categorised into eight different types based on structural arrangements involving reduction or oxidation such as hydroxylation, dehydration and cyclisation between different oxygenated groups. Abietic acid type abietane, is characterized by the presence of a carboxylic acid in the compound, while levopimaric acid type abietane is characterised by a double bond in ring C. Ferruginol and carnosol type abietanes are characterised by the presence of phenolic hydroxyl groups in ring C, except that the presence of a lactone ring could extend across ring B at positions C-7 to C-10 in carnosol type abietanes which differentiate them from ferruginol type abietanes. Callicarpone type abietanes are based on the epoxide ring at position C-12 and the presence of a hydroxy isopropyl group attached to C-15 with unsaturated ketone groups in rings B and C. The royleanones have a benzoquinone ring C. Tanshinone abietanes consist of highly oxidised rings where rings, A and/or B are aromatic, and ring C usually contains two adjacent α, β-unsaturated systems and a furan ring present as ring D. Fichtelite closely resembles the abietane skeletal structure and sometimes referred to as a norabietane due to the absence of the methyl group at position C-4. These are also characterised by the presence of a double bond at position C-4 in the chemical structure.

https://etd.uwc.ac.za/

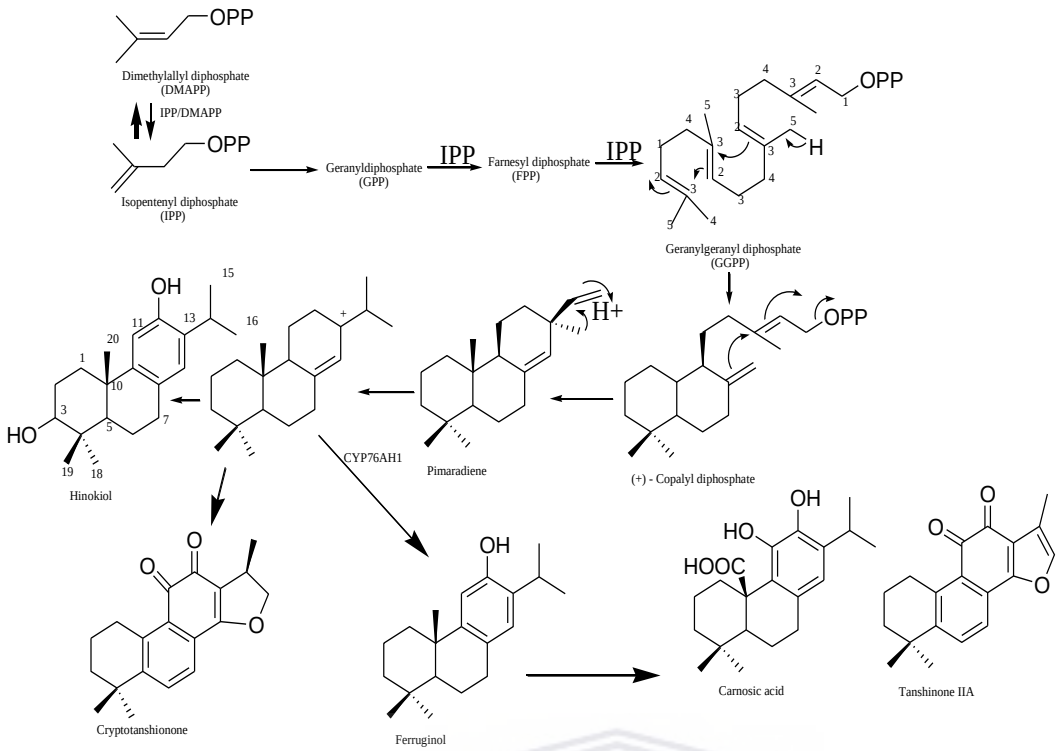

Figure 2.13: Biosynthesis of abietane diterpenes

Abietane diterpenes have also been reported to display a broad spectrum of biological activities including anticancer, antiviral, antimicrobial, antileishmanial, antiplasmodial, antifungal, antitumour, cytotoxicity, antiulcer, cardiovascular, antioxidant, anti-inflammatory and antidiabetic (Gonzalez, 2015). However, abietane type diterpenes such as carnosic acid derivatives has been reported to be very efficient in the management of diabetes complications by improving insulin secretion (Song, et al., 2018) as well as glucose homeostasis or stimulate glucose uptake by increasing peripheral glucose clearance in tissues thereby alleviate pathological effects related with the hyperglycaemic state (Lipina & Hundal, 2014). Carnosol stimulates glucose uptake (Vlavcheski, et al., 2018), improves diabetes and its complications by the regulation of oxidative stress and inflammatory responses (Samarghandian, et al., 2017). This review serves as background information for the *in-vitro* and *in-vivo* antidiabetic activity of abietane diterpenes isolated from different plant species.

https://etd.uwc.ac.za/

2.9 *In vitro* models

The therapeutic approach to manage type 2 DM is to decrease the postprandial glucose levels through the inhibition of alpha-glucosidase enzyme by reducing the rate of carbohydrate digestion or delaying the carbohydrates absorbance in the intestine. The *in-vitro* bio-evaluation revealing the ability of various plant-derived abietanoids from *Plectranthus madagascariensis*, *Metasequoia glyptostroboides*, *Rosmarinus officinalis*, *Salvia* species to inhibit *alpha*-glucosidase activity (Nazaruk & Borzym-Kluczyk, 2015). Taxoquinone, isolated from *Metasequoia glyptostroboides* showed moderate inhibitory activity against *alpha*-glucosidase with the percentage of inhibition ranging from 9.24 to 51.32 % at the concentration range from 100 to 3.0 μg/mL (Bajpai, et al., 2015).

Protein tyrosine phosphatases (PTP 1B) are enzymes directly involved in the modulation of cellular signalling and metabolism. They are involved in the dephosphorylation process of the receptor *β*-subunit. Therefore, the inhibition of PTP 1B can potentially improve insulin resistance; regulate plasma glucose and insulin levels without inducing hypoglycaemia (Nazaruk & Borzym-Kluczyk, 2015). Few natural tanshinones such as cryptotanshinone, tanshinol B and dehydrodanshenol A isolated from *Salvia miltiorrhiza* (Lamiaceae) exhibited potent protein tyrosine phosphatase 1B (PTP1B) inhibition with IC_{50} values of 5.5 ± 0.9, 4.7 ± 0.4 and 8.5 ± 0.5 μM, respectively as shown in Table 2.1 (Kim, et al., 2017).

Diacylglycerol acyltransferase (DGCT) is well known to be involved in the catalytic reaction of acyl residue transfer from acyl-CoA to diacylglycerol to form triacylglycerol (Tabata, et al., 1997). It plays a crucial t in the metabolism of cellular diacylglycerol and is vital for triglyceride metabolism such as intestinal fat absorption, lipoprotein assembly, modulation of plasma triglyceride concentrations, and fat storage in adipocytes (Dahlqvist, et al., 2000). However, triglycerides accumulation, when above threshold level in certain tissues, can lead to serious diseases such as atherosclerosis, diabetes, metabolic disorders. Diacylglycerol

https://etd.uwc.ac.za/

acyltransferase (DGAT) is involved in triacylglycerol formation and thus is expected to be an effective target of inhibition for the treatment and prevention of these abovementioned diseases (Yang & Nickels, 2015). The inhibition of DGAT has been studied and the results suggested that abietane-type diterpenes isolated from *R. officinalis* possess moderate DGAT1 inhibition activity and carnosol is one of the major components that exhibits the highest inhibitory activity on *de novo* intracellular triglyceride synthesis on human hepatocyte HepG2 cells (Cui, et al., 2012). Carnosol also suppressed cAMP/CREB-induced gene expression mediated by the glucose-6-phosphatase (G6Pase) promoter, which indicate that it possesses the potential to lower fasting blood glucose levels by suppressing gluconeogenesis *via* inhibition of the cAMP/PKA/CREB pathway (Yun, et al., 2013). Additionally, carnosol activates glucose uptake in L6 myotubes in dose- and time-dependent manner, without affecting protein kinase B (Akt). It is increased the activation of the energy sensor AMP-activated kinase (AMPK) phosphorylation and plasma membrane GLUT4 levels (Vlavcheski, et al., 2018).

UNIVERSITY of the
WESTERN CAPE

Peroxisome proliferator-activated receptors (PPARs) are ligand-activated transcription factors of nuclear hormone receptor superfamily. The activation of PPAR-γ causes insulin sensitization and enhances glucose metabolism. PPARs are prominent therapeutic targets for numerous obesity-related problems such as overt type 2 diabetes, atherosclerosis, and the metabolic syndrome. Christensen, et al. (2010), have reported that 12-*O*-methyl carnosic acid significantly activates nuclear receptor peroxisome proliferator-activated receptor PPAR-γ by exerting its beneficial effect on lipid and glucose homeostasis through PPAR-γ-mediated pathways.

Glucose-6-phosphatase (G6Pase) is an enzyme, which is mainly found in the liver and the kidneys, and it plays a critical role in blood glucose homoeostasis. However, inhibitors of glucose-6-phosphate translocase (G6P T1) are directly involved in the control of abnormal

https://etd.uwc.ac.za/

glucose levels (Schaftingen & Gerin, 2002). Abietic acid and dehydroabietic acid decrease the activity of G6Pase and stimulates Glycogen Synthase (GS). (Nachar, et al., 2015). Promoters for cytosolic phosphoenolpyruvate carboxykinase (PEPCK-C) and glucose-6-phosphate (G6Pase) play a vital role in the homeostatic regulation of blood glucose levels. Hence, the suppression of cAMP/protein kinase response of the PEPCK-C or G6Pase gene may significantly contribute to the antihyperglycemic activity. Abietane diterpenes such as 7-O-methylrosmanol royleanonic acid and carnosol isolated from Rosemary have been reported to suppress forskolin (FSK)-induced luciferase expression when monitored by cAMP/response element (CRE), PEPCK-C and G6Pase gene promoters (Yun, et al., 2013). Tanshinone I and 16-dihydrotanshinone I have been report to increase the activity of insulin on the tyrosine phosphorylation of the insulin receptor (IR) in addition to the activation of the downstream kinases Akt, ERK1/2, and GSK3beta. The insulin-sensitizing activities demonstrated by these compounds may be very useful for developing new anti-diabetic agents as specific insulin receptor activators (Jung, et al., 2009)

UNIVERSITY of the
WESTERN CAPE

Table 2.2: In vitro antidiabetic activity of some abietane diterpenes

Compound	Biological activity	references
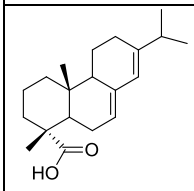 Abietic acid	Decreases the activity of G6Pase Stimulates Glycogen Synthase (GS)	(Nachar, et al., 2015)
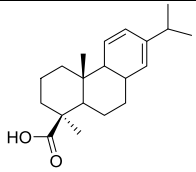 Dehydroabietic acid	Reduces MCP-1, TNF-α, and NO productions by activated macrophages and differentiated adipocytes Improves inflammatory changes associated with obesity-related diabetes	(Kang, et al., 2008)
	Regulation of liver cell glucose homeostasis	(Nachar, et al.,

https://etd.uwc.ac.za/

		2015)
	Improves diabetic wound healing.	(Wang, et al., 2014)
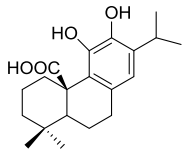 Carnosic acid	Activates Nrf2/ARE and Inhibition of NF-κB pathway	(Xie, et al., 2018)
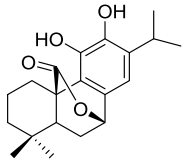 Carnosol	Inhibition of DGAT activity with IC_{50} = 62.5 ± 2.1 µM Suppress cAMP/CREB induce gene expression	(Cui, et al., 2012)
	Stimulates glucose uptake in L6 myotubes Inhibition of the pancreatic lipase activity	(Yun, et al., 2013)
	Regulation of glucose homeostasis	(Vlavcheski, et al., 2018)
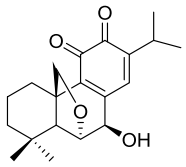 7β-hydroxy-20-deoxo-rosmaquinone	Inhibitor of Diacyl glycerol acyl transferase (DGAT)	(Cui, et al., 2012)
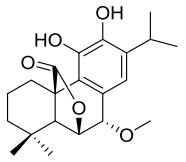 7α-methoxyrosmanol	Inhibitor of DGAT	(Cui, et al., 2012)
	Suppress cAMP/CREB induced gene expression	(Yun, et al., 2013)
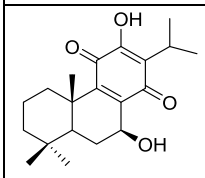 Taxoquinone	Alpha-glucosidase inhibitor	(Bajpai, et al., 2015)

UNIVERSITY of the WESTERN CAPE
https://etd.uwc.ac.za/

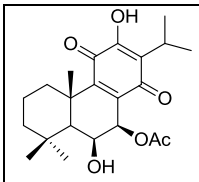 7β-acetoxy-6β-hydroxyroyleanone	Alpha-glucosidase inhibitor	(Kubínová, et al., 2014)
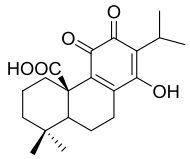 Royleanonic acid	Suppress cAMP/CREB induced gene expression mediated by the G6Pase promoter	(Yun, et al., 2013)
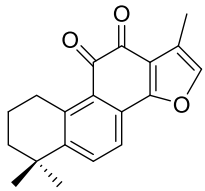 Tanshinone IIA *Salvia miltiorrhiza*	Down regulation of the expression levels of VEGF and ICAM-1	(Fan, et al., 2017)
	Delays the promotion of diabetic nephropathy via inhibiting oxidative stress and inflammatory reaction	(Chen, et al., 2017)
	Protect against diabetes-induced impairment of endothelium-dependent vasorelaxation	(Li, et al., 2015)
	Renoprotective activity.	(Cao, et al., 2017)
	Regulates adipocyte differentiation and lipid accumulation Enhances Akt and GSK-3β phosphorylation Inhibits NF-κB phosphorylation	(Kim, et al., 2009)
	Cardioprotective in the context of diabetic cardiomyopathy through kinin B2 receptor-Akt-GSK-3β dependent pathway	(Sun, et al., 2011)
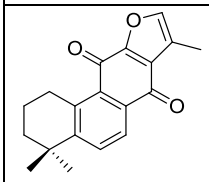 Isotanshinone IIA	Non-competitive inhibitor of PTP1B	(Han, et al., 2005)
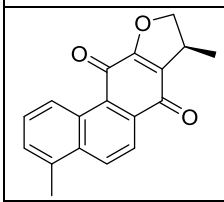	Non-competitive inhibitor of PTP1B	(Han, et al., 2005)

https://etd.uwc.ac.za/

Dihydroisotanshinone I		
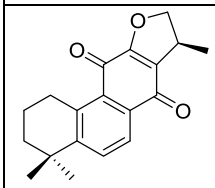 Isocryptotanshinone	Non-competitive inhibitor of PTP1B	(Han, et al., 2005)
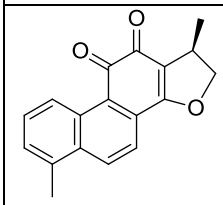 16-Dihydrotanshinone I	Insulin receptor activators	(Jung, et al., 2009)
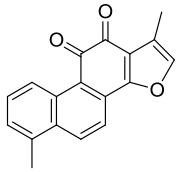 Tanshinone I	Insulin receptor activators	(Jung, et al., 2009)
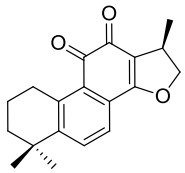 Cryptotanshinone	Inhibitor of protein tyrosine phosphatase	(Kim, et al., 2017)
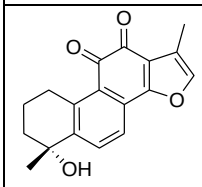 Tanshinol B	Inhibitor of protein tyrosine phosphatase	(Kim, et al., 2017)

UNIVERSITY of the WESTERN CAPE

https://etd.uwc.ac.za/

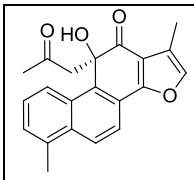 Dehydrodansheno l A	Inhibitor of protein tyrosine phosphatase	(Kim, et al., 2017)
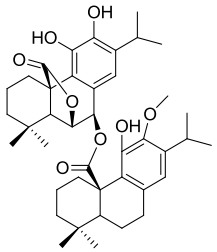 Epirosmanol ester of 12-*O*-methyl carnosic acid	Activation of the nuclear receptor peroxisome proliferator-activated receptor PPARγ.	(Christensen, et al., 2010)

2.10 *In vivo* models/animal models

Several studies have been conducted on the evaluation of the antidiabetic properties of abietane diterpenes in animal models using rats and mice. Some abietane diterpenes demonstrate remarkable antidiabetic activity when administrated to rats or mice as shown in Table 2.3.

Tanshinone I demonstrated a significant decrease of blood glucose level, body weight loss and higher insulin resistance in T2DM rats. Additionally, tanshinone I significantly reduced total cholesterol, free fatty acids, total triglyceride (TG), total low density lipoprotein cholesterol (LDL-C) and insulin receptor substrate 1 (IRS-1) expression when administrated in T2DM rats (Wei, et al., 2017).

Non-alcoholic fatty liver disease (NAFLD) is defined as an accumulation of liver fat in people who drink little or no alcohol. It comprises a spectrum of liver damage characterized by abnormal hepatic fat accumulation and inflammatory response. The dominant feature of NAFLD is the abundant accumulation of hepatic triglycerides (TGs). NAFLD is rapidly

UNIVERSITY of the WESTERN CAPE
https://etd.uwc.ac.za/

becoming a serious global health concern due to its prevalence, which has rapidly increased with the prevalence of obesity and type 2 diabetes (T2D). Hence, carnosic acid isolated from *R. officinalis*, suppresses inflammation and lipogenesis in mice administrated to a high fat diet through myristoylated alanine-rich C-kinase substrate regulation regulation (Song, et al., 2018).

Carnosic acid at 30 mg/kg decreases the levels of fasting plasma glucose (15.6%), total cholesterol (14.1%) and triglyceride (47.8%) at 15 weeks (Ou, et al., 2018). Carnosol ameliorates the level of serum glucose in the diabetic group of rats after streptozotocin (STZ) administration of 60 mg/kg for induction of diabetes (Samarghandian, et al., 2017).

The Oral administration of Sodium tanshinone IIA silate (STS) for 10 days evolved in the activation of AMP-activated protein kinase in aortas from *ob/ob* or *db/db* mice (Ou, et al., 2018). Tanshinone IIA attenuated neuronal apoptosis and improved learning and memory by suppressing endoplasmic reticulum (ER) stress activation in the hippocampus of diabetic rats after streptozotocin administration for induction of diabetes (Chen, et al., 2018). Additionally, Tanshinone IIA administration significantly reduced myocardial infarct size, improved left ventricular ejection fraction, decreased myocardial apoptotic death compared with I/R group. TSN treatment enhanced Akt phosphorylation and inhibited NF-kappaB phosphorylation in cardiac tissues (Zhang, et al., 2010). Dehydroabietic acid (DAA) has been reported to decrease plasma glucose and insulin levels as well as plasma triglyceride (TG) and hepatic TG levels by suppressing the production of monocyte chemoattractant protein-1 (MCP-1) and tumor necrosis factor-alpha (TNF-α) (proinflammatory cytokines) and increase that of adiponectin (an anti-inflammatory cytokine). In addition, the treatment of DAA improves the levels of plasma glucose, plasma insulin, plasma triglyceride, and hepatic triglyceride through the decrease in the macrophage infiltration into adipose tissues, suggesting that DAA is a helpful food-derived compound for treating obesity-related diseases (Kang, et al., 2009).

https://etd.uwc.ac.za/

Table 2.3: In vivo antidiabetic activity of some abietane diterpenes

Compound	Biological activity	References
Tanshinone I	Decreases blood glucose level in T2DM rats.	(Wei, et al., 2017)
Carnosic acid	Protective effect against streptozotocin-induced oxidation, glycation, inflammation and microbiota imbalance in diabetic rats	(Ou, et al., 2018)
	Protective effect in mitigating diabetic symptoms in rats. Suppresses inflammation and lipogenesis in mice	(Song, et al., 2018)
	Attenuates collagen-induced arthritis in db/db mice via inflammation suppression by regulating ROS-dependent p38 pathway	(Xia, et al., 2017)
	Stimulates glucose uptake in rat skeletal L6 myotubes,	(Lipina, 2014)
	Inhibition of ROS, Caspases and NF-κBsignaling pathway in mice	(Li, et al., 2016)
Dehydroabietic acid	Improves diabetes and hyperlipidemia in obese diabetic KK-Ay mice	(Kang, et al., 2009)
Tanshinone IIA	Alleviates neuropathic pain and inhibits the NF-κB signaling pathway in diabetic rats.	(Feng & Qiu, 2018)
	Reduces infarct size and improves cardiac dysfunction after I/R injury in diabetic rats	(Zhang, et al., 2010)
	Decreases glucose, BUN, and 24-h urine protein excretion in a STZ-induced DN rat model. Inhibition of the expressions of AGEs, Ang II, TGFb1, collagen IV, and ED-1.	(Gong, et al., 2009)
	Exerts neuroprotective effects on hippocampus-dependent cognitive impairments in diabetic rats	(Chen, et al., 2018)

UNIVERSITY of the WESTERN CAPE
https://etd.uwc.ac.za/

Carnosol	Improves diabetes and its complications by modulation of oxidative stress and inflammatory responses.	(Samarghandian, et al., 2017)
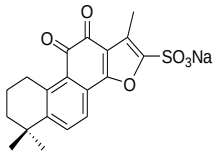 Sodium tanshinone IIA silate (STS)	Inhibits high glucose-induced vascular smooth muscle cell proliferation and migration through activation of AMP-activated protein kinase	(Wu, et al., 2014)

2.11. Conclusion

Natural products are still considered as potential sources for drug discovery and play a crucial role in drug development programs. Moreover, many medicinal herbs are rich sources of bioactive compounds with no undesirable side effects and display powerful pharmacological actions. However, abietane diterpenes are classes of compounds which are mainly found in *Salvia* species, and they possess a broad spectrum of biological activities especially antioxidant and antidiabetic. Hence, efforts have been made to optimize the procedure of screening natural products isolated from different plants for the discovery of new natural anti-diabetic compounds. Additionally, these natural products can be used as an alternative to synthetic oral hypoglycemic drugs with less side effects. This review highlighted the different mode of action of various types of abietane diterpenes in the prevention and management of type 2 diabetes complications, obesity and other related diseases.

UNIVERSITY of the WESTERN CAPE
https://etd.uwc.ac.za/

References

Bajpai, V.K., Park, Y.H., Na, M and Kang, S.C. (2015). Alpha-glucosidase and tyrosinase inhibitory effects of an abietane type diterpenoid taxoquinone from *Metasequoia glyptostroboides*. *BMC Complementary and Alternative Medicine*, 15.84.

Cao, A; Tang, Y and Liu, Y. (2012). Novel fluorescent biosensor for alpha-glucosidase inhibitor screening based on cationic conjugated polymers. *ACS Applied Materials and Interfaces, 4*, 3773−3778.

Cao, L., Huang, B., Fu, X., Yang, J., Lin, Y and Lin, F. (2017). Effects of tanshinone IIA on the regulation of renal proximal tubular fibrosis. Molecular Medicine Reports, 15(6), 4247-4252.

Chen, J., Bi, Y., Chen, L., Zhang, Q and Xu, L. (2018). Tanshinone IIA exerts neuroprotective effects on hippocampus-dependent cognitive impairments in diabetic rats by attenuating ER stress-induced apoptosis. *Biomedicine and Pharmacotherapy*, 104:530-536.

Christensen, K.B., Jørgensen, M., Kotowska, D., Petersen, R.K., Kristiansen, K and Christensen, LP. (2010). Activation of the nuclear receptor PPARγ by metabolites isolated from sage (*Salvia officinalis* L.). *Journal of Ethnopharmacology*, 132(1), 127-33.

Cui, L., Kim, M.O., Seo, J.H., Kim, S., Kim, N.Y., Lee, S.H., Park, J., Kim, J and Lee, H.S. (2012). Abietane diterpenoids of *Rosmarinus officinalis* and their diacylglycerol acyltransferase-inhibitory activity. *Food Chemistry*, 132(4), 1775–1780.

Dahlqvist, , A., Ståhl, U., Lenman, M., Banas, A., Lee, M., Sandager, L., Ronne, H and Stymne, S. (2000). Phospholipid:diacylglycerol acyltransferase: An enzyme that catalyzes the acyl-CoA-independent formation of triacylglycerol in yeast and plants. *Proceedings of the National Academy of Sciences of the United States of America*, 97(12): 6487–6492

Fan, K., Li, S., Liu, G., Yuan, H., Ma, L and Lu, P. (2017). Tanshinone IIA inhibits high glucose-induced proliferation, migration and vascularization of human retinal endothelial cells. *Molecular Medicine Report*, 16(6), 9023-9028.

Feng, F.B and Qiu, H.Y. (2018). Neuroprotective effect of tanshinone IIA against neuropathic pain in diabetic rats through the Nrf2/ARE and NF-κBsignaling pathways. *Kaohsiung Journal of Medical Sciences*, 34(8),428-437.

Gonzalez, M. (2015). Aromatic abietane diterpenoids: Their biological activity and synthesis. *Natural Product Reports*, 32(5), 684-704.

Gong, Z., Huang, C., Sheng, X., Zhang, Y., Li, Q., Wang, M.W., Peng, L and Zang, Y.Q. (2009). The role of tanshinone IIA in the treatment of obesity through peroxisome proliferator- activated receptor gamma antagonism. *Endocrinology*, 150(1):104-13.

Han, Y.M., Oh, H., Na, M., Kim, B.S., Oh, W.K., Kim, B.Y., Jeong, D.G., Ryu, S.E., Sok, D.E and Ahn, J.S. (2005). PTP1B inhibitory effect of abietane diterpenes isolated from *Salvia miltiorrhiza*. *Biological and Pharmaceutical Bulletin*, 28(9), 1795-7.

https://etd.uwc.ac.za/

Jung, S.H., Seol, H.J., Jeon, S.J., Son, K.H and Lee, J.R. (2009). Insulin-sensitizing activities of tanshinones, Diterpene compounds of the root of Salvia miltiorrhiza Bunge Salvia miltiorrhiza Bunge. *Phytomedicine*, 16(4), 327-35.

Kang, M.S., Hirai, S., Goto, T., Kuroyanagi, K., Lee, J.Y., Uemura, T., Ezaki, Y., Takahashi, N and Kawada, T. (2008). Dehydroabietic acid, a phytochemical, acts as ligand for PPARs in macrophages and adipocytes to regulate inflammation. *Biochemical and Biophysic Research Communication*. 369(2), 333-8.

Kang, M.S., Hirai, S., Goto, T., Kuroyanagi, K., Kim, Y.I., Ohyama, K., Uemura, T., Lee, J.Y., Sakamoto, T., Ezaki, Y., Yu, R., Takahashi, N and Kawada, T. (2009). Diterpene, improves diabetes and hyperlipidemia in obese diabetic KK-Ay mice. *Biofactors*, 35(5), 442-8.

Kim, S.K., Jung, K.H and Lee, B.C. (2009). Protective effect of Tanshinone IIA on the early stage of experimental diabetic nephropathy. *Biological and Pharmaceutical Bulletin*, 32(2):220-4.

Kim, D.H., Paudel, P., Yu, T., Ngo, T.M., Kim, J.A., Jung, H.A., Yokozawa, T and Choi, J.S. (2017). Characterization of the inhibitory activity of natural tanshinones from *Salvia miltiorrhiza* roots on protein tyrosine phosphatase 1B. *Chemico Biological Interaction*, 278, 65-73.

Kubínová, R., Pořízková, R., Navrátilová, A., Farsa, O., Hanáková, Z., Bačinská, A., Cezek, A and Valentova, M. (2014). Antimicrobial and enzyme inhibitory activities of the constituents of *Plectranthus madagascariensis* (Pers.) Benth. *Journal of Enzyme Inhibition and Medicinal Chemistry*, 29, 5, 749-752

Li, H., Sun, J.J., Chen, G.Y., Wang, W.W., Xie, Z.T., Tang, G.F and Wei, S.D. (2016). Carnosic acid nanoparticles suppress liver ischemia/reperfusion injury by inhibition of ROS, caspases and NF-κBsignaling pathway in mice. *Biomedicine and Pharmacotherapy*, 82, 237-46

Li, Y.H., Xu, Q., Xu, W.H., Guo, X.H., Zhang, S and Chen, Y.D. (2015). Mechanisms of protection against diabetes-induced impairement of endothelium-dependent vasorelaxation by Tanshinone IIA. *Biochimica et Biophysica Acta*, 1850(4), 813-23

Lipina, C and Hundal, H.S. (2014). Carnosic acid stimulates glucose uptake in skeletal muscle cells via a PME-1/PP2A/PKB signalling axis. *Cell Signal*, 26(11), 2343-9.

Lorenzati, B., Zucco, C., Miglietta, S., Lamberti, F and Bruno, G. (2010). Oral hypoglycemic drugs: Pathophysiological basis of their mechanism of action. *Pharmaceuticals* 3, 3005–3020.

Marín-Peñalver, J.J., Martín-Timón, I., Sevillano-Collantes, C and del Cañizo-Gómez, F.J. (2016). Type 2 diabetes and cardiovascular disease: Have all risk factors the same strength. *World Journal of Diabetes*, 7, 354-395.

https://etd.uwc.ac.za/

Mamun-or-Rashid, A.N.M., Hossain, M.S., Hassan, N., Dash, B.K., Sapon, M.A and Kumer Sen, M. (2014). A review on medicinal plants with antidiabetic activity. *Journal of Pharmacognosy and Phytochemistry, 3*(4), 149-159.

Mohammed, A., Ibrahim, M.A and Islam, M.S. (2014). African medicinal plants with antidiabetic potentials: A review. *Planta Medica,* 80, 354-377.

Nachar, A., Saleem, A., Arnason, J.T., Haddad, P.S. (2015). Regulation of liver cell glucose homeostasis by dehydroabietic acid, abietic acid and squalene isolated from balsam fir (*Abies balsamea* (L.) Mill.) a plant of the Eastern James Bay Cree traditional pharmacopeia. *Phytochemistry*, 117, 373-379.

Nazaruk, J and Borzym-Kluczyk, M. (2015). The role of triterpenes in the management of diabetes mellitus and its complications. *Phytochemistry Review*, 14(4), 675–690.

Ou, J., Huang, J., Zhao, D., Du, B and Wang, M . (2018). Protective effect of rosmarinic acid and carnosic acid against streptozotocin-induced oxidation, glycation, inflammation and microbiota imbalance in diabetic rats. *Food and Function,* 9(2), 851-860.

Samarghandian, S., Borji, A and Farkhondeh, T. (2017). Evaluation of antidiabetic activity of carnosol (phenolic diterpene in rosemary) in Streptozotocin-induced diabetic rats. *Cardiovasc Hematol Disord Drug Targets*, 17(1), 11-17.

Schaftingen, E.V and Gerin, I. (2002). The glucose-6-phosphatase system. *Biochemical Journal*, 362, 513–532

Sofowora, A., Ogunbodede, E and Onayade, A. (2013). The role and place of medicinal plants in the strategies for disease prevention. *African Journal of Traditional Complementary and Alternative Medecine*, 10,210–229

Song, H.L., Li, X., Liu, Y.Y., Lu, W.P., Cui, Z.H., Zhou, L., Yao, D and Zhang, H.M. (2018). Carnosic acid protects mice from high-fat diet-induced NAFLD by regulating MARCKS. *International Journal of Molecular Medecine*, 42, 193-207.

Sun, D., Shen, M., Li, J., Li, W., Zhang, Y., Zhao, L., Zhang, Z., Yuan, Y., Wang, H and Cao, F. (2011). Cardioprotective effects of tanshinone IIA pretreatment via kinin B2 receptor-Akt-GSK-3β dependent pathway in experimental diabetic cardiomyopathy. *Cardiovascular Diabetology*, 10,4.

Tabata, N., Ito, M., Tomoda, H and Omura, S. (1997). Xanthohumols diacylglycerol acyltransferase inhibitors, from humulus lupulus. *Phytochemisrry*, 46(4), 683487

Tripathy, J.P. (2018). Burden and risk factors of diabetes and hyperglycemia in India: Findings from the Global Burden of Disease Study 2016, *Diabetes Metab Syndr Obes*, 11, 381-387

Ullah, A., Khan, A and Khan, I. (2016). Diabetes mellitus and oxidative stress -A concise review. *Pharmaceutical Journal*, 24, 547-553.

UNIVERSITY of the WESTERN CAPE
https://etd.uwc.ac.za/

Vlavcheski, F., Baron, D., Vlachogiannis, I.A., MacPherson, R.E.K and Tsiani, E. (2018). Carnosol increases skeletal muscle cell glucose uptake *via* AMPK-Dependent GLUT4 glucose transporter translocation. *International Journal of Molecular Sciences*, 29, 19(5).

Wang, X.W., Yu, Y and Gu, L. (2014). Dehydroabietic acid reverses TNF-α-induced the activation of FOXO1 and suppression of TGF-β1/Smadsignaling in human adult dermal fibroblasts. *International Journal of Clinical and Experimental Pathology*, 7(12), 8616-26.

Wei, Y., Gao, J., Qin, L., Xu, Y., Wang, D., Shi, H., Xu, T and Liu, T. (2017). Tanshinone I alleviates insulin resistance in type 2 diabetes mellitus rats through IRS-1 pathway. *Biomedicine and Pharmacotherapy*, 93, 352-358.

Wu, W.Y., Yan, H., Wang, X.B., Gui, Y.Z., Gao, F., Tang, X.L., Qin, X.L., Su, M., Chen, T and Wang, Y.P. (2014). Sodium tanshinone IIA silate inhibits high glucose-induced vascular smooth muscle cell proliferation and migration through activation of AMP-activated protein kinase. *PLOS ONE*, 9(4), 94957.

Xia, G., Wang, X., Sun, H., Qin, Y and Fu, M. (2017). Carnosic acid (CA) attenuates collagen-induced arthritis in db/db mice *via* inflammation suppression by regulating ROS-dependent p38 pathway. *Free Radical Biology and Medicine*, 108, 418-432.

Xie, Z., Zhong, L., Wu, Y., Wan, X., Yang, H., Xu, X and Li, P. (2018). Carnosic acid improves diabetic nephropathy by activating Nrf2/ARE and inhibition of NF-κB pathway. *Phytomedicine*, 47, 161-173.

Yang, M and Nickels, J.T. (2015). MOGAT2: A new therapeutic target for metabolic syndrome. *Diseases*, 3(3), 176–192.

Yun, Y.S., Noda, S., Shigemori, G., Kuriyama, R., Takahashi, S., Umemura, M., Takahashi, Y and Inoue, H. (2013). Phenolic diterpenes from rosemary suppress cAMP responsiveness of gluconeogenic gene promoters. *Phytotherapy Research*, 27(6), 906-10.

Zhang, Y., Wei, L., Sun, D., Cao, F., Gao, H., Zhao, L., Du, J., Li, Y and Wang, H. (2010). Tanshinone IIA pretreatment protects myocardium against ischaemia/reperfusion injury through the phosphatidylinositol 3-kinase/Akt-dependent pathway in diabetic rats. *Diabetes Obesity and Metabolism*, 12(4), 316-22.

https://etd.uwc.ac.za/

CHAPTER THREE

PHYTOCHEMICAL ISOLATION AND BIOLOGICAL INVESTIGATION OF *SALVIA AFRICANA -LUTEA*

3.1 Abstract

The phytochemical investigation of a methanolic extract of *Salvia africana-lutea* collected from the Cape Floristic Region, South Africa (SA), afforded four new abietane diterpenes namely 19-acetoxy-12-methoxy carnosic acid (**1**), 3β-acetoxy-7α-methoxyrosmanol (**2**), 19-acetoxy-7α-methoxyrosmanol (**3**), 19-acetoxy-12-methoxy carnosol (**4**), and two known named clinopodiolides A (**5**) and B (**6**), in addition to four known triterpenes, oleanolic and ursolic acids (**7**, **8**), 11,12-dehydroursolic acid lactone (**9**) and β-amyrin (**10**). The chemical structural elucidation of the isolated compounds was determined on the basis of 1D and 2D NMR, high resolution mass spectrometry (HRMS), ultra violet (UV), fourier transform infrared (IR), raman spectroscopy and in comparison with literature data. The in vitro bio-evaluation against alpha-glucosidase showed strong inhibitory activities of **8**, **10** and **7** with IC_{50} values of 11.3 ± 1.0, 17.1 ± 1.0 and 22.9 ± 2.0 µg/mL respectively while **7** demonstrated the strongest in vitro alpha-amylase inhibitory activity among the tested compounds with IC_{50} of 12.5 ± 0.7 µg/mL. Additionally, some of the compounds showed significant antioxidant capacities. The methanolic extract of *S. africana-lutea* is a rich source of terpenoids especially abietane diterpenes with strong antioxidant and anti-diabetic activities that can be helpful to modulate the redox status of the body, and could therefore be an excellent candidate for the prevention of the development of diabetes, a disease where oxidase stress plays an important role.

https://etd.uwc.ac.za/

3.2 Background information

Lamiaceae plants have been used since time immemorial for curing numerous human afflictions. They are known to be the main source of health-promoting substances because they possess secondary metabolites such as polyphenols, flavonoids, terpenoids, alkaloids, carotenoids, vitamins and several other phytochemicals, which are responsible for a wide spectrum of pharmaceutical applications including diabetes (Sofowora, et al., 2013).

Salvia africana-lutea, commonly known as bruinsalie or beach sage is widely distributed form Namaquland to the Eastern Cape Province of South Africa [in the South-Western part of South Africa]. It is traditionally used to treat different kind of ailments and/or diseases such as coughs, sexual debility, mental and nervous conditions, throat inflammation, chronic bronchitis, tuberculosis, influenza, stomach ache, diarrhea and urticarial (Amabeoku, et al., 2001; Manning & Goldblatt, 2012).

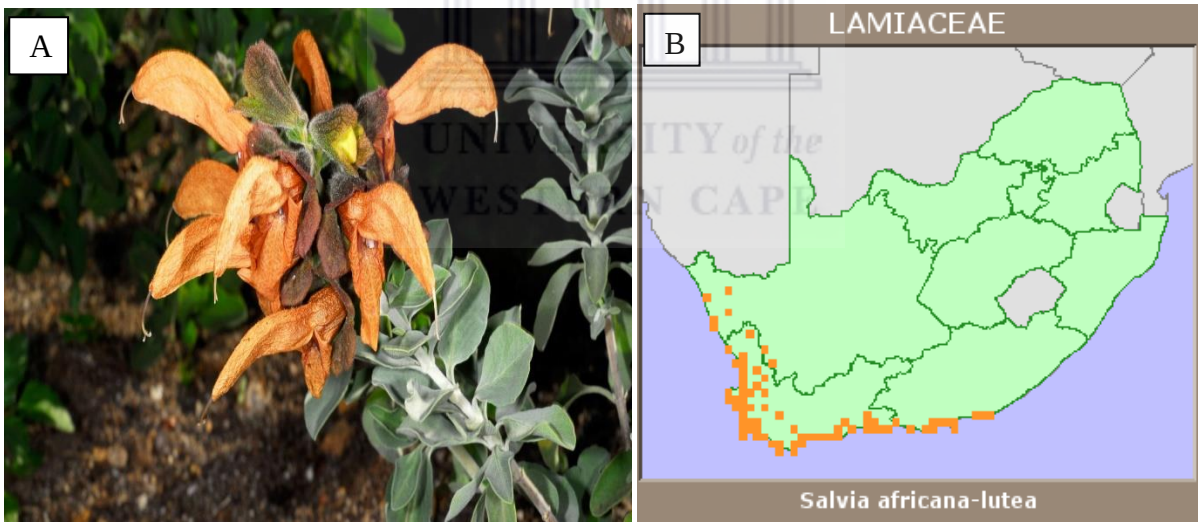

Retrieved from: http://redlist.sanbi.org/species.php?species=1685-3

Figure 3.1: *Salvia africana lutea* description (**A**) distribution along South African coastal (**B**)

https://etd.uwc.ac.za/

This chapter describes:

- Isolation of the different chemical constituents present in the methanolic extract of *S. africana lutea* using different chromatographic methods.
- Structural elucidation of each compound using different spectroscopic techniques.
- In-vitro bio-evaluation of alpha-glucosidase and alpha-amylase inhibitory activities of the isolated compounds.
- In-vitro bio-evaluation of the antioxidant capacities of the isolated compounds.

CHEMICAL CHARACTERIZATION OF *SALVIA AFRICANA-LUTEA* CONSTITUENTS

3.3 General experiment procedure

3.3.1 Reagents and solvents

Organic solvents such as methanol (HPLC grade), ethanol, ethyl acetate, dichloromethane, n-hexane, vanillin, and deuterated chloroform were supplied by Merck (Cape Town, South Africa). Sulphuric acid was secured from kimix (Cape Town, South Africa).

UNIVERSITY of the
WESTERN CAPE

3.3.2 Chromatography

3.3.2.1 Thin layer chromatography (TLC)

Pre-coated plates of silica gel 60 F_{254} (Merck, Germany) was utilised for TLC analysis. Visualization of TLC plates was conducted by observing the bands “spots” after development under UV at wavelengths 254 and 366 nm using UV lamp (CAMAG, Switzerland), followed by vallinin/sulphuric acid spray reagent and then heated for phytochemical identification. The solvent systems commonly used for the TLC development of *Salvia africana-lutea* fractions are indicated in Table 3.1.

https://etd.uwc.ac.za/

Table 3.1: TLC solvent systems

Solvent system	Ratio	Assigned code
Hex - EtOAc	9:1	A
Hex - EtOAc	7:3	B
DCM - MeOH	9.5:0.5	C
DCM - MeOH	9:1	D
DCM - MeOH	7:3	E

Hex: hexane; EtOAc: ethylacetate; DCM: dichloromethane; MeOH: methanol

3.3.2.2 Column chromatography

The column chromatography (different diameters) was performed using silica gel 60 H (0.040-0.063 mm particle size, Merck, South Africa) and sephadex LH-20 (Sigma-Aldrich, South Africa) as stationary phases.

3.3.2.3 Semi-preparative high-pressure liquid chromatography (HPLC)

Final purification was performed using Agilent Technologies 1200 series, equipped with UV detector, manual injector, quaternary pump (G1311A), vacuum degasser (G1322A), column compartment (G1316A) and reversed phase C18 column SUPELCO (25 x 1.0 cm, 5 μm). The flow rate was set at 1.5 mL/min, and all experiments were done at room temperature.

UNIVERSITY of the
WESTERN CAPE

3.3.3 Spectroscopy

3.3.3.1 Nuclear magnetic resonance (NMR) spectroscopy

NMR spectra were recorded at 20^{o}C, using deuterated chloroform on a Bruker Avance 400 MHz NMR spectrometer (Germany), chemical shifts of ^{1}H (δ_{H}) and ^{13}C (δ_{C}) in ppm were determined relative to tetramethylsilane (TMS) as internal reference.

3.3.3.2 Mass spectroscopy

Liquid chromatography mass spectrometry (LCMS) analysis. A Waters Synapt G2 Quadrupole time-of-flight (QTOF) mass spectrometer (MS) connected to a Waters Acquity ultra-performance liquid chromatograph (UPLC) (Waters, Milford, MA, USA) was used for

https://etd.uwc.ac.za/

high-resolution UPLC-MS analysis. Electrospray ionization was used in negative mode with a cone voltage of15V, desolvation temperature of 275 °C, desolvation gas at 650 L/h, and the rest of the MS settings optimized for best resolution and sensitivity.

3.3.3.3 Fourier transform infrared (FTIR) spectroscopy

Attenuated total internal reflectance FTIR measurements were conducted using Spectrum 100 (Perkin Elmer Corp). Spectra recording were accomplished using the interface (Spectrum). Methanol was used to dissolve the samples.

3.3.3.4 Raman spectroscopy

Raman spectrum was recorded with Renishaw inVia^{TM} quontor confocal Raman Microscope system equipped with diode cobolt Fandango 514 nm line, a leica microscope, an electrically cooled CCD (charge-coupled device) detector Renishaw centrus 1024 x 256 puxels and notch filter to eliminate elastic scattering. The spectrum was obtained using 50 x super long working distance. The laser power output was 1 mw and the spectral resolution was 2 cm^{-1}.

3.3.3.5 Ultra violet (UV) spectroscopy

UV Nicolet Evolution (EV-100 ver. 4.60) spectrophotometer (Therma Electron Corporation, Madison, USA) was used for measurement of absorbance maxima between the wavelengths 200-400 nm.

3.3.4 Optical rotation measurement

The optical rotation measurements were carried out using Autupol III Polarimeter (Rudolph research analytical, Hackettstown, MA, USA).

3.4 Collection and identification of plant material

The aerial part of *Salvia africana-lutea* used in this study was collected in April 2017, from the Cape Flats Nature Reserve, University of the Western Cape, South Africa. A voucher specimen was identified at the Compton Herbarium, Kirstenbosch by Prof. Christopher Cupido, with herbarium number NBG1465544-0.

https://etd.uwc.ac.za/

3.5 Extraction and Fractionation of the total extract

The aerial part of *Salvia africana-lutea* (2.5 kg) were blended and extracted with methanol (4.5 L) at room temperature (25 ^{o}C) for 24 h. The methanol extract was filtered and evaporated to dryness under reduced pressure at 40 ^{o}C to yield 97.77 g (3.9%). The total extract (97 g) was applied to a silica gel column (30 x 18 cm) and eluted using gradient of Hex and EtOAc in order of increasing polarity as indicated in Table 3.2. Eighty (80) fractions (500 mL each) were collected and combined according to their TLC profiles to yield eighteen fractions labelled I-XVIII as shown in Table 3.2.

Table 3.2: Fractionation of the extract of *S. africana lutea*

Solvent system	Solvent volume	Fraction collected
Hex	2L	1-4
Hex - EtOAc (95:5)	2L	5-8
Hex - EtOAc (90:10)	2L	9-12
Hex - EtOAc (85:15)	2L	13-16
Hex - EtOAc (80:20)	2L	17-20
Hex - EtOAc (75:25)	2L	21-24
Hex - EtOAc (70:30)	2L	25-28
Hex - EtOAc (65:45)	2L	29-32
Hex - EtOAc (60:40)	2L	33-36
Hex - EtOAc (55:45)	3L	37-42
Hex - EtOAc (50:50)	3L	43-48
Hex - EtOAc (40:60)	3L	49-54
Hex - EtOAc (30:70)	3L	55-60
Hex - EtOAc (20:80)	3L	61-66
Hex - EtOAc (10:80)	3L	67-72
EtOAc	4L	73-80

UNIVERSITY of the WESTERN CAPE

https://etd.uwc.ac.za/

The collected fractions (1-80) were concentrated and combined according to their TLC profiles using solvent system C to yield 18 main fractions (Fig. 3.2). The roman numbers (I-XVIII) were used as to code the obtained fractions and the results are summarized in Table 3.3

Table 3.3: Fractions obtained upon fractionation of total extract of *S. africana lutea*

Combined fraction	Designated number	Code	Weight of fractions (mg)
1-5	I	SAL-I	5462.2
6-8	II	SAL-II	2444.5
9-10	III	SAL-III	616.5
11-14	IV	SAL-IV	1181.4
15-18	V	SAL-V	742.5
19	VI	SAL-VI	183.8
20-23	VII	SAL-VII	910.4
24-26	VIII	SAL-VIII	727.4
27-28	IX	SAL-IX	477.6
29-31	X	SAL-X	531.2
32-37	XI	SAL-XI	1273.9
38-40	XII	SAL-XII	1894.1
41-44	XIII	SAL-XIII	1349.5
45-49	XIV	SAL-XIV	2352.2
50-53	XV	SAL-XV	1615.5
54-58	XVI	SAL-XVI	3538.3
59-68	XVII	SAL-XVII	1499.8
69-79	XVIII	SAL-XVIII	920.1

UNIVERSITY of the
WESTERN CAPE

https://etd.uwc.ac.za/

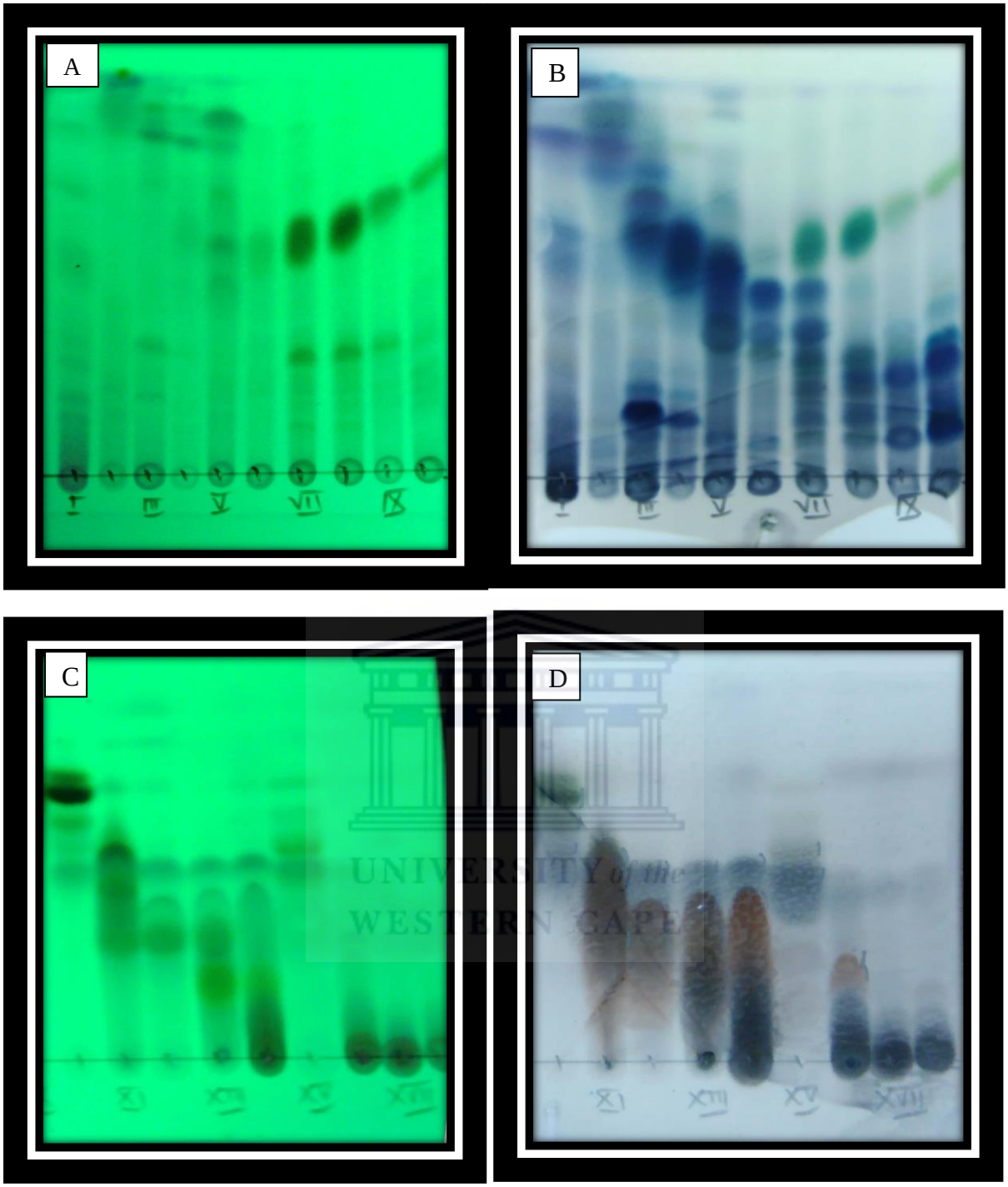

Figure 3.2: TLC plate (silica gel) of combined fractions under UV (254 nm; A&C), and after spraying with H_2SO_4/vanillin and then heated (B&D). TLC was developed using solvent system C

https://etd.uwc.ac.za/

3.6 Isolation of pure compounds

3.6.1 Isolation of compound 1

Main fraction XVII (1490 mg) was subjected to successive silica gel column using Hex/EtOAc gradient (7:3 and 100%), fraction of 100 mL was collected and evaporated using rotary evaporator. Fractions obtained were developed on TLC using solvent system C and the fractions that displayed same profiles on the TLC plate were combined as indicated in Table 3.4.

Table 3.4: Fractions grouped from the column

Fraction	Weight (mg)	Assigned code
1 -25	3.3	SAL-XVII-0
26-29	33.2	SAL-XVII-1
30-33	56.1	SAL-XVII-2
34-38	69.2	SAL-XVII-3
39-41	155.8	SAL-XVII-4
42-44	195.2	SAL-XVII-5
45-46	26.3	SAL-XVII-6
47-50	205.8	SAL-XVII-7
51-54	63.8	SAL-XVII-8
55-57	12.5	SAL-XVII-9
58-63	21.4	SAL-XVII-10
64-67	11.2	SAL-XVII-11
68-73	155.2	SAL-XVII-12

UNIVERSITY of the WESTERN CAPE

https://etd.uwc.ac.za/

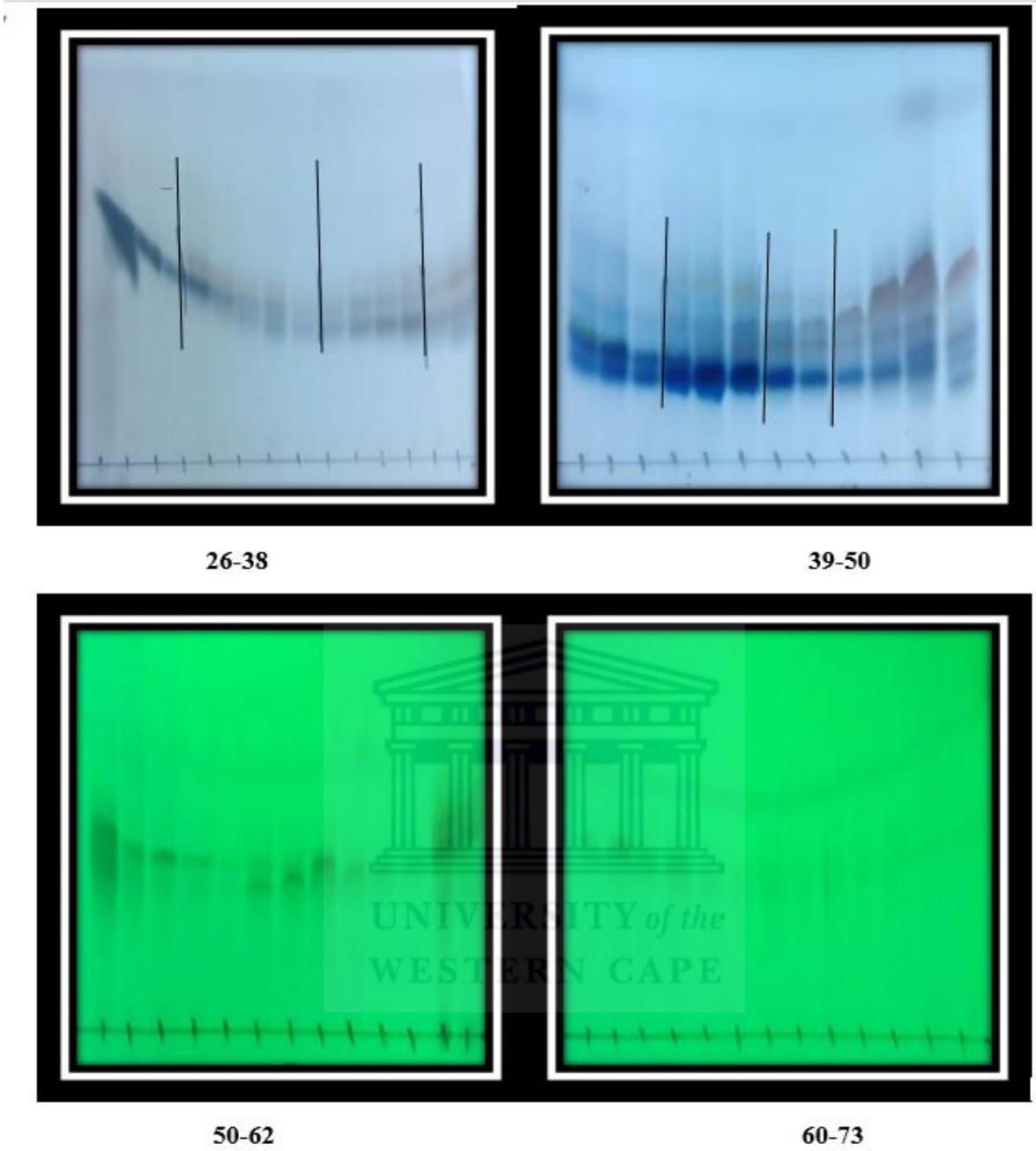

Figure 3.3: TLC plate of collected fractions of SAL-XVII

The sub-fractions SAL-XVII-7 (205.8 mg) were subjected then to sephadex (using 95% aqueous ethanol). Fractions of 5 mL each were collected and evaporated using rotary evaporator. The collected fractions (24-31) were pooled together, evaporated and re-spotted using solvent system C to further confirm the purity of the combined fractions. The TLC

https://etd.uwc.ac.za/

showed only single spot after development and confirmed the purity (Fig. 3.4) and labelled the compound as **1** (44.1 mg, 0.017%).

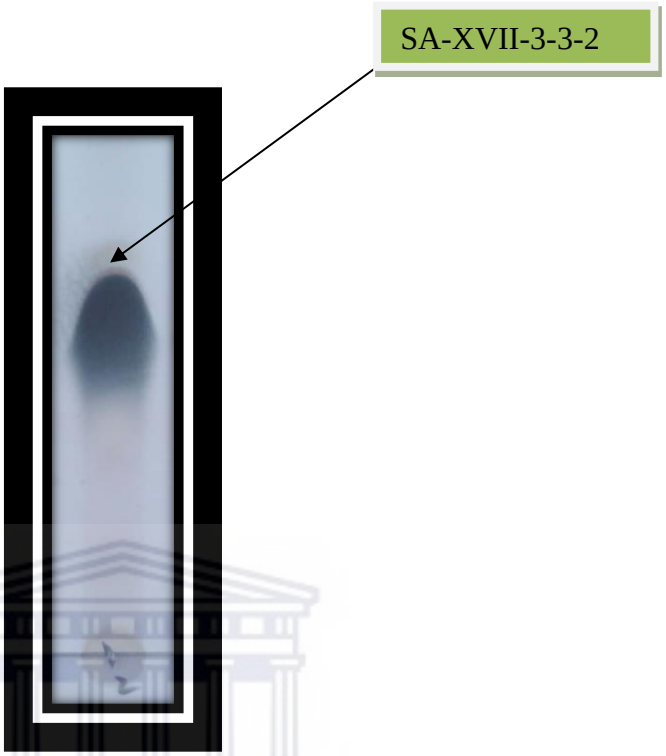

Figure 3.4: TLC plate of SAL-XVII-3-3-2

UNIVERSITY of the
WESTERN CAPE

https://etd.uwc.ac.za/

3.6.2 Isolation of compound 2

Main fraction XI (1205 mg) was subjected to successive silica gel column using Hex/EtOAc gradient (7:3 and 100%), then sephadex (using 95% aqueous ethanol). Fractions of 5 mL each were collected and evaporated using rotary evaporator. Fractions obtained were developed on TLC using solvent system C and the fractions that displayed same profiles on the TLC plate were combined as indicated in Table 3.5.

Table 3.5: Fractions grouped from the column

Fraction	Weight (mg)	Assigned code
1-5	2.7	SAL-XI-0
6-9	133.2	SAL-XI-1
10-13	156.1	SAL-XI-2
14-19	321.4	SAL-XI-3
20-27	211.2	SAL-XI-4
28-35	55.2	SAL-XI-5

Sub fraction XI-5 (55 mg) was injected to the HPLC and eluted using gradient solvent system of MeOH and de-ionized water (75:25 to 100% MeOH in 45 min), which afforded prominent peak as shown in Figure 3.5B, collected and labelled as **SAL-XI-5-5**. After spotting and developing the collected fractions on TLC plate using solvent system C, a single spot suspected to be a pure compound was observed (Fig. 3.5A). The fraction that afforded this single spot was labelled as **2** (R_t 19.67 min, 9.9 mg, 0.004%).

UNIVERSITY of the WESTERN CAPE
https://etd.uwc.ac.za/

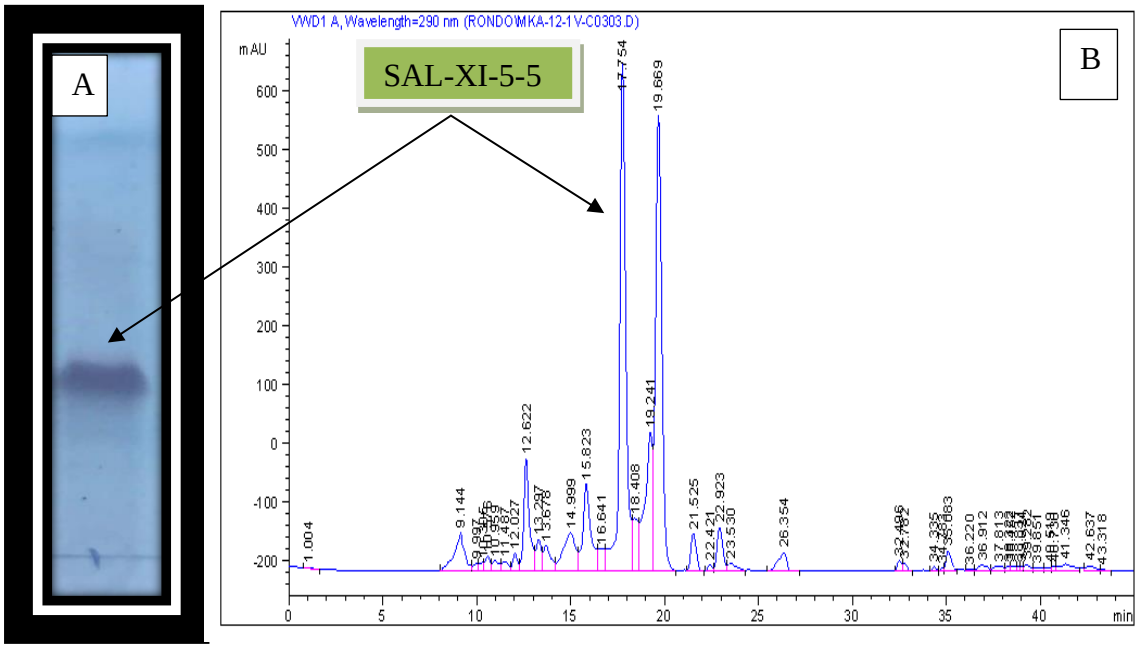

Figure 3.5: TLC plate of SAL-XI-5-5 (Fig. 3.5A) and HPLC chromatogram of sub fraction XI-5 (Fig. 3.5B).

***Conditions**

Solvent	MeOH:DIW 75:25 to 100% in 45 min
Column	SUPELCO, RP-18 (25 x 1 cm)
Flow rate	1.5 mL/min
Detection	UV at 290 nm

UNIVERSITY of the WESTERN CAPE

3.6.3 Isolation of compound 3 and 10

Main fraction XIII (1340 mg) was rinsed with a mixture of Hex/EtOAc (1:1) to remove the white powder, which was spotted and developed on TLC plate using solvent system B. A single spot suspected to be a pure compound was observed and labelled as SAL-XIII-A, **10** (304.4 mg, 0.12%). Main fraction XIII (1040 mg) was subjected to successive silica gel column using Hex/EtOAc gradient (7:3 and 100%), then sephadex (using 95% aqueous ethanol). Fractions of 5 mL each were collected and evaporated using rotary evaporator. Fractions obtained were developed on TLC using solvent system C and the fractions that displayed same profiles on the TLC plate (Fig. 3.6) were combined as indicated in Table 3.6.

https://etd.uwc.ac.za/

Table 3.6: Fractions grouped from the column

Fraction	Weight (mg)	Assigned code
1-4	1.7	SAL-XIII-0
5-9	33.2	SAL-XIII-1
10-15	94.5	SAL-XIII-2
16-20	169.2	SAL-XIII-3
21-23	255.8	SAL-XIII-4
24-31	195.2	SAL-XIII-5
32-41	45.3	SAL-XIII-6
42-43	65.4	SAL-XIII-7
44-51	74.2	SAL-XIII-8
52-69	36.3	SAL-XIII-9

Figure 3.6: TLC plate of combined fractions of SAL-XIII

Sub fraction XIII-3 (169.2 mg) was injected to the HPLC and eluted using gradient solvent system of MeOH and de-ionized water (75:25 to 100% MeOH in 45 min), which afforded prominent peak as known in Figure 3.7B, collected and labelled as SAL-XIII-3-7. After spotting and developing the collected fractions on TLC plate using solvent system C, a single spot suspected to be a pure compound was observed (Fig 3.7A). The fraction that afforded this single spot was labelled as **3** (R_t 23.62 min, 9.1 mg, 0.0036%).

https://etd.uwc.ac.za/

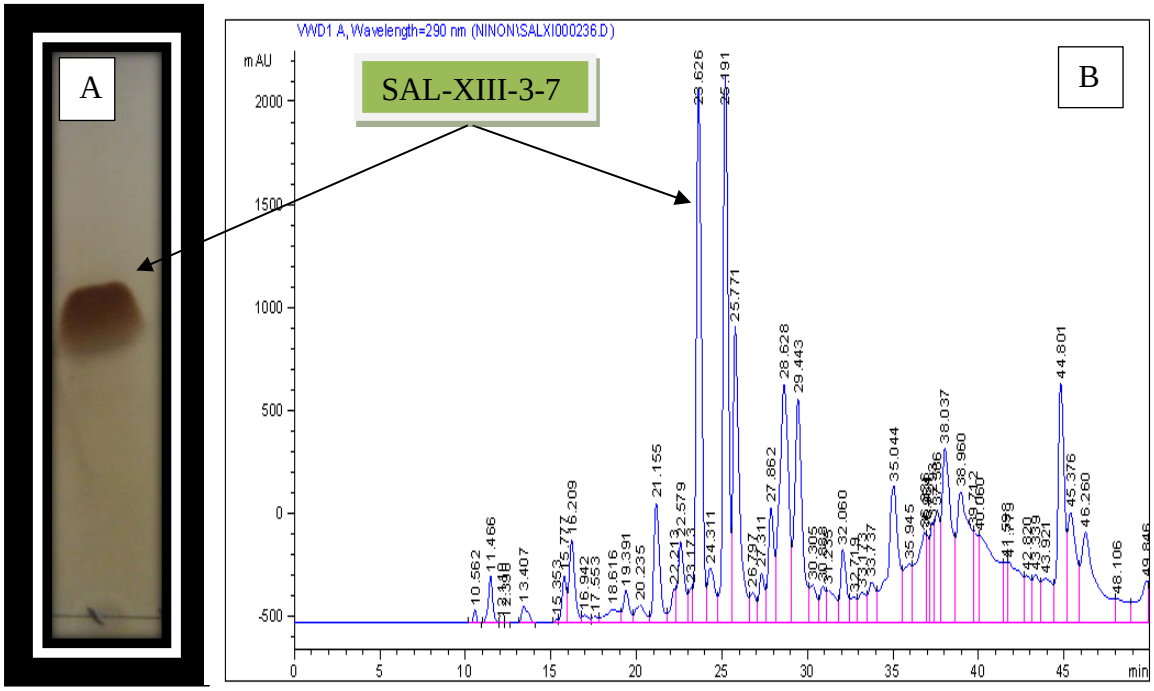

Figure 3.7: TLC plate of SAL-XIII-3-7 (Fig. 3.7A) and HPLC chromatogram of sub fraction XIII-3 (Fig. 3.7B).

***Conditions**

Solvent	MeOH:DIW 75:25 to 100% in 45 min
Column	SUPELCO, RP-18 (25 x 1 cm)
Flow rate	1.5 mL/min
Detection	UV at 290 nm

UNIVERSITY of the
WESTERN CAPE

3.6.4 Isolation of compound 4

Sub fraction XIII-2 (94.5 mg) was injected to the HPLC and eluted using gradient solvent system of MeOH and de-ionized water (75:25 to 100% MeOH in 45 min), which afforded prominent peak as shown in Figure 3.8B, collected and labelled as **SAL-XIII-2-10**. After spotting and developing the collected fractions on TLC plate using solvent system C, a single spot suspected to be a pure compound was observed (Fig 3.8A). The fractions that afforded this single spot were pooled together and labelled as **4** (R_t 17.9 min, 11.17 mg, 0.0045%).

https://etd.uwc.ac.za/

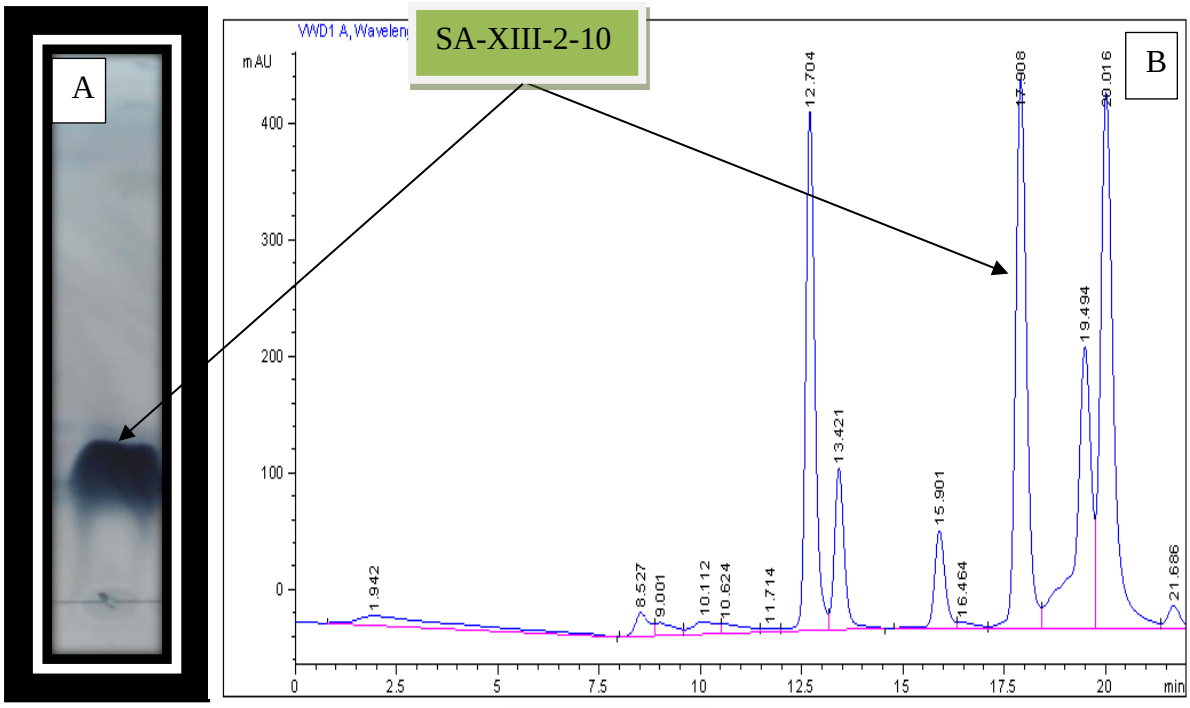

Figure 3.8: TLC plate of SAL-XIII-2-10 (Fig. 3.8 A) and HPLC chromatogram of sub fraction XIII-2 (Fig. 3.8B).

***Conditions**

Solvent	MeOH:DIW 75:25 to 100% in 45 min
Column	SUPELCO, RP-18 (25 x 1 cm)
Flow rate	1.5 mL/min
Detection	UV at 290 nm

UNIVERSITY of the
WESTERN CAPE

3.6.5 Isolation of compound 5

Sub fraction XIII-4 (124.5 mg) was injected to the HPLC and eluted using gradient solvent system of MeOH and de-ionized water (75:25 to 100% MeOH in 45 min) which afforded prominent peak labelled as shown in Figure 3.9B, collected and labelled as SAL-XIII-4-5. After spotting and developing the collected fractions on TLC plate using solvent system C, a single spot suspected to be a pure compound was observed (Fig 3.9A). The fraction that afforded this single spot was labelled as **5** (R_t 32.17 min, 46.3 mg, 0.018%)

https://etd.uwc.ac.za/

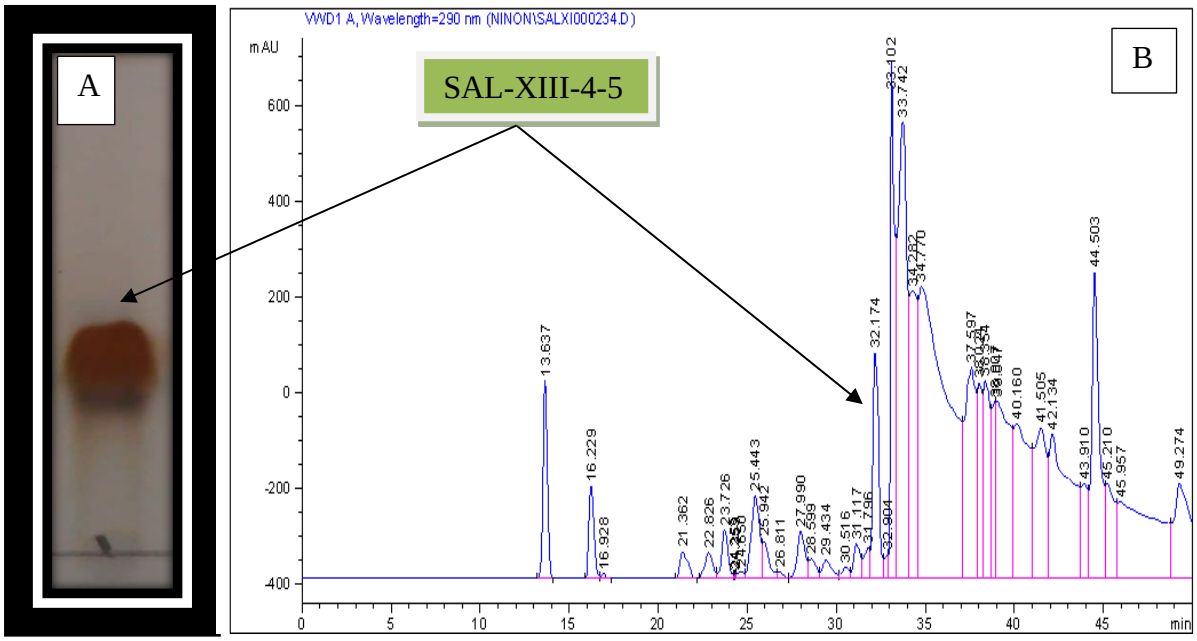

Figure 3.9: TLC plate of SAL-XIII-4-5 (Fig. 3.9 A) and HPLC chromatogram of sub fraction XIII-4 (Fig. 3.9B).

***Conditions**

Solvent	MeOH:DIW 75:25 to 100% in 45 min
Column	SUPELCO, RP-18 (25 x 1 cm)
Flow rate	1.5 mL/min
Detection	UV at 290 nm

UNIVERSITY of the
WESTERN CAPE

3.6.6 Isolation of compound 6

Sub fraction XIII-5 (54.5 mg) was injected to the HPLC and eluted using gradient solvent system of MeOH and de-ionized water (75:25 to 100% MeOH in 45 min) which afforded a prominent peak labeled **SAL-XIII-5-5** as shown in figure 3.10B. After spotting and developing the fractions on TLC plate using solvent system C, a single spot suspected to be a pure compound was observed (Fig 3.10A). The fractions that afforded this single spot were pooled together and labelled as **6** (R_t 12.75 min, 40.1 mg, 0.016%).

https://etd.uwc.ac.za/

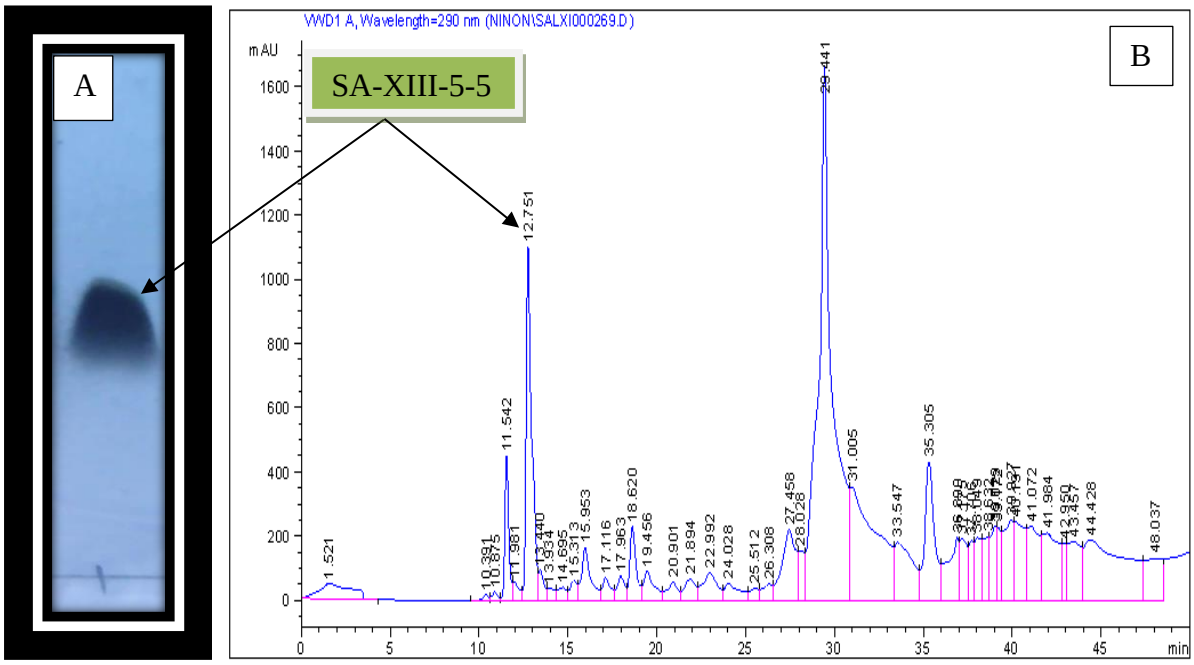

Figure 3.10: TLC plate of SAL-XIII-5-5 (Fig. 3.10A) and HPLC chromatogram of sub fraction XIII-5 (Fig. 3.10B).

***Conditions**

Solvent	MeOH:DIW 75:25 to 100% in 45 min
Column	SUPELCO, RP-18 (25 x 1 cm)
Flow rate	1.5 mL/min
Detection	UV at 290 nm

UNIVERSITY of the WESTERN CAPE

3.6.7 Isolation of compound 7

Main fraction X (530 mg) was subjected to successive silica gel column using Hex/EtOAc gradient (7:3 and 100%), then chromatographed on sephadex column (5% aqueous ethanol). Fractions of 5 mL each were collected and evaporated using rotary evaporator. Fractions obtained were developed on TLC using solvent system C and the fractions that displayed same profiles on the TLC plate were combined together. After re-spotting and developing the combined fractions on TLC plate using solvent system C, a single spot suspected to be a pure compound was observed (Fig 3.11). The fractions that afforded this single spot labelled as **7** (69.6 mg; 0.028%).

https://etd.uwc.ac.za/

Figure 3.11: TLC plate of SAL-X

3.6.8 Isolation of compound 8

Main fraction IX (450 mg) was subjected to successive silica gel column using Hex/EtOAc gradient (7:3 and 100%), then chromatographed on sephadex column (5% aqueous ethanol). Fractions of 5 mL each were collected and evaporated using rotary evaporator. Fractions obtained were developed on TLC using solvent system C and the fractions that displayed same profiles on the TLC plate were combined. After spotting and developing the fractions on TLC plate using solvent system C, a single spot suspected to be a pure compound was observed (Fig 3.12). The fractions that afforded this single spot labelled as to produce **8** (34.6 mg; 0.014%).

https://etd.uwc.ac.za/

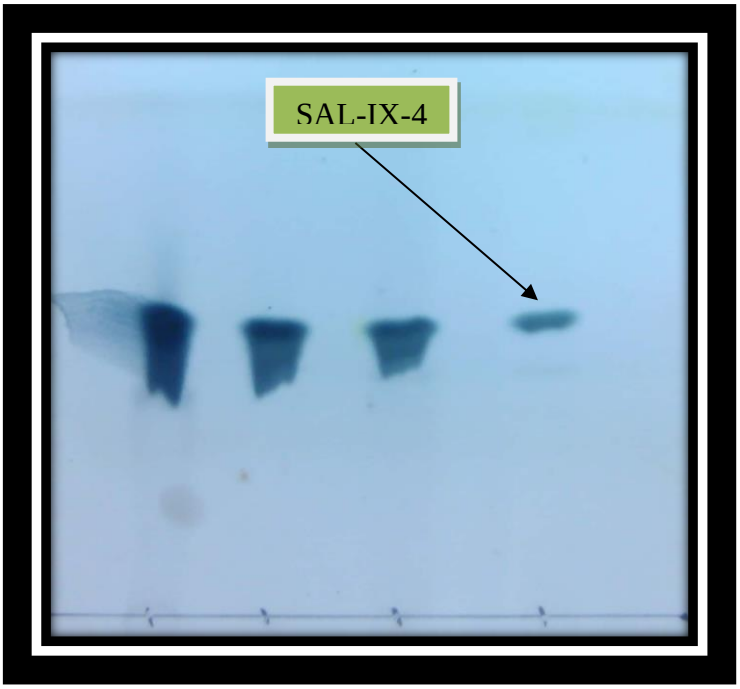

Figure 3.12: TLC plate of SAL-IX-4

3.6.9 Isolation of compound 9

Sub fraction XI-4 (211.2 mg) was injected to the HPLC and eluted using gradient solvent system of MeOH and de-ionized water (75:25 to 100% MeOH in 45 min) which afforded a prominent peak labelled **SAL-XI-4-5** as shown in figure 3.13A. After spotting and developing the fractions on TLC plate using solvent system C, a single spot suspected to be a pure compound was observed (Fig 3.13B). The fraction that afforded this single spot was labelled as **9** (R_t 23.22 min, 12.5 mg, 0.005%).

UNIVERSITY of the WESTERN CAPE

https://etd.uwc.ac.za/

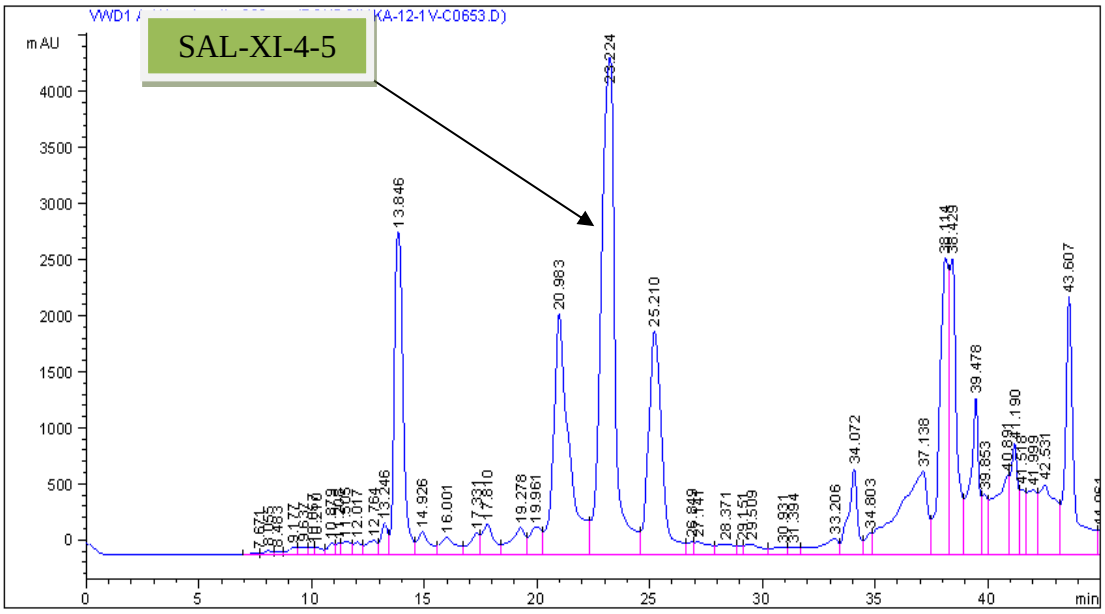

Figure 3.13: HPLC chromatogram of sub fraction XI-4

UNIVERSITY of the
WESTERN CAPE

https://etd.uwc.ac.za/

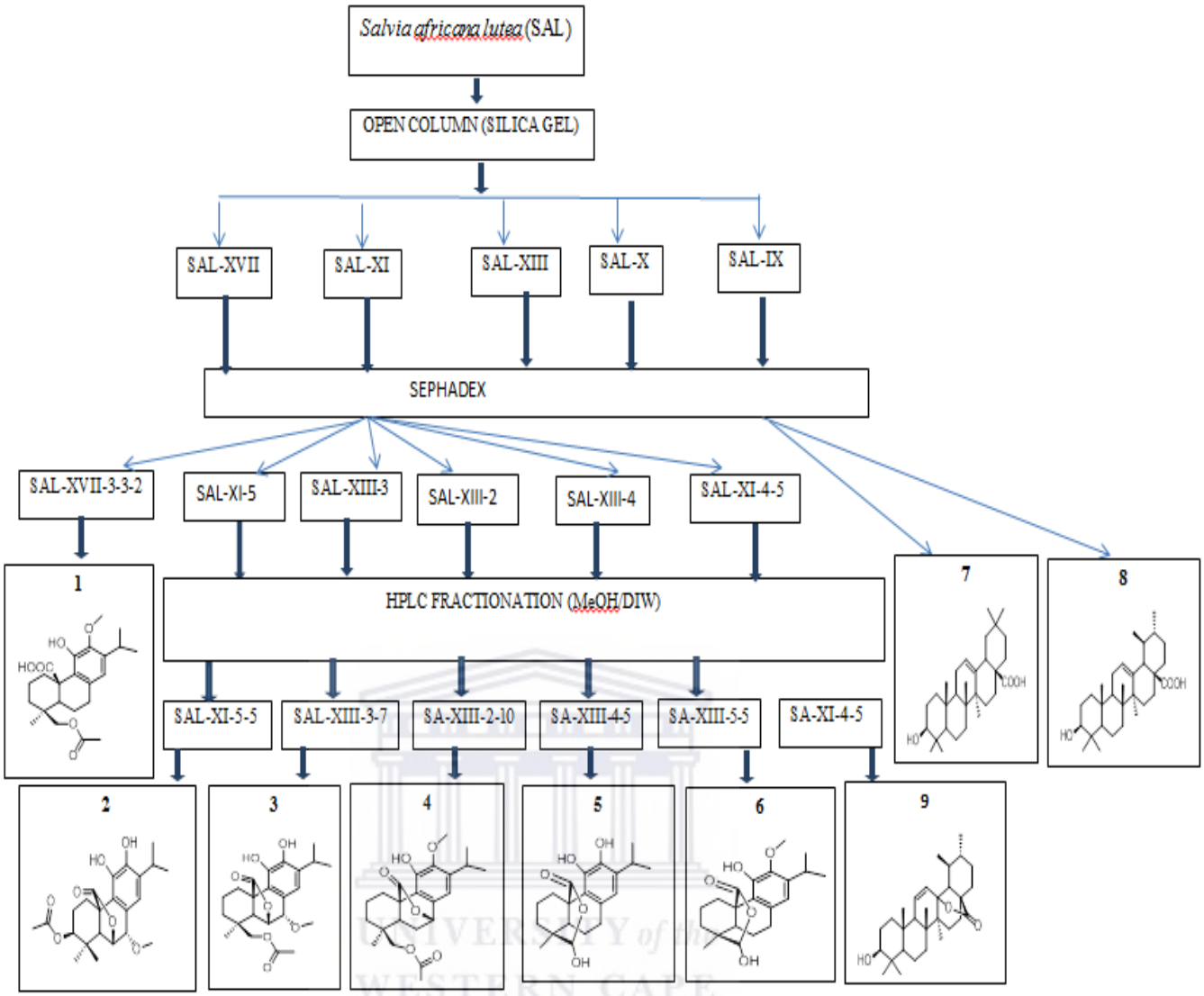

Scheme 3.1: A flow diagram of experimental procedure for the isolation of compounds from *S. africana lutea*

https://etd.uwc.ac.za/

BIOLOGICAL CHARACTERIZATION OF SALVIA AFRICANA CONSTITUENTS

3.7 General experimental procedure for biological assays

3.7.1 Reagents

EGCG (Epigallocatechin gallate), trolox (6-hydroxyl-2, 5, 7, 8- tetramethylchroman-2-carboxylic acid), and other reagents including ABTS (2,2- azino-bis (3-ethylbenzo thiazoline-6-sulfonic acid) diammonium salt), potassium peroxodisulphate, fluorescein sodium salt, AAPH (2,2-Azobis (2-methylpropionamidine) dihydrochloride, perchloric acid, TPTZ (2,4,6-tri[2-pyridyl]-s-triazine, iron (III) chloride hexahydrate, copper sulphate, hydrogen peroxide, alpha-glucosidase (*Saccharomyces cerevisiae*), α-amylase (procaine pancreas) and 3, 5, di-nitro salicylic acid (DNS), 4-nitro-phenyl-α-D-glucopyranoside (pNPG), sodium carbonate (Na_2CO_3), sodium dihydrogen phosphate, di-sodium hydrogen phosphate secured purchased from Sigma-Aldrich, South Africa.

3.7.2 Alpha-glucosidase inhibitory activity

Alpha-glucosidase inhibitory activity of the isolated compounds was carried out according to the standard method with slight modification (Telagari & Hullatti, 2015). In a 96-well plate, the reaction mixture containing 50 µL of phosphate buffer (100 mM, pH = 6. 8), 10 µL alpha-glucosidase (1 U/mL), and 20 µL of varying concentrations (133.33 - 4.17 µg/mL) of isolated compounds was pre-incubated at 37°C for 15 min. Then, 20 µL of PNPG (5 mM) was added as a substrate and incubated further at 37 °C for 20 min. The reaction was stopped by adding 50 µL of sodium carbonate Na_2CO_3 (0.1 M). The absorbance of the released p-nitrophenol was measured at 405 nm using Multiplate Reader (Multiskan thermo scientific, version 1.00.40, Vantaa, Finland). Acarbose at various concentrations was included as a standard. Each experiment was repeated three times. The results were expressed as percentage inhibition, which was calculated using the formula,

Inhibitory activity (%) = $(1 - A/B) \times 100$

https://etd.uwc.ac.za/

Where, A is the absorbance in the presence of test substance and B is the absorbance of control.

3.7.3 Alpha-amylase inhibitory activity

The alpha-amylase inhibitory activity of the isolated compounds was carried out according to the standard method with slight modification (Telagari & Hullatti, 2015). In a 96-well plate, the reaction mixture containing 50 µl of phosphate buffer (100 mM, pH = 6.8), 10 µl alpha–amylase (2 U/mL), and 20 µL of varying concentrations (100 - 31.2 µg/mL) of isolated compounds was pre-incubated at 37 °C for 20 min. Then, 20 µL of 1% soluble starch (100 mM phosphate buffer pH 6.8) was added as a substrate and incubated further at 37°C for 30 min. A volume of 100 µL of the color reagent (DNS) was added and then boiled for 10 min. The absorbance of the resulting mixture was measured at 540 nm using Multiplate Reader (Multiskan thermo scientific, version 1.00.40, Vantaa, Finland). Acarbose at various concentrations was used as a standard. Each experiment was repeated three times. The results were expressed as percentage inhibition, which was calculated using the formula,

UNIVERSITY of the
WESTERN CAPE

Inhibitory activity (%) = $(1 - A/B) \times 100$

Where, A is the absorbance in the presence of test substance and B is the absorbance of control.

3.7.4 Antioxidant Assays

3.7.4.1 Ferric-ion reducing antioxidant power (FRAP) assay

The FRAP assay was carried out in accordance to the method described previously (Benzie & Strain, 1996). In a 96-well plate, 10 µL of the stock solution (1 mg/mL w/v) of the isolated compounds (**1-10**) were mixed with 300 µL FRAP reagent. The FRAP reagent was prepared by mixing (10:1:1, v/v/v) of acetate buffer (300 mM, pH 3.6), tripyridyl triazine (TPTZ) (10 mM in 40 mM HCl) and $FeCl_3.6H_2O$ (20 mM), Incubation commenced at room temperature for 30 min, and the plate was read at a wavelength of 593 nm in a Multiskan spectrum plate

https://etd.uwc.ac.za/

reader (Thermo Fisher Scientific). L-Ascorbic (Sigma Aldrich, South Africa) was used as a standard with concentrations varying between 0 and 1000 μM. Further dilutions were done to the samples that were highly concentrated and such dilution factors were recorded and used for calculations of the affected samples. The results were expressed as μM ascorbic acid equivalents per milligram dry weight (μM AAE/g) of the test samples.

3.7.4.2 Automated oxygen radical absorbance capacity (ORAC) assay

ORAC assay was done according to the previous method with slight modifications (Cao & Prior, 1998). The method measures the antioxidant scavenging capacity of thermal decomposition generated by peroxyl radical of 2,2-azobis (2-amino-propane) dihydrochloride (AAPH) as peroxyradical (ORAC $_{ROO^{\cdot}}$) generator. The loss of fluorescence of fluorescein (probe) was an indication of the extent of its oxidation through reaction with the peroxyl radical. The protective effect of an antioxidant was measured by assessing the fluorescence area under the curve (AUC) plot relative to that of blank in which no antioxidant was present. The analyzer was programmed to record the fluorescence of fluorescein every 2 minutes after AAPH was added. The fluorescein solution and sample were added in the wells of an illuminated 96 well plate, 12 μL of each of sample (in stock solution of 1 mg/mL was combined with 138 μL of a fluorescein working solution followed by addition of 50 μL of 150 mg of AAPH prepared in-situ in 6 mL phosphate buffer. Absorbance was measured with Fluoroskan spectrum plate reader with the excitation wavelength set as 485 nm and the emission wavelength at 530 nm. A calibration curve was used, using a trolox stock solution of concentration in the range of 83 - 417 μM (R^2=0.9514). The ORAC values were calculated using a regression equation ($Y = a + bX + Cx^2$) between Trolox concentration (Y in μM) and the net area under the fluorescence decay curve (X). ORAC values were expressed as μMTE/mg of test sample. Samples without perfect curve were further diluted and the dilution factors were used for the calculation of such samples.

UNIVERSITY of the WESTERN CAPE
https://etd.uwc.ac.za/

3.7.4.3 Trolox equivalent absorbance capacity (TEAC) assay

The total antioxidant activity of the test sample was measured using previously described methods (Pellegrini, et al., 1999). The stock solutions which contain 7 mM ABTS and 140 mM $K_2S_2O_8$ was prepared and kept at -2 ^oC. The working solution was then prepared by adding 88 µL $K_2S_2O_8$ solution to 5 mL ABTS solution. The two solutions were mixed and allowed to react for 24 hours at room temperature in the dark. Trolox was used as the standard with concentrations ranging between 0 and 500 µM. After 24 hours, the ABTS mix solution was diluted with ethanol to read a start-up absorbance (control) of approximately 2.0 (±0.1). The stock solution (1 mg/mL) of a methanol extract (SC) and purified compounds (25 µL) were allowed to react with 300 µL ABTS in the dark at room temperature for 30 min. The absorbance was read at 734 nm at 25 ^oC in the plate reader. The results were expressed as µM trolox equivalents per milligram dry weight (µM/TE/g) of the test samples.

3.8 Statistical Analysis

All the measurements were repeated three times and IC_{50} values were calculated using GraphPad Prism 5 version 5.01 (Graph pad software, Inc., La Jolla, CA, USA.) statistical software. The data presented are means ± SD obtained from 96 well plate readers for all in vitro experiments

3.9 Results and discussion: Chemical characterization

Chromatographic purification of a methanolic extract of *S. africana-lutea* using different techniques including semi Prep-HPLC yielded ten pure terpenoids (Fig. 3.14), four of them reported for the first time from the natural source and six of them isolated for the first time from *S. africana-lutea*.

https://etd.uwc.ac.za/

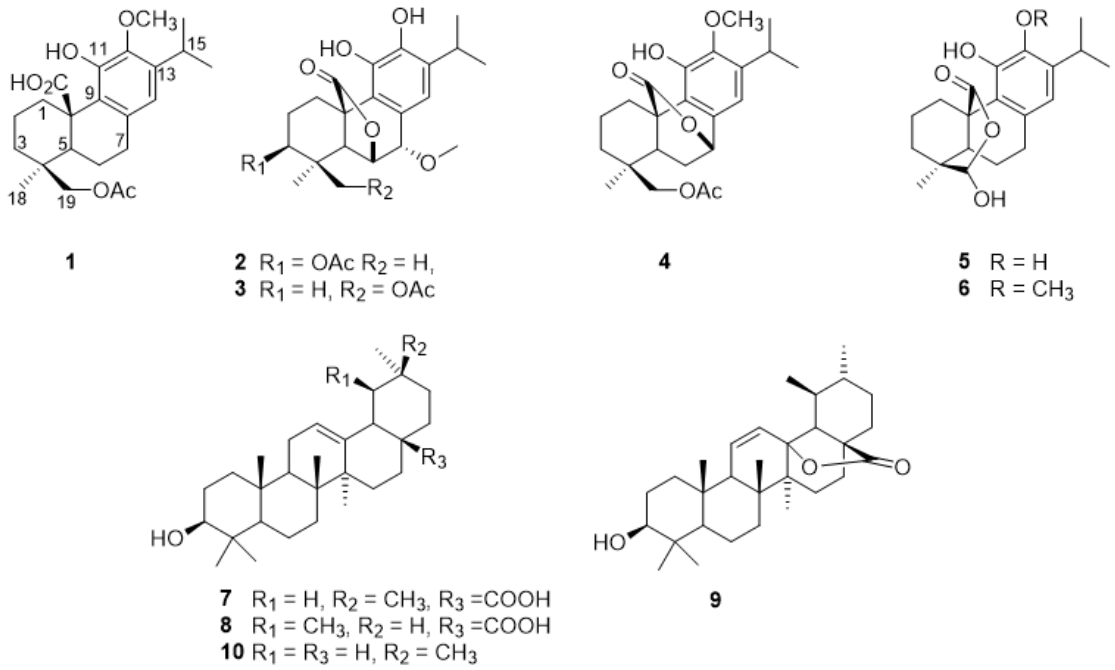

Figure 3.14: Chemical structures of the isolated compounds (**1-10**) from *S. africana-lutea*

3.9.1 Structure elucidation of 19-acetoxy-12-methoxy carnosic acid (**1**)

Compound **1** was isolated as amorphous yellowish-brown powder. The HRMS data indicated a molecular ion peak at $[M]^+$ 403.2115 *m/z* suggesting a possible chemical formula of $C_{23}H_{32}O_6$ ((Fig. 3.24). The UV spectrum showed two absorptions at 210 and 280 nm (Fig. 3.25). Its IR spectrum exhibited bands at 1725 cm^{-1} for a carbonyl group as well as 3324 and 3445 cm^{-1} attributed to hydroxyl groups (Fig. 3.26). The proton nuclear magnetic resonance (^{1}H NMR) spectra (Table 3.7) showed signals of 3 methyls at 1.19 ppm (*d*, *J* = 6.8 Hz), 1.17 (*d*, *J* = 6.8 Hz) and 1.06 (s); an aromatic proton at 6.46 (*s*); an oxygenated methylene proton at 3.97 and 4.24 (*d*/each, *J* = 11.4 Hz); a multiplet signal at 3.17 (*sept*, *J* = 6.8 Hz); in addition to acetoxyl and a methoxyl groups at 1.86 and 3.75. The ^{13}C NMR, DEPT-135 and HSQC spectra showed 23 carbons (Table 3.7) and classified as five methyls including acetoxyl (20.7), methoxyl (61.1) groups; six methylenes; three methines, one of them aromatic (117.8); and nine quaternary carbons including a carbonyl group (181.7); and five aromatic (126.8, 133.8, 148.9, 143.7, and 139.6) in addition to the acetoxyl group (172.5, 20.7). The

UNIVERSITY of the WESTERN CAPE
https://etd.uwc.ac.za/

NMR data indicated an abietane diterpene with similar structure to carnosic acid, previously isolated from the same source (Hussein, et al., 2007), with the only difference b the presence of extra acetoxyl and methoxyl groups. The methoxyl group was allocated at C-12 from the HMBC spectra which showed correlations (among others) between the methoxyl protons and C-12 (143.7). The acetoxyl group was allocated at C-19 due to the presence of a methylene signal at 3.97 and 4.24, and both protons showed HMBC correlations with the acetoxyl's carbonyl groupand C-4/C-5, and C-3. Other 2D data [HMBC and NOESY] confirmed the structure of **1** as 19β-acetoxy-12-methoxy carnosic acid. The absolute configuration of the compound is proposed to belong to the normal abietane skeleton based on biosynthetic bases, because normal abietane diterpene derivatives were isolated from the same source previously and directly related to the isolated compounds (Gao, et al., 2018; Hussein, et al., 2007).

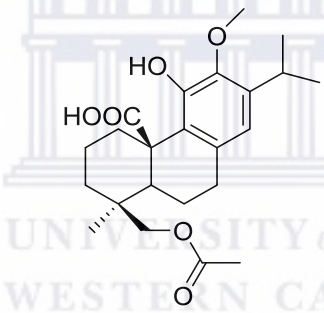

UNIVERSITY of the
WESTERN CAPE

19β-acetoxy-12-methoxy carnosic acid

Figure 3.15: Chemical structure of **1**

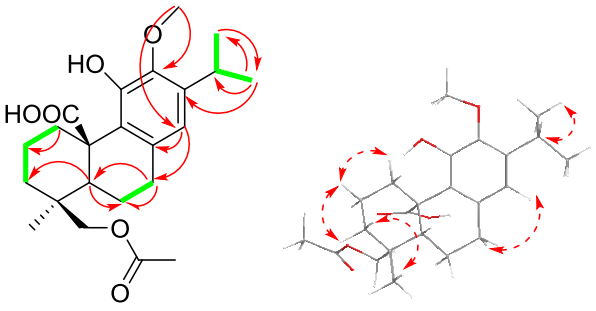

1

Figure 3.16: Key $^{1}H-^{1}H$ COSY, HMBC and NOESY correlations of **1**

https://etd.uwc.ac.za/

Table 3.7: ^{1}H and ^{13}C NMR spectroscopic data assignments (400 MHz) for compound **1** (δ in ppm, m, *J* in Hz) in $CDCl_3$

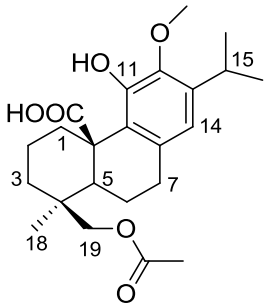

		1		
N^{O}	δ_H (*J* in Hz)	^{13}C	Multiplicity	HMBC
1	3.47 d (10.7) 1.16 d (10.7)	34.6	CH_2	3, 10, 20
2	2.42 m 1.48 d (8.6)	19.7	CH_2	1
3	1.66 d (14.1) 1.19 s	37.1	CH_2	
4		36.9	C	
5	1.58 d (12.0)	44.3	CH	
6	1.47 d (14.1) 1.93 d (14.1)	20.0	CH_2	
7	2.75 d (5.0)	32.9	CH_2	6, 5, 14, 8, 9
8		126.8	C	
9		133.8	C	
10		49.0	C	
11		148.9	C	
12		143.7	C	
13		139.6	C	
14	6.46 s	117.8	CH	11, 12, 8, 7, 15
15	3.17 sept (6.8)	26.5	CH	16, 14, 13, 12
16	1.19 d (6.8)	23.5	CH_3	17, 15, 13
17	1.17 d (6.8)	23.5	CH_3	13
18	1.06 s	27.6	CH_3	4, 19, 3
19	3.97 d (11.4) 4.24 d (11.4)	68.7	CH_2	18
20		181.7	C	
$\underline{COO}CH_3$		172.5	C	
$COO\underline{CH_3}$	1.86 s	20.7	CH_3	
OCH_3	3.75 s	61.1	CH_3	12

UNIVERSITY of the WESTERN CAPE

https://etd.uwc.ac.za/

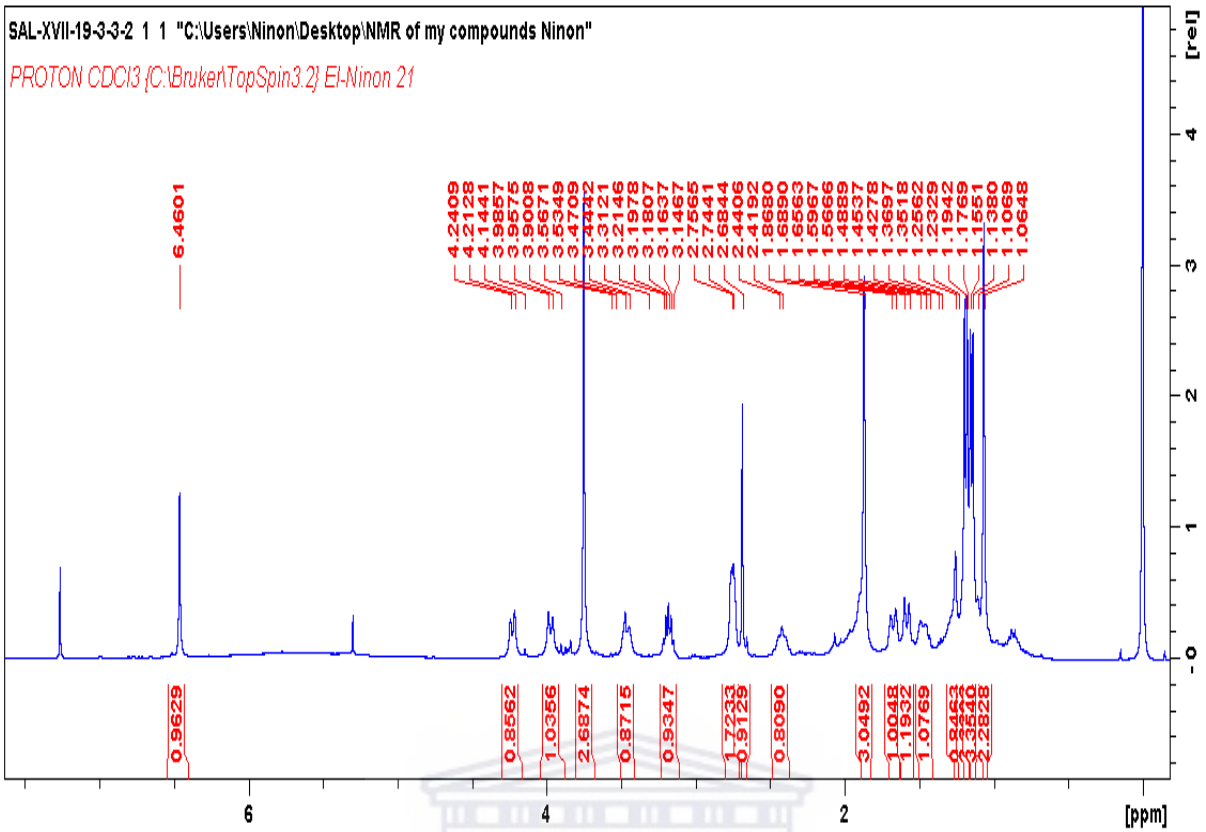

Figure 3.17: ^{1}H NMR (400 MHz, CDCl3) spectrum of **1**

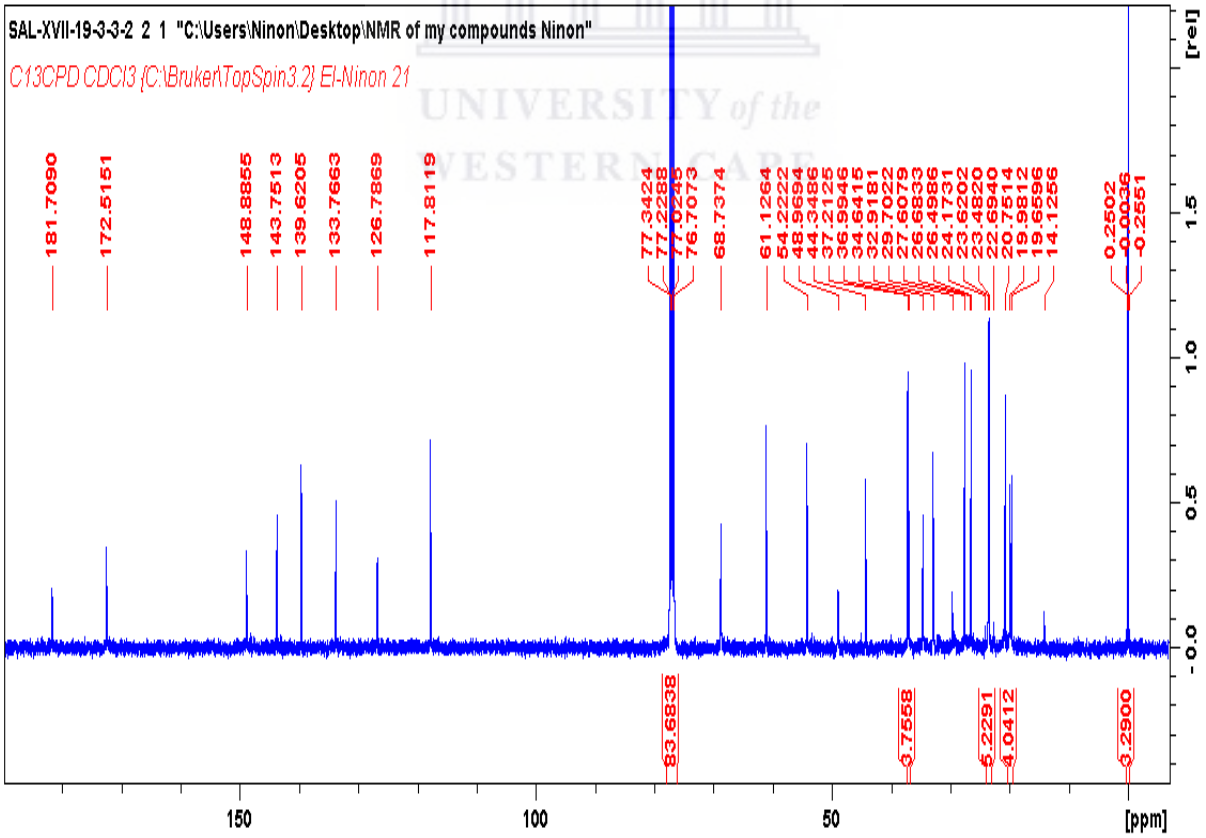

Figure 3.18: ^{13}C NMR (400 MHz, CDCl3) spectrum of **1**

https://etd.uwc.ac.za/

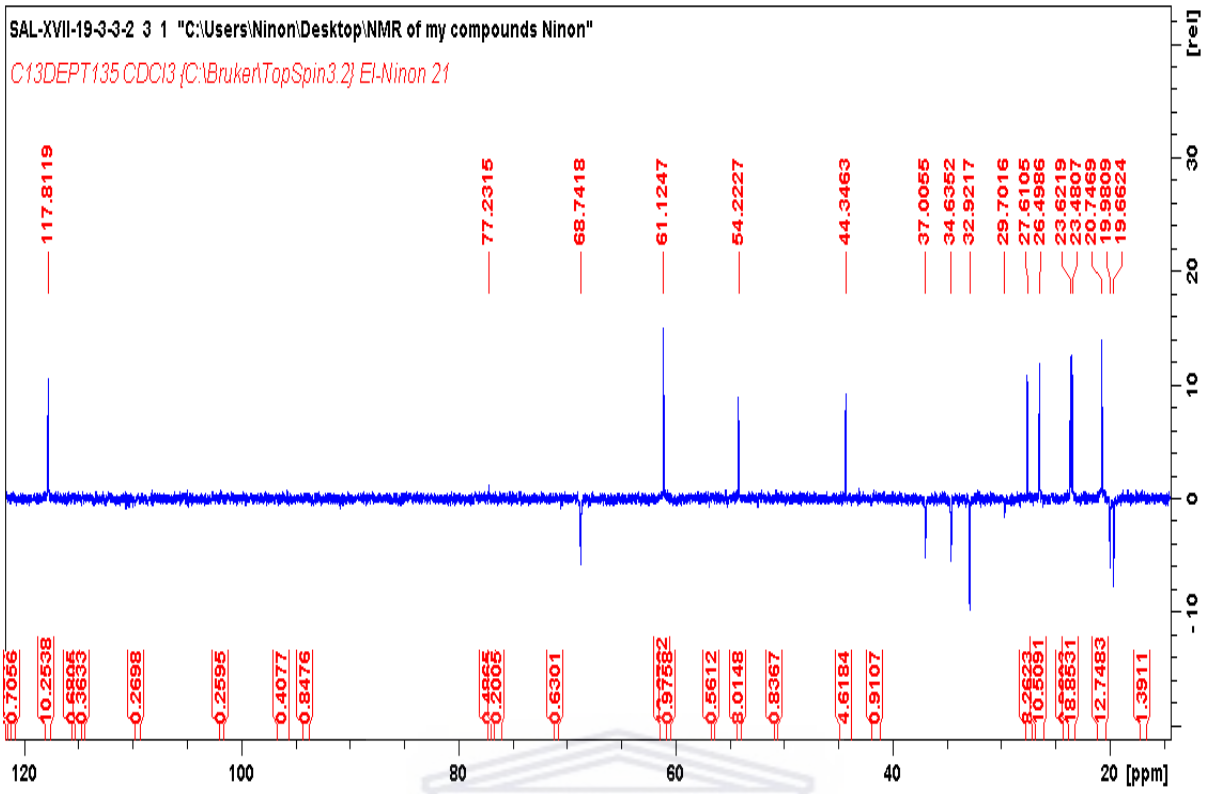

Figure 3.19: DEPT NMR (400 MHz, CDCl3) spectrum of **1**

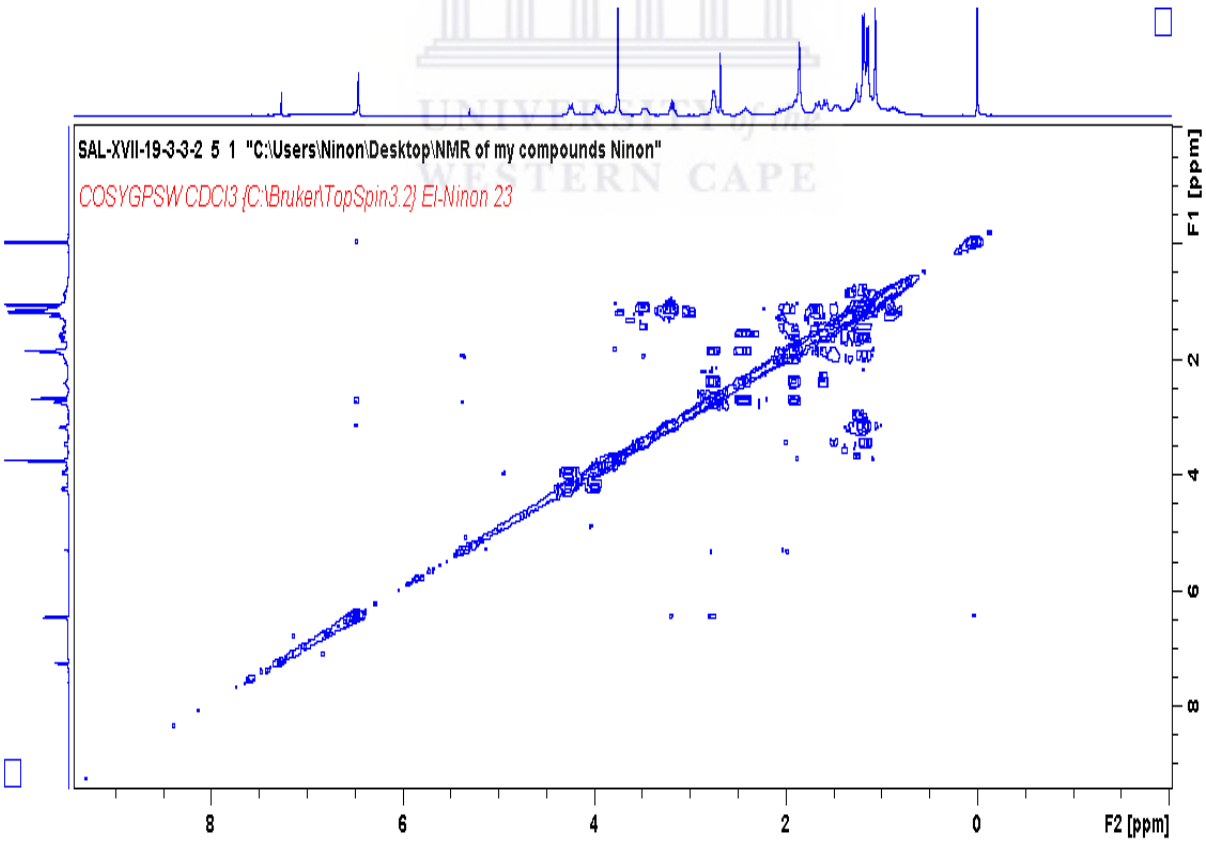

Figure 3.20: COSY (400 MHz, CDCl3) spectrum of **1**

https://etd.uwc.ac.za/

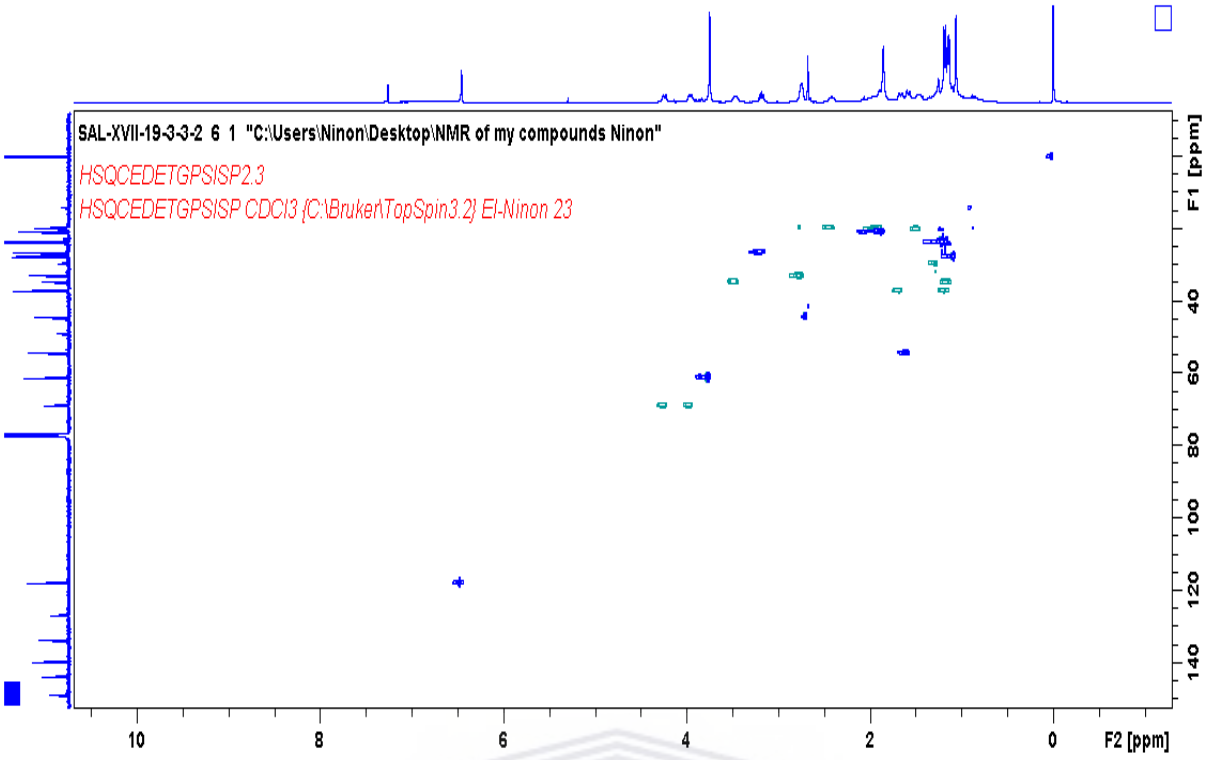

Figure 3.21: HSQC (400 MHz, CDCl3) spectrum of **1**

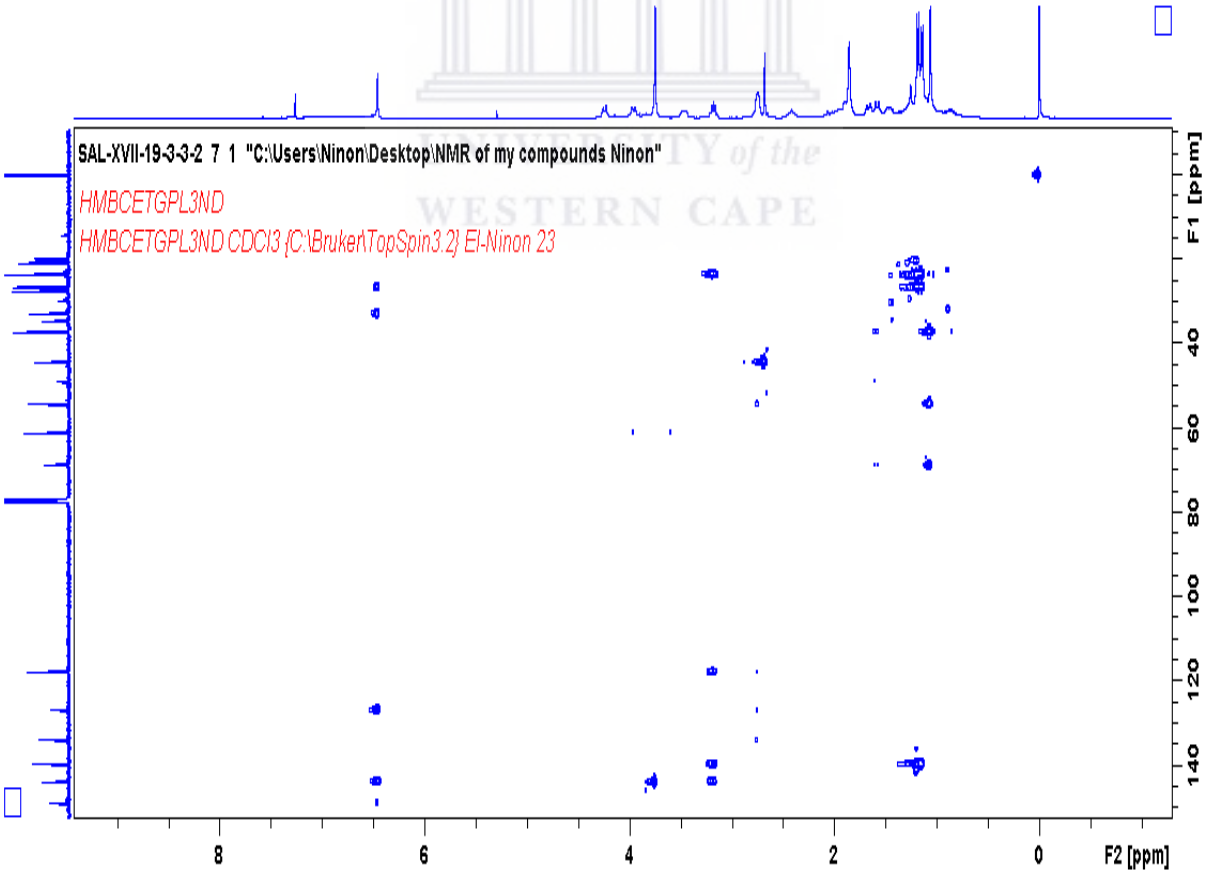

Figure 3.22: HMBC (400 MHz, CDCl3) spectrum of **1**

https://etd.uwc.ac.za/

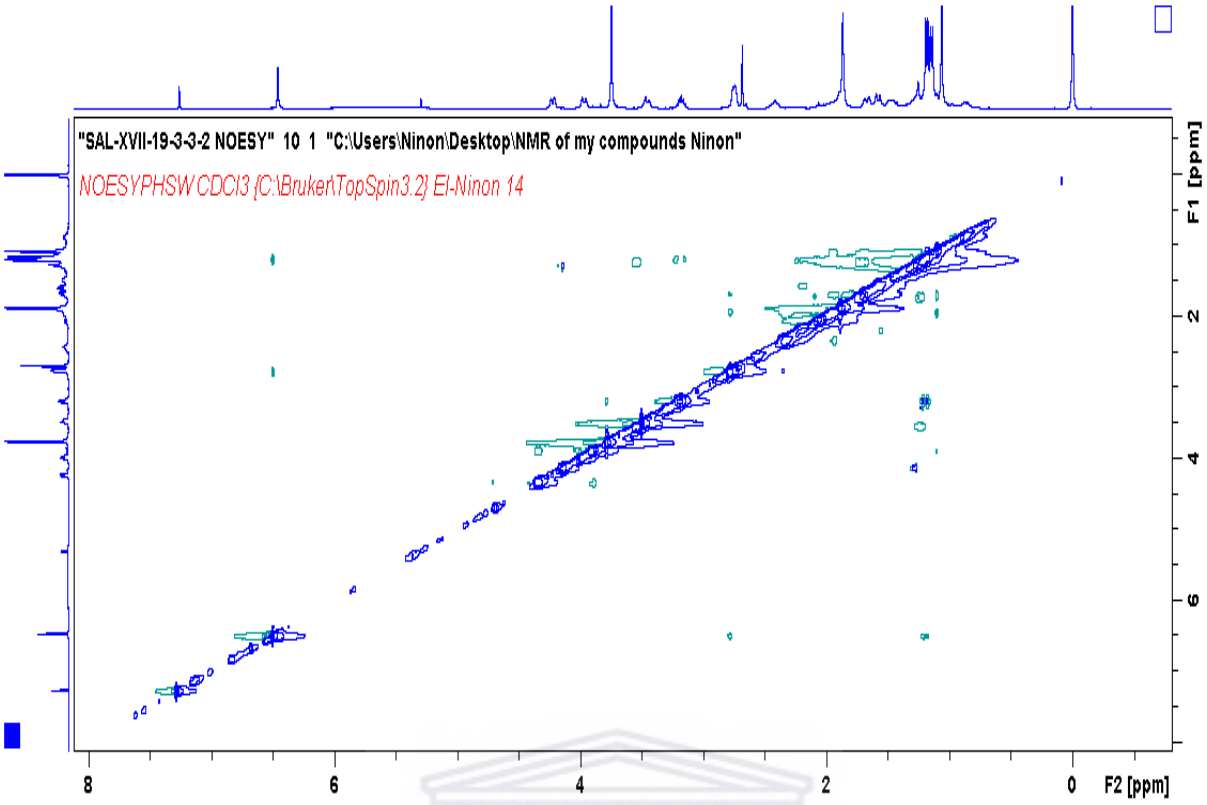

Figure 3.23: NOESY (400 MHz, CDCl3) spectrum of **1**

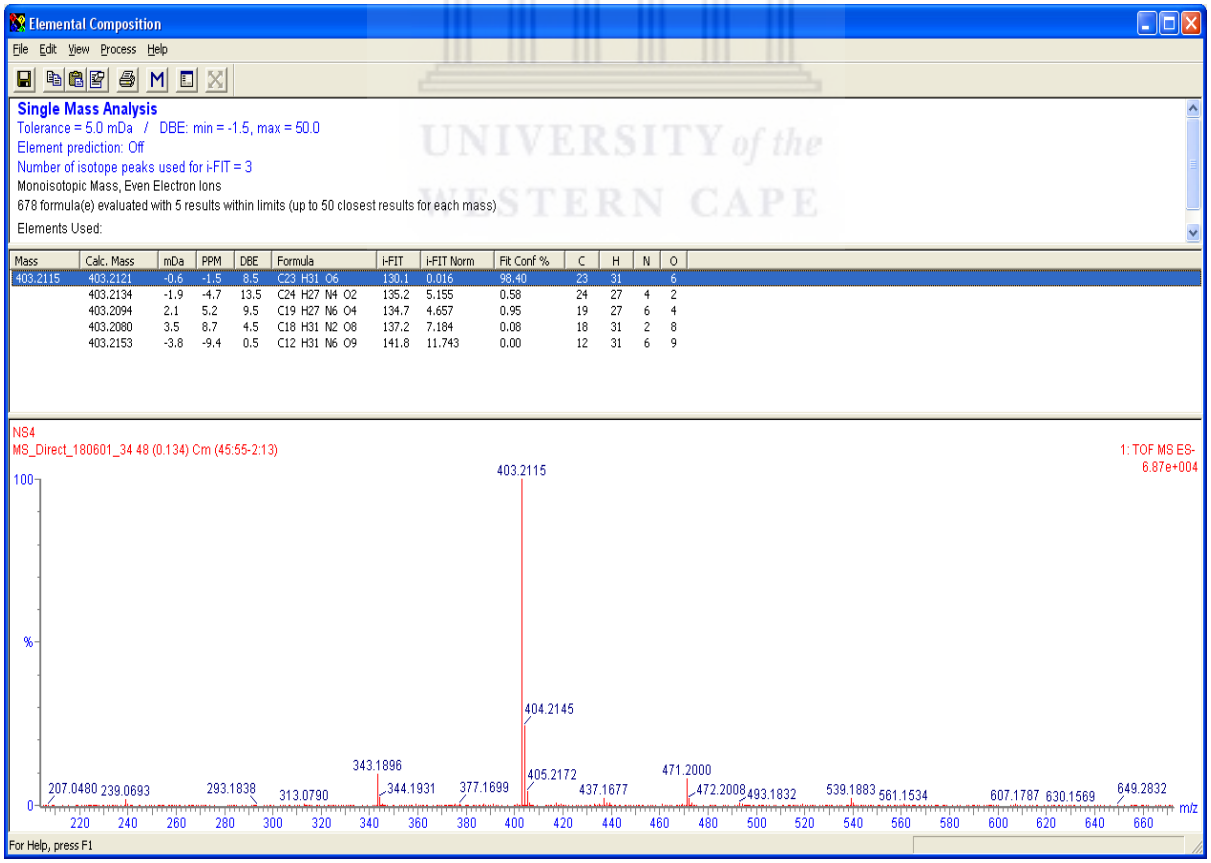

Figure 3.24: HRMS spectrum of **1**

https://etd.uwc.ac.za/

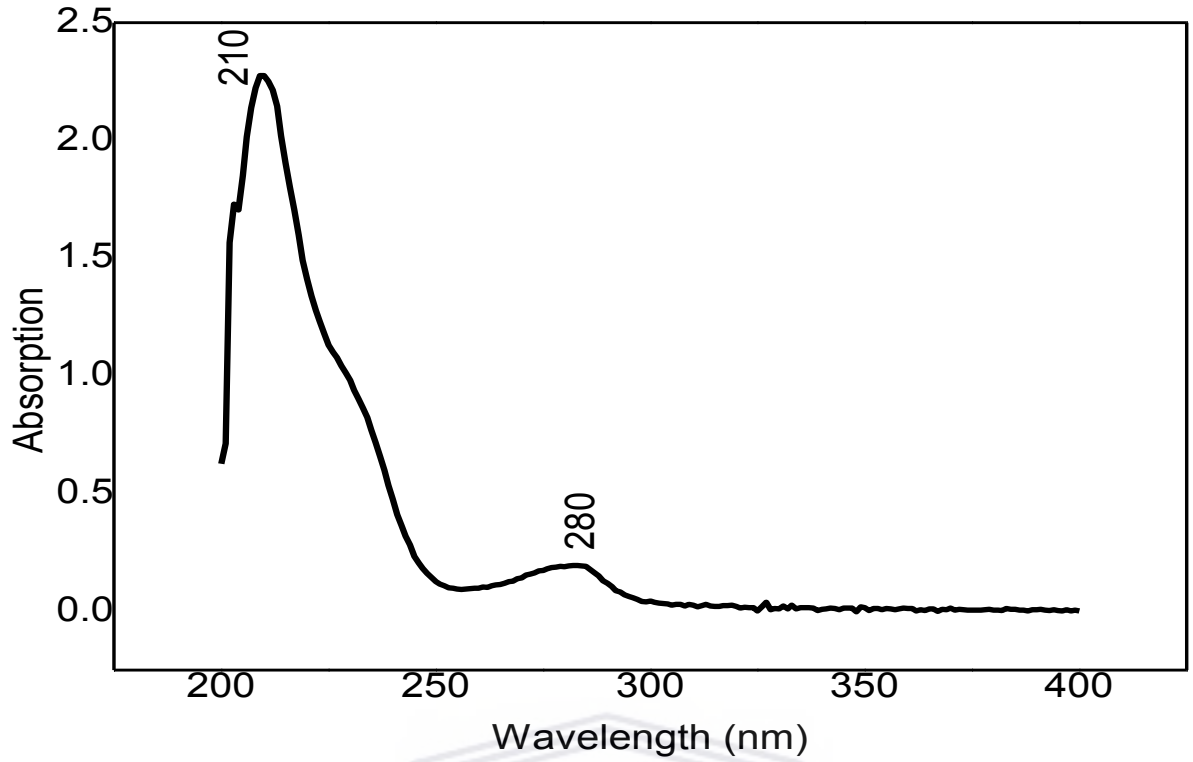

Figure 3.25: UV spectrum of **1**

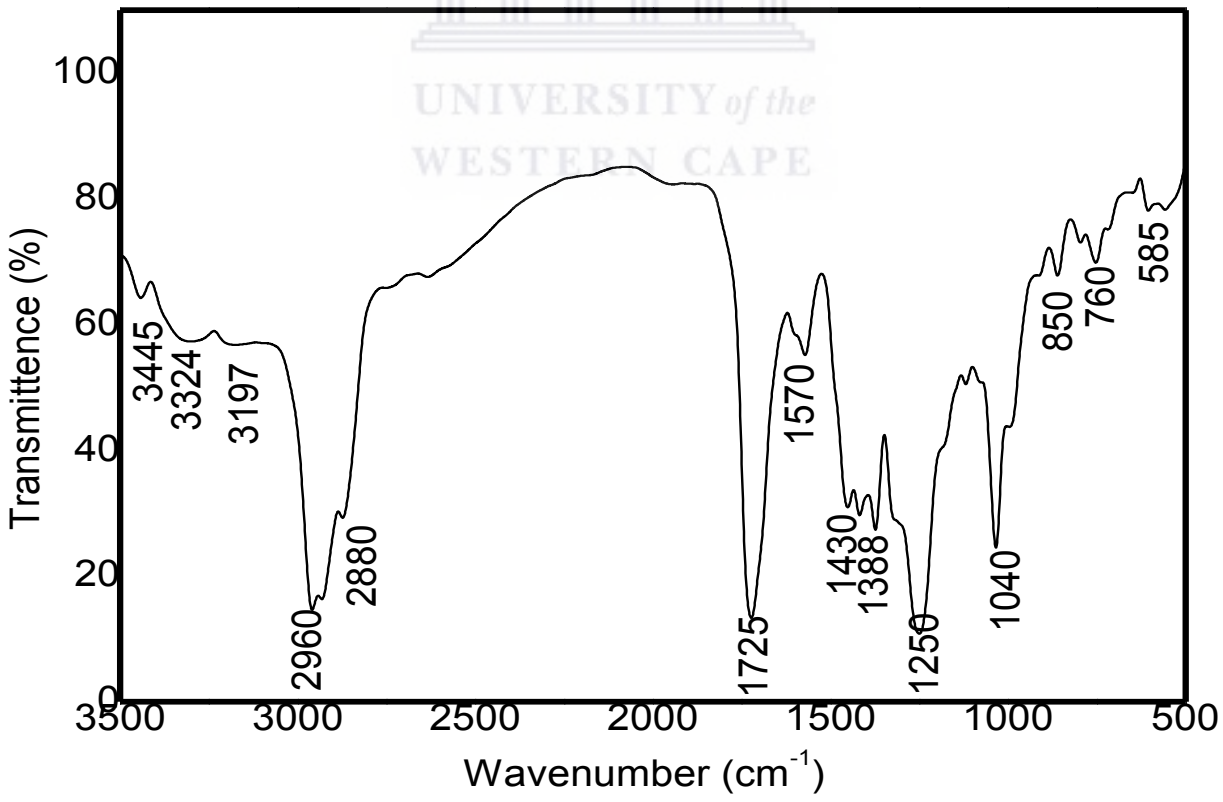

Figure 3.26: FTIR spectrum of **1**

https://etd.uwc.ac.za/

3.9.2 Structure elucidation of 3β-acetoxy-7-methoxy rosmanol (**2**)

Compound **2** was isolated as a red brownish powder. The HRMS data indicated the molecular ion peak at $[M]^+$ 417.1907 m/z suggesting a possible formula of $C_{23}H_{30}O_7$ (Fig. 3.36). The UV spectrum showed two peaks at 212 and 287 nm (Fig. 3.37). Its IR spectrum exhibited bands at 1727 cm^{-1} for an ester as well as at 3447 cm^{-1} and 3300 cm^{-1} attributed to hydroxyl groups (Fig. 3.38). The Raman spectrum featured characteristic bands at 1372 cm^{-1} and 1598 cm^{-1}, which are related to the CH_3 bond vibrations and the deformation vibrations of C-C groups respectively (Fig. 3.39) (Belt, et al., 2017; Chain, et al., 2015; Raschi, et al., 2014). Analysis of the ^1H NMR data (Table 3.8) showed the presence of an isopropyl group [a proton at δ_H = 3.04 (*sept, J* = 6.5 Hz); two methyls at 1.23, 1.25 (*d*/both)]; an aromatic proton (δ_H = 6.79, *s*); three separated protons attached to three oxygenated carbons at 4.66 (*dd, J* = 3.6 Hz), 4.74 (*d, J* = 3.2 Hz), and 4.29 (*d, J* = 3.1 Hz); in addition to four methyl signals at 0.99 and 1.01 (*s* each), 2.07 (*s*, acetoxy) and 3.66 (*s*, methoxy). The ^{13}C NMR, DEPT-135 and HSQC showed 23 carbons and classified as four methyls at (16.2, 26.7, 22.3 and 22.4), an acetoxy (21.2), a methoxy (58.4); two methylene groups (25.3, 24.3); six methines, (one of them is aromatic); nine quaternary carbons including two carbonyls (170.7, 178.1); and five aromatics (126.6, 123.4, 141, 141.8 and 134.7)]. According to HSQC, the proton resonating at 4.66 attached to carbon at 74.0 showed HMBC correlations with C's at 174 (CO acetoxy), 77.4 (C-7), 51.5 (C-5) and 46.5 (C-10), which indicates the presence of a lactone ring at position 6. Additionally, the proton at 4.29 (H-7) showed HMBC correlations with carbons at 74.0 (C-6), 126.6 (C-8), 123.4 (C-9) and 120.4 (C-14) as shown in Table 3.8. On the other hand, the spectroscopic data of **2** showed close similarity with methoxyrosmanol, the only difference is the presence of an extra acetoxyl signal at (2.07/170.7). The position of the acetate group was located at C-3 (from HMBC and NOESY correlations). Other 2D spectra

https://etd.uwc.ac.za/

confirmed the structure of **2** as 3β-acetoxy-7α-methoxyrosmanol (Bajpai & Kang, 2015; Nickavar, et al., 2008).

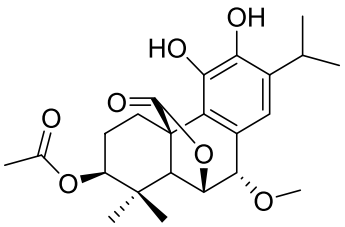

3β-acetoxy-7-methoxy rosmanol

Figure 3.27: Chemical structure of **2**

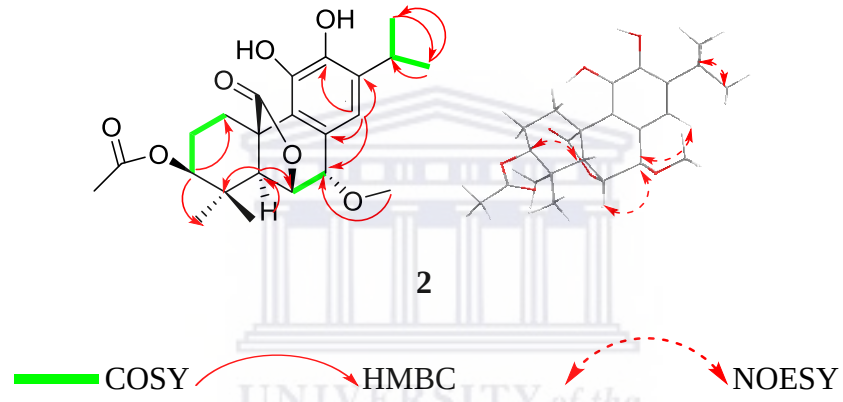

Figure 3.28: Key $^{1}H-^{1}H$ COSY, HMBC, and NOESY correlations of **2**

https://etd.uwc.ac.za/

Table 3.8: ^{1}H and ^{13}C NMR spectroscopic data assignments (400 MHz) for compound **2** (δ in ppm, m, *J* in Hz) in $CDCl_3$

	2			
N^{O}	δ_H (*J* in Hz)	^{13}C	Multiplicity	HMBC
1	3.28 d (15.2) 2.27 d (5.3)	25.3	CH_2	10
2	1.81 m 1.62 m	24.3	CH_2	
3	4.66 dd (3.6, 3.6)	77.5	CH	18, 1
4		36.0	C	
5	2.42 s	51.5	CH	18, 4, 10, 3
6	4.74 d (3.2)	74.0	CH	5, 23, 7, 14, 9, 8
7	4.29 d (3.1)	77.4	CH	4, 10, 5, 20
8		126.6	C	
9		123.4	C	
10		46.5	C	
11		141.0	C	
12		141.8	C	
13		134.7	C	
14	6.79 s	120.4	CH	15, 7, 9, 12, 8
15	3.04 sept (6.5)	27.4	CH	16
16	1.23 s	22.4	CH_3	17, 15
17	1.25 s	22.3	CH_3	13
18	1.01 s	16.2	CH_3	19, 5, 3
19	0.99 s	26.7	CH_3	18, 4, 5, 3
20		178.1	C	
$\underline{COO}CH_3$		170.7	C	
$COO\underline{CH_3}$	2.07 s	21.2	CH_3	
OCH_3	3.66 s	58.4	CH_3	7

UNIVERSITY of the
WESTERN CAPE

https://etd.uwc.ac.za/

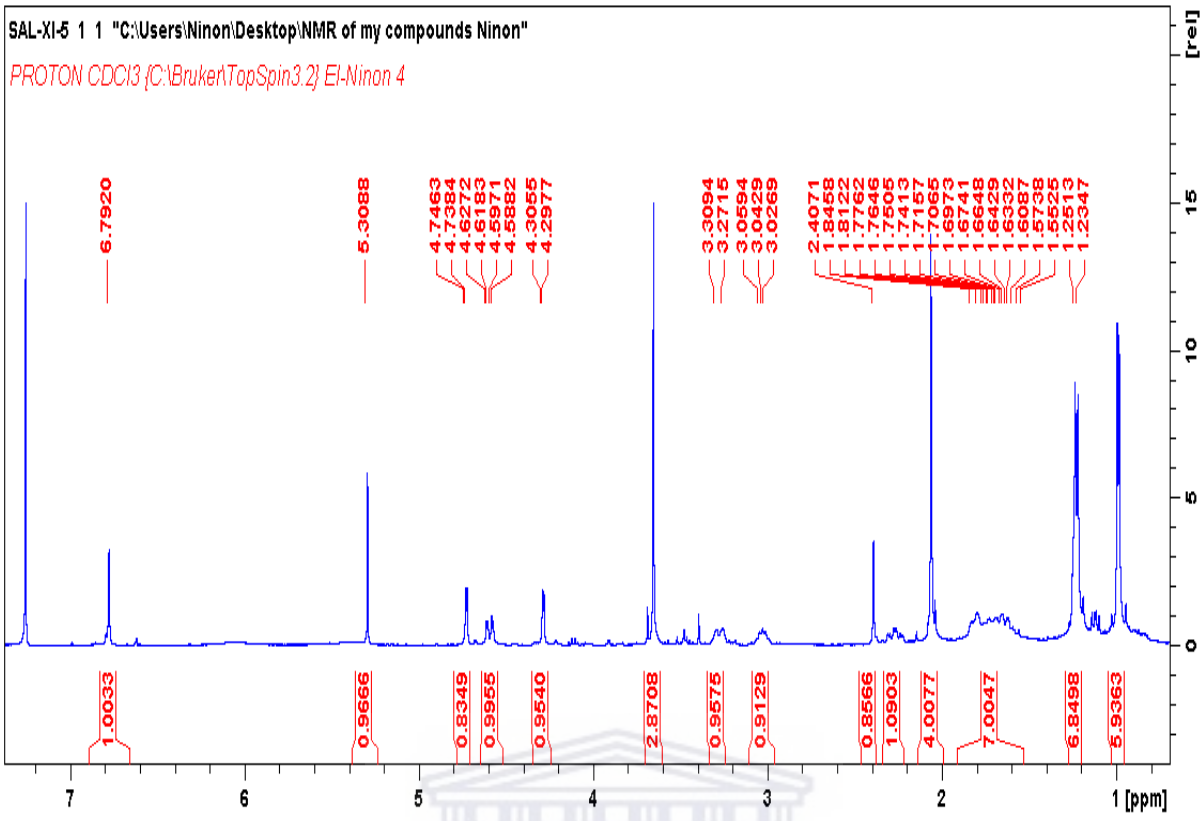

Figure 3.29: ^{1}H NMR (400 MHz, CDCl3) spectrum of **2**

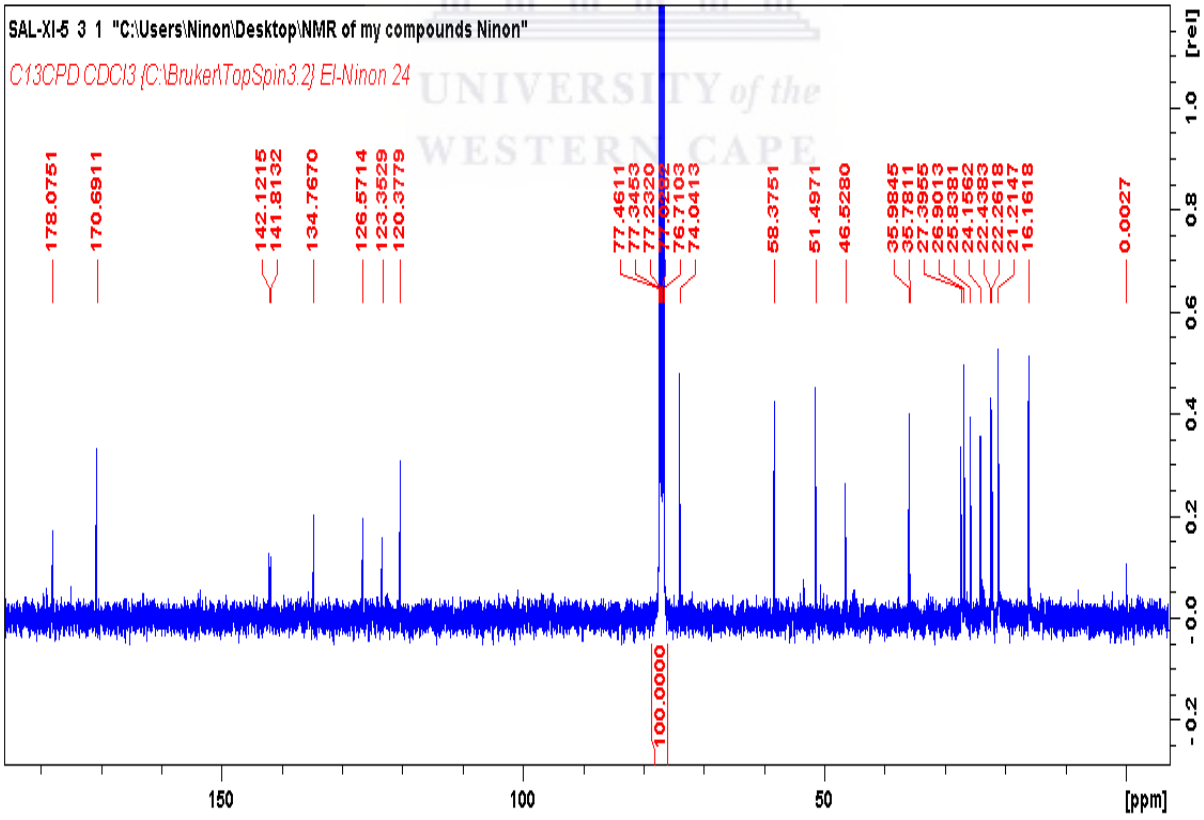

Figure 3.30: ^{13}C NMR (400 MHz, CDCl3) spectrum of **2**

https://etd.uwc.ac.za/

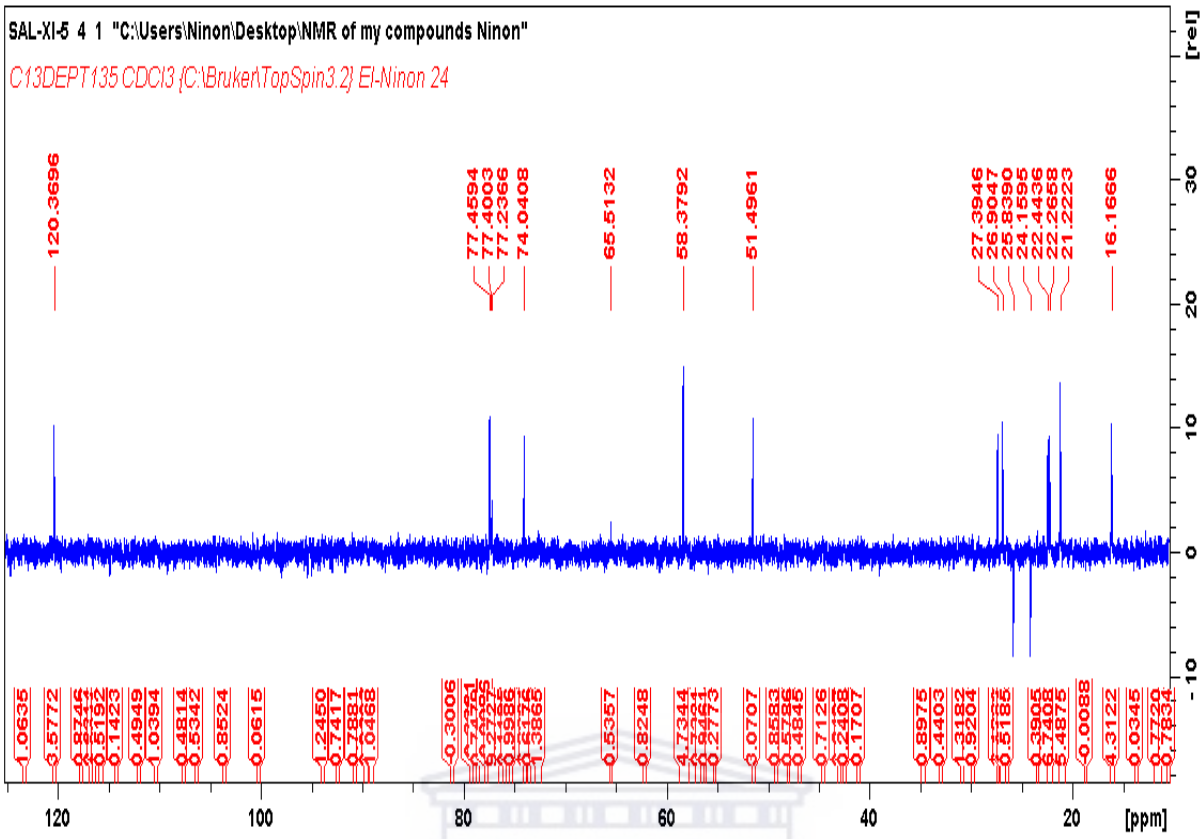

Figure 3.31: DEPT NMR (400 MHz, CDCl3) spectrum of **2**

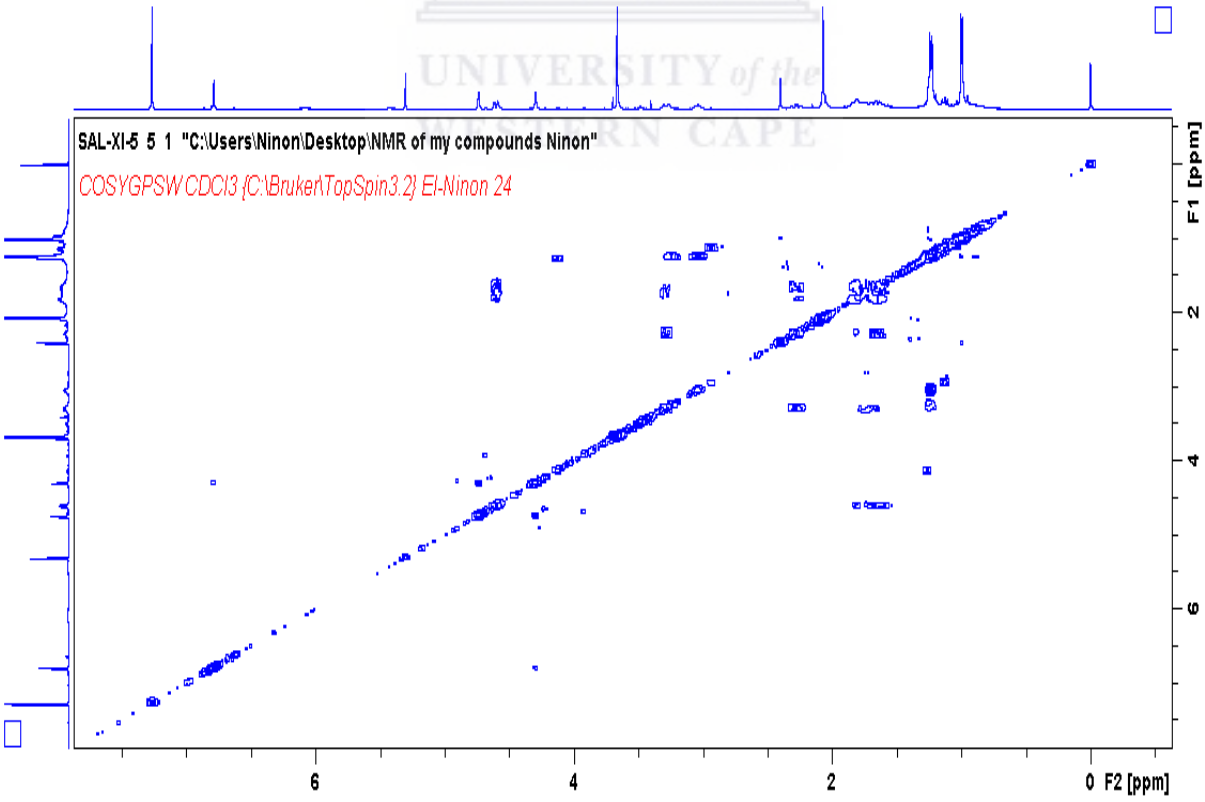

Figure 3.32: COSY (400 MHz, CDCl3) spectrum of **2**

https://etd.uwc.ac.za/

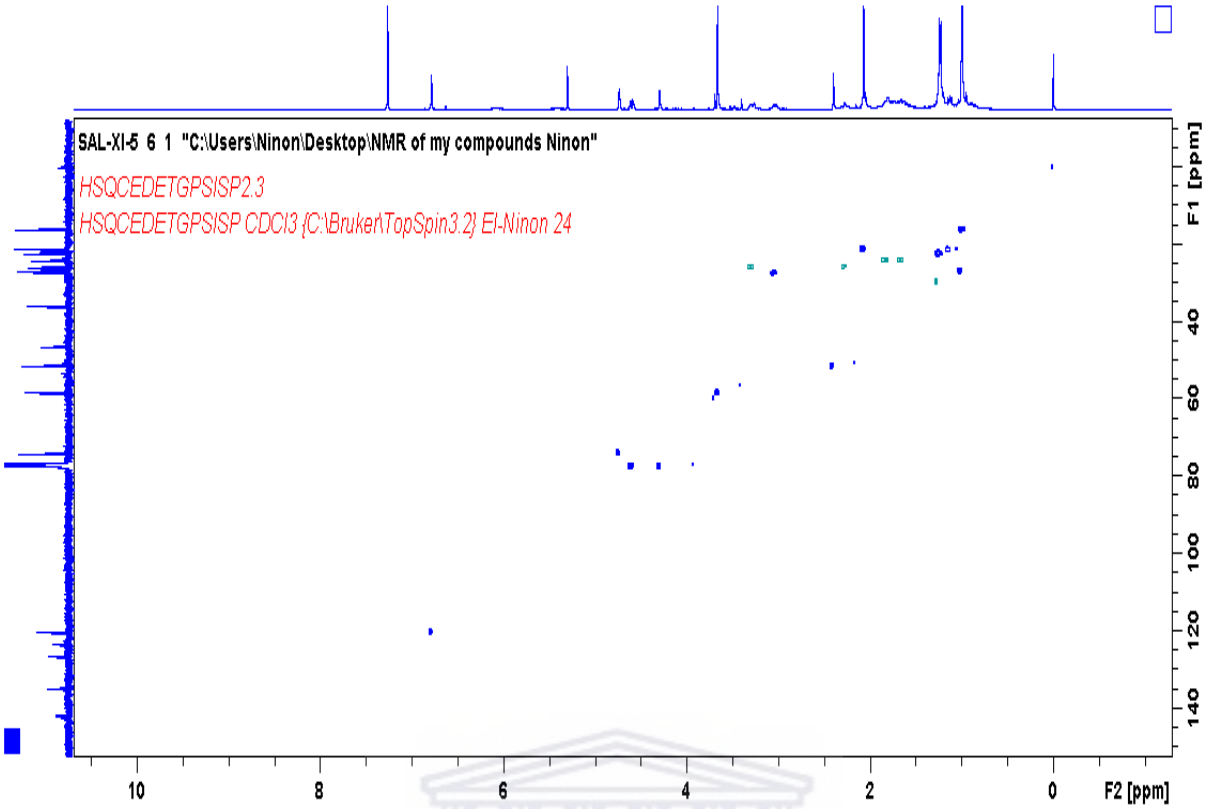

Figure 3.33: HSQC (400 MHz, CDCl3) spectrum of **2**

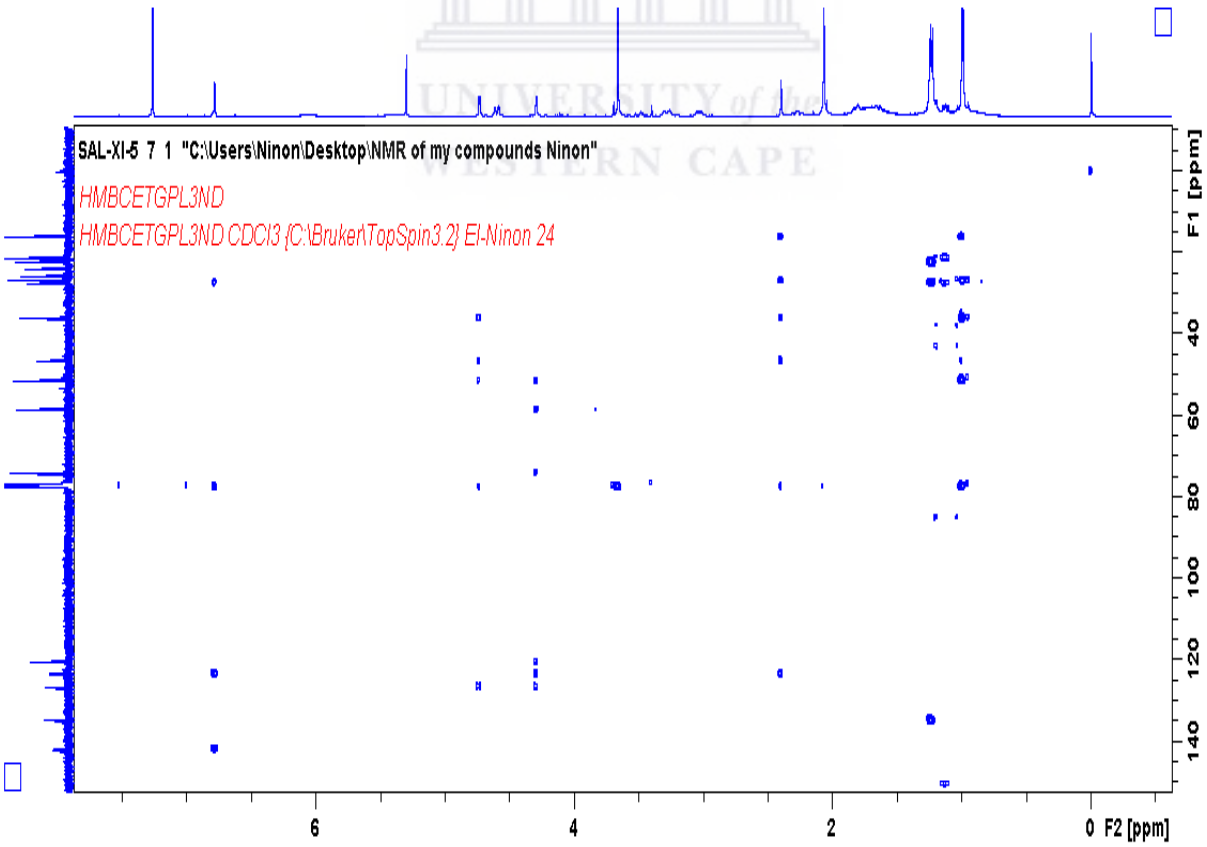

Figure 3.34: HMBC (400 MHz, CDCl3) spectrum of **2**

https://etd.uwc.ac.za/

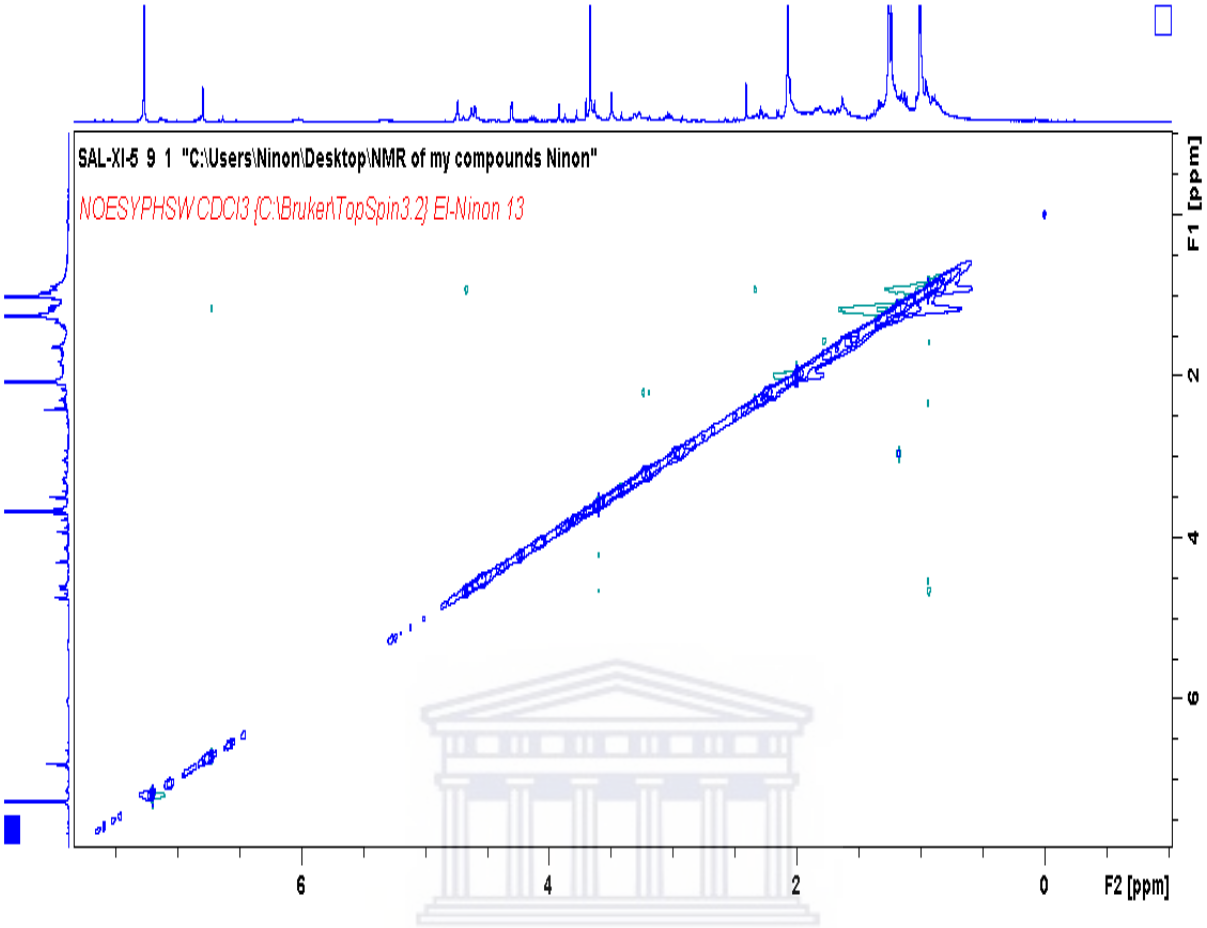

Figure 3.35: NOESY (400 MHz, CDCl3) spectrum of **2**

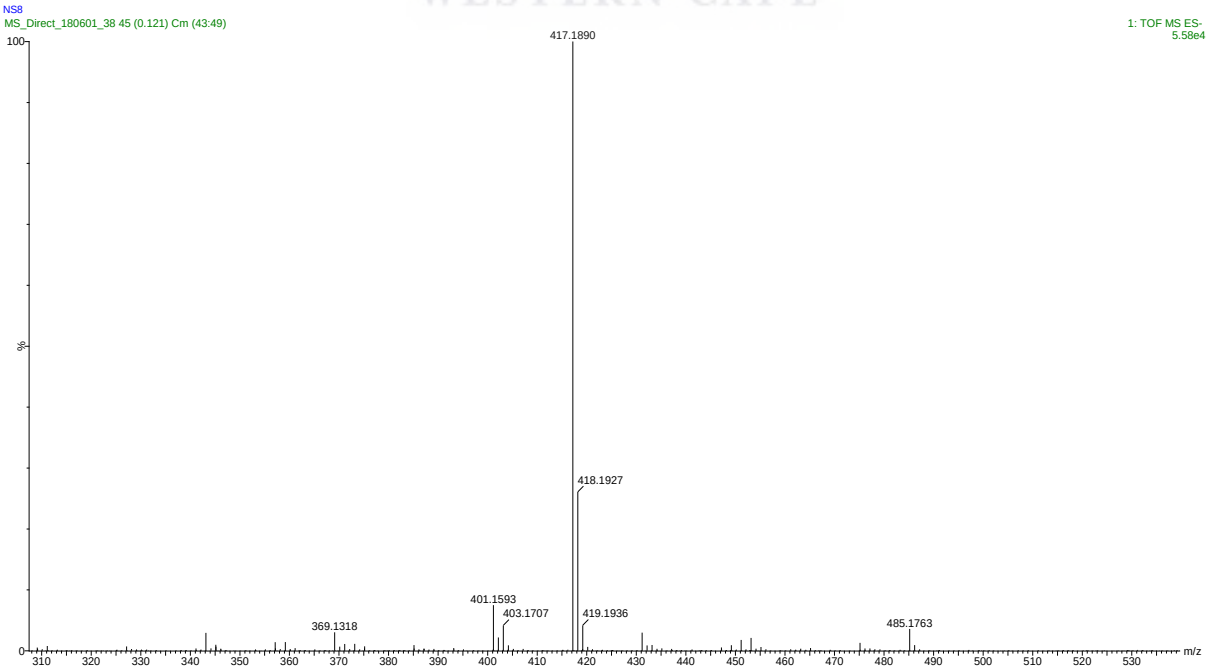

Figure 3.36: HRMS spectrum of **2**

https://etd.uwc.ac.za/

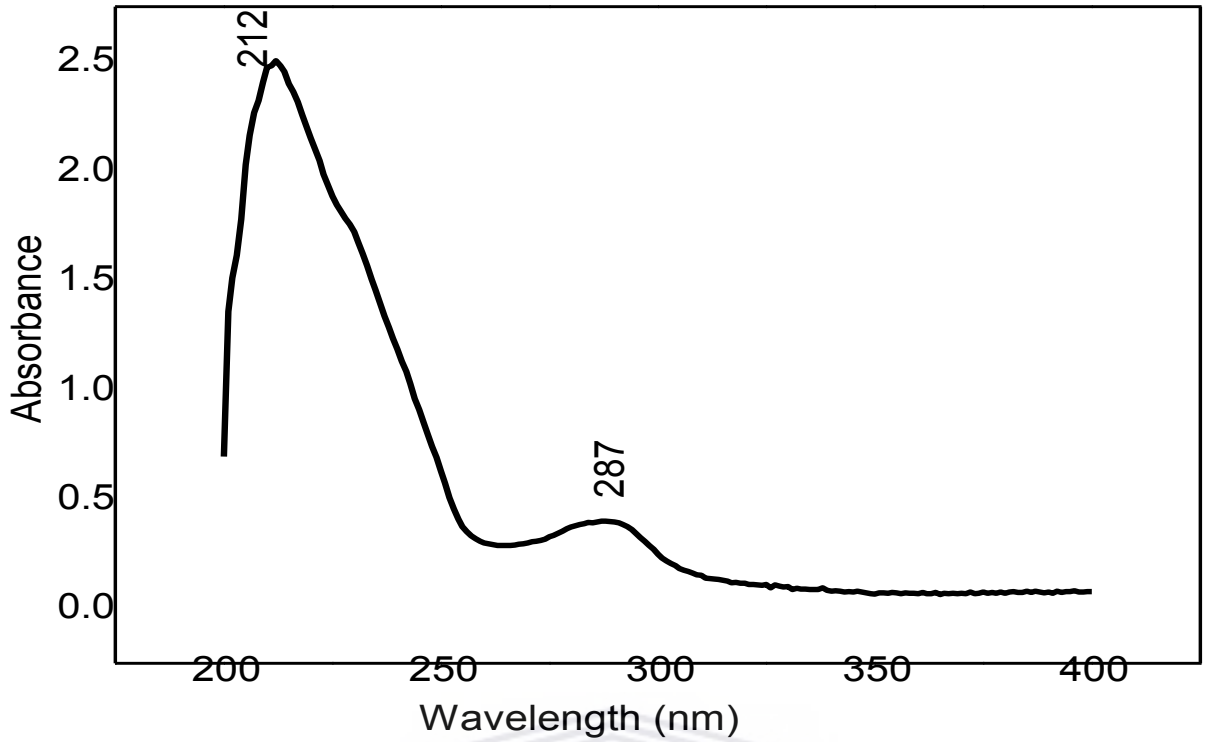

Figure 3.37: UV spectrum of **2**

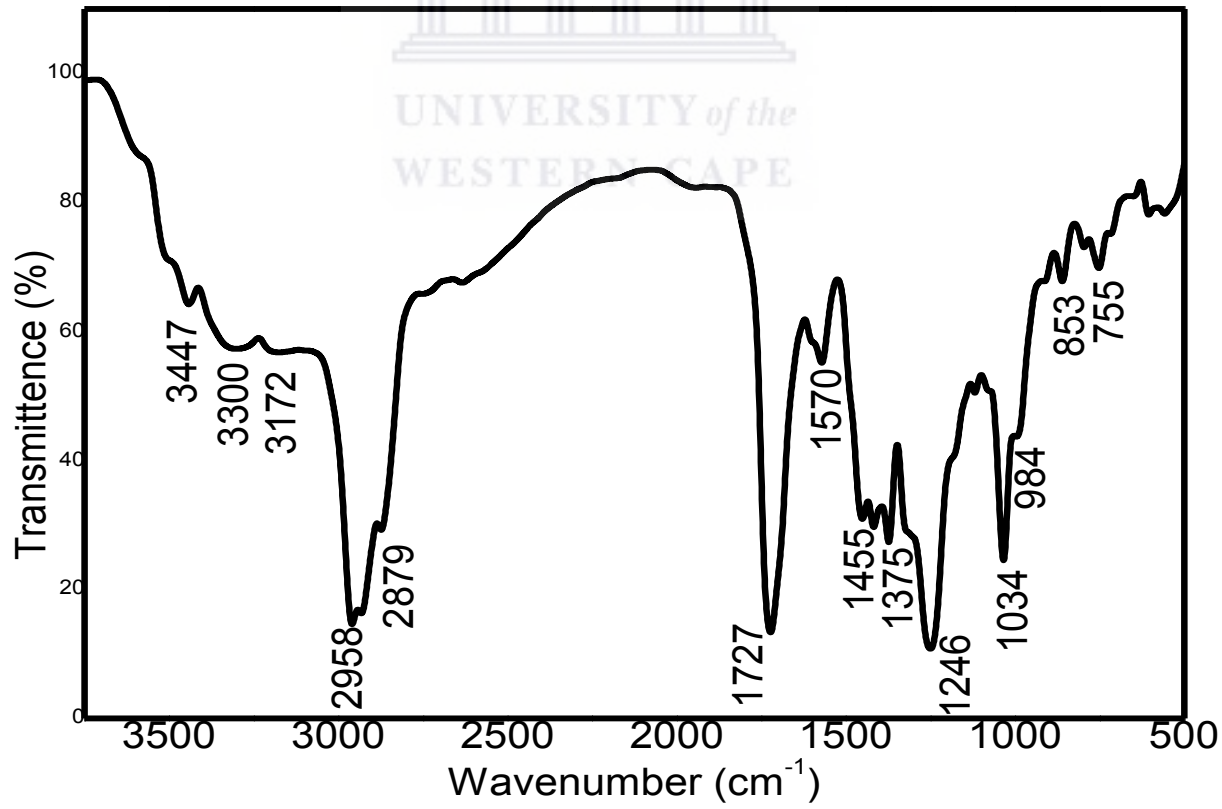

Figure 3.38: FTIR spectrum of **2**

https://etd.uwc.ac.za/

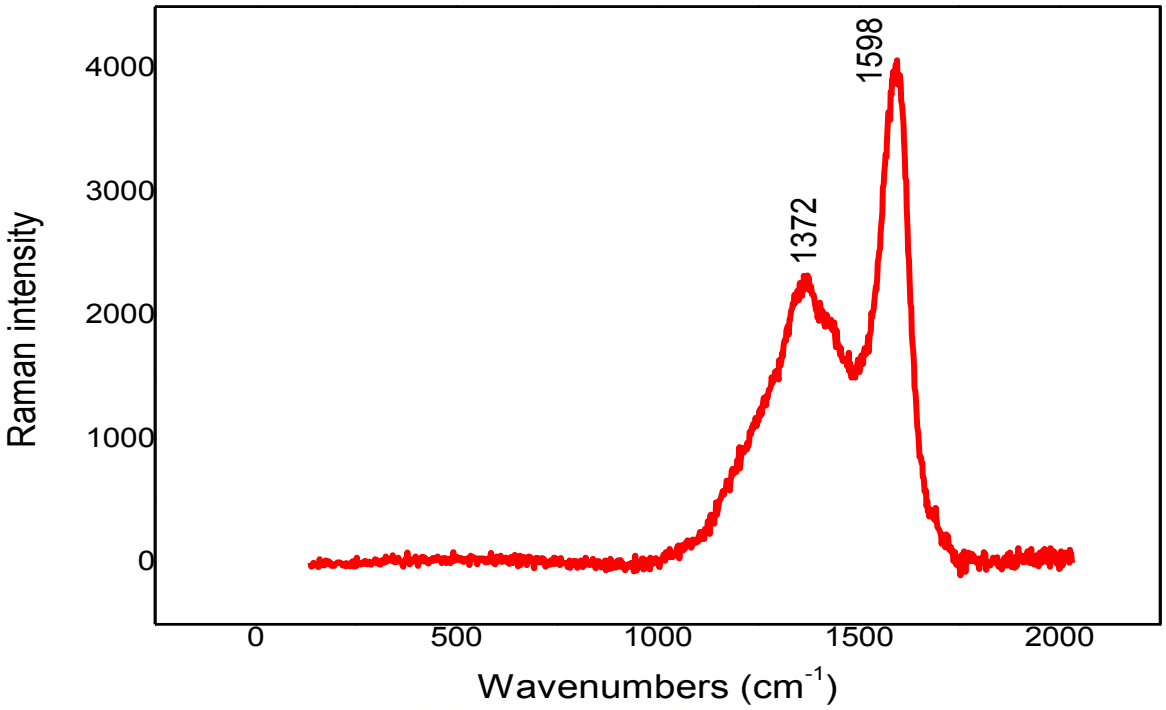

Figure 3.39: Raman spectrum of **2**

RAMAN	Intensity	Assignments
1372	n	CH_2/CH_3 deformation
1598	s	C-C deformation

3.9.3 Structure elucidation of 19-acetoxy-7α-methoxyrosmanol (3)

Compound **3** was isolated as a brown amorphous powder. The HRMS data indicated the molecular ion with a large peak at $[M]^+$ = 417.1907 *m/z* suggesting a possible formula of $C_{23}H_{30}O_7$ (Fig. 3.46). The UV spectrum showed two peaks at 210 and 295 nm (Fig. 3.47). Its IR spectrum exhibited bands at 1769 cm^{-1} for an ester and 3450 cm^{-1} attributed to hydroxyl group (Fig. 3.48). The NMR data of Compound **3** showed close similarity to compound **2**. The ^1H NMR showed the absence of the C-3 methine signal at 4.66 (Table 3.9) and appearance of signal of methylene protons (4.05, s) attached to an acetoxyl group (from HMBC spectra). The acetoxyl group is attached to C-19 because the NOESY and HMBC correlations showed cross-peaks between the acetoxy methyl/C-19, in addition to CH_2-19/C-3; C-4 and C-5. Other 2D data confirmed the structure of **3** as 19-acetoxy-7α-methoxyrosmanol (Gao, et al., 2018).

https://etd.uwc.ac.za/

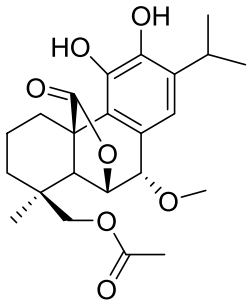

19-acetoxy-7α-methoxyrosmanol

Figure 3.40: Chemical structure of the **3**

Table 3.9: ^{1}H and ^{13}C NMR spectroscopic data assignments (400 MHz) for compound **3** (δ in ppm, m, *J* in Hz) in $CDCl_3$

		3		
N^{O}	δ_H (*J* in Hz)	^{13}C	Multiplicity	HMBC
1	3.22 d, 2.06 d (14.7, 5.5)	27.09	CH_2	2, 10
2	1.53 t 1.69 d (3.7, 3.4)	18.45	CH_2	
3	4.66 dd (3.6, 3.6)	33.2	CH_2	1, 2
4		51.04	C	
5	2.42 s	50.88	CH	18, 10, 19, 20
6	4.26 d (3.2)	77.4	CH	23, 4, 7, 8, 9, 14
7	4.9 d (3.1)	73.91	CH	8, 20
8		126.07	C	
9		123.85	C	
10		47.01	C	
11		142.4	C	
12		141.8	C	
13		134.8	C	
14	6.82 s	119.1	CH	7, 9, 11
15	3.06 sept (6.9)	27.34	CH	16, 13, 14
16	1.23 s	22.21	CH_3	17, 15, 13
17	1.24 s	22.45	CH_3	15, 13
18	1.05 s	25.99	CH_3	3, 4, 19
19	4.05 s	66.17	CH_2	18, 3, 4, 1
20		178.5	C	
$\underline{COO}CH_3$		170.79	C	
$COO\underline{CH_3}$	2.09 s	20.93	CH_3	18, 19,
OCH_3	3.66 s	58.4	CH_3	5, 6

UNIVERSITY of the WESTERN CAPE

https://etd.uwc.ac.za/

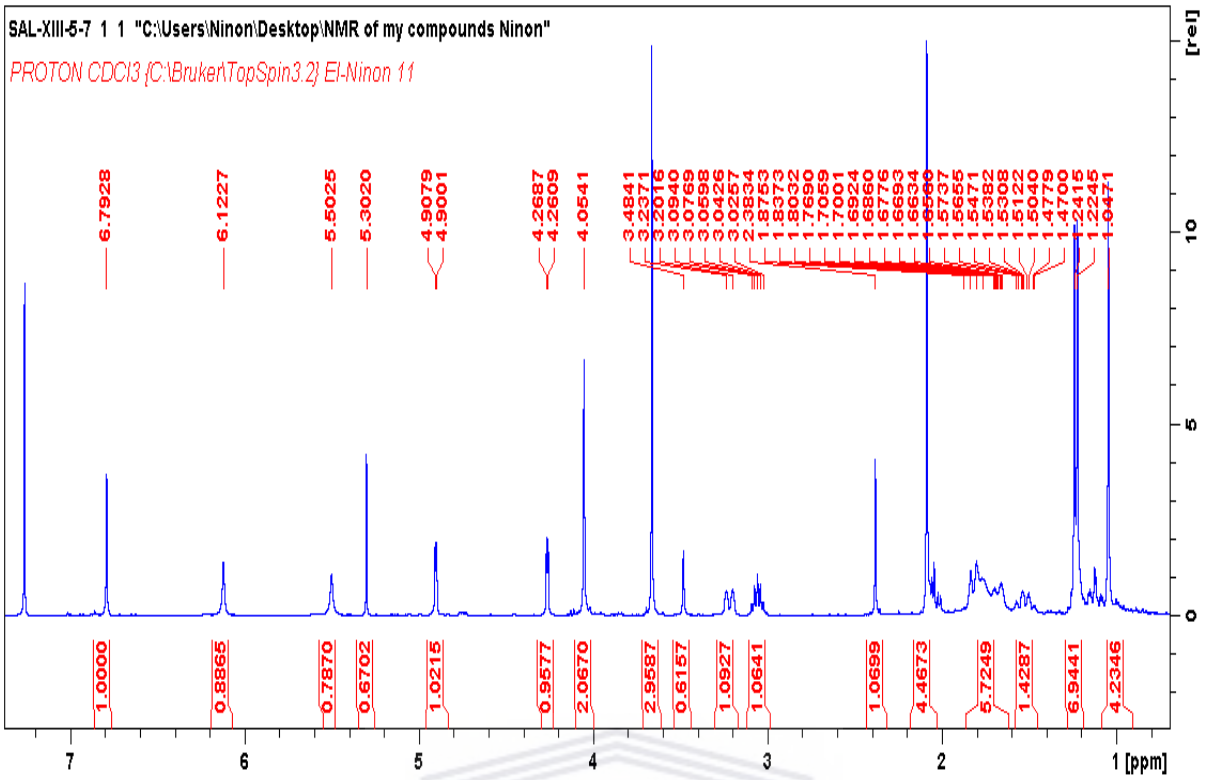

Figure 3.41: ^{1}H NMR (400 MHz, CDCl3) spectrum of **3**

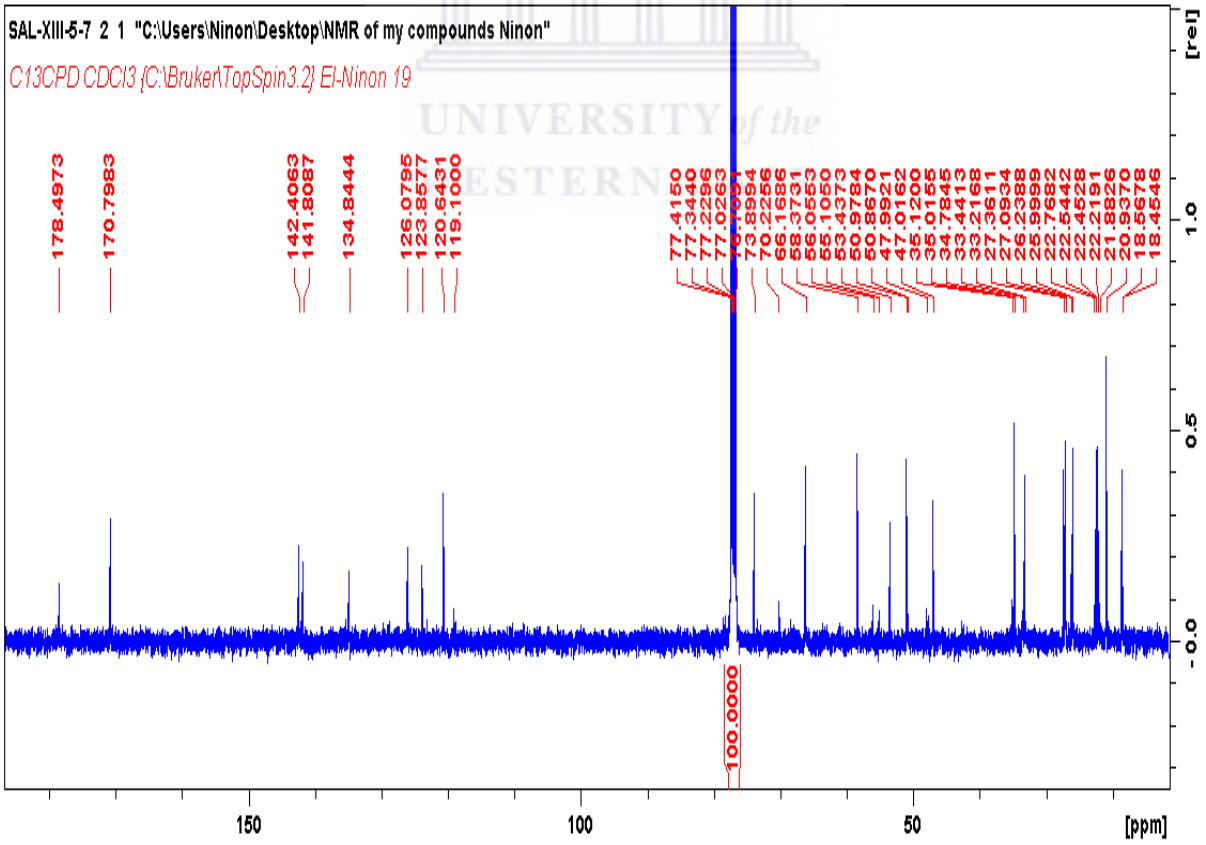

Figure 3.42: ^{13}C NMR (400 MHz, CDCl3) spectrum of **3**

https://etd.uwc.ac.za/

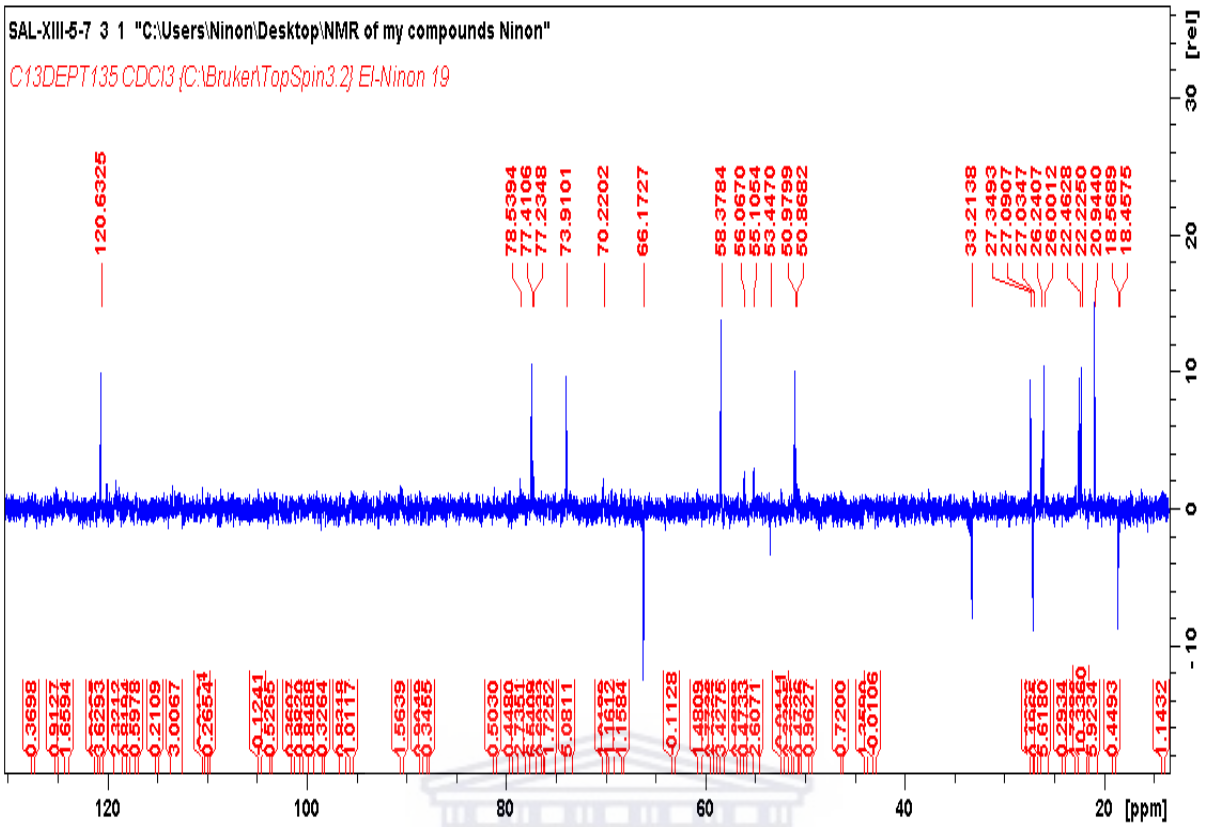

Figure 3.43: DEPT NMR (400 MHz, CDCl3) spectrum of **3**

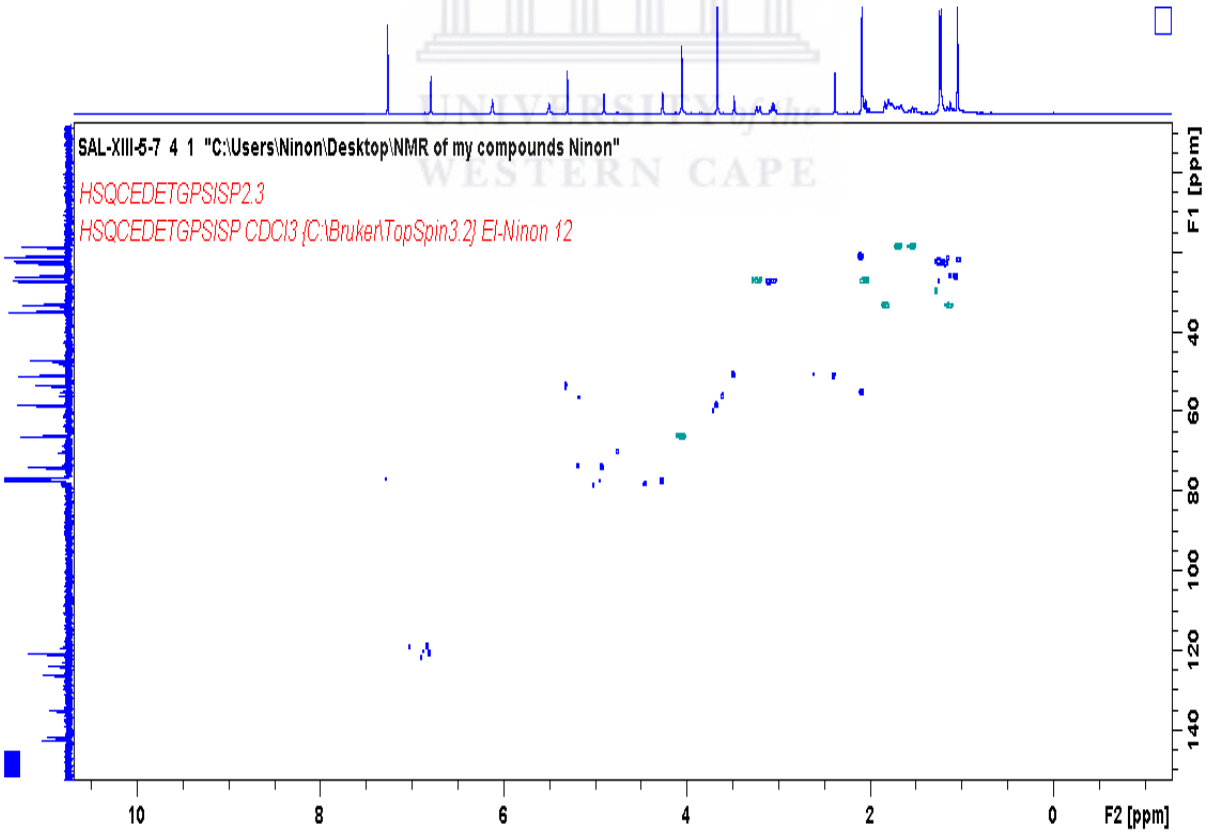

Figure 3.44: HSQC (400 MHz, CDCl3) spectrum of **3**

https://etd.uwc.ac.za/

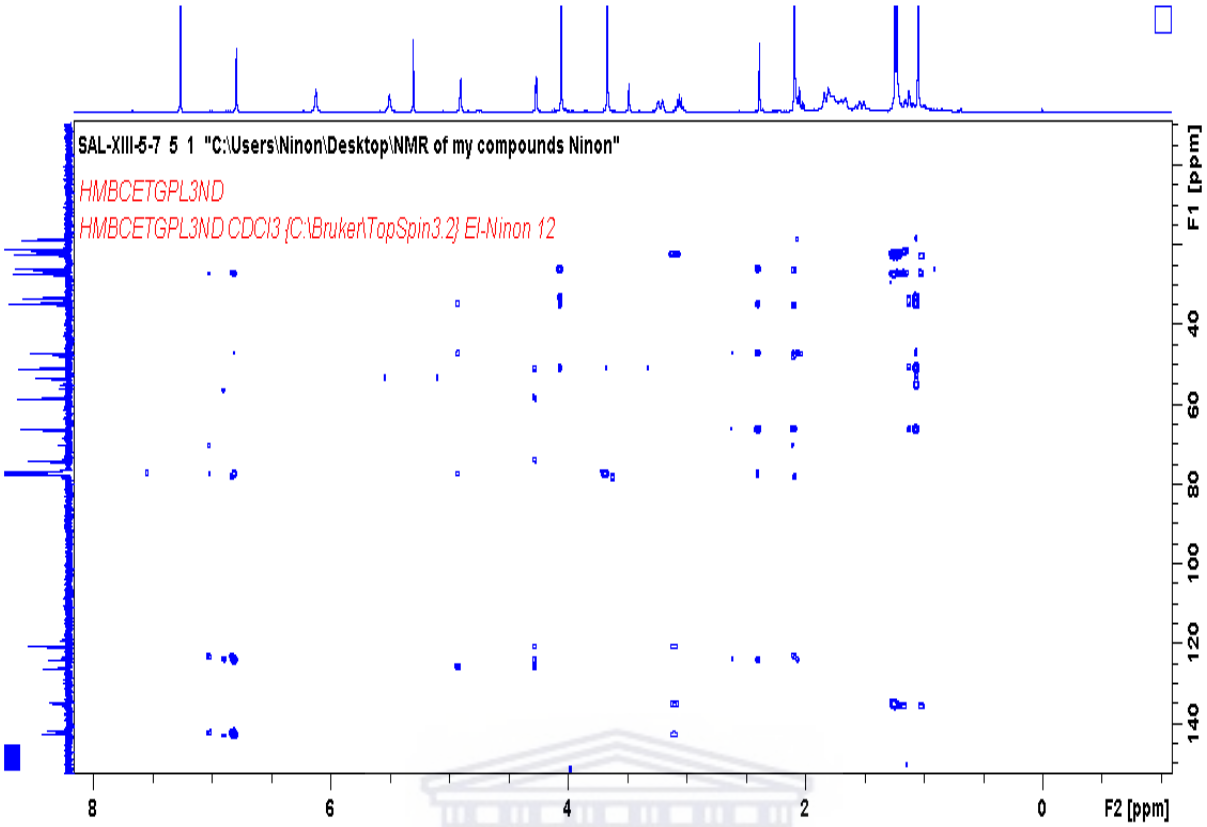

Figure 3.45: HMBC (400 MHz, CDCl3) spectrum of **3**

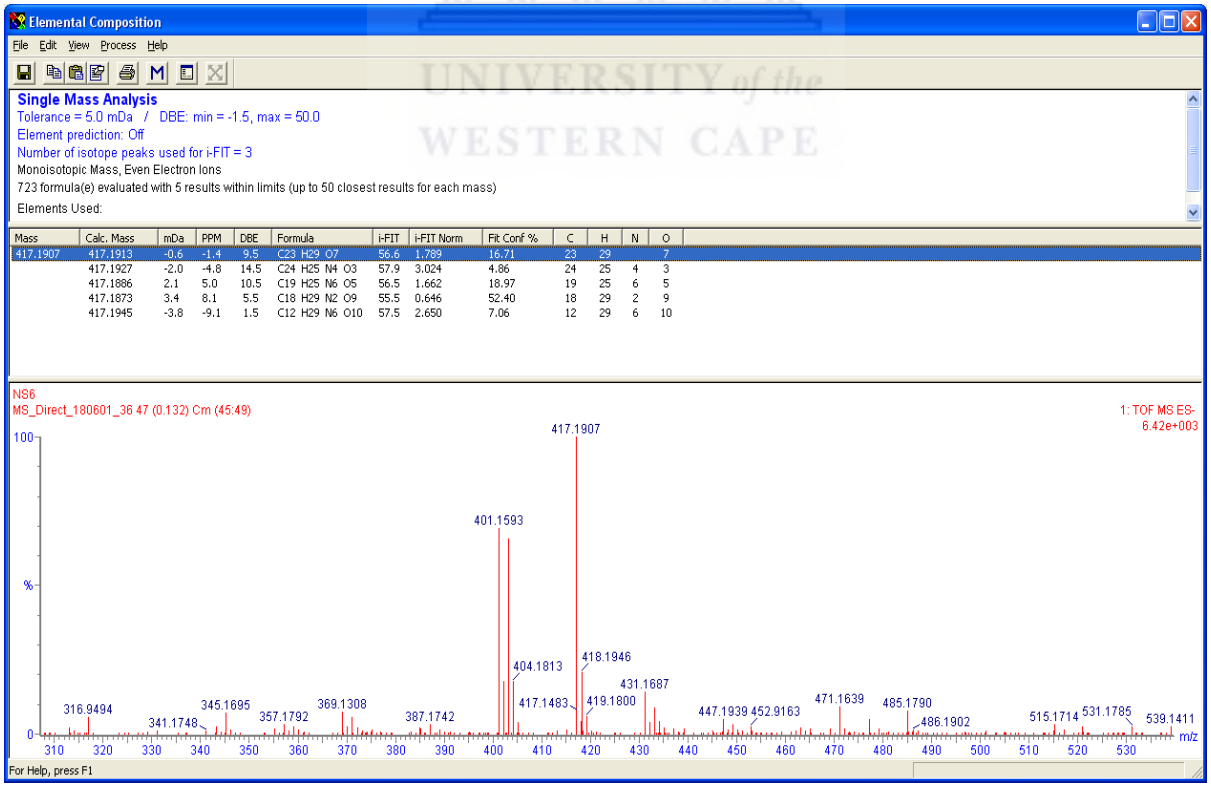

Figure 3.46: HRMS spectrum of **3**

https://etd.uwc.ac.za/

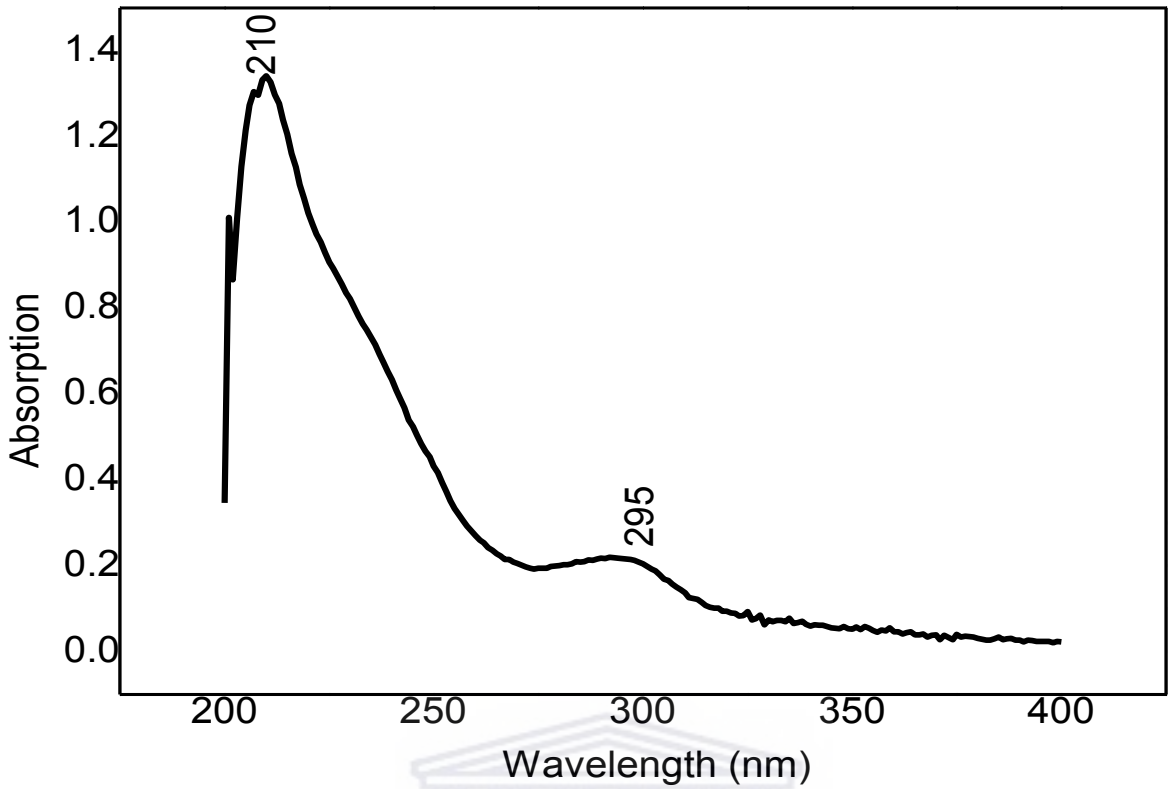

Figure 3.47: UV spectrum of **3**

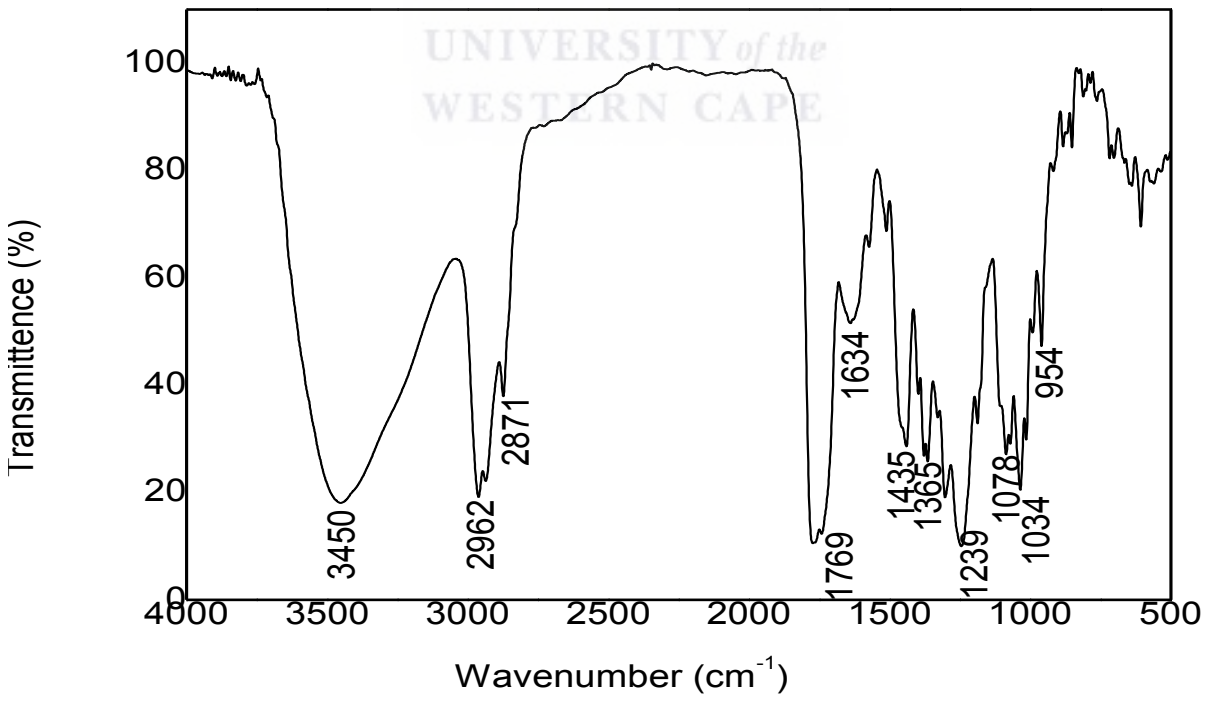

Figure 3.48: FTIR spectrum of **3**

https://etd.uwc.ac.za/

3.9.4 Structure elucidation of 19-acetoxy-12-methoxy carnosol (**4**)

Compound **4** was isolated as a yellow amorphous powder. The HRMS data indicated the molecular ion with a large peak at $[M]^+$ 417.1907 m/z suggesting a possible formula of $C_{23}H_{30}O_7$ (Fig. 3.56). The UV spectrum showed two peaks at 210 and 281 nm (Fig. 3.57). Its IR spectrum exhibited bands at 1750 cm^{-1} for an ester and 3330 cm^{-1} attributed to hydroxyl group (Fig. 3.58). The Raman spectrum featured characteristic bands at 1605 cm^{-1} related to C=C stretching, 1566 cm^{-1} (C-C stretching), 1412 cm^{-1} related to the deformation vibration of the CH_2, 1265 cm^{-1} related to C-H deformation in unconjugated cis-double bond, 1235 cm^{-1} related to the deformation of the hydroxyl group (O-H) (Fig. 3.59) (Belt, et al., 2017; Chain, et al., 2015; Raschi, et al., 2014). The NMR of **4** showed close similarity with carnosol and compounds **2** and **3** except the absence of C-6α(OH)/C-7α(OH) system and appearing C-20/C-7α lactone ring, in addition to a methoxy group and was located at C-12 as shown in Table 3.10. The HMBC spectra showed correlation between H6/C-7; C-5; C-4; C-8 and H7/C-6; C-8; C-13; C-9. Other 2D data confirmed the structure of **4** as 19-acetoxy-12-methoxy carnosol (Etsassala, et al., 2019).

UNIVERSITY of the
WESTERN CAPE

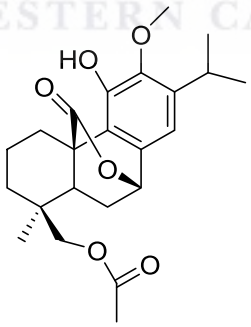

19-acetoxy-12-methoxy carnosol

Figure 3.49: Chemical structure of **4**

https://etd.uwc.ac.za/

Table 3.10: ^{1}H and ^{13}C NMR spectroscopic data assignments (400 MHz) for compound **4** (δ in ppm, m, *J* in Hz) in $CDCl_3$

	4		
N^{O}	δ_H (*J* in Hz)	^{13}C	Multiplicity
1	3.22 d (6.2) 1.64 dd (2.4)	28.3	CH_2
2	1.40 d (4.3)	20.9	CH_2
3	3.28 d (5.2) 1.64 d (5.6)	28.3	CH_2
4		45.0	C
5	1.91 d (2.9)	51.8	CH
6	1.37 d (4.8) 1.92 m	21.0	CH
7	4.6 d (3.3)	78.7	CH
8		133.7	C
9		119.1	C
10		44.0	C
11		147.9	C
12		143.0	C
13		140.2	C
14	6.54 s	117.8	CH
15	3.22 sept (6.9)	26.5	CH
16	1.21*	22.7	CH_3
17	1.22*	23.5	CH_3
18	1.19 s	25.5	CH_3
19	4.16 d (11.6) 4.24 d (11.1)	65.7	CH_2
20		174.3	C
$\underline{COO}CH_3$		170.9	C
$COO\underline{CH_3}$	2.08 s	20.9	CH_3
OCH_3	3.76 s	61.9	CH_3

UNIVERSITY of the WESTERN CAPE

https://etd.uwc.ac.za/

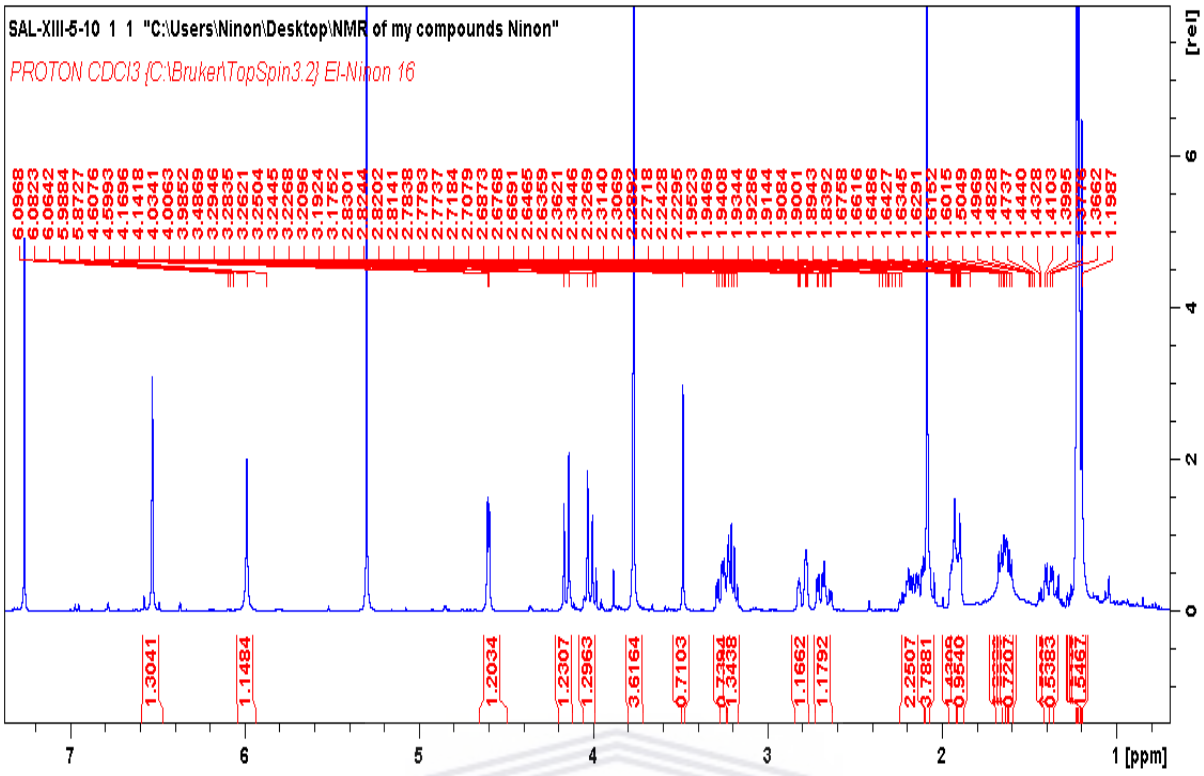

Figure 3.50: ^{1}H NMR (400 MHz, CDCl3) spectrum of **4**

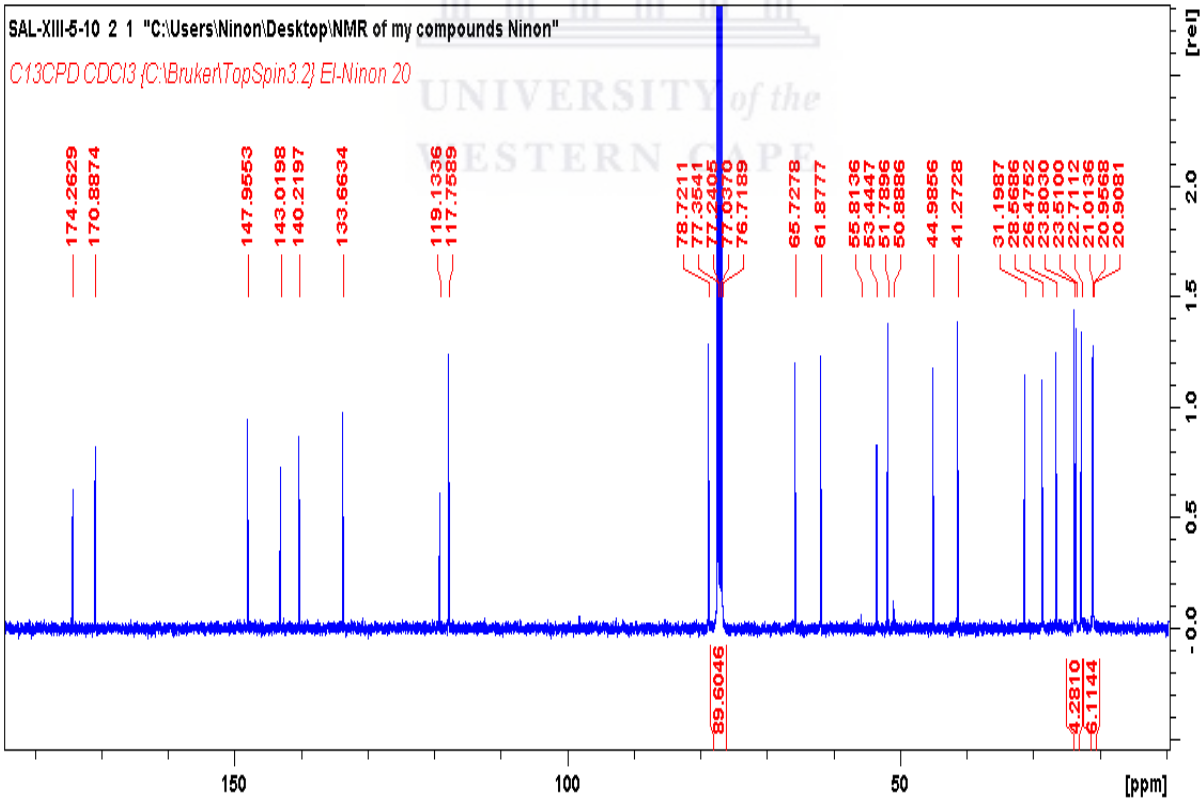

Figure 3.51: ^{13}C NMR (400 MHz, CDCl3) spectrum of **4**

https://etd.uwc.ac.za/

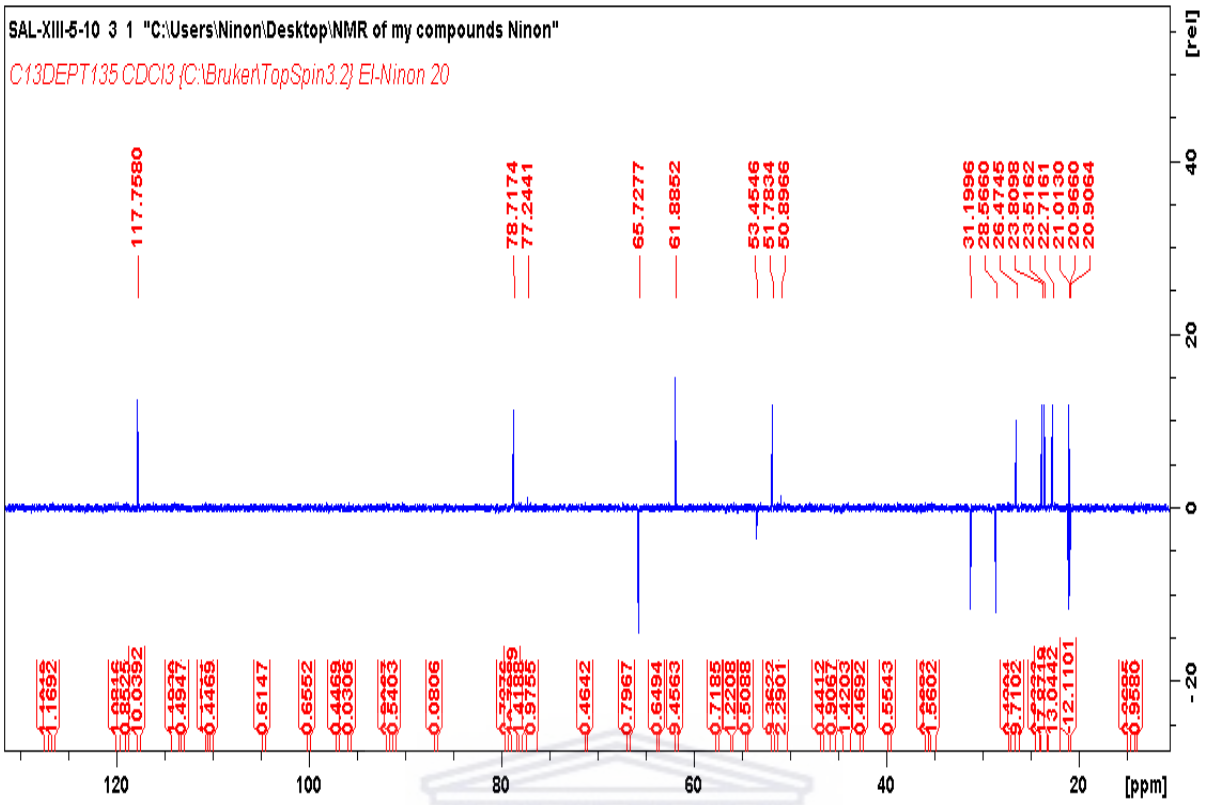

Figure 3.52: DEPT NMR (400 MHz, CDCl3) spectrum of **4**

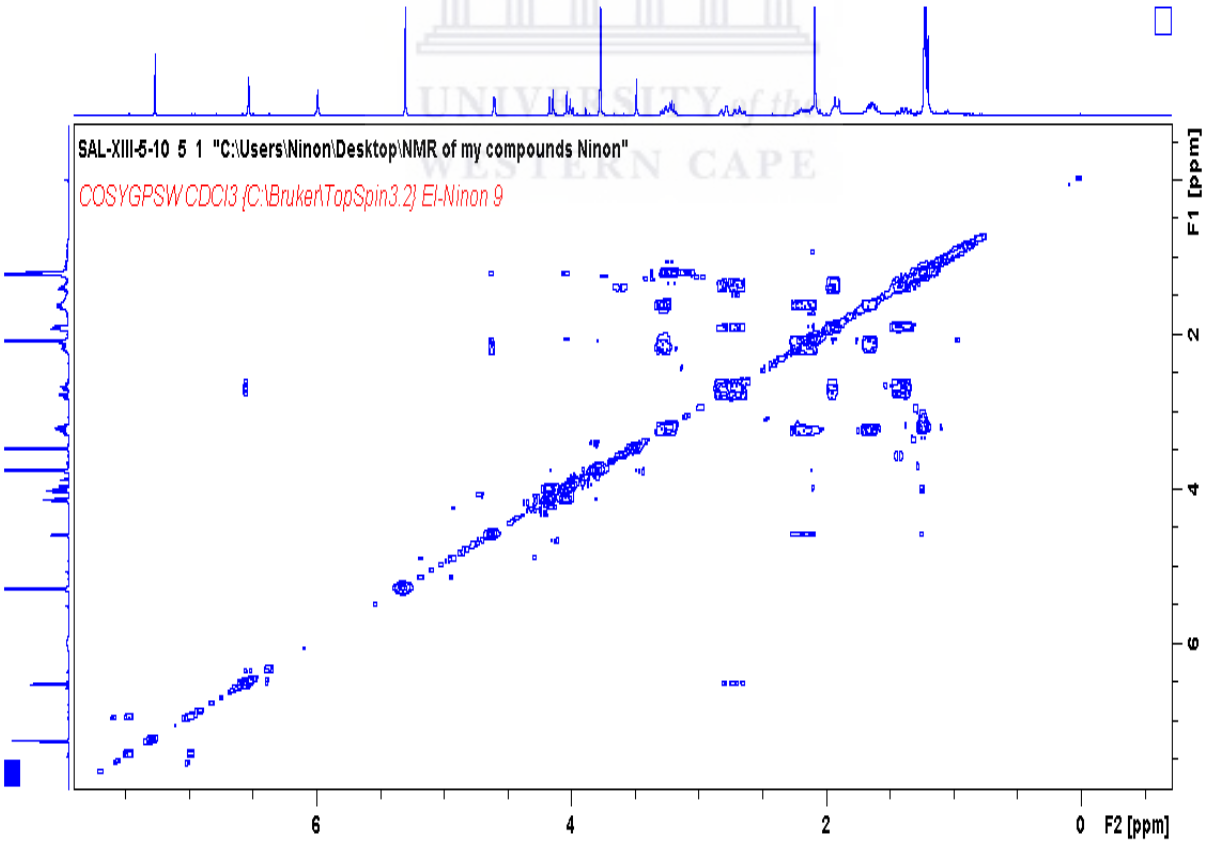

Figure 3.53: COSY (400 MHz, CDCl3) spectrum of **4**

https://etd.uwc.ac.za/

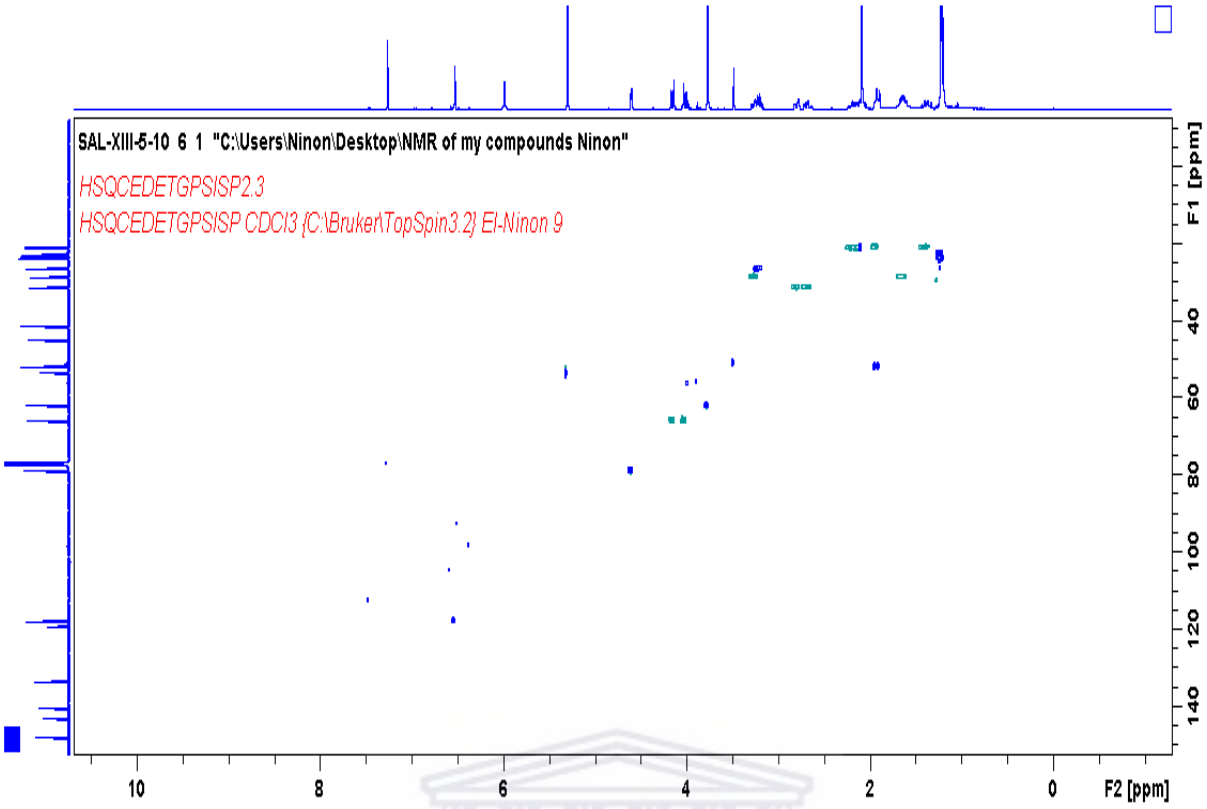

Figure 3.54: HSQC (400 MHz, CDCl3) spectrum of **4**

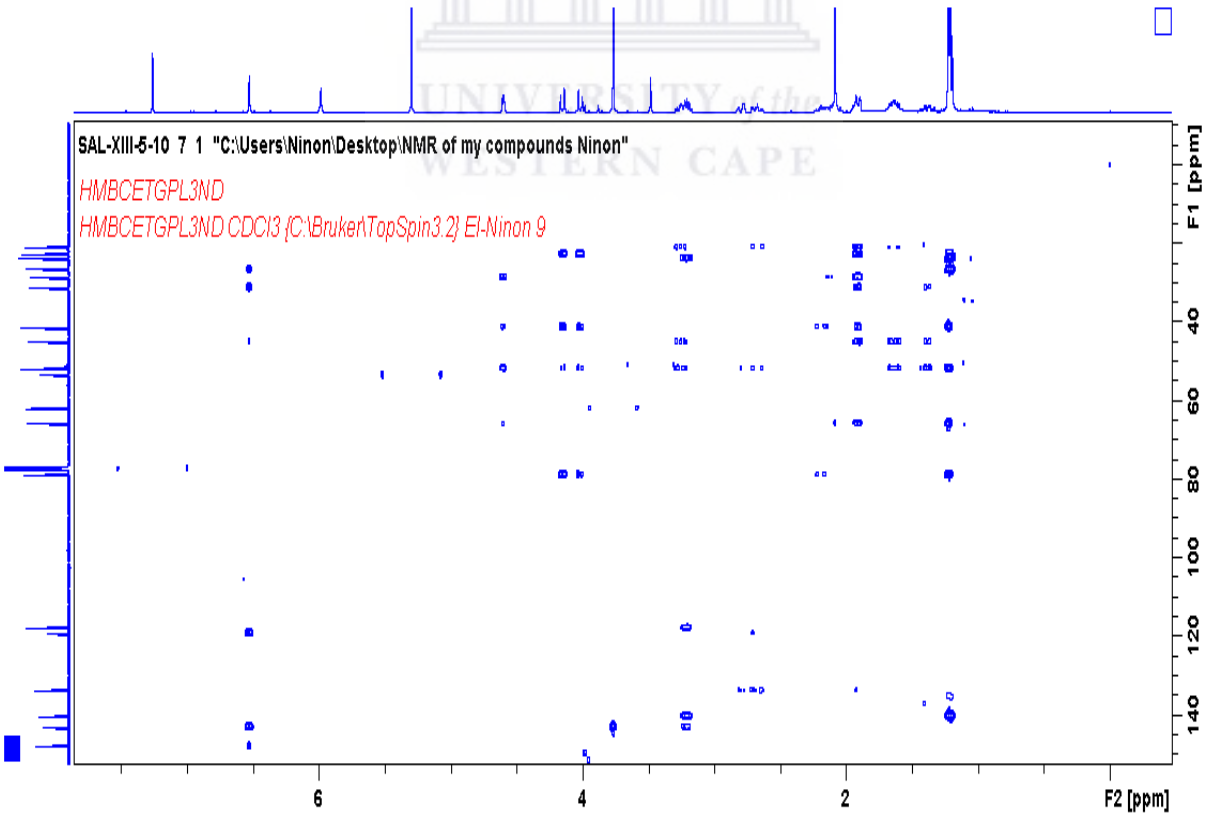

Figure 3.55: HMBC (400 MHz, CDCl3) spectrum of **4**

https://etd.uwc.ac.za/

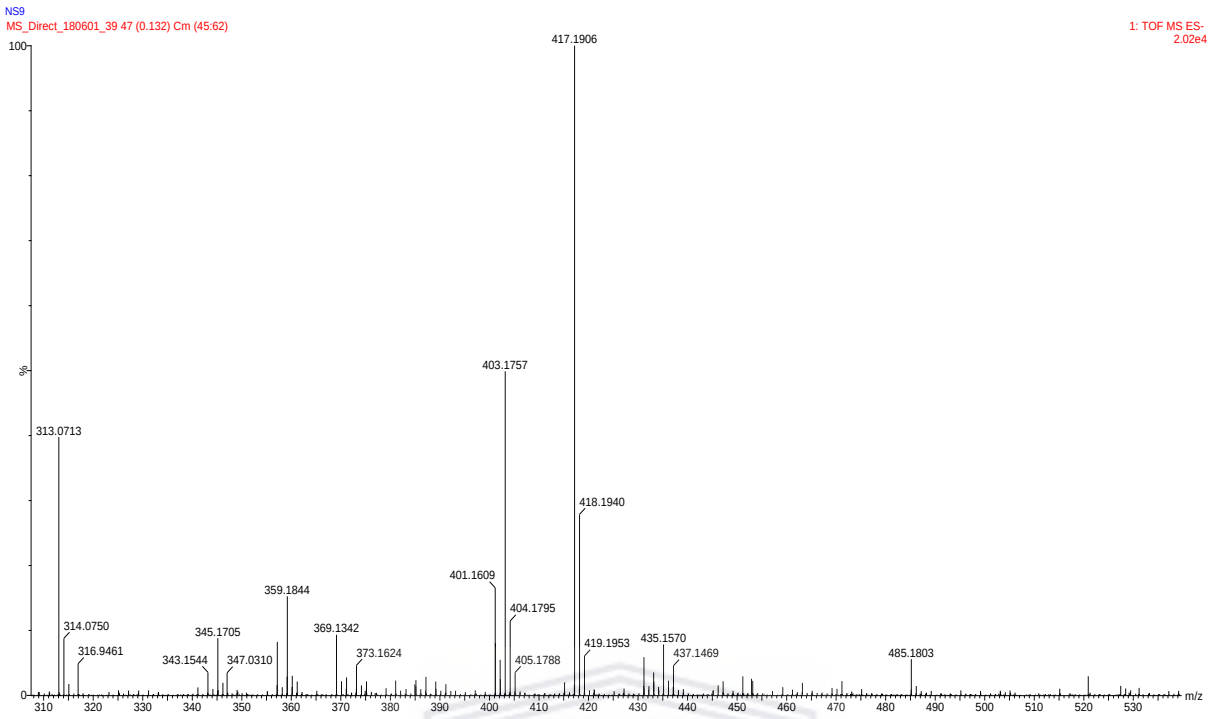

Figure 3.56: HRMS spectrum of **4**

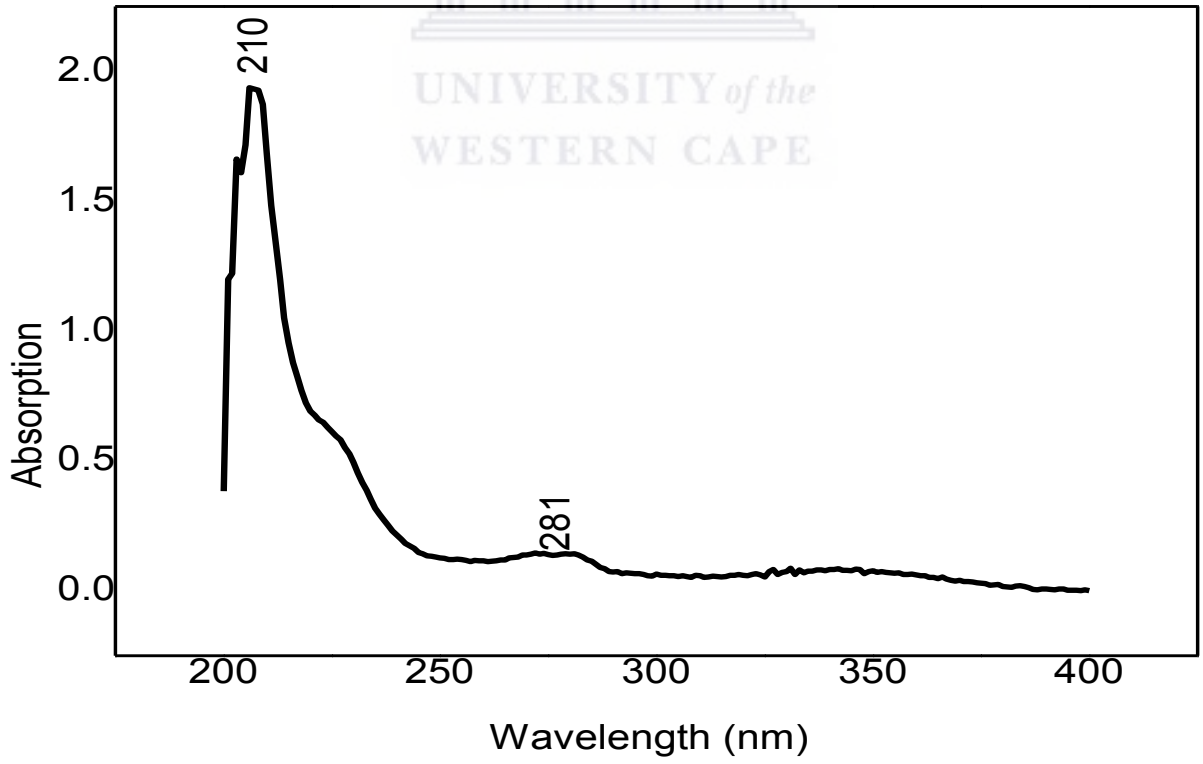

Figure 3.57: UV spectrum of **4**

UNIVERSITY of the WESTERN CAPE
https://etd.uwc.ac.za/

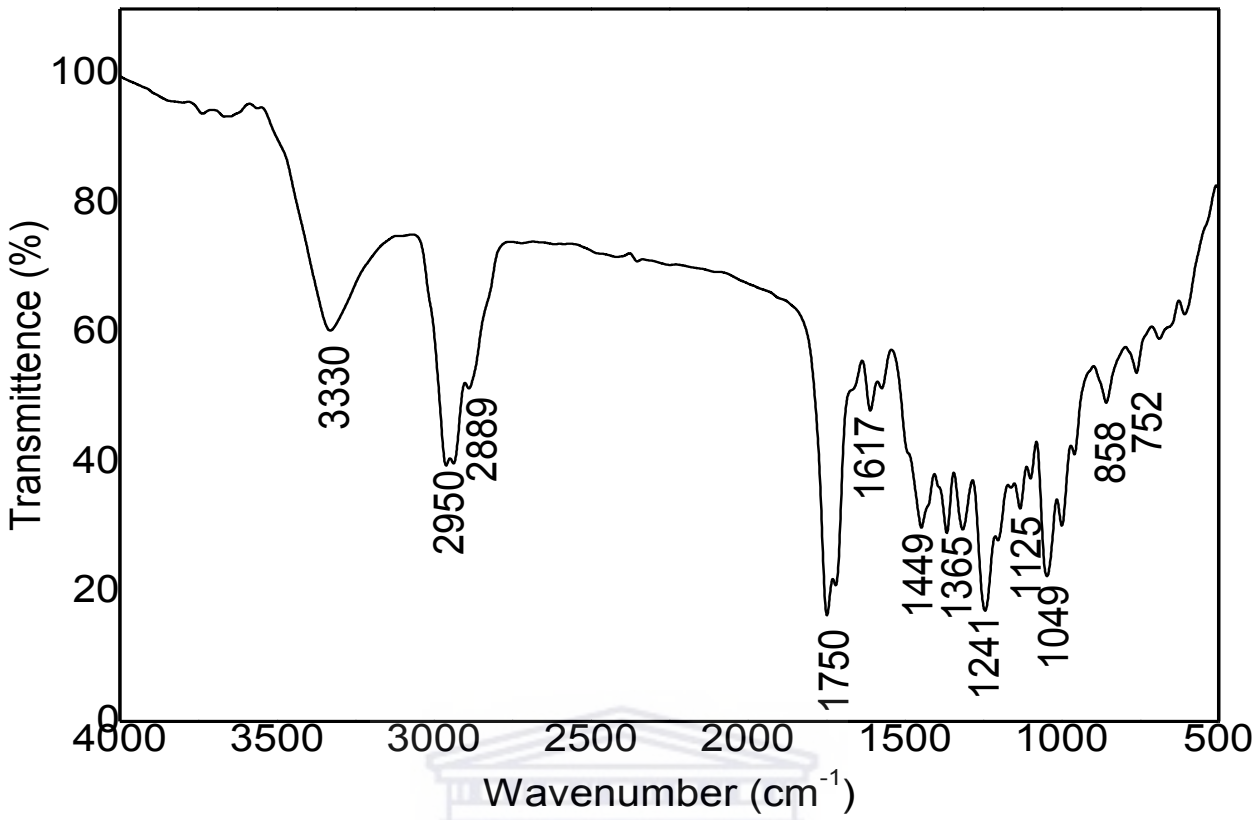

Figure 3.58: FTIR spectrum of **4**

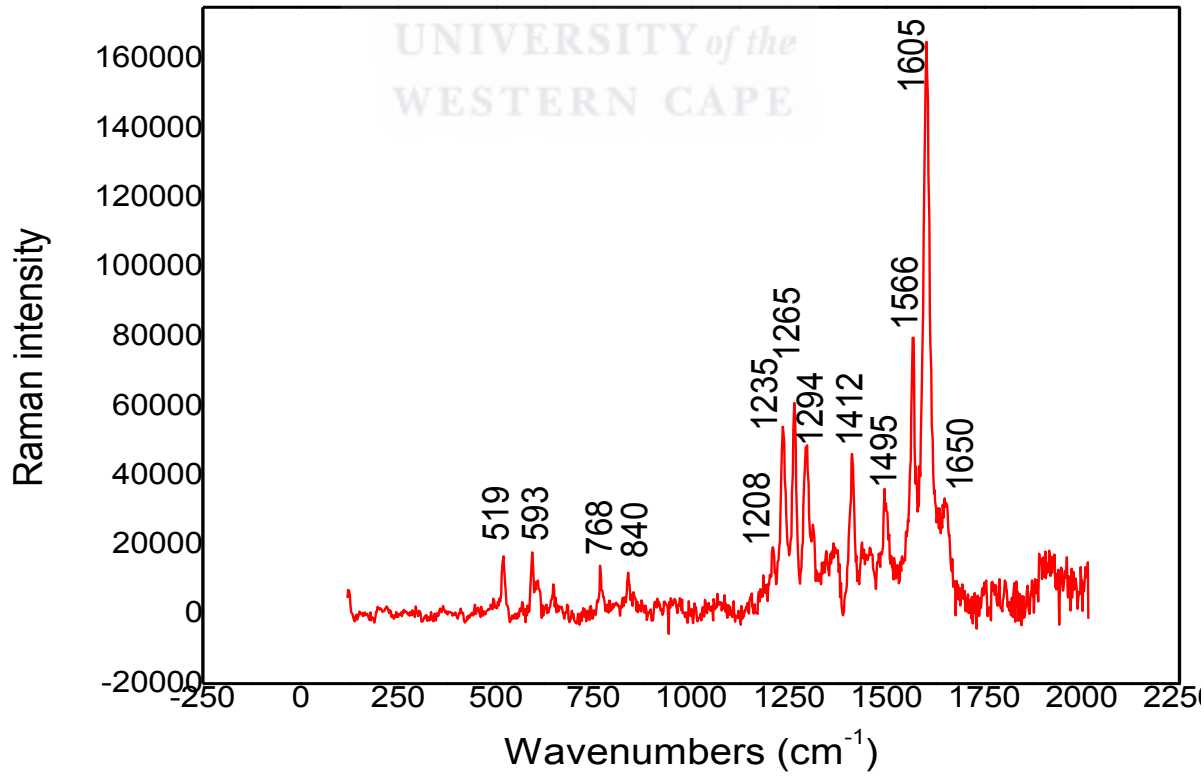

Figure 3.59: Raman spectrum of **4**

https://etd.uwc.ac.za/

RAMAN	Intensity	Assignments
519	w	Deformation ring
593	w	C-C-O deformation
768	w	Skeletal vibration
840	w	CH_2 torsion
1235	n	O-H deformation
1265	n	C-H deformation
1294	n	CH_2/CH_3 deformation
1412	n	CH_2 deformation
1495	n	CH_3 deformation
1566	n	C-C stretching
1605	s	C=C stretching
1650	w	C=C stretching

3.9.5 Structure elucidation of clinopodiolide A (**5**)

Compound 5 was isolated as a white powder. The HRMS data indicated an ion peak at 345.1694 *m/z* corresponding to $[M]^+$ suggesting the molecular chemical formula of $C_{20}H_{28}O_6$ (Fig. 3.68). The UV spectrum showed two peaks at 208 and 284 nm (Fig. 3.69). Its IR spectrum exhibited bands at 1675 cm^{-1} for an ester as well as at 3500 and 3210 cm^{-1} attributed to hydroxyl groups (Fig. 3.70). The Raman spectrum featured characteristic bands at 1688 and 1618 cm^{-1} related to C=C stretching, 1578 cm^{-1} (C-C stretching), 1449 cm^{-1} related to the deformation vibration of the CH_2, 1358 cm^{-1} related to the CH_3 bond vibrations, 1314 cm^{-1} (CH_2 wagging), 1195 cm^{-1} (C-C-O stretching), 1109 cm^{-1} and 1002 (C-C aromatic ring), 986 and 822 cm^{-1} (C-H deformation) (Fig 3.71) (Belt, et al., 2017; Chain, et al., 2015; Raschi, et al., 2014). The NMR spectra of **5** (Table 3.11) showed similar signals to compound **1**, the difference between them is the absence of the acetoxyl and methoxy1 groups and the appearance of dihydroxy-carbon signal at 102.8 (C-19) attached to a singlet proton at 5.61, which form the lactone group with the carbon at position C-20 (180.0). In particular, the HMBC showed correlations between a proton at 5.61 (H-19) and the C-20 (180.0)/C-4 (37.0)/C-5 (50.3). Other 2D spectra in comparison with literature data confirmed the structure of **5** as clinopodiolide A. The occurrence of the lactol moety at C-19-C-20 is very unusual in nature and it has been recently isolated for the first time from *Salvia clinopodioide* (Bustos-

https://etd.uwc.ac.za/

brito, et al., 2019). This is the first report on the isolation of clinopodiolide A from *S. africana lutea.*

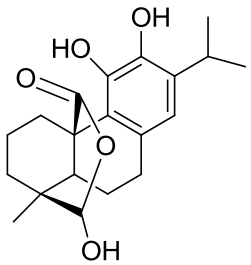

Clinopodidlide A

Figure 3.60: Chemical structure of **5**

Table 3.11: ^{1}H and ^{13}C NMR spectroscopic data assignments (400 MHz) for compound **5** (δ in ppm, m, *J* in Hz) in $CDCl_3$

	5		
N^{O}	δ_H (*J* in Hz)	^{13}C	Multiplicity
1	3.34 m 1.47 d (13.2)	35.4	CH_2
2	1.74 m	21.2	CH_2
3	2.3 m, 1.47 d (5.7)	32.5	CH_2
4		37.0	C
5	3.51 s	50.3	CH
6	2.11 d (2.3) 1.31 d (5.7)	21.6	CH_2
7	2.77 m	30.7	CH_2
8		122.3	C
9		128.0	C
10		49.8	C
11		143.4	C
12		142.1	C
13		133.9	C
14	6.55 s	118.9	CH
15	3.24 sept (6.9)	27.2	CH
16	1.12*	22.3	CH_3
17	1.21*	24.1	CH_3
18	1.15 s	24.1	CH_3
19	5.61 s	102.8	CH
20		180.0	C

UNIVERSITY of the WESTERN CAPE

https://etd.uwc.ac.za/

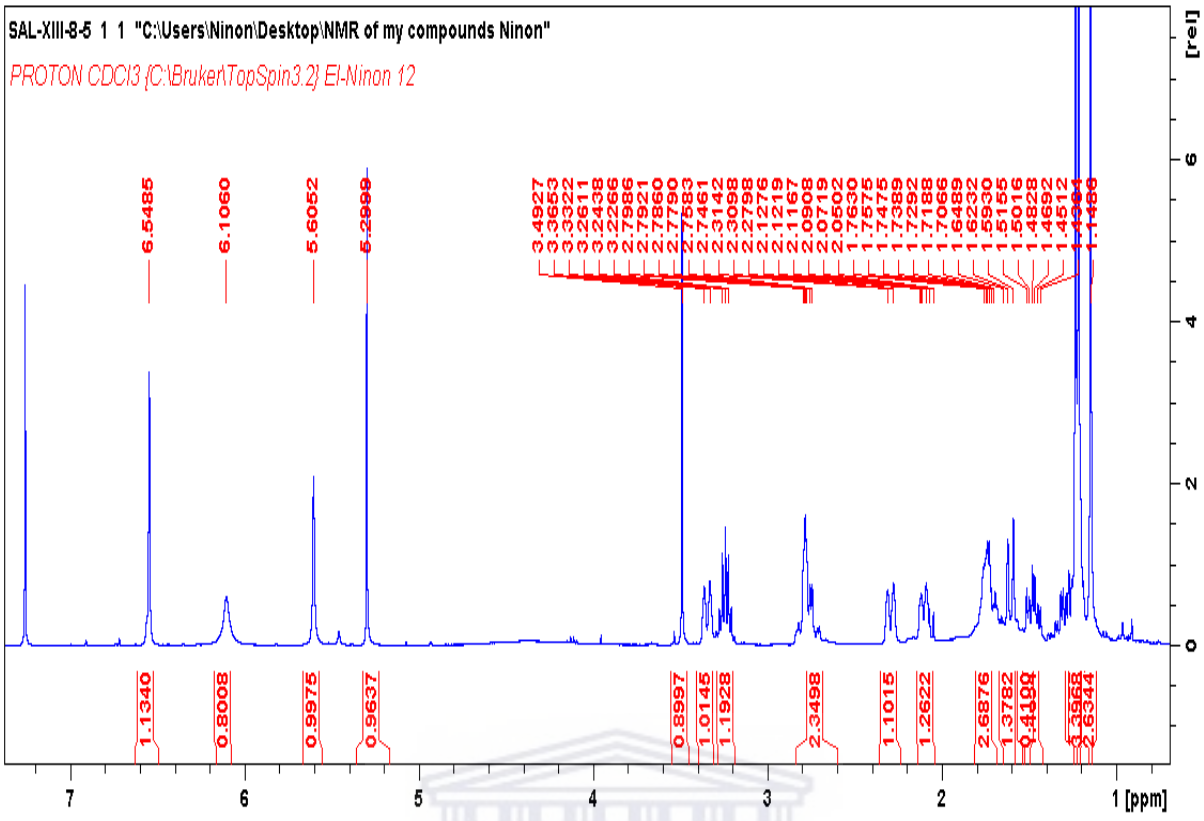

Figure 3.61: ^{1}H NMR (400 MHz, CDCl3) spectrum of **5**

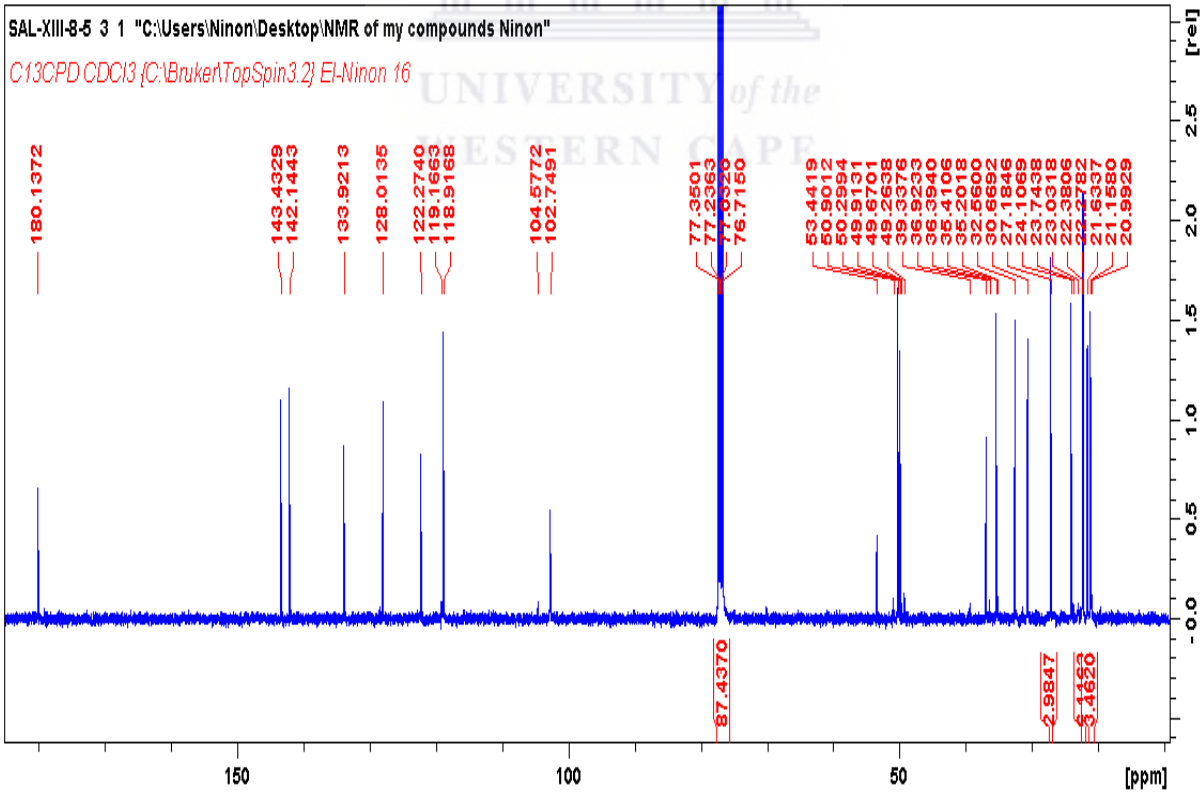

Figure 3.62: ^{13}C NMR (400 MHz, CDCl3) spectrum of **5**

https://etd.uwc.ac.za/

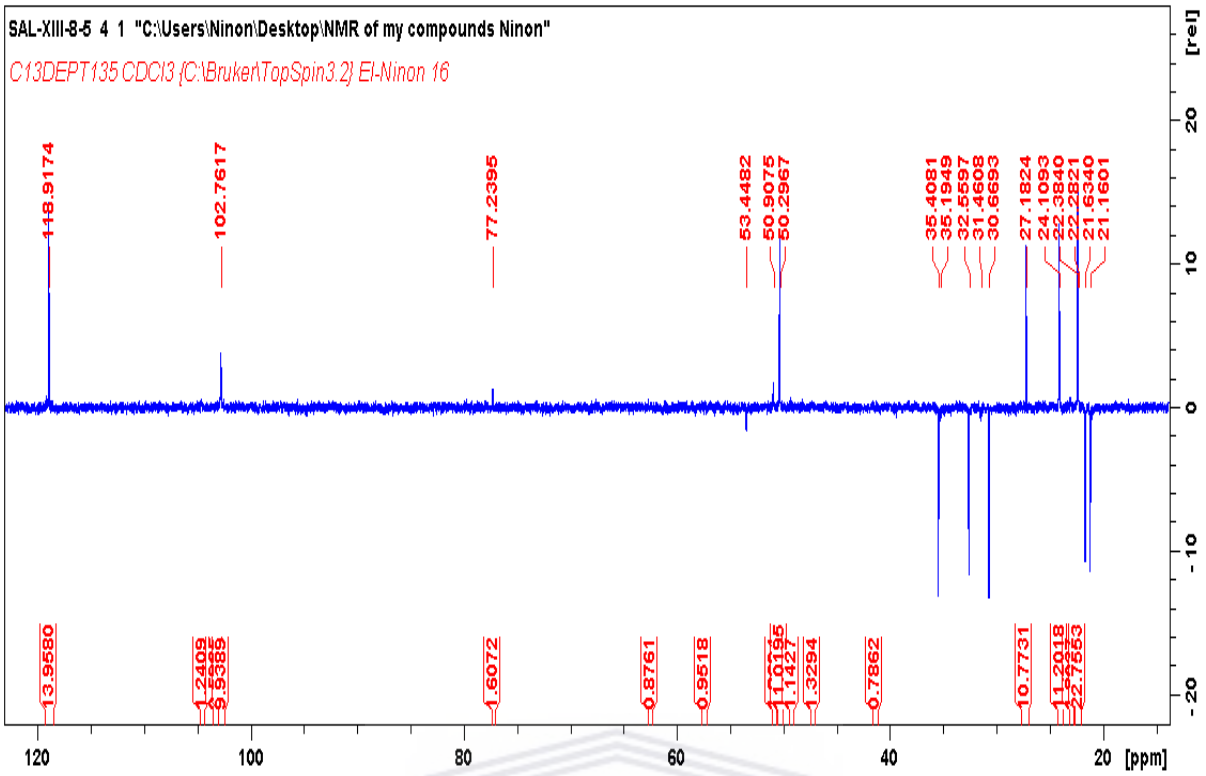

Figure 3.63: DEPT NMR (400 MHz, CDCl3) spectrum of **5**

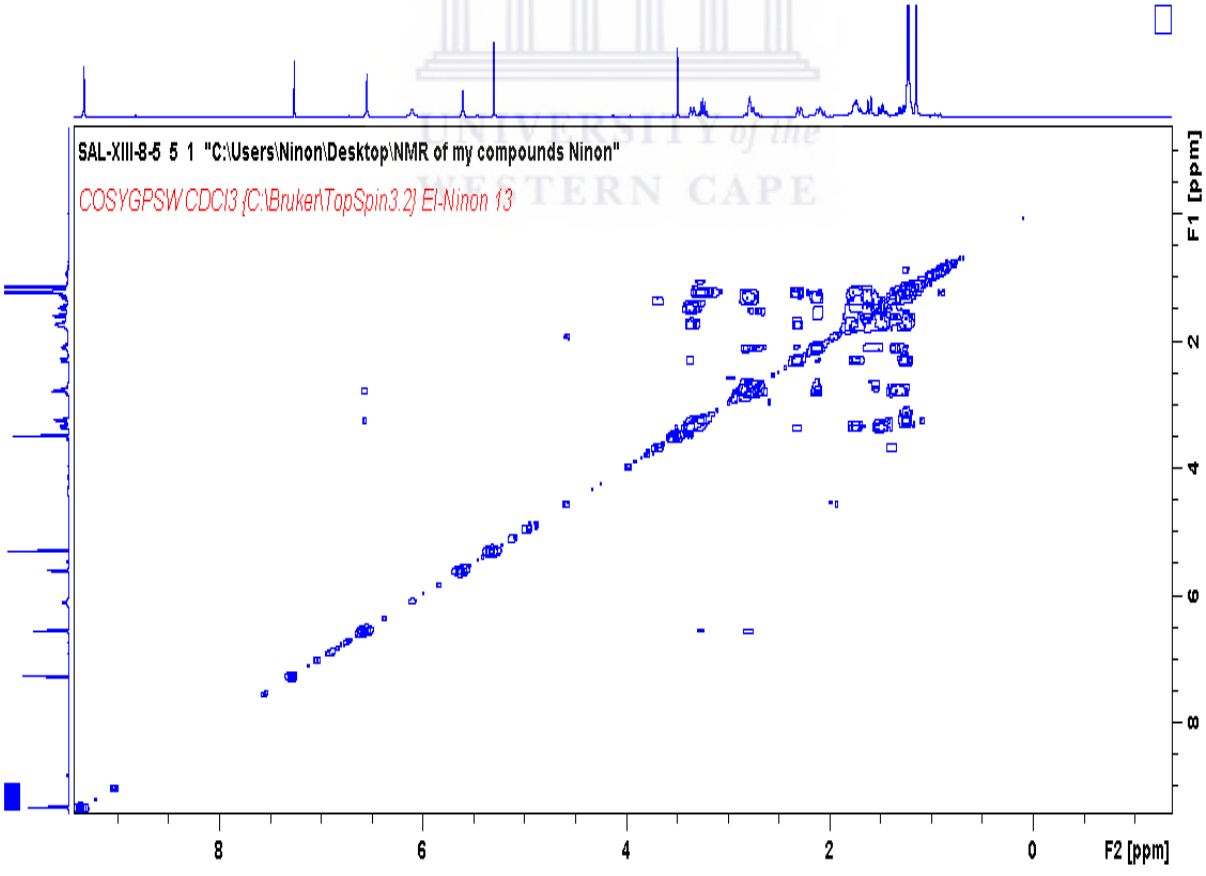

Figure 3.64: COSY (400 MHz, CDCl3) spectrum of **5**

https://etd.uwc.ac.za/

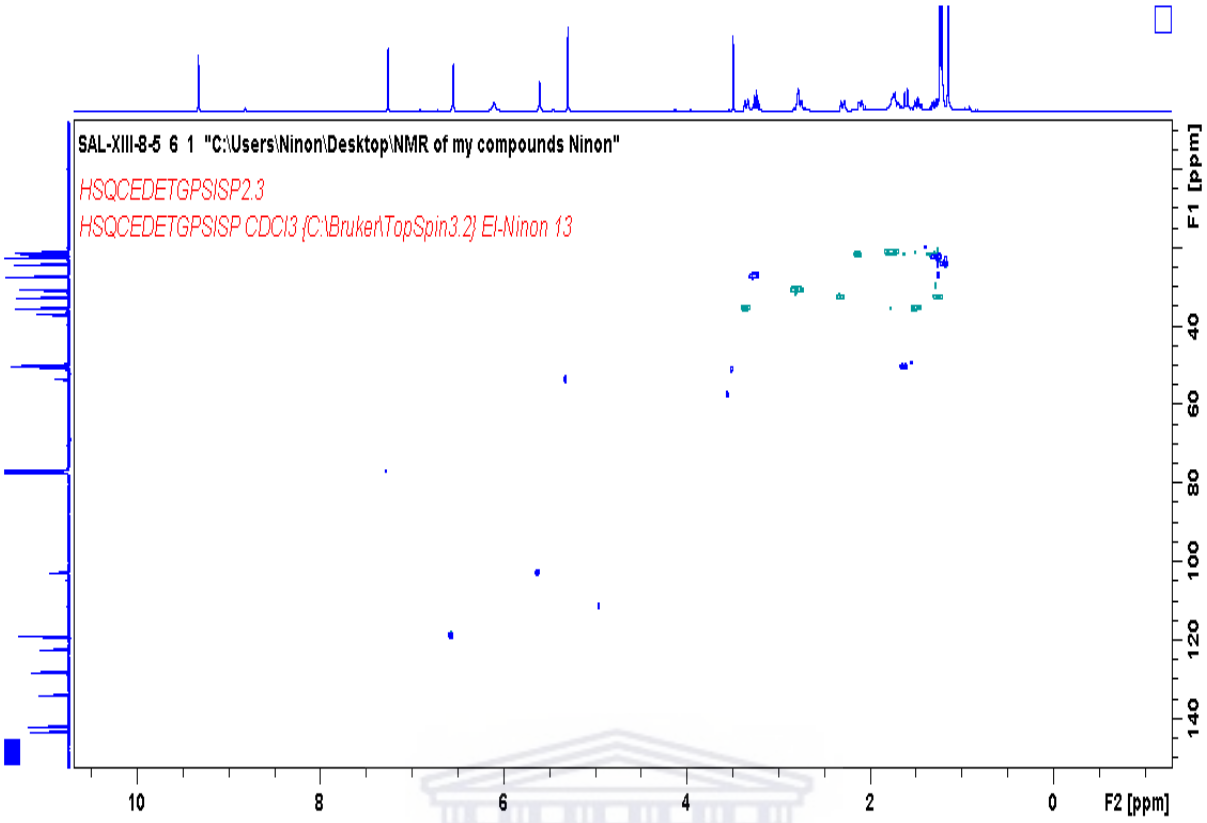

Figure 3.65: HSQC (400 MHz, CDCl3) spectrum of **5**

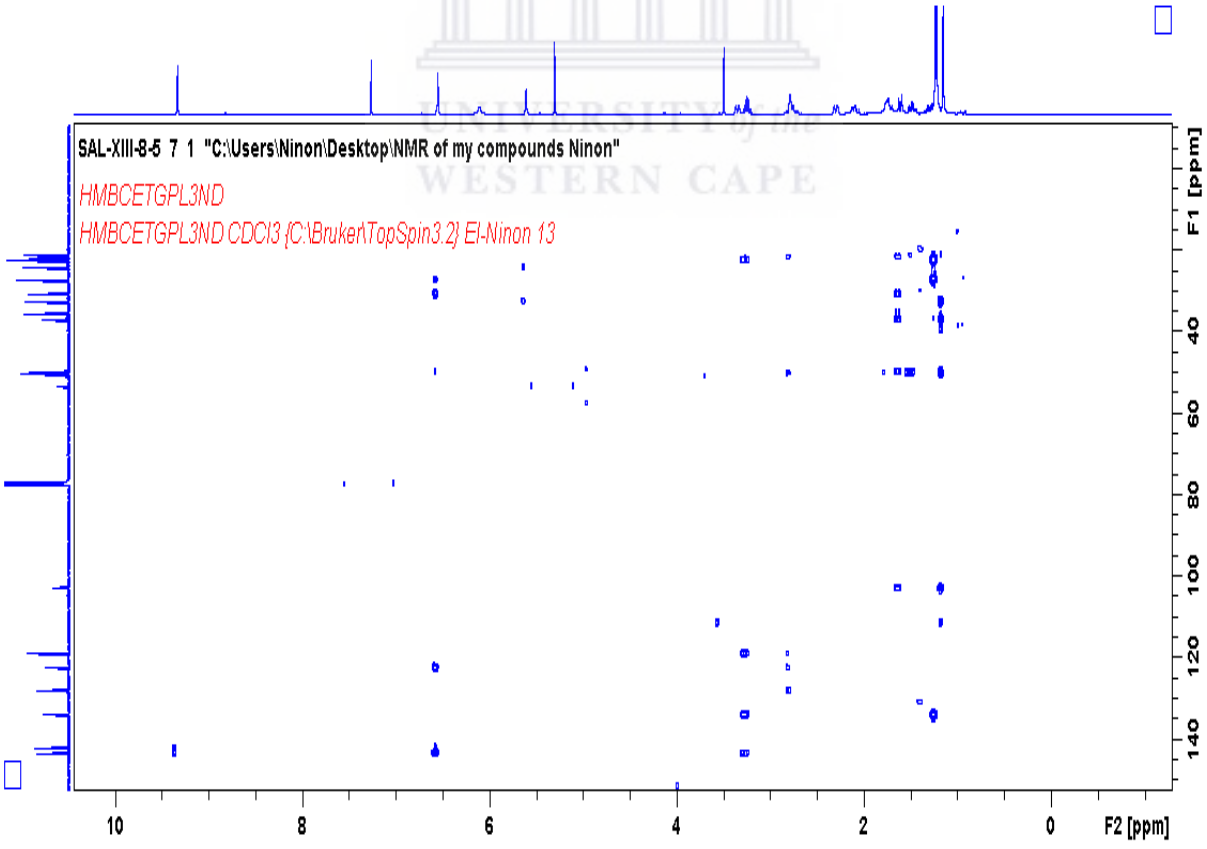

Figure 3.66: HMBC (400 MHz, CDCl3) spectrum of **5**

https://etd.uwc.ac.za/

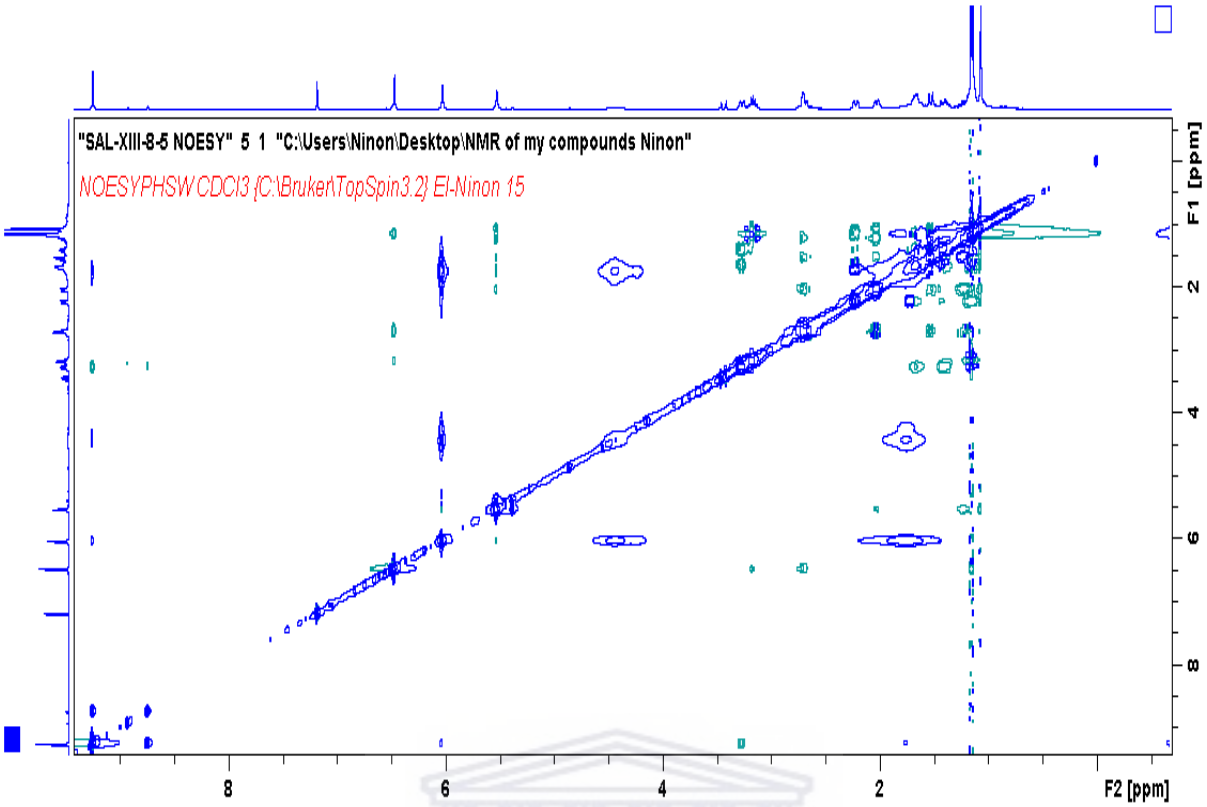

Figure 3.67: NOESY (400 MHz, CDCl3) spectrum of **5**

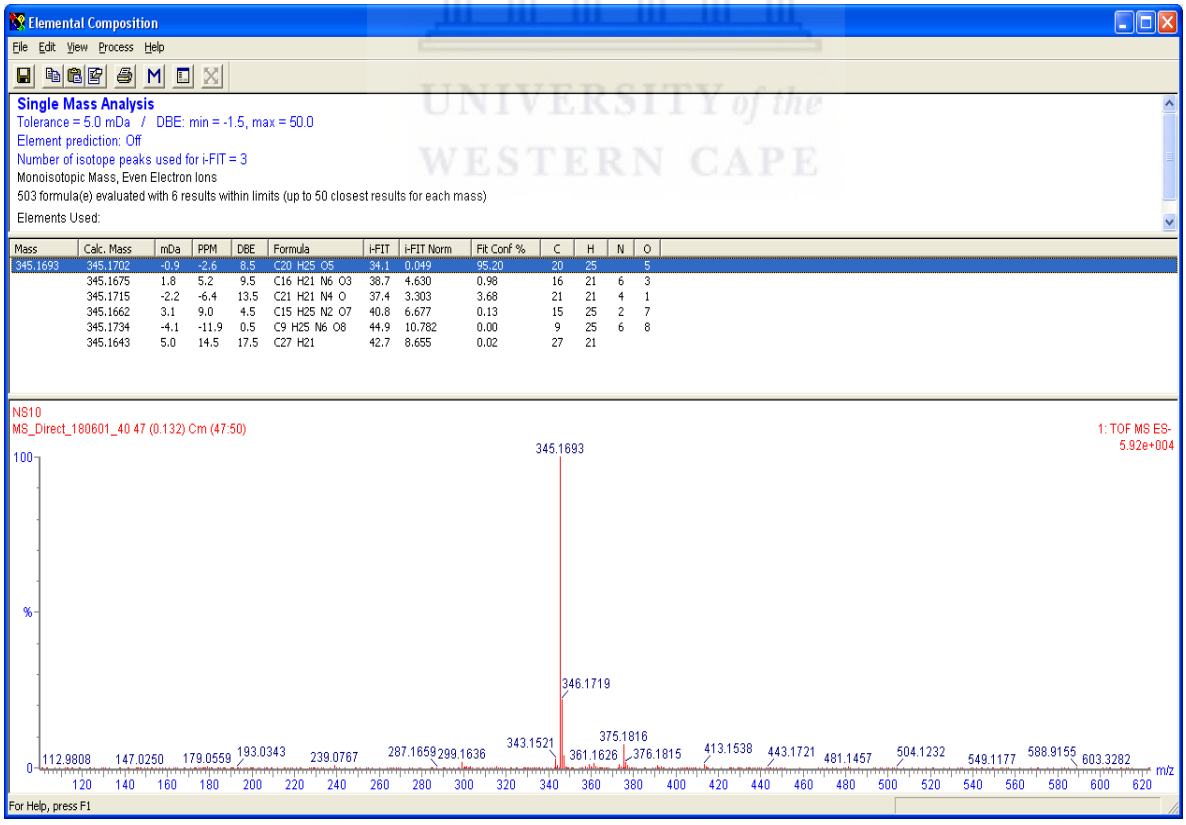

Figure 3.68: HRMS spectrum of **5**

https://etd.uwc.ac.za/

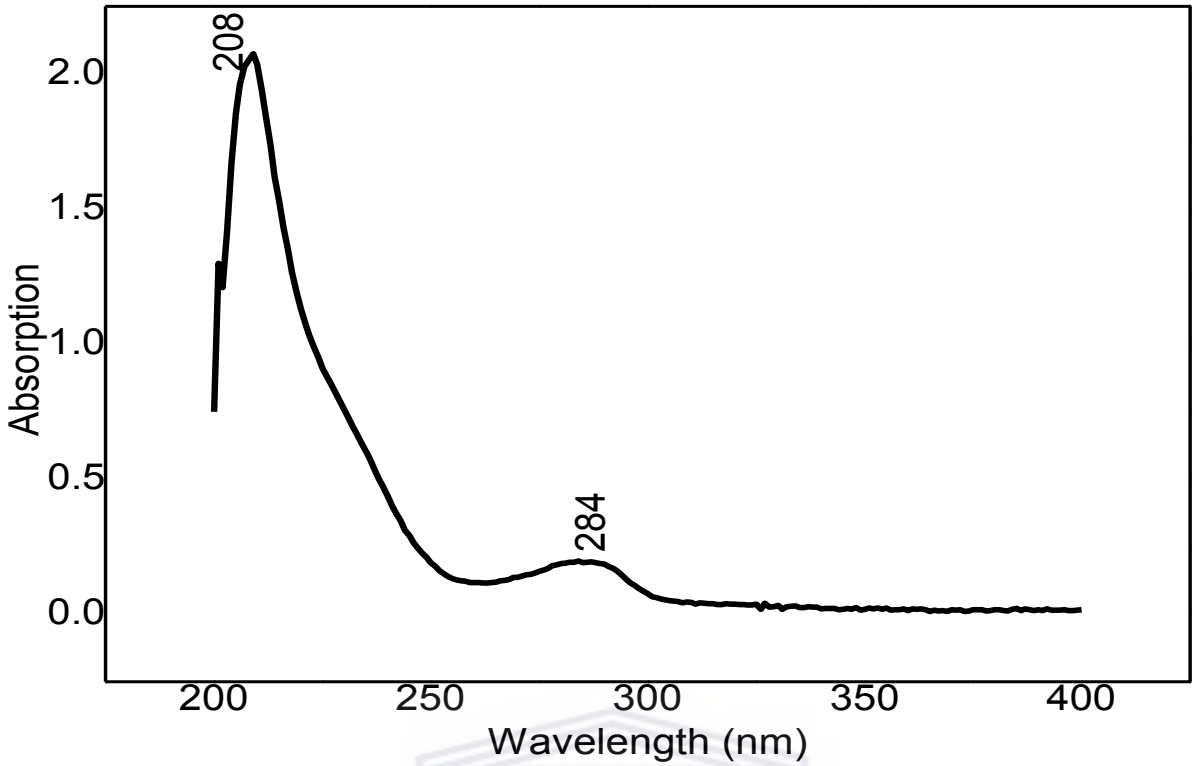

Figure 3.69: UV spectrum of **5**

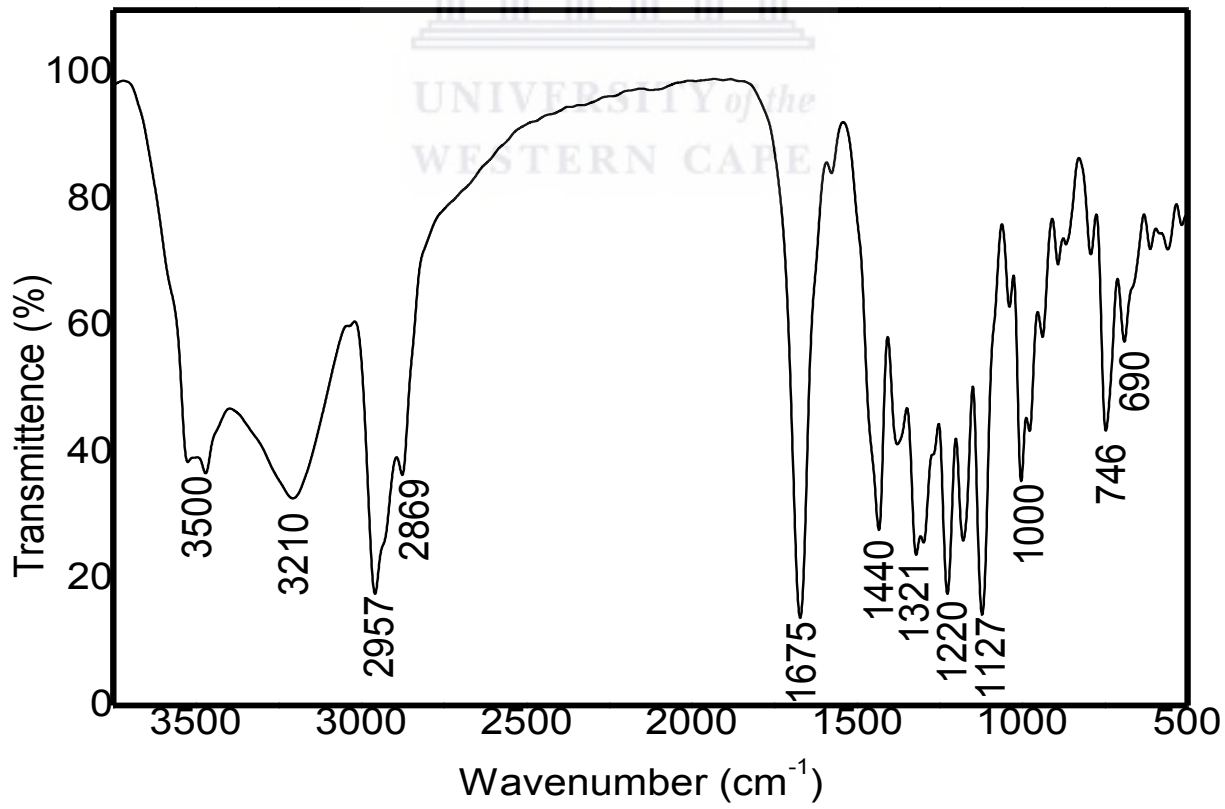

Figure 3.70: FTIR spectrum of **5**

https://etd.uwc.ac.za/

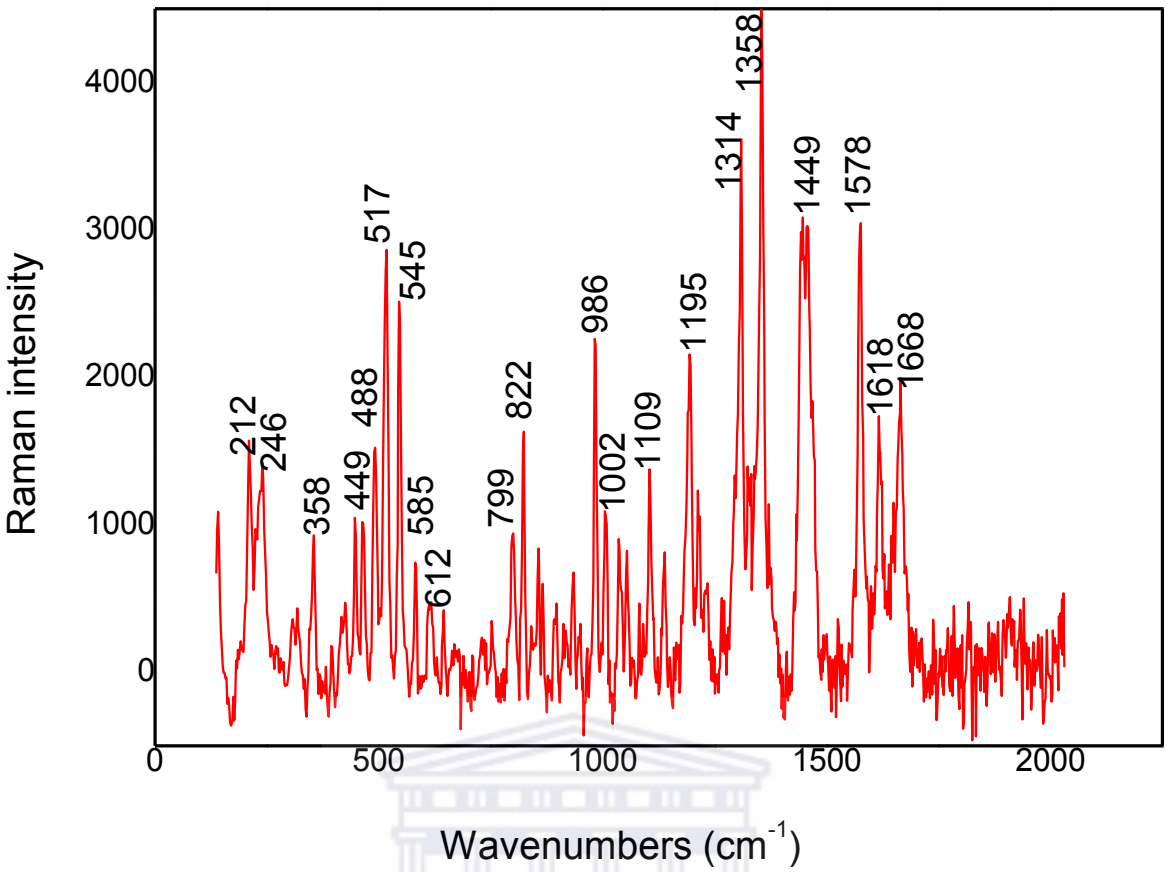

Figure 3.71: Raman spectrum of **5**

RAMAN	Intensity	Assignment
212	w	C-C-C deformation
246	w	C-C-C deformation
517	n	C-C-C deformation
545	n	C-C-O deformation
822	n	C-H deformation
986	n	C-H deformation
1002	w	C-C aromatic ring
1109	w	C-C aromatic ring
1195	n	C-C-O stretching
1314	s	CH_2 wagging
1358	s	CH_2 wagging
1449	s	CH3/CH_2 deformation
1578	s	C-C stretching
1618	n	C=C stretching
1688	n	C=C stretching

https://etd.uwc.ac.za/

3.9.6 Structure elucidation of clinopodiolide B (**6**)

Compound 6 was isolated as a grey powder. The The HRMS data indicated the molecular ion with a large ion peak at 359.1864 *m*/*z* corresponding to $[M]^+$ suggesting the molecular chemical formula of $C_{21}H_{27}O_6$ (Fig. 3.78). The UV spectrum showed two peaks at 211 and 282 nm (Fig. 3.79). Its IR spectrum exhibited bands at 1678 cm^{-1} for an ester as well as at 3375 cm^{-1} and 3212 cm^{-1} attributed to hydroxyl groups (Fig. 3.80). The Raman spectrum featured characteristic bands at 1612 related to C=C stretching, 1562 cm^{-1} related to C-C stretching, 1466 and 1449 cm^{-1} related to the deformation vibration of the CH_2/CH_3, 1308 cm^{-1} (CH_2 wagging), 1038 and 1031 cm^{-1} attributed to C-C aromatic ring, 562 cm^{-1} related to the deformation of C-C-O (Fig. 3.81) (Belt, et al., 2017; Chain, et al., 2015; Raschi, et al., 2014). The NMR signals of **6** showed typical NMR signals similar to the one of compound **5** (Table 3.12) except the presence of an extra methoxyl signal, which was placed on C-12 from the HMBC correlations. Other 2D spectra in comparison with literature data confirmed the structure of **C6** as clinopodiolide B (Bustos-brito, et al., 2019). This is the first report on the isolation of **C6** from *S. africana lutea.*

UNIVERSITY of the
WESTERN CAPE

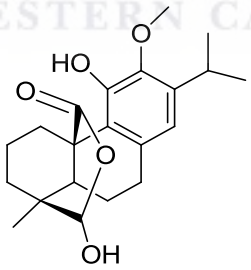

Clinopodiolide B

Figure 3.72: Chemical structure of **6**

https://etd.uwc.ac.za/

Table 3.12: ^{1}H and ^{13}C NMR spectroscopic data assignments (400 MHz) for compound **6** (δ in ppm, m, *J* in Hz) in $CDCl_3$

	6		
N^{O}	δ_H (*J* in Hz)	^{13}C	Multiplicity
1	3.42 (13.6) 1.46 d (4.2)	35.0	CH_2
2	1.73 m	21.0	CH_2
3	2.3 d, 1.21 s (12.5)	32.7	CH_2
4		36.9	C
5	1.57 d (12.5)	50.2	CH
6	2.11 d (11.2) 1.43 d (4.1)	21.4	CH_2
7	2.8 m	30.9	CH_2
8		123.8	C
9		133.3	C
10		49.4	C
11		149.7	C
12		146.3	C
13		141.8	C
14	6.56 s	118.4	CH
15	3.28 sept (7.4)	26.7	CH
16	1.2*	23.5	CH_3
17	1.19*	23.3	CH_3
18	1.13 s	24.1	CH_3
19	5.61 s	103.3	CH
20		180.0	
OCH_3	3.86 s	58.6	CH_3

UNIVERSITY of the
WESTERN CAPE

https://etd.uwc.ac.za/

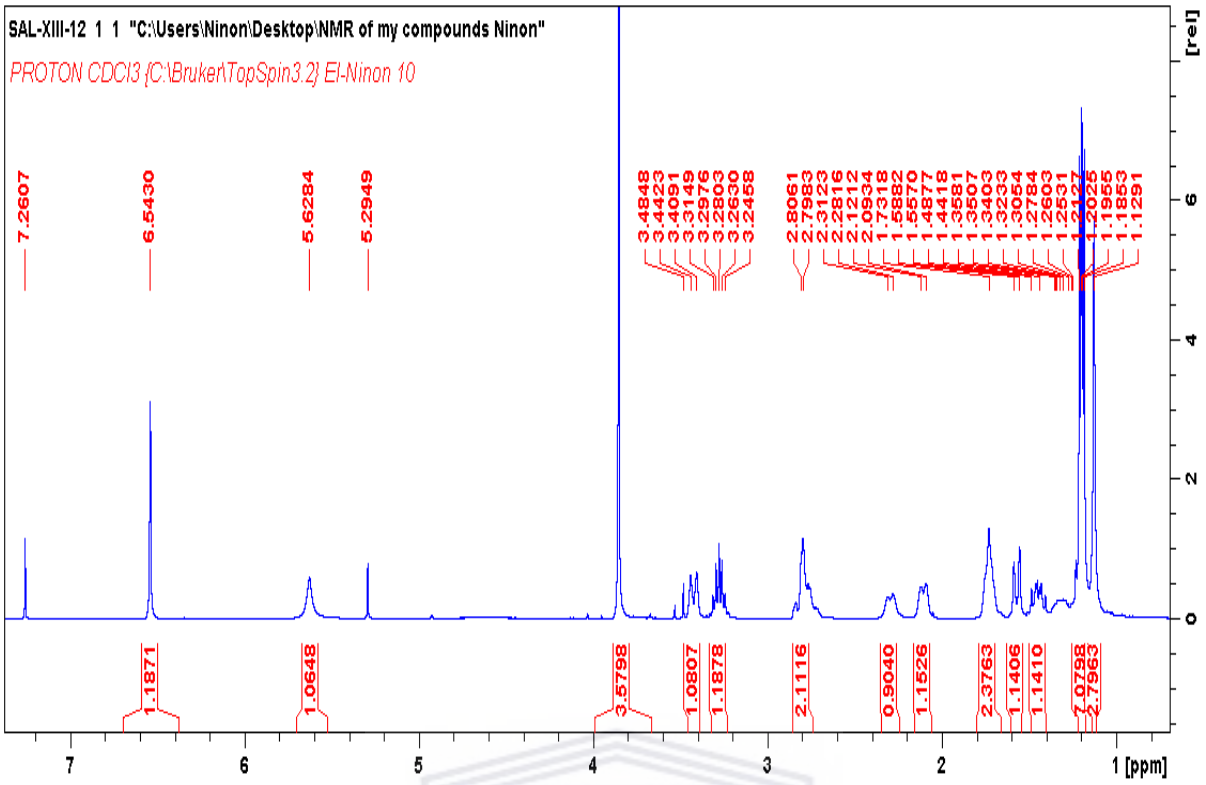

Figure 3.73: ^{1}H NMR (400 MHz, CDCl3) spectrum of **6**

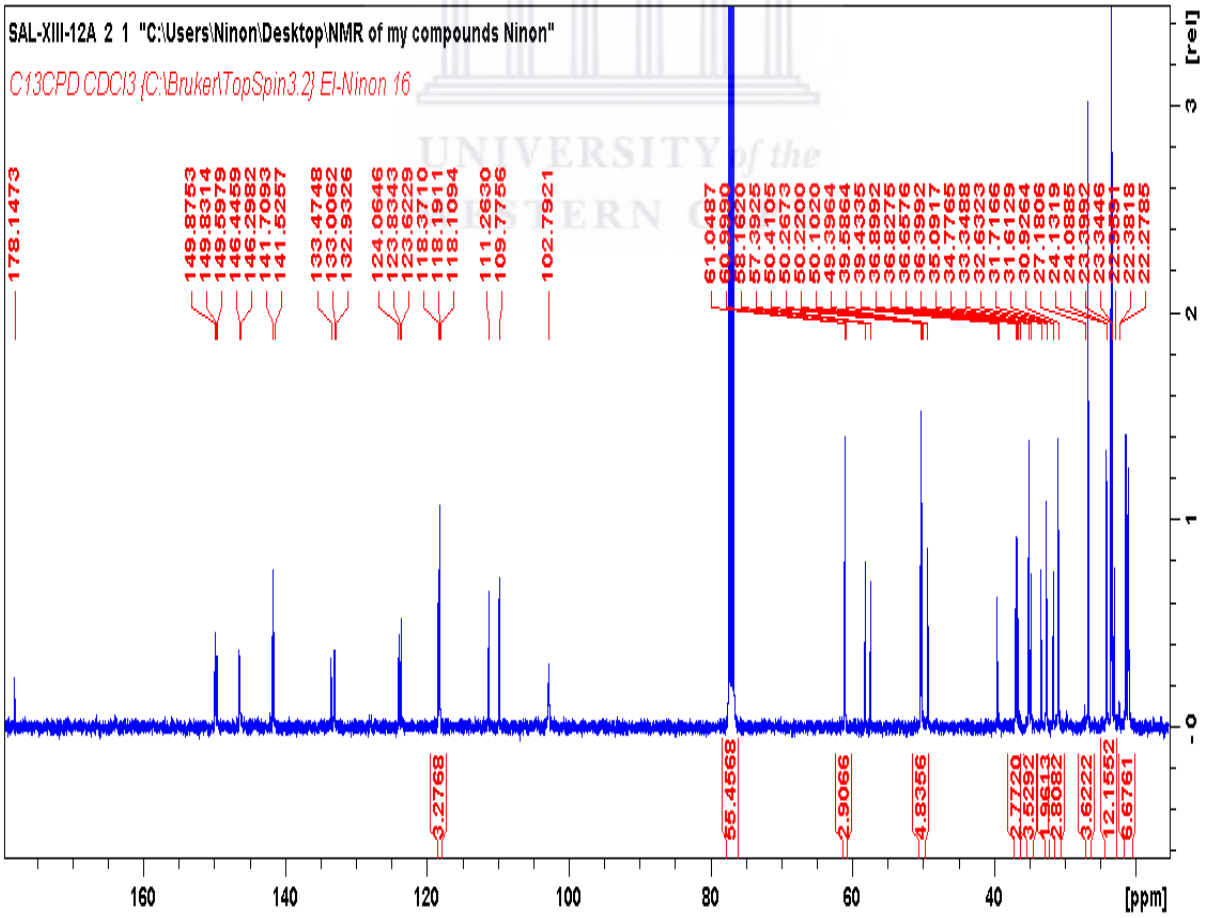

Figure 3.74: ^{13}C NMR (400 MHz, CDCl3) spectrum of **6**

https://etd.uwc.ac.za/

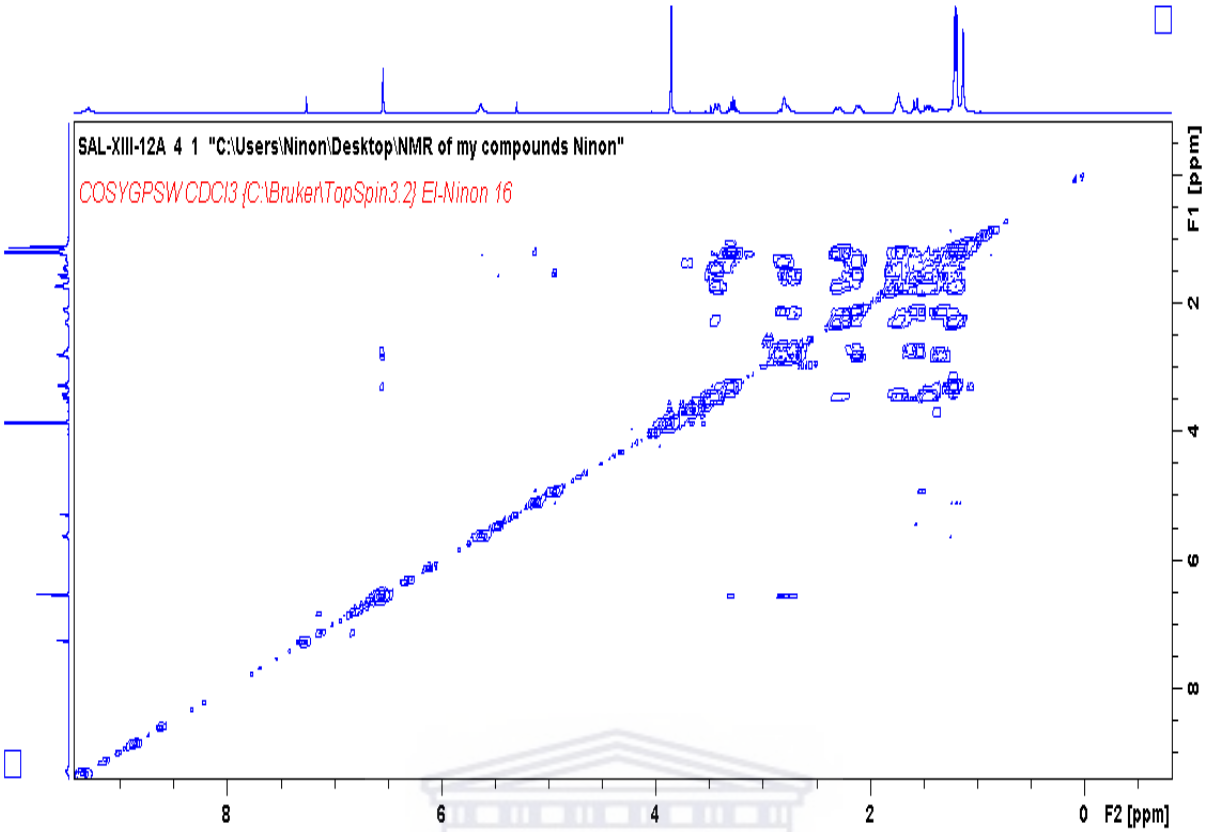

Figure 3.75: COSY (400 MHz, CDCl3) spectrum of **6**

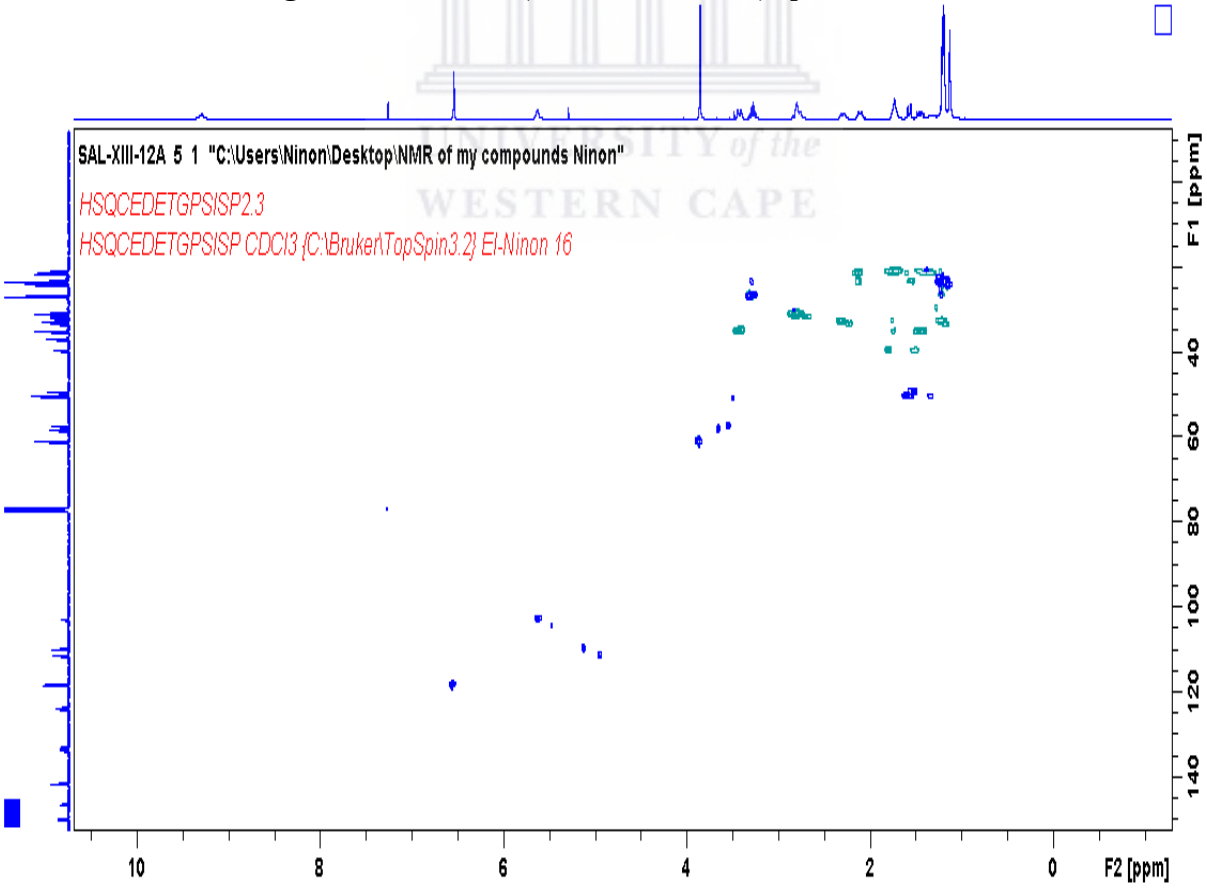

Figure 3.76: HSQC (400 MHz, CDCl3) spectrum of **6**

https://etd.uwc.ac.za/

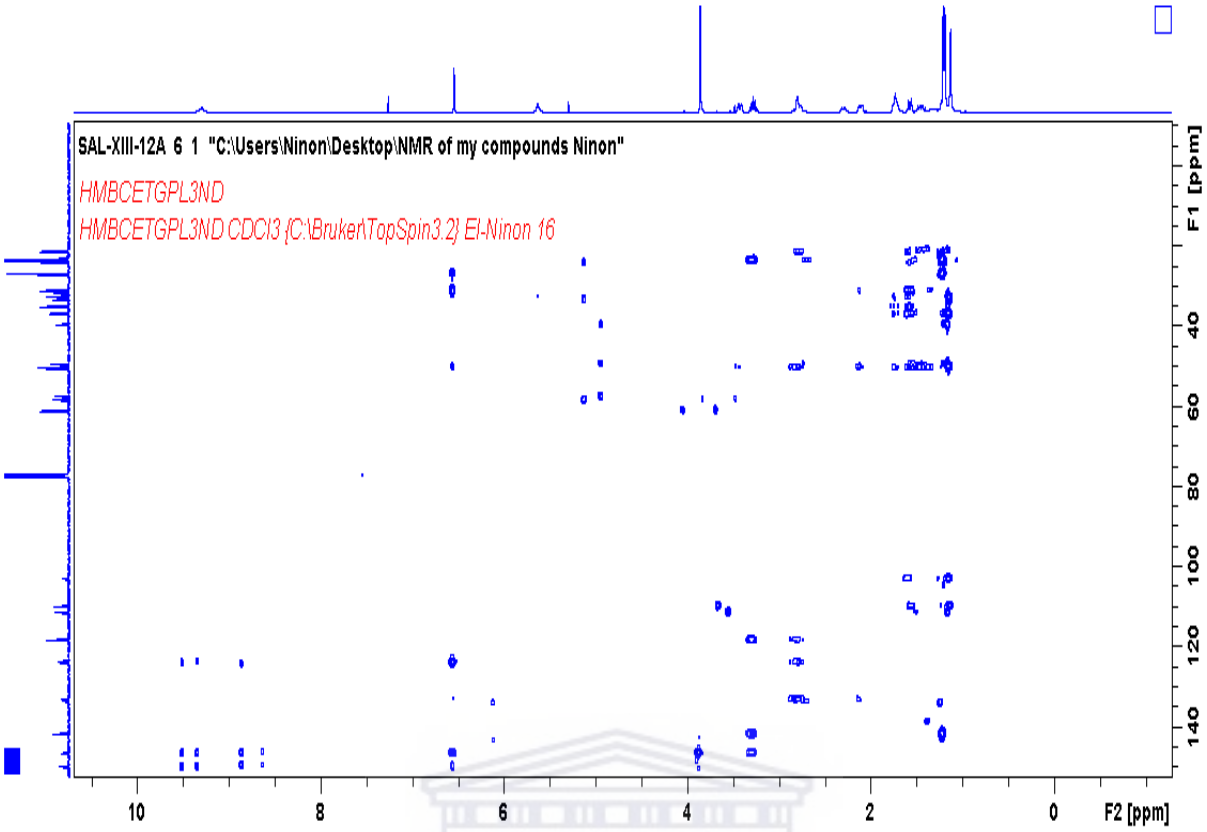

Figure 3.77: HMBC (400 MHz, CDCl3) spectrum of **6**

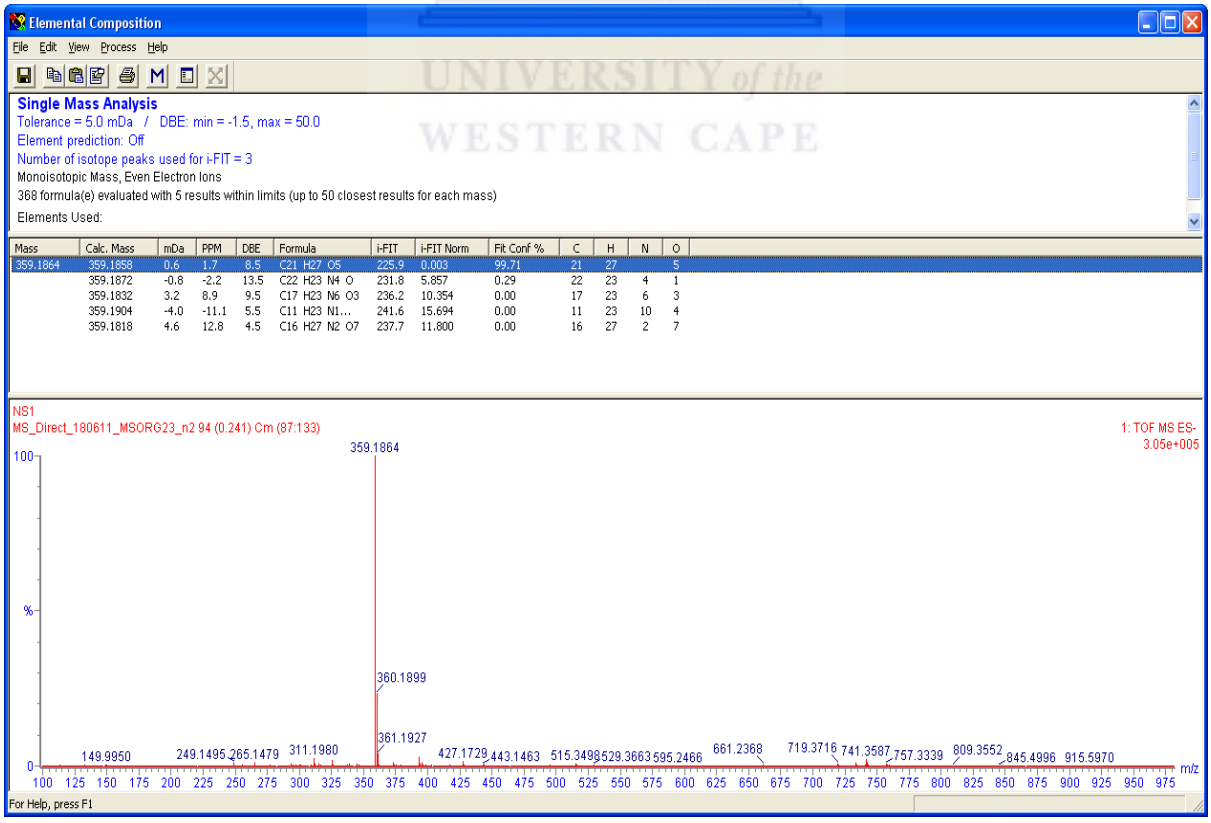

Figure 3.78: HR-MS spectrum of **6**

https://etd.uwc.ac.za/

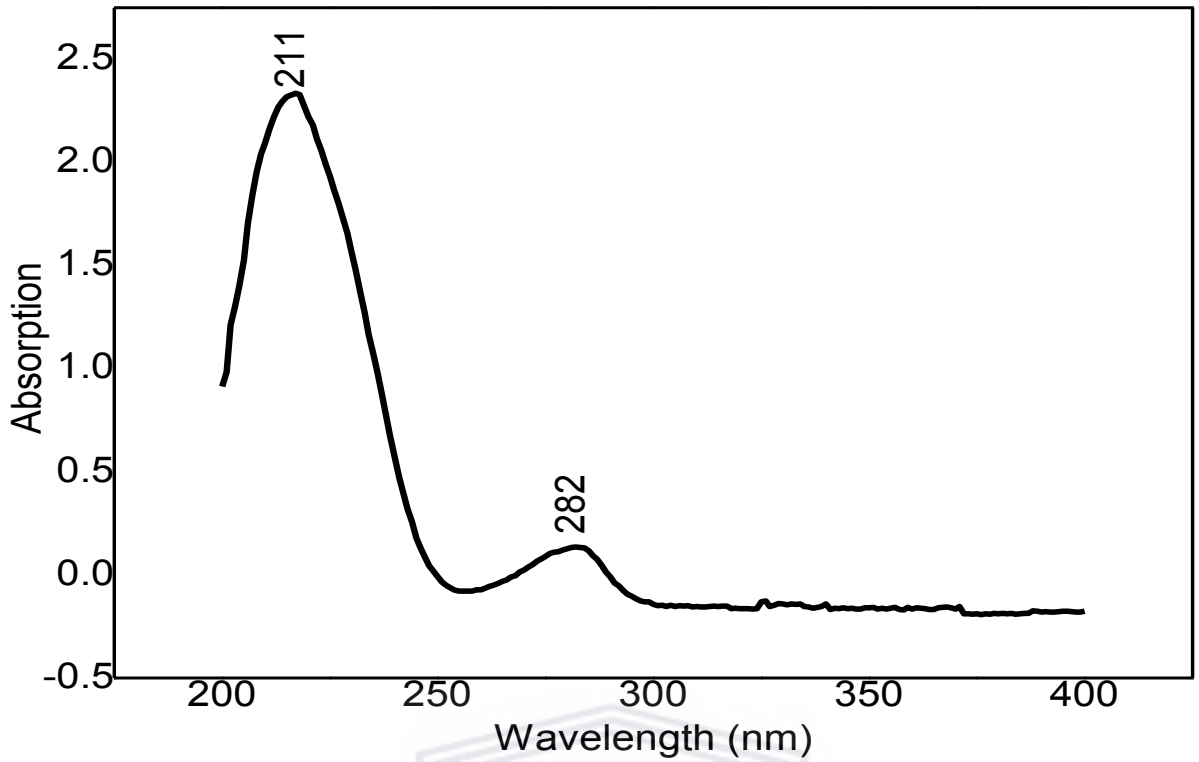

Figure 3.79: UV spectrum of **6**

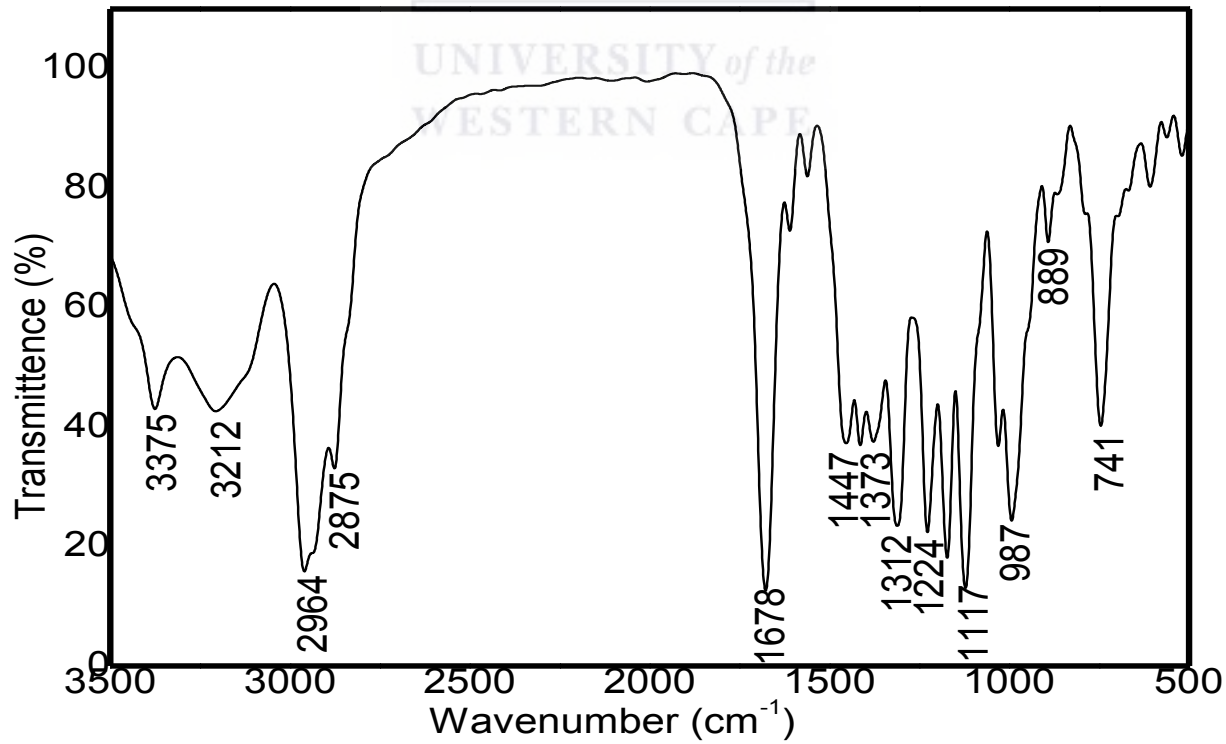

Figure 3.80: FTIR spectrum of **6**

https://etd.uwc.ac.za/

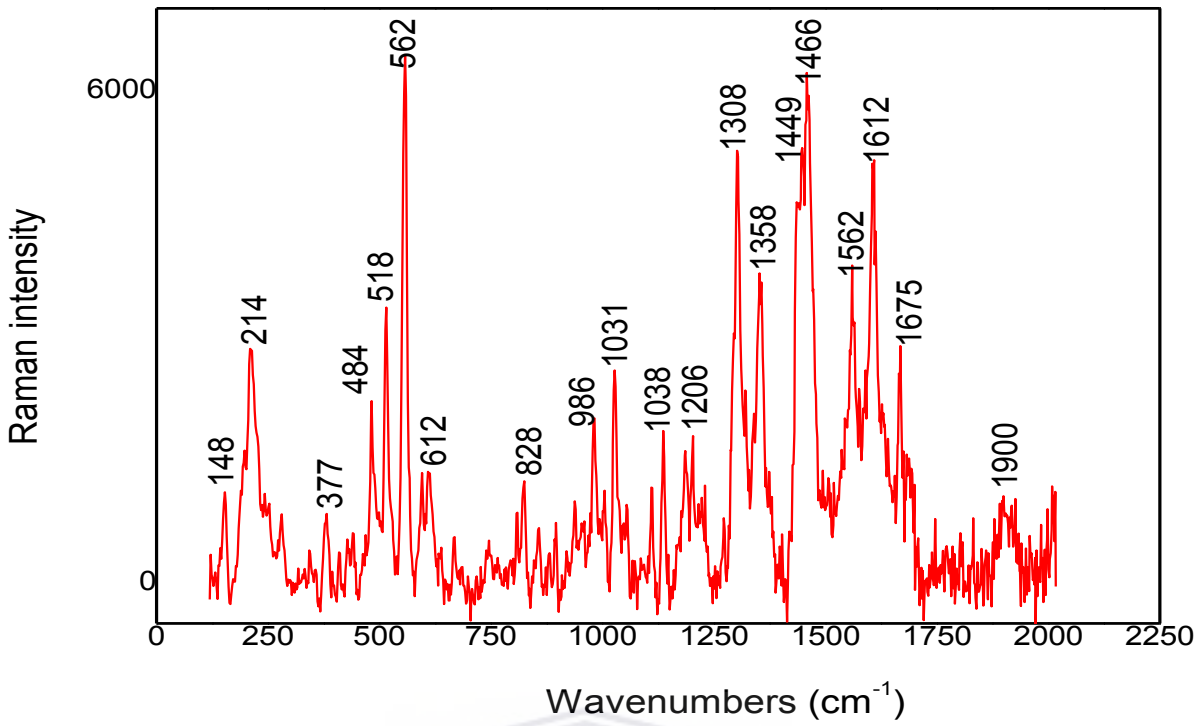

Figure 3.81: Raman spectrum of **6**

RAMAN	Intensity	Assignments
214	n	C-C-C deformation
484	n	C-C-C deformation
518	n	Deformation ring
562	s	C-C-O deformation
1031	n	C-C aromatic ring
1038	w	C-C aromatic ring
1206	w	O-H deformation
1308	s	CH_2 wagging
1358	n	CH_2 wagging
1449	s	CH_3 deformation
1466	s	CH_2 deformation
1562	n	C-C stretching
1612	s	C=C stretching
1675	n	C=C stretching

https://etd.uwc.ac.za/

3.9.7 Structure elucidation of oleanolic acid (**7**)

Compound 7 was isolated as a white powder. The HRMS data indicated a molecular ion peak at $[M]^+$ 456.3545 *m*/*z* suggesting a possible chemical formula of $C_{30}H_{48}O_3$ (Fig. 3.86). Its IR spectrum exhibited bands at 1694 cm^{-1} for the carbonyl group (C=O), 2933 and 2870 cm^{-1} for the carbon-hydrogen stretching (C-H) as well as at 3416 cm^{-1} attributed hydroxyl group (OH) (Fig. 3.87), which is in agreement the report data (Ribeiro, et al., 2018). The Raman spectrum featured characteristic bands at 1911 cm^{-1} related to C-H stretching, 1661 cm^{-1} related to C=C stretching, 1460 cm^{-1} related to the deformation vibration of the CH_2 group, 1096 and 1035 related to attributed to C-C aromatic ring (Fig. 3.88) (Mello, et al., 2006; Yu, et al., 2007). It was identified as oleanolic acid based on its NMR data, which showed typical triterpene signals. The ^{13}C NMR and DEPT spectra (Fig. 3.84, 85) confirmed the presence of thirty carbons consisted of eight quaternaries, five tertiaries, ten secondary and seven methyls carbons. ^1H NMR showed signals for an olefinic proton ($C_{12\text{-}13}$) at 5.25 (*t*, *J* = 3.7 Hz), a carbinolic proton (3 β-OH) at 3.22 (*dd*, *J* = 5.0, 10.3 Hz), carboxylic group (C-28). The identity of the compound was confirmed by comparing the experimental data with literature (Ayatollahi, et al., 2011). This is the first report on the isolation of **7** from *S. africana lutea*.

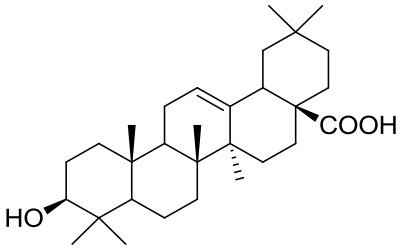

Oleanolic acid

Figure 3.82: Chemical structure of **7**

https://etd.uwc.ac.za/

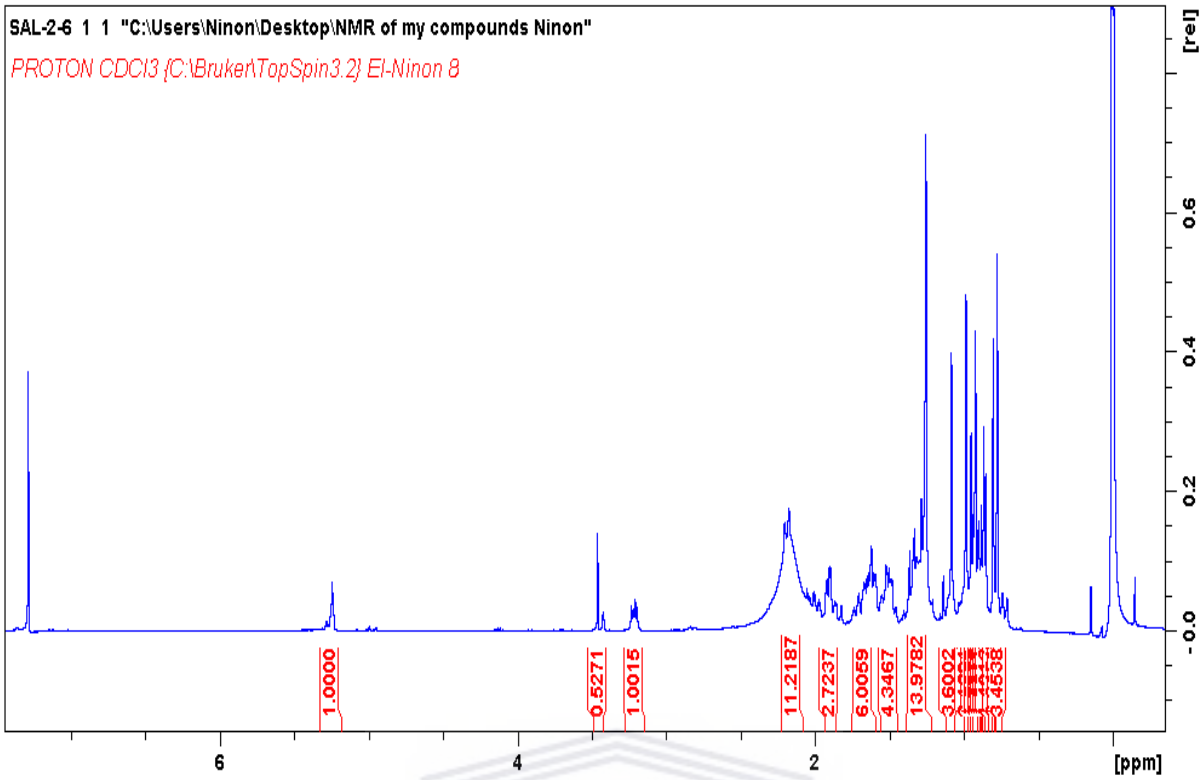

Figure 3.83: ^{1}H NMR (400 MHz, CDCl3) Spectrum of **7**

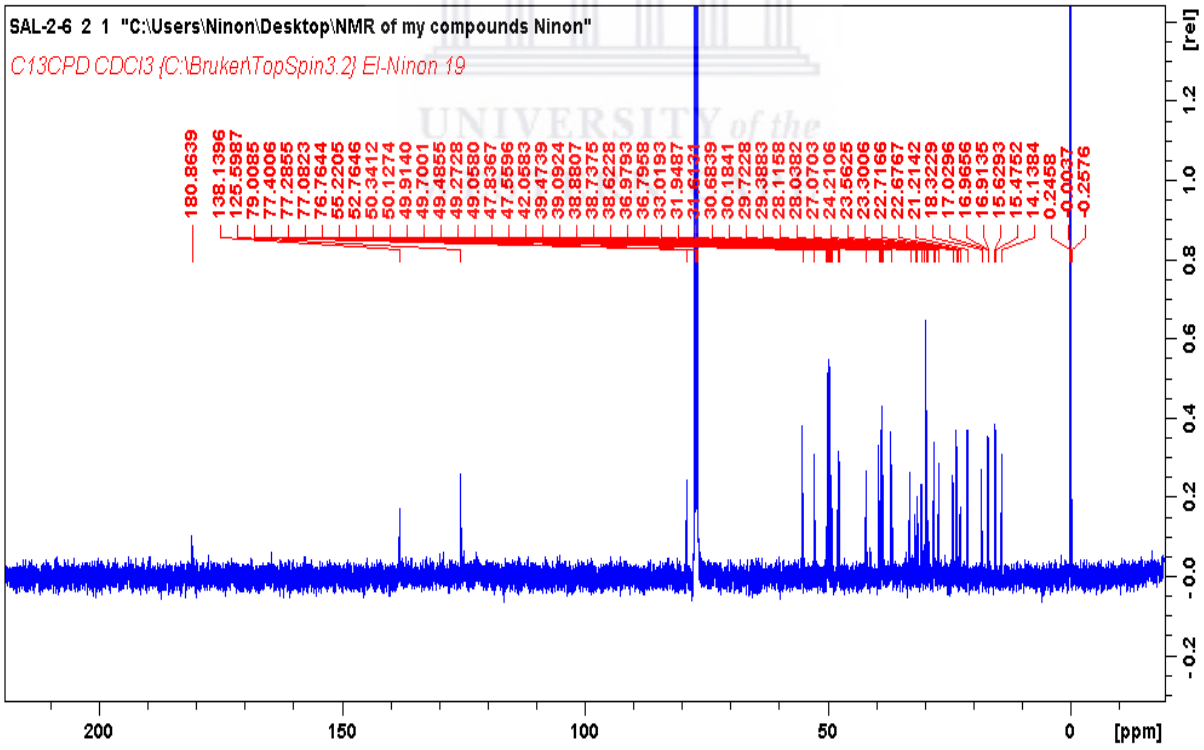

Figure 3.84: ^{13}C NMR (400 MHz, CDCl3) Spectrum of **7**

https://etd.uwc.ac.za/

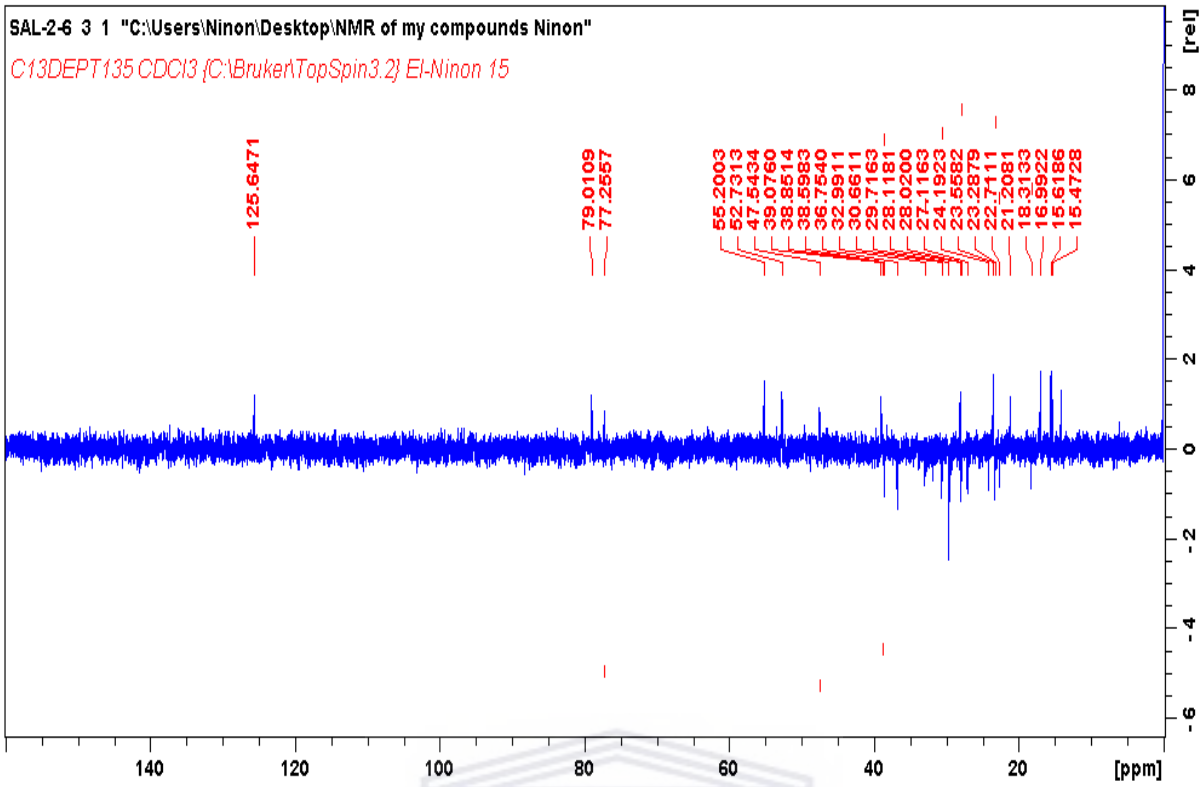

Figure 3.85: DEPT NMR (400 MHz, CDCl3) Spectrum of **7**

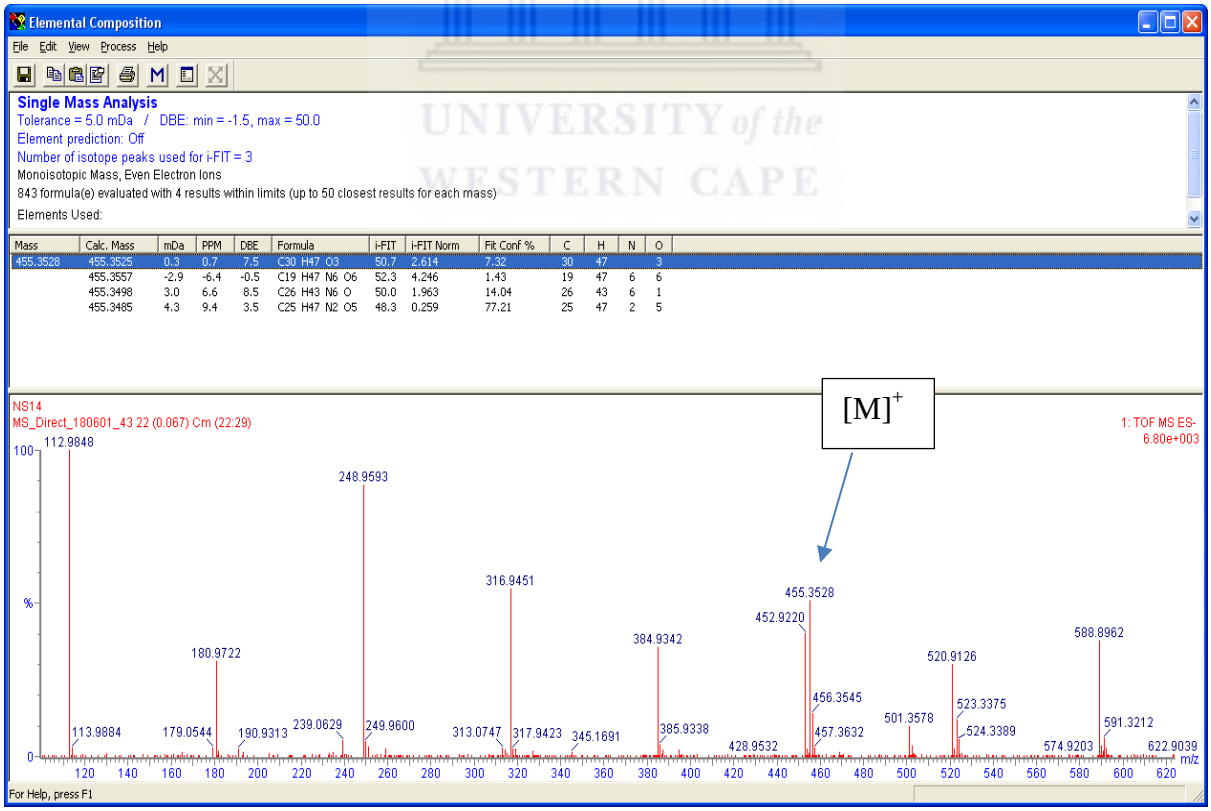

Figure 3.86: HRMS spectrum of **7**

https://etd.uwc.ac.za/

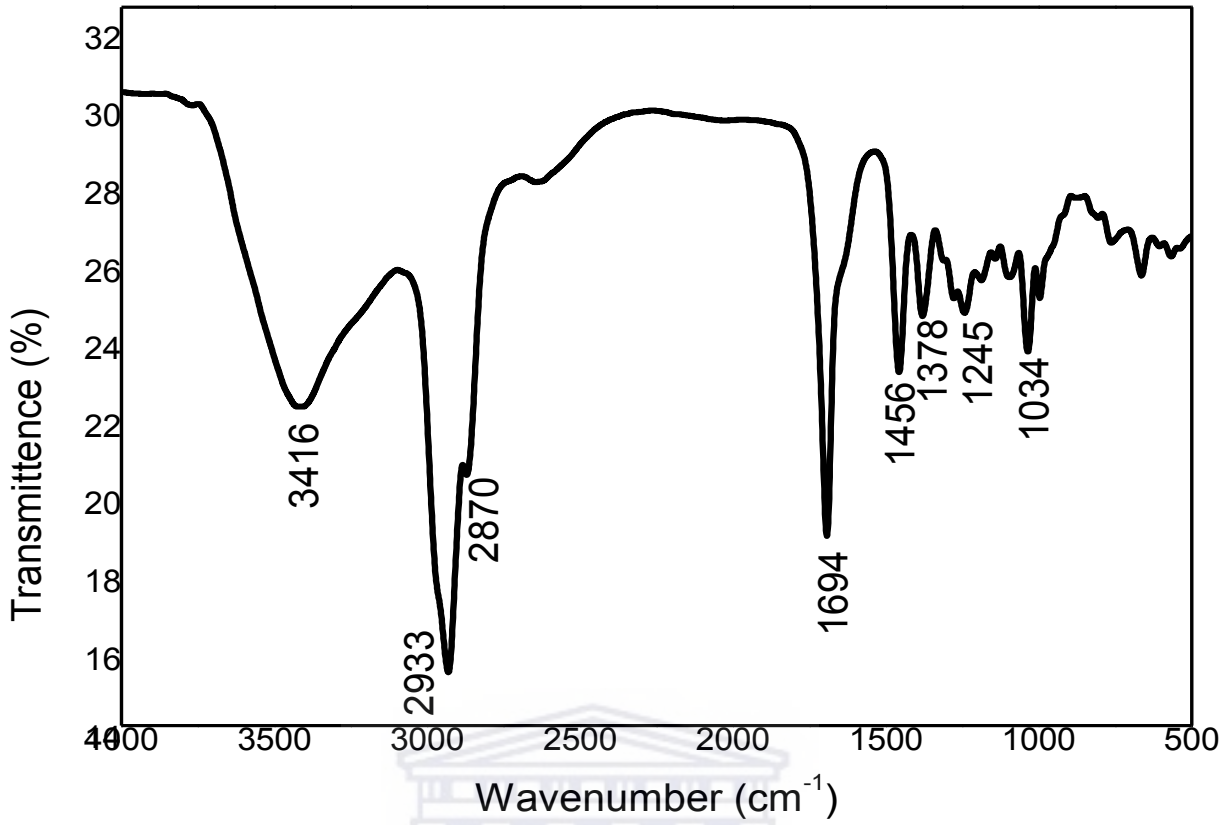

Figure 3.87: FTIR spectrum of **7**

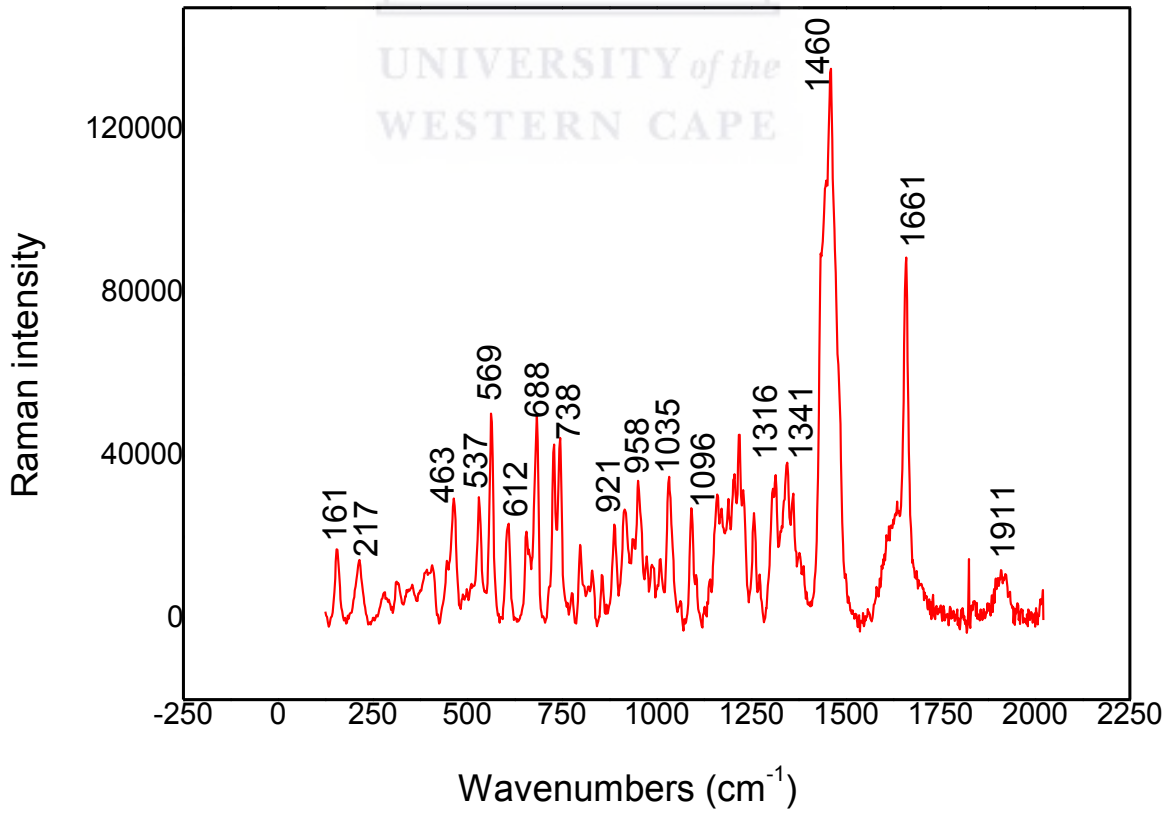

Figure 3.88: Raman spectrum of **7**

UNIVERSITY of the WESTERN CAPE
https://etd.uwc.ac.za/

RAMAN	Intensity	Assignments
537	n	Deformation ring
612	n	C-C ring deformation
1035	n	C-C aromatic ring
1096	n	C-C aromatic ring
1316	n	CH_2 wagging
1341	n	CH_2 wagging
1460	s	CH_2/CH_3 deformation
1661	s	C=C stretching
1911	w	C-H stretching

3.9.8 Structure elucidation of ursolic acid (**8**)

Compound 8 was isolated as a white powder. The HRMS data indicated a molecular ion peak at $[M]^+$ 456.3545 *m/z* suggesting a possible chemical formula of $C_{30}H_{48}O_3$ (Fig. 3.92). Its IR spectrum exhibited bands at 1694 cm^{-1} for the carbonyl group (C=O), 2933 and 2863 cm^{-1} for the carbon-hydrogen stretching (C-H) as well as at 3405 cm^{-1} attributed hydroxyl group (OH) (Fig. 3.93), which is in agreement the report data (Naika, et al., 2016). The ^{13}C NMR and DEPT spectra (Fig. 3.91, 92) revealed the presence of 30 carbon resonances distinguished into seven methyls (15.3, 15.5, 17.0, 17.1, 23.6, 25.9, and 28.1 ppm), nine methylene (18.3, 22.9, 23.4, 27.0, 27.2, 27.7, 32.4, 32.6, and 38.4 ppm), seven methine (38.7, 38.8, 47.5, 52.7, and 55.2 ppm), in addition to two carbon resonances at 79.0 and 122.6 ppm representing one oxygenated aliphatic (C-3) and one olefinic (C-12) carbons respectively, together with seven quaternary carbons (37.0, 38.7, 40.0, 41.6, 46.5, 143.6, and 182.9 ppm). In addition, the appearance of 79.0 indicate the presence of an oxygenated aliphatic [(C-3; β-OH], and the occurence of δ_c 143.6 and 122.6 revealed the presence of the double bond at position $C_{12\text{-}13.}$ The most downfield signal at 182.9 indicates the carboxylic function allocated in position C-28 according to the HMBC. The ^1H NMR showed signals for an olefinic proton ($C_{12\text{-}13}$) at 5.28 (*t, J* = 3.3 Hz), a carbinolic proton (3 β-OH) at of 3.22 (*dd, J* = 4.28, 15.4 Hz), carboxylic group (C-28).

https://etd.uwc.ac.za/

The identity of the compound confirmed by comparing the experimental data with literature (Ayatollahi, et al., 2011; Guvenalp, et al., 2006). This is the first report on the isolation of **8** from *S. africana lutea*.

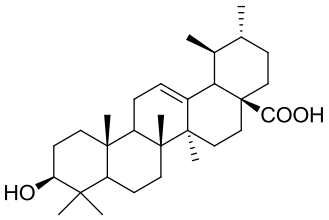

Ursolic acid

Figure 3.89: Chemical structure of **8**

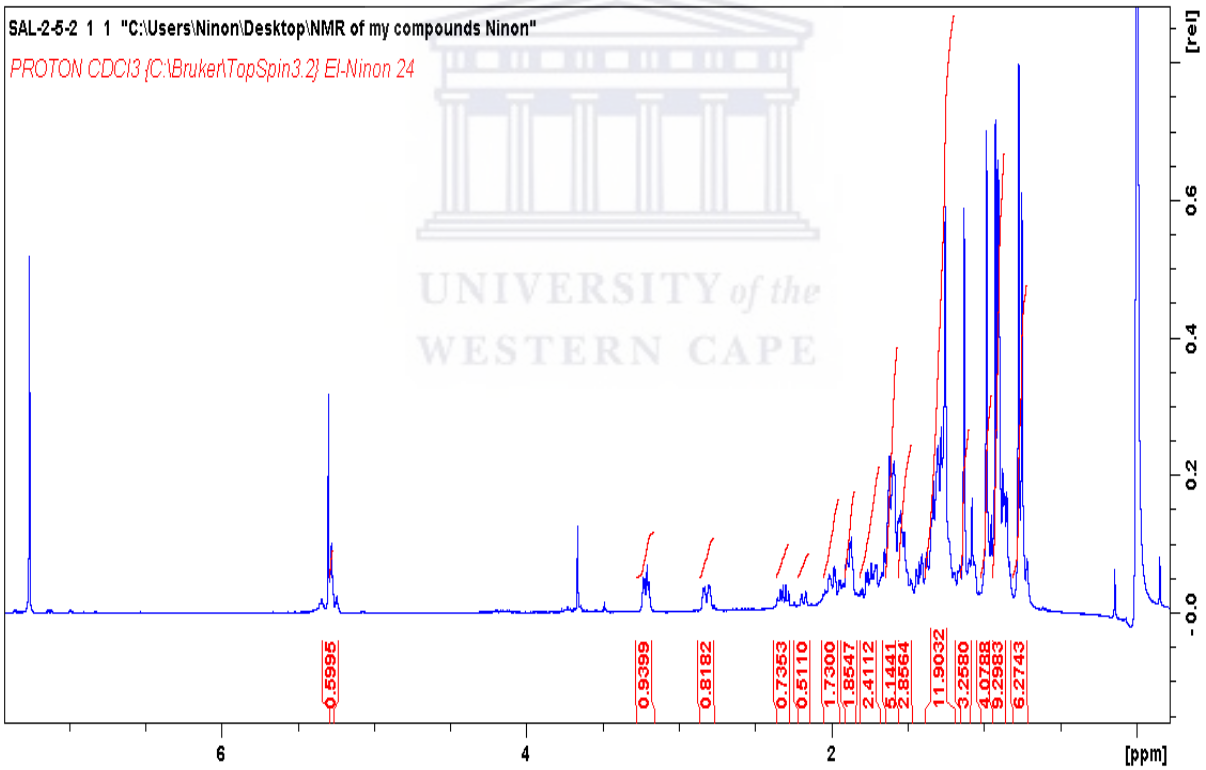

Figure 3.90: ^{1}H NMR (400 MHz, CDCl3) Spectrum of **8**

https://etd.uwc.ac.za/

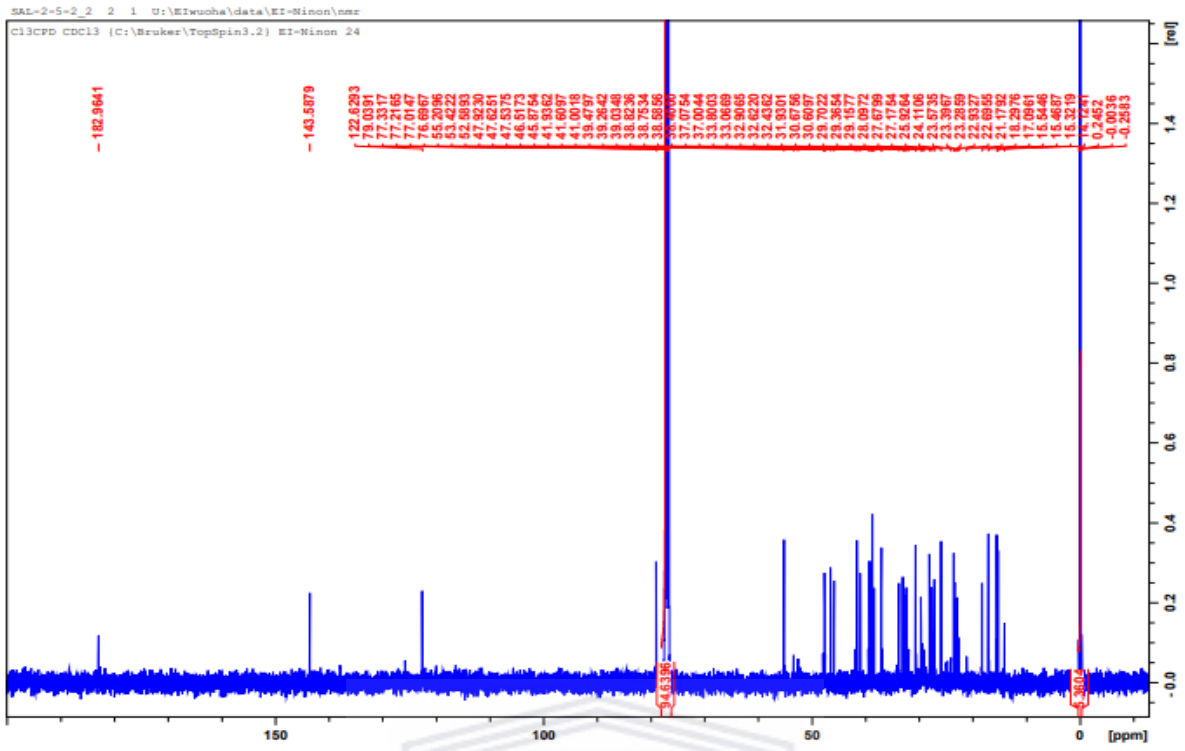

Figure 3.91: ^{13}C NMR (400 MHz, CDCl3) Spectrum of **8**

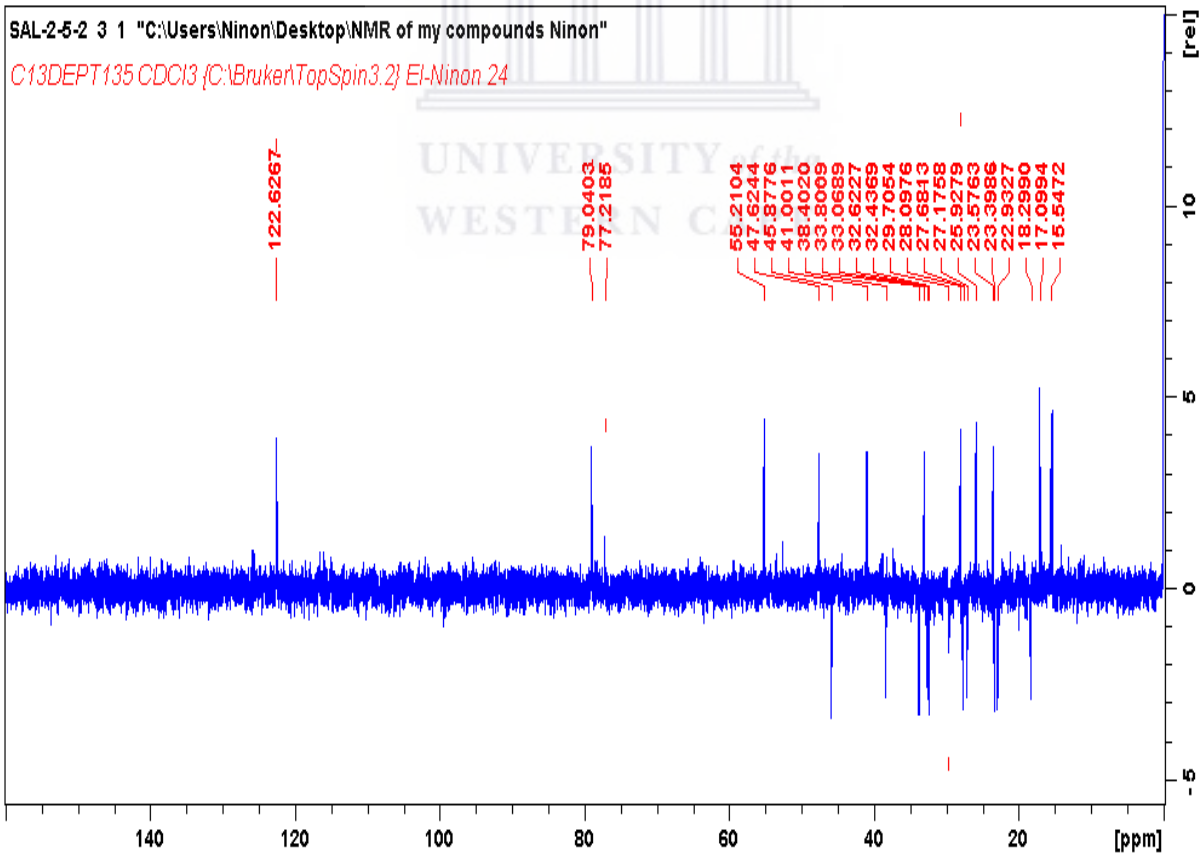

Figure 3.92: DEPT NMR (400 MHz, CDCl3) Spectrum of **8**

https://etd.uwc.ac.za/

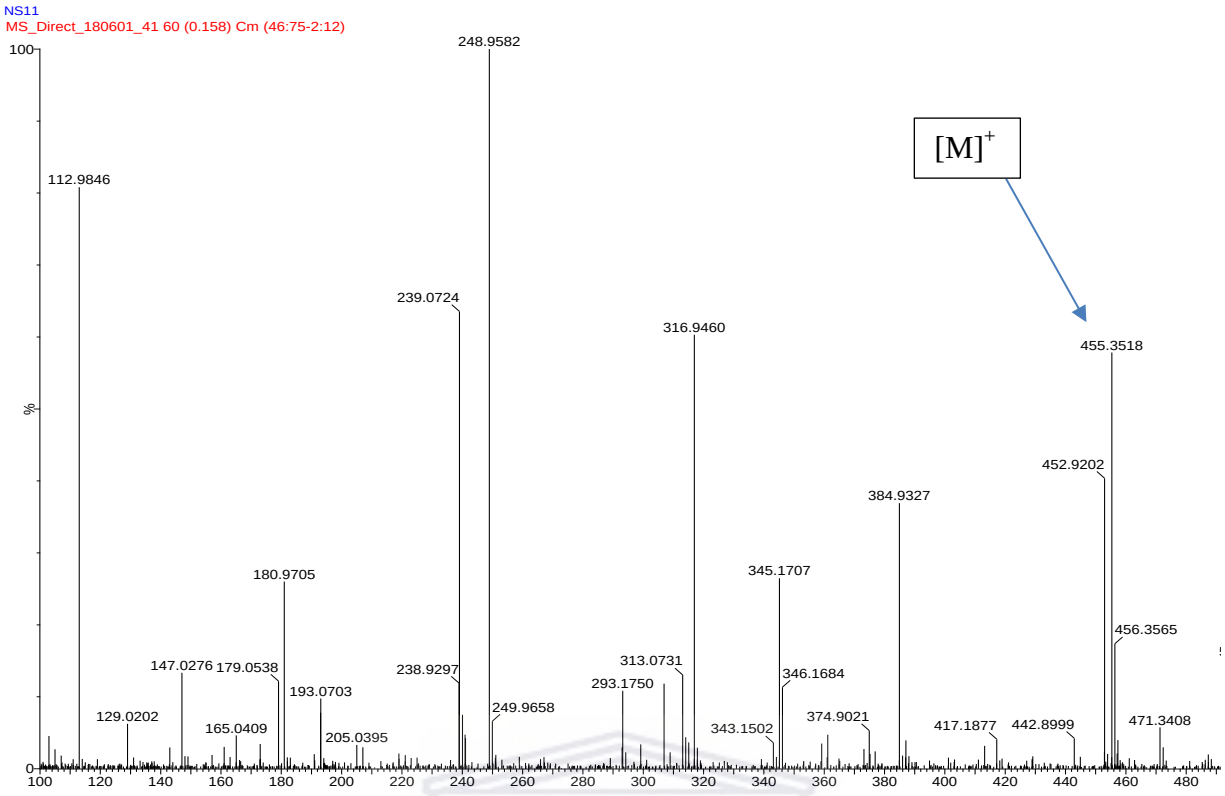

Figure 3.93: HRMS spectrum of **8**

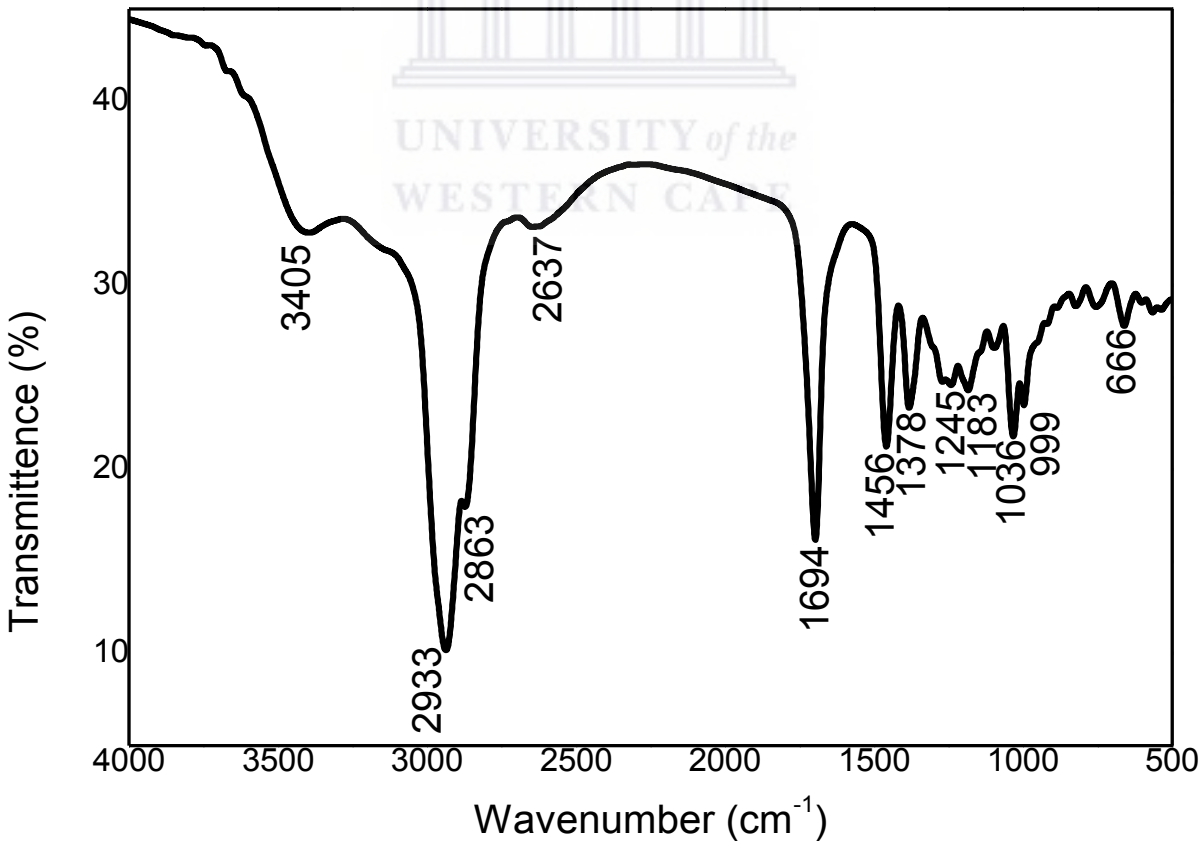

Figure 3.94: FTIR spectrum of **8**

UNIVERSITY of the WESTERN CAPE
https://etd.uwc.ac.za/

3.9.9 Structure elucidation of 11,12-dehydroursolic acid lactone (**9**)

Compound 9 was isolated as a white powder. It was identified as 11,12-dehydroursolic acid lactone based on its NMR data (see annexe), which showed close similarity with ursolic acid expect the presence of the lactone ring at 175.6 pm and the shift of the double bond from position $C_{12\text{-}13}$ at ursolic acid to $C_{11\text{-}12}$ at 11,12-dehydroursolic acid lactone. The identity of the compound confirmed by comparing the experimental data with literature (Sidan, et al., 2012). This is the first report on the isolation of **9** from *S. africana lutea*.

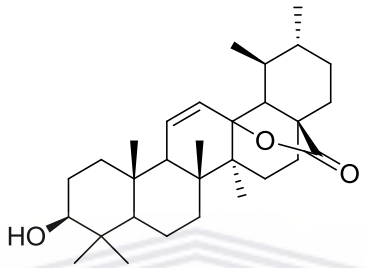

11,12-dehydroursolic acid lactone

Figure 3.95: Chemical structure of **9**

3.9.10: Structure elucidation of β-amyrin (**10**)

Compound 10 was isolated as a white powder. Its IR spectrum exhibited bands at 1693 cm^{-1} for the carbonyl lactone group (C=O), 2925 and 2870 cm^{-1} for the carbon-hydrogen stretching (C-H) as well as at 3408 cm^{-1} attributed hydroxyl group (OH) (Fig. 3. 102). It was identified as β-amyrin based on its NMR data (see annexe), which showed close similarity with ursolic acid expect the absence of the carboxylic group. The identity of the compound confirmed by comparing the experimental data with literature (Hossain & Ismail, 2013). This is the first report on the isolation of **10** from a *S. africana lutea*.

https://etd.uwc.ac.za/

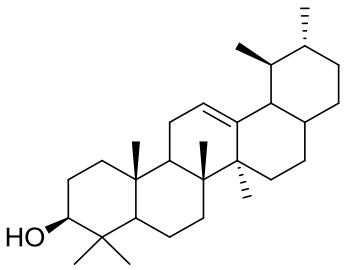

β-amyrin

Figure 3.96: Chemical structure of **10**

3.10 Biological evaluation: Results and discussion

3.10.1 Alpha-glucosidase and alpha-amylase activities

Alpha-glucosidase is an enzyme located in the brush border of the small intestine epithelium, which catalyzes the breaking down of the reaction of disaccharides and starch to glucose. Glucosidase inhibitors reduce the rate of carbohydrate digestion and delay the carbohydrate absorption from the alimentary tract (Bajpai & Kang, 2015). Alpha-amylase is one of the main enzymes in human that are directly involved in the breakdown of starch to simpler sugars (Nickavar, et al., 2008).

It hydrolyses complex polysaccharides to produce oligosaccharides and disaccharides which are then hydrolysed by alpha-glycosidase to monosaccharide which are absorbed through the small intestines into the hepatic portal vein and increase postprandial glucose levels. The inhibitory mechanisms of these enzymes are characterized by delaying the carbohydrate digestion and reducing the rate of glucose absorption (Thilagam, et al., 2013).

The bio-evaluation of natural resources for the antidiabetic properties has been intensified, and a great deal of research is being carried out to identify plants with potent anti-diabetic activity with emphasis on the inhibition of the two enzymes, alpha-glucosidase and alpha-amylase. In this study, the inhibitory activity of isolated compounds from *S. africana lutea* was investigated and the results showed that **8** demonstrated the highest alpha-glucosidase

https://etd.uwc.ac.za/

inhibitory activity with IC_{50} value of 11.3 ± 1.0 µg/mL, followed by **10** and **7** with IC_{50} values of 17.1 ± 1.0 and 22.9 ± 2.0 µg/mL respectively as indicated in Table 3. The IC_{50} value of compound **8** is in agreement with the reported value of 12.1 ± 1.0 µM (Zhang, et al., 2017). The fact that **8** exhibited stronger inhibitory activity than **7** suggested that the shift of C-29 methyl group from C-20 to C-19 could enhance the inhibition of alpha-glucosidase (Zhang, et al., 2017). In addition, the lowest alpha-glucosidase inhibitory activity demonstrated by **10** among the tested triterpenes might be due to the absence of the carboxylic group in its chemical skeleton. Among all the tested abietane diterpenes, only **6** demonstrated moderate alpha-glucosidase inhibitory activity with IC_{50} value of 81.7 ± 2.1 µg/mL. Remarkably, **7** demonstrated the strongest alpha-amylase inhibitory activity among the tested compounds with IC_{50} value of 12.5 ± 0.7 µg/mL followed by **8** and **10** with IC_{50} values of 66.1 ± 2.0 and 76.6 ± 2.8 µg/ml respectively. None of the tested abietane diterpenes showed alpha amylase inhibitory activity as shown in Table 3. Several surveys were carried out on the evaluation of the alpha glucosidase and inhibitory activity of triterpenes including **7**, **8** and **10**, the results revealed that these compounds are competitive inhibitors of alpha glucosidase with the ability to bind to the enzyme or substrate (López, et al., 2015). Additionally, our results corroborate with the reported data. (Kakarla, et al., 2016; Poongunran, et al., 2016; Zhang, et al., 2017).

UNIVERSITY of the
WESTERN CAPE

https://etd.uwc.ac.za/

Table 3.13: Inhibitory activities of the isolated compounds on alpha-glucosidase and alpha-amylase

Items	Alpha-glucosidase IC_{50} (µg/mL)	Alpha-amylase IC_{50} (µg/mL)
1	NA	NA
2	NA	NA
3	NA	NA
4	NA	NA
5	NA	NA
6	81.7 ± 2.1	NA
7	22.9 ± 2.0	12.5 ± 0.7
8	11.3 ± 1.0	66.1 ± 2.0
9	85.8 ± 2.3	NA
10	17.1 ± 1.0	76.6 ± 2.1
Crude extract	286.7 ± 2.9	NA
Acarbose	610.4 ± 1.0	10.2 ± 0.6

NA not active at the tested concentrations. The results are expressed as mean ±SEM for n = 3

3.10.2 Antioxidant activity

It is well known that oxidative stress is one of the main causes of diabetes complications due to over-accumulation of free radicals, which cause mitochondrial superoxide overproduction, diabetes tissue damage, insulin resistance, β-cell dysfunction, and impaired glucose tolerance (Yatoo, et al., 2016). The *in vitro* antioxidant activity of the isolated compounds of the methanolic extract of *S. africana-lutea* were investigated by evaluating their FRAP, TEAC and ORAC activities. The TEAC and FRAP are assays based on single electron transfer (SET) mechanism in which the antioxidant transfers an electron to the corresponding cationic radical to neutralize it (Pérez-Fons, et al., 2010), while ORAC is based on a hydrogen atom transfer (HAT) mechanism in which the antioxidant exhibits the potential health-beneficial roles via transferring hydrogen atom (s) to the reactive species, thereby deactivating them (Apak, et al., 2016). The results demonstrated that **1** and **5** exhibited strong activity on ORAC (2588.18 ± 10.10; 2357.18 ± 0.1) µM TE/g respectively. Compounds **5** and **6** showed strong activities on TEAC (862.2 ± 1.36; 705.5 ± 1.99) µM TE/g, whereas **5** and **2** demonstrated significant inhibitory activity on FRAP (2262.89 ± 11.01; 2200.95 ± 14.22) µM AAE/g when

https://etd.uwc.ac.za/

compared to the reference antioxidant epigallocatechingallate (EGCG) as shown in Table 4. The crude extract of *S. africana lutea* exhibited significant antioxidant activity when tested on ORAC (4427.62 ± 4.6), TEAC (1062 ± 2.1 µM TE/g) and FRAP (464.4 ± 4.5 µM AAE/g), which can be related to synergistic effects. Phenolic compounds have been reported to be responsible for the antioxidant activity of numerous plant species by stabilization of radicals by donating electrons or by metal ion complexation among other mechanisms. Nevertheless, other aspects can be considered for example, the presence of vicinal hydroxyl groups is essential in a pronounced antioxidant activity (Souza de Oliveira, et al., 2015). Abietane diterpenes are known to have strong antioxidant activity due to the presence of ortho-dihydroxyl groups/vicinal hydroxyls in the aromatic ring that serve as hydrogen and/or electron donating agents to the corresponding reactive species leading to the formation of the stable quinone derivatives (Brewer, 2011). It has been shown that the phenolic group at the 11 position is more implicated in the antioxidant activity (Masuda, et al., 2005). In general, phenolic compounds expected to transfer electrons or donate protons to the reactive radicals because of the resonance stability of phenoxy radical (Özgen, et al., 2011). Hence, the structure-activity relationship (SAR) of **5** could be related to the presence of ortho-dihydroxyl groups/vicinal hydroxyls in the aromatic ring as well as the presence of the free hydroxyl group in its chemical structure which are responsible for the high activity demonstrated when compared to **6**. However, the substitution of the free OH at position C-12 by a methoxyl group is directly related to the decrease of the activity observed. This observation is in agreement with the reported data where **5** exhibits stronger inhibition effects than **6** in the TBARS assay with an IC_{50} value of 5.9 ± 0.4 µM as well as in DPPH assay with IC_{50} value of 24.8 ± 1.2 µM (Bustos-brito, et al., 2019). The presence of an acetoxy group in **1** could be responsible of its high capacity of hydrogen atom transfer demonstrated in the ORAC assay. Although, the antioxidant activity of 2 demonstrated in FRAP is high because of the highly-

https://etd.uwc.ac.za/

stress lactone ring which may open during the course of chemical reaction leading to extension of conjugation and formation of p-quininoidal structure.

Table 3.14: Antioxidant activities of the isolated compounds

Items	ORAC (µmole TE/g)	TEAC (µmole TE/g)	FRAP (µM AAE/g)
1	2588.18 ± 10.10	694 ± 1.63	1217.4 ± 2.93
2	2233.86 ± 7.97	635.7 ± 0.85	2200.95 ± 14.22
3	735.41 ± 1.98	124.4 ± 0.57	1440.37 ± 9.13
4	559.66 ± 15.17	440.1 ± 1.48	1257.04 ± 6.71
5	2357.16 ± .011	862.2 ± 1.36	2262.89 ± 11.01
6	1502.50 ± 21.22	724.9 ± 1.3	1480.01 ± 3.95;
7	NA	NA	347.82 ± 3.72
9	NA	NA	283.41 ± 3.9
8	NA	NA	778.9 ± 6.80
10	NA	NA	412.23 ± 12.97
Crude extract	4427.62 ± 4.6	1062.2 ± 2.1	464.4 ± 4.5
EGCG	3976.82 ± 3.82	4146.4 ± 19.77	7524.98 ± 4.94

NA not active at the test concentrations; EGCG: Epigallocatechingallate. The results are expressed as mean ±SEM for n = 3

Compound 1: yellow, amorphous solid; $[\alpha]^{28}_{D}$ +70.43 (0.1, MeOH); UV (MeOH) λ_{max} (log ε) 210 (4.31), 280 (3.79); nm; IR (KBr) ν_{max} 3447, 3320, 2954, 1725, 1570, 1381, 1250, 1039cm^{-1}; ^{1}H and ^{13}C NMR data, see Table 1 and 2; positive-ion HRESIMS [M -H] $^{+}$ *403.2115*(calcd for $C_{23}H_{32}O_6$, 404.2199).

Compound 2: red brownish powder; $[\alpha]^{28}_{D}$ +22.92 (0.2, MeOH); UV (MeOH) λ_{max} (log ε) 212 (4.32), 287 (4.09); nm; IR (KBr) ν_{max} 3447, 3300, 2958, 1727, 1575, 1246, 1034 cm^{-1}; ^{1}H and ^{13}C NMR data, see Table 1 and 2; positive-ion HRESIMS [M -H] $^{+}$ *417.1890*(calcd for $C_{23}H_{32}O_6$, 418.1932).

Compound 3: brown amorphous powder; $[\alpha]^{28}_{D}$ +49.04 (0.07, MeOH); UV (MeOH) λ_{max} (log ε) 210 (4.31), 295 (3.92); nm; IR (KBr) ν_{max} 3450, 2962, 1769, 1634, 1435, 1239, 1034 cm^{-1}; ^{1}H and ^{13}C NMR data, see Table 1 and 2; positive-ion HRESIMS [M -H] $^{+}$ *417.1907*(calcd for $C_{23}H_{32}O_6$, 418.20).

Compound 4: yellow amorphous powder; $[\alpha]^{28}_{D}$ -53.27 (0.03, MeOH); UV (MeOH) λ_{max} (log ε) 210 (4.31), 281 (4.13); nm; IR (KBr) ν_{max} 3330, 2950, 1750, 1617, 1446, 1243, 1050 cm^{-1}; ^{1}H and ^{13}C NMR data, see Table 1 and 2; positive-ion HRESIMS [M -H]$^{+}$ 401.1609 (calcd for $C_{23}H_{32}O_6$, 402.2042).

https://etd.uwc.ac.za/

Compound 5: white powder; $[\alpha]^{28}_{D}$ -81.52 (0.1, MeOH); UV (MeOH) λ_{max} (log ε) 208 (3.81), 284 (4.13); nm; IR (KBr) ν_{max} 3500, 3210, 2957, 1675, 1440, 1321, 1220, 1127, 1000 cm^{-1}; ^{1}H and ^{13}C NMR data, see Table 1 and 2; positive-ion HRESIMS [M – (H_2O)] $^{+}$ *346.1723*(calcd for $C_{20}H_{28}O_6$, 364.19).

Compound 6: grey powder; $[\alpha]^{28}_{D}$ -86.36 (0.1, MeOH); UV (MeOH) λ_{max} (log ε) 211 (4.31), 282 (4.13); nm; IR (KBr) ν_{max} 3375, 3212, 2964, 1678, 1312, 1117, 985 cm^{-1}; ^{1}H and ^{13}C NMR data, see Table 1 and 2; positive-ion HRESIMS [M – (H_2O)] $^{+}$ 359.1864 (calcd for $C_{20}H_{28}O_6$, 378.2).

3.11 Conclusion

The phytochemical and biological investigation of *S. africana –lutea* methanolic extract revealed that this plant is a rich source of abietane diterpenes and triterpenes with significant alpha glucosidase and alpha amylase inhibitory activities as well as remarkable antioxidant activity when considering the FRAP, TEAC, ORAC assays. The present work is the first scientific report on alpha glucosidase and alpha amylase inhibitory activities of novel abietane diterpenes from *S. africana –lutea* and the results suggest that the methanolic extract of this plant and/or its individual constituents might become prominent natural therapeutic agents for the inhibition of alpha glucosidase and alpha amylase enzymes and oxidative stress, which are both playing an important role in the development of diabetic related diseases. Therefore, compounds with high antioxidant and antidiabetic activities are the most logical choice for reducing diabetes-induced ROS.

UNIVERSITY of the WESTERN CAPE
https://etd.uwc.ac.za/

References

Amabeoku, G.J., Eagles, P., Scott, G., Mayeng, I and Springfield, E. (2001). Analgesic and antipyretic effects of *Dodonaea angustifolla* and *Salvia africana lutea*. *Journal of Ethnopharmacology,* 75, 117-124.

Apak, R., Ozyurek, M and Güclu, K. (2016). Antioxidant activity/capacity measurement hydrogen atom transfer (HAT)-based, mixed-mode (electron transfer (ET)/HAT), and lipid peroxidation assays. *Journal of Agricultural and Food Chemistry, 64*(1028−1045), 64, 1028−1045.

Ayatollahi, A.M., Ghanadian, M., Afsharypour, S., Abdella, O.M., Mirzai, M and Askari, G. (2011). Pentacyclic triterpenes in Euphorbia microsciadia with their T-cell proliferation activity. *Iran Journal of Pharmaceutical Research,* 10(2): 287–294.

Bajpai, V.K and Kang, S.C. (2015). Tyrosinase and alpha-glucosidase inhibitory effects of an abietane type diterpenoid taxodone from *Metasequoia glyptostroboides*. *National Academy Science Letters*, 38(5), 399–402.

Belt, T., Keplinger, T., Hänninen, T., Rautkari, L. (2017). Cellular level distributions of Scots pine heartwood and knot heartwood extractives revealed by Raman spectroscopy imaging. *Industrial Crops and Products*, 108, 327-335.

Benzie, I.F.F and Strain, J.J. (1996). The ferric reducing ability of plasma (FRAP) as a measure of "antioxidant power": The FRAP Assay. *Analytical Biochemistry, 238*, 70-76.

Brewer, M. (2011). Natural antioxidants: Sources, compounds, mechanisms of action, and potential applications. *Comprehensive Reviewsin Food Science and Food Safety*, 10, 221-246.

UNIVERSITY of the WESTERN CAPE

https://etd.uwc.ac.za/

Bustos-brito, C., Joseph-Nathan, P., Burgueno-Tapia, E., Martinez-Otero, D., NieTO-Camacho, A., Calzada, F., Yepez-Mulia, L., Esquivel, B and Quijano, L. (2019). Structure and absolute configuration of abietane diterpenes fom *Salvia clinopodidides*: Antioxidant, antiprotozoal and antipropulsive activities. *Journal of Natural Products*, 82, 1207-1216.

Cao, G and Prior, R.L. (1998). Measurement of oxygen radical absorbance capacity in biological samples. *Methods in Enzymology, 22*(5), 749-760.

Chain, F.E., Leyton, P., Paipa, C., Fortuna, M and Brandán, S.A. (2015). FT-IR, FT-Raman, UV-visible, and NMR spectroscopy and vibrational properties of the labdane-type diterpene 13-epi-sclareol. *Spectrochimica Acta part A Molecular and Biomolecular Spectroscopy*, 138, 303-13.

Etsassala, N.G.E.R., Adeloye, A.O., El-Halawany, A., Hussein, A.A and Iwuoha, E.I. (2019). Investigation of in-vitro antioxidant and electrochemical activities of isolated compounds from *Salvia chamelaeagnea* P.J.Bergius extract. *Antioxidants*, 8, 98.

Gao, J.B., Yang, S.J., Yan, Z.R., Zhang, X.J., Pu, D.B., Wang, L.X., Li, X.L., Zhang, R.H and Xiao,W.L.J.. (2018). Isolation, characterization, and structure-activity relationship analysis of abietane diterpenoids from *Callicarpa bodinieri* as spleen tyrosine kinase inhibitors. *Natural Products*, 81, 998−1006.

Guvenalp, Z., Kilic, N., Kazaz, C., Kaya, Y and Demirezer, O. (2006). Chemical constituents of *Galium tortumense*. *Turkey Journal of Chemisty,* 30, 515 – 523.

Hossain, M.A and Ismail, Z. (2013). Isolation and characterization of triterpenes from the leaves of *Orthosiphon stamineus*. *Arabian Journal of Chemistry*, 6(3), 295-298.

Hussein, A., Meyer, J.M., Jimeno, M.L and Rodrıguez, B. (2007). Bioactive diterpenes from *Orthosiphon labiatus* and *Salvia africana-lutea*. *Journal of Natural Products*, 70, 293-295.

UNIVERSITY of the WESTERN CAPE

https://etd.uwc.ac.za/

Kakarla, L., Katragadda, S.B., Tiwari, A.K., Kotamraju, K.S., Madhusudana, K., Kumar, D.A and Botlagunta, M. (2016). Free radical scavenging, alpha-glucosidase inhibitory and anti-inflammatory constituents from *Indian sedges*, *Cyperus scariosus* R.Br and *Cyperus rotundus* L. *Pharmacognosy Magazine*, 488-S496.

López, D., Cherigo, L., Spadafora, L., Loza-Mejía, M.A., Martínez-Luis, S. (2015). Phytochemical composition, antiparasitic and alpha-glucosidase inhibition activities from *Pelliciera rhizophorae*. *Chemistry Central Journal*, 9: 53.

Manning, J and Goldblatt, P. (2012). Plants of the greater Cape Floristic Region 1: The core Cape flora. *Strelitzia 29. South African National Biodiversity Institute, Pretoria.*, 29.

Masuda, T., Kirikihira, T and Takeda, Y. (2005). Recovery of antioxidant activity from carnosol quinone: Antioxidants obtained from a water-promoted conversion of carnosol quinone. *Journal of Agriculture and Food Chemistry*, 53, 6831-6834.

Mello, C., Crotti, A.E.M., Vessecchi, R., Cunha, W.R. (2006). 2D Raman spectroscopy as an alternative technique for distinguishing oleanoic acid and ursolic acid. *Journal of Molecular Structure*, 799(1-3), 141-145.

Naika, R.H., Bhavana, S., Teixeira, D.A., Silva, J.A., Lingaraju, K., Mohan, V.C and Krishna, V. (2016). In silico and in vivo wound healing studies of ursolic acid isolated from *Clematis gouriana* against GSK-3 beta. *Nusantara Bioscience*, 8(2), 232-244.

Nickavar, B., Abolhasani, L and Izadpanah, H. (2008). Alpha-amylase inhibitory activities of six tivities of six *Salvia* Species. *Iranian Journal of Pharmaceutical Research*, 7, 297-303.

Özgen, U., Mavi, A., Terzi, Z., Kazaz, C., Asci, A., Kaya, Y and Secen, H. (2011). *Records of Natural Products*, 5,12-21.

UNIVERSITY of the WESTERN CAPE

https://etd.uwc.ac.za/

Pellegrini, N., Re, R., Yang, M and Rice-Evans, C.A (1999). Screening of dietary carotenoid rich fruit extracts for antioxidant activities applying ABTS radical cation decolorisation assay. *Methods in Enzymology, 299,* 379-389.

Pérez-Fons, L., Garzón, M.T and Micol, V. (2010). Relationship between the antioxidant capacity and effect of rosemary (*Rosmarinus officinalis* L.) polyphenols on membrane phospholipid order. *Journal of Agriculture and Food Chemistry, 58*(1), 161-71.

Poongunran, J., Perera, H.K., Jayasinghe, L., Fernando, I.T., Sivakanesan, R., Araya, H and Fiyimoto, Y. (2016). Bioassay-guided fractionation and identification of alpha-amylase inhibitors from *Syzygium cumini* leaves. *Journal of Pharmaceutical Biology*, 55,1.

Raschi, A.B., Romano, E., Castillo, M.V., Leyton, P., Paipa, C., Maldonado, L.M and Brandán, S.A. (2014). Vibrational study of caffeic acid phenethyl ester, a potential anticancer agent, by infrared, Raman, and NMR spectroscopy. *Vibrational Spectroscopy*, 70, 100-109.

Ribeiro, N.C., Demuner, A.J., Dos Santos, M.H., Maltha, C.R.A., de Alvarenga, E.A and Komarnytsky, S. (2018). Metals complexes formed with oleanolic acid. *International Journal of Organic Chemistry*, 8, 160-169.

Sidan, J., Singh, S., Arora, S.K., Foley, W.J and Singh, I.P. (2012). Terpenoidal constituents of *Eucalyptus loxophleba* ssp. lissophloia. *Pharmaceutical Biology*, 50,7, 823-827.

Sofowora, A., Ogunbodede, E and Onayade, A. (2013). The Role and place of medicinal plants in the strategies for disease prevention. *African Journal of Traditional Complementary and Alternative Medecine*, 10,210–229.

Souza de Oliveira, F.F., Aguiar, P.N.C., Ribeiro, G.J.G., Lozer de Amorim, M.L., Guimarães, P.S.S., Filho, C.V.M., Sivieri, R.R.G., Brandão, M.G.L., Pio dos Santos, W.T and Grael,

UNIVERSITY of the WESTERN CAPE
https://etd.uwc.ac.za/

C.F.F. (2015). Antioxidant activity and phytochemical screening of extracts of *Erythroxylum suberosum* A.St.-Hil (Erythroxylaceae). *Research Journal of Phytochemistry, 9*(2), 9, 68-78.

Telagari, M and Hullatti,K. (2015). In-vitro alpha-amylase and alpha-glucosidase inhibitory activity of *Adiantum caudatum* Linn. and *Celosia argentea* Linn. extracts and fractions. *Indiam Journal of Pharmacology*, 47, 425-429.

Thilagam, E., Parimaladevi, B., Kumarappan, C and Mandal, S.C.J. (2013). Alpha-glucosidase and alpha-amylase inhibitory activity of *Senna surattensis*. *Acupuncture Meridian Studies*, 6, 24-30.

Yatoo, M.I., Dimri, U., Gopalakrishan, A., Saminathan, M., Dhama, K., Mathesh, K., Saxena, A., Gopinath, D and Husain, S. (2016). Antidiabetic and oxidative stress ameliorative potential of ethanolic extract of *Pedicularis longiflora Rudolph*. *International Journal of Pharmacology*, 12 (3), 177-187.

Yu, M.M.L., Schulze, H.G., Jetter, R., Blades, M.W and Turner, R.F.B. (2007). Raman microspectroscopic analysis of triterpenoids found in plant *Cuticles*. *Applied Spectroscopy*, 61(1), 32-37.

Zhang, B.W., Xing, Y., Wen, C., Yu, X.X., Sun, W.L., Xiu, Z.L and Dong, Y.S. (2017). Pentacyclic triterpenes as alpha-glucosidase and alpha-amylase inhibitors: Structure- activity relationships and the synergism with acarbose. *Bioorganic & Medicinal Chemistry Letters*, 27, 5065–5070.

UNIVERSITY of the WESTERN CAPE

https://etd.uwc.ac.za/

CHAPTER FOUR

PHYTOCHEMICAL AND BIOLOGICAL INVESTIGATION OF SALVIA AURITA

4.1 Abstract

The phytochemical investigation of *Salvia aurita* collected from Hogobach pass, Eastern Cape, South Africa (SA), afforded four known abietane diterpenes namely carnosol (**11**), rosmanol (**12**), 7-methoxyrosmanol (**13**), 12-methoxycarnosic acid (**14**) and one flavonoid named 4,7-dimethylapigenin (**15**). The chemical structural elucidation of the isolated compounds was determined on the basis of 1D and 2D NMR, FTIR, Raman spectroscopy and in comparison with literature data. All the compounds were isolated for the first time from *S. aurita*. The *in vitro* bio-evaluation against alpha-glucosidase showed strong inhibitory activities for **13** and **12** with IC_{50} values of 4.2 ± 0.7 and 16.4 ± 1.1 µg/mL respectively while **14** and **11** demonstrated strong *in vitro* alpha-amylase inhibitory activity among the tested compounds with IC_{50} of 16.2 ± 0.3 and 19.8 ± 1.4 µg/mL. Additionally, excellent total antioxidant capacities were demonstrated by **12**, **11** and **13** respectively as ORAC (25789.9 ± 10.5; 23961.8 ± 14.1; 23939.3 ± 2.4) µM TE/g; **11** and **12** as FRAP (3917.8 ± 2.1; 1522.3 ± 0.9) µM AAE/g; **15** and **12** as TEAC (3190.4 ± 2.8; 2055.0 ± 2.6) µM TE/g. The methanolic extract of *S. aurita is* a rich source of abietane diterpenes with strong antioxidant and anti-diabetic activities that can be helpful to regulate oxidative stress, and could therefore be excellent candidates for the prevention and management of diabetes complications. This is the first scientific report on the phytochemical isolation and in vitro bio-evaluation of alpha glucosidase and alpha amylase inhibitory activities of *Salvia aurita*.

https://etd.uwc.ac.za/

4.2 Background information on *Salvia aurita*

Salvia aurita (Lamiaceae, Salvia), commonly known as African blue sage, is an herbaceous perennial shrub native to South Africa. It is widely distributed in the Cape floristic region, KwaZulu-Nataland and Swaziland, where it grows up to 1.2 m (3.9 ft) tall on streambanks. The flowers are typically characteristic of sage with a two-lipped corolla and ranges from pale blue to lilac, white and white blushed with pink. The flowering time is mainly in spring and summer. *S. aurita* grows at altitudes of 5-1405 m in moist areas in valleys, open hillsides, renosterveld or along streams and in forests. *Salvia aurita* L.f, has demonstrated potential pharmaceutical application as antimicrobial, anti-oxidant, anti-inflammatory, antiplasmodial, cytotoxicity, antituberculosis (Kamatou, et al., 2008)

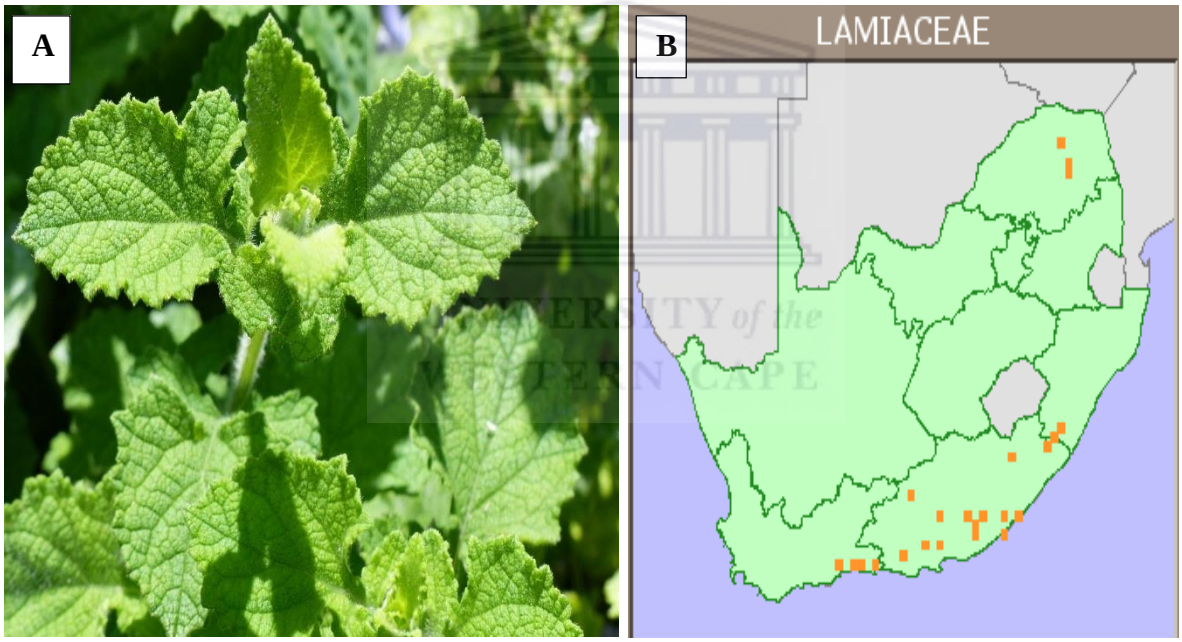

Retrieved from: http://pza.sanbi.org/salvia-aurita-var-aurita

Figure 4.1: *Salvia aurita* description (**A**), distribution along South African coastal (**B**)

https://etd.uwc.ac.za/

This chapter describes:

- Isolation of the different chemical constituents present in the methanolic extract of *Salvia aurita* using different chromatographic methods.
- Structural elucidation of each isolated compound using different spectroscopic techniques.
- In-vitro bio-evaluation of alpha-glucosidase and alpha-amylase inhibitory activities of the isolated compounds.
- Evaluation of the antioxidant capacities of the isolated compounds.

CHEMICAL CHARACTERIZATION OF *SALVIA AURITA* CONSTITUENTS

4.3 General experiment procedure

4.3.1 Reagents and solvents

All organic solvents described in section 3.3.1 were used

4.3.2 Thin layer chromatography (TLC)

Unless otherwise stated, the solvent systems generally used for the TLC development of *S. aurita* fractions are indicated in Table 4.1.

UNIVERSITY of the
WESTERN CAPE

Table 4.1: TLC solvent systems

Solvent system	Ratio	Assigned code
Hex - EtOAc	9:1	A
Hex - EtOAc	7:3	B
DCM - MeOH	9.5:0.5	C
DCM - MeOH	9:1	D
DCM - MeOH	7:3	E

Hex: hexane; EtOAc: ethylacetate; DCM: dichloromethane; MeOH: methanol

All other chromatographic of TLC, column, and HPLC techniques and procedures described in section 3.3.2 were followed.

https://etd.uwc.ac.za/

4.3.3 Spectroscopy

All analytical procedure of spectroscopic (NMR) techniques described in section 3.3.3 were followed.

4.4 Plant material

The aerial part of the plant material used in this study was collected in June 2017 from Eastern Cape, South Africa. A voucher specimen was identified at the Compton Herbarium, Kirstenbosch by Prof. Christopher Cupido

4.5 Extraction and purification of chemical constituents

The aerial part of the fresh plant material (855.1 g) were blended and extracted with methanol (4.5 L) at room temperature (25 ^{o}C) for 24 h. The methanol extract was filtered and evaporated to dryness under reduced pressure at 40 ^{o}C to yield 64.62 g (5.6 %). The total extract (62 g) was applied to a silica gel column (25 x 18 cm) and eluted using gradient of Hex and EtOAc in order of increasing polarity. Sixty-two (62) fractions (500 mL each) were collected and combined according to their TLC profiles to yield seventeen fractions labelled I-XVII as shown in Table 4.2.

UNIVERSITY of the
WESTERN CAPE

https://etd.uwc.ac.za/

Table 4.2: Fractionation of the extract of *S. aurita*

Solvent system	Solvent volume	Fraction collected
Hex	2L	1-4
Hex - EtOAc (95:5)	2L	5-8
Hex - EtOAc (90:10)	2L	9-12
Hex - EtOAc (85:15)	2L	13-16
Hex - EtOAc (80:20)	2L	17-20
Hex - EtOAc (75:25)	2L	21-24
Hex - EtOAc (70:30)	2L	25-28
Hex - EtOAc (65:45)	2L	29-32
Hex - EtOAc (60:40)	2L	33-36
Hex - EtOAc (55:45)	2L	37-40
Hex - EtOAc (50:50)	2L	41-44
Hex - EtOAc (40:60)	2L	45-48
Hex - EtOAc (20:80)	2L	49-52
Hex - EtOAc (10:90)	2L	53-56
EtOAc	3L	57-62

UNIVERSITY of the
WESTERN CAPE

The collected fractions (1-62) were concentrated and combined according to their TLC profiles using solvent system C to yield seventeen (17) main fractions (Fig 4.2). The roman numbers (I-XVII) were used as to code the obtained fractions and the results are summarized in Table 4.3.

https://etd.uwc.ac.za/

Table 4.3: Fractions obtained upon fractionation of total extract of *S. aurita*

Combined fraction	Designated number	Code	Weight of fractions (mg)
1-3	I	SA-I	5462.2
4-5	II	SA-II	2444.5
6-7	III	SA-III	616.5
8-9	IV	SA-IV	1181.4
10-12	V	SA-V	742.5
13-14	VI	SA-VI	183.8
15-17	VII	SA-VII	910.4
18-20	VIII	SA-VIII	727.4
21-22	IX	SA-IX	675.1
23-24	X	SA-X	2162.4
25-27	XI	SA-XI	1504.3
28-29	XII	SA-XII	258.8
30-33	XIII	SA-XIII	1045.3
34-37	XIV	SA-XIV	1077.9
38-41	XV	SA-XV	441.4
42-46	XVI	SA-XVI	397.1
47-62	XVII	SA-XVII	199.8

UNIVERSITY of the WESTERN CAPE

https://etd.uwc.ac.za/

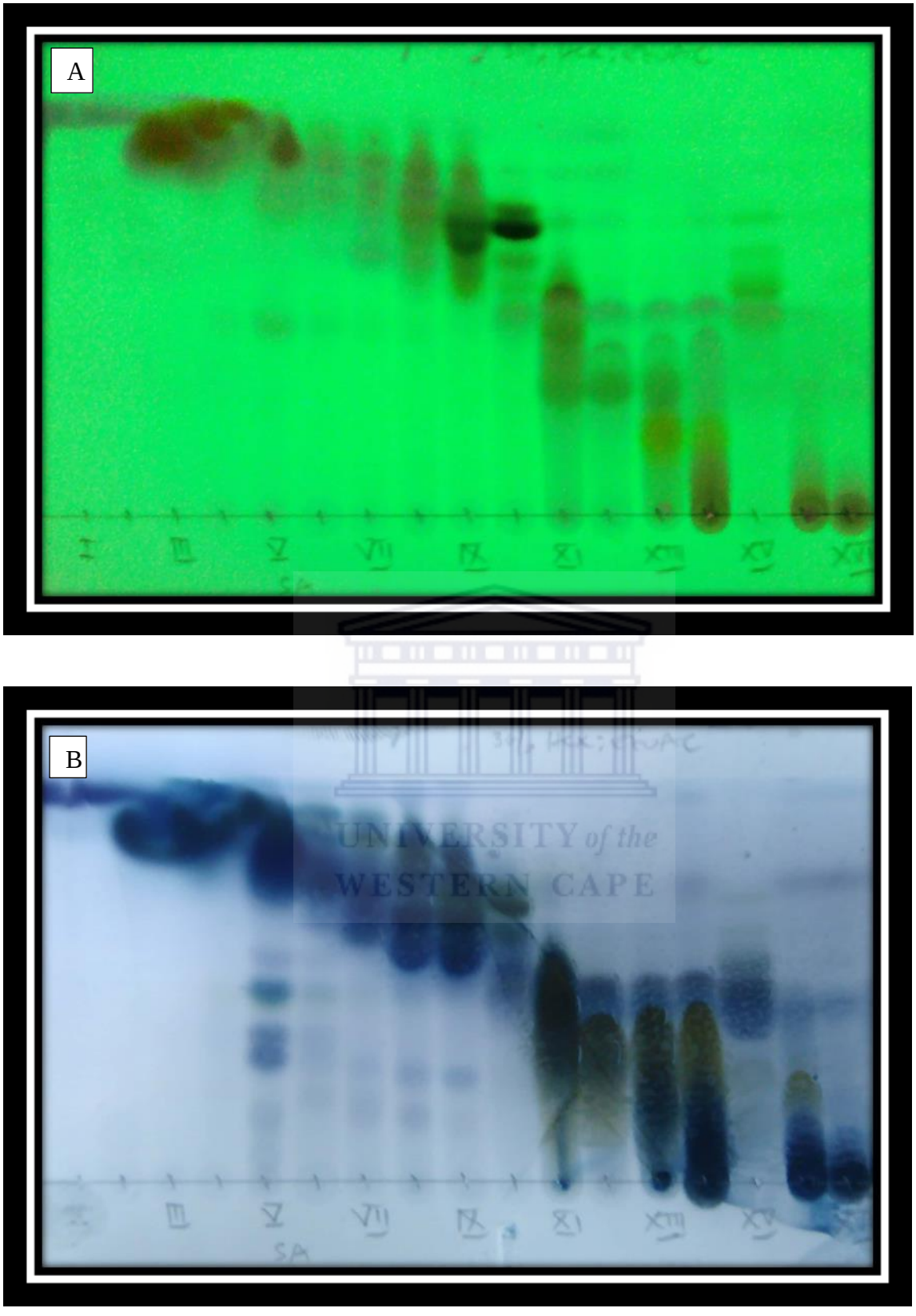

Figure 4.2: TLC plate (silica gel) of combined fractions under UV (254 nm; A), and after spraying with H_2SO_4/vanillin and then heated (B). TLC was developed using solvent system C

UNIVERSITY of the WESTERN CAPE
https://etd.uwc.ac.za/

4.6 Isolation of pure compounds

4.6.1 Isolation of compound 11

Main fraction XIII (1040 mg) was subjected to successive silica gel column using Hex/EtOAc gradient (7:3 and 100%), then sephadex (using 95% aqueous methanol). Fractions of 5 mL each were collected and evaporated using rotary evaporator. Fractions obtained were developed on TLC using solvent system C and the fractions that displayed the same profiles on the TLC plate were combined as indicated in Table 4.4.

Table 4.4: Fractions grouped from the column

Fraction	Weight (mg)	Assigned code
1-3	33.2	SA-XIII-1
4-6	94.5	SA-XIII-2
7-10	169.2	SA-XIII-3
11-15	255.8	SA-XIII-4
16-19	154.5	SA-XIII-5

UNIVERSITY of the
WESTERN CAPE

https://etd.uwc.ac.za/

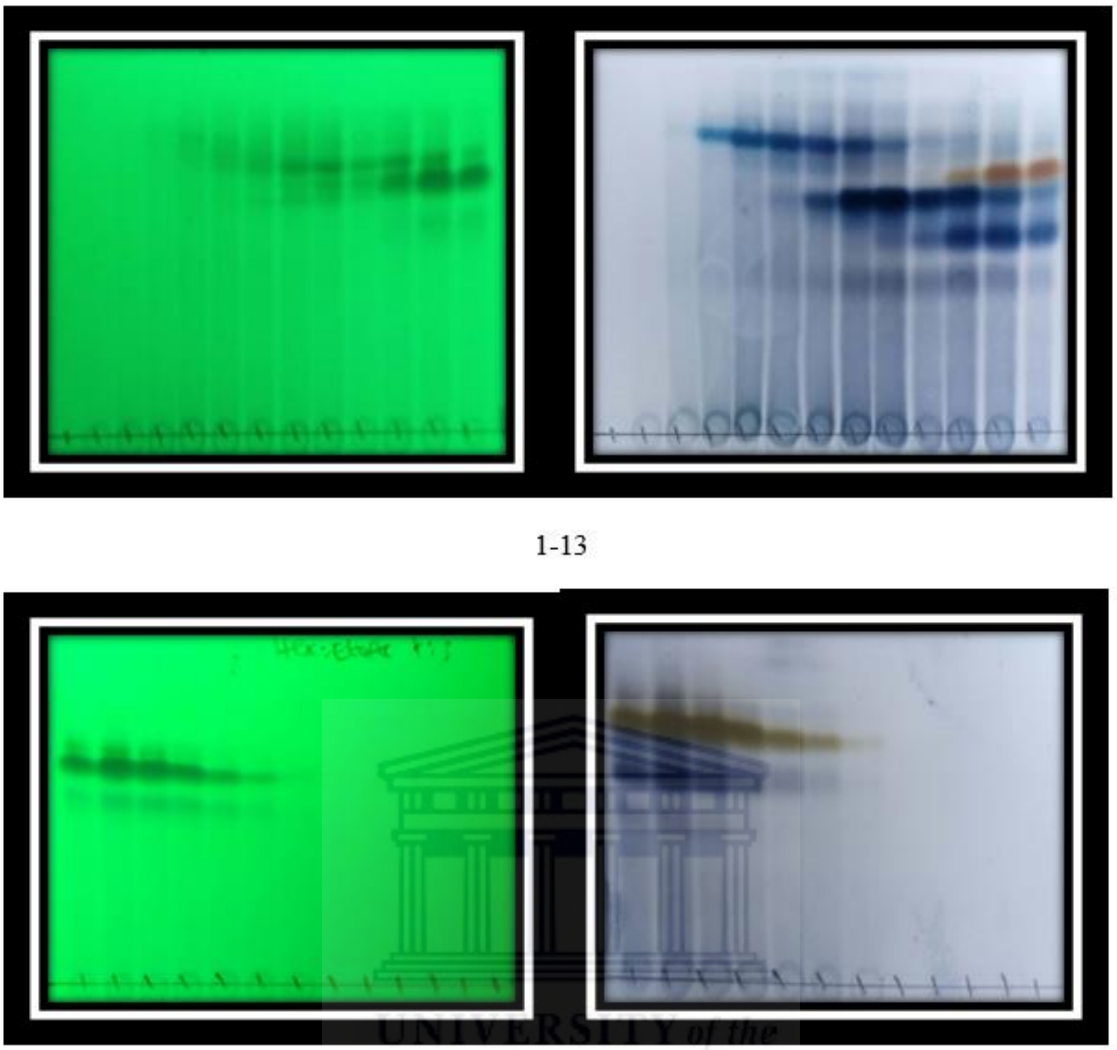

UNIVERSITY of the
WESTERN CAPE

Figure 4.3: TLC plate of combined fractions of SA-XIII

Sub fraction XIII-5 (154.5 mg) was injected to the HPLC and eluted using gradient solvent system of MeOH and de-ionized water (70:30 to 100% MeOH in 45 min), which afforded a prominent peak as shown in Figure 4.4B, collected and labelled as **SA-XI-5-2**. After spotting and developing the collected fractions on TLC plate using solvent system C, a single spot suspected to be a pure compound was observed (Fig 4.4A). The fraction that afforded this single spot was labelled as **11** (R_t 14.06 min, 19.9 mg, 0.023%).

https://etd.uwc.ac.za/

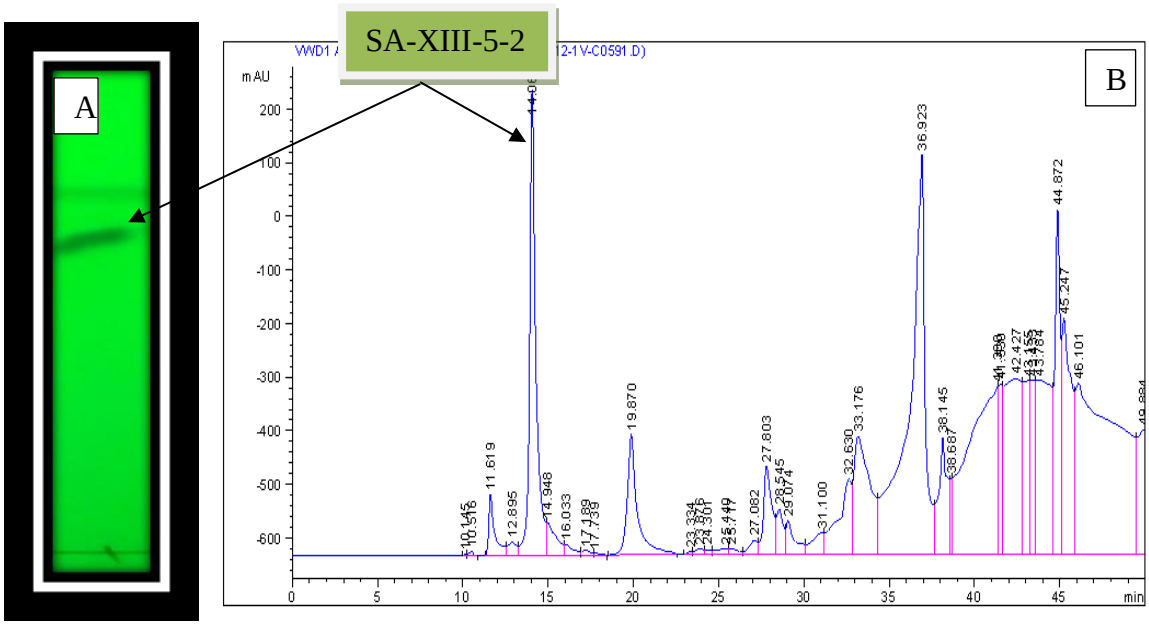

Figure 4.4: TLC plate of SA-XIII-5-2 (Fig. 4.4A), solvent system C and HPLC chromatogram of sub fraction XIII-5 (Fig. 4.4B).

***Conditions**

Solvent	MeOH:DIW 70:30 to 100% in 45 min
Column	SUPELCO, RP-18 (25 x 1 cm)
Flow rate	1.0 mL/min
Detection	UV at 290 nm

4.6.2 Isolation of compound 12

Sub fraction XIII-4 (255 mg) was injected to the HPLC and eluted using gradient solvent system of MeOH and de-ionized water (70:30 to 100% MeOH in 45 min), which afforded prominent peak as shown in Figure 4.5B, collected and labelled as **SA-XIII-4-6**. After spotting and developing the collected fractions on TLC plate using solvent system C, a single spot suspected to be a pure compound was observed (Fig 4.5A). The fraction that afforded this single spot was labelled as **12** (R_t 27.09 min, 11.2 mg, 0.013%).

https://etd.uwc.ac.za/

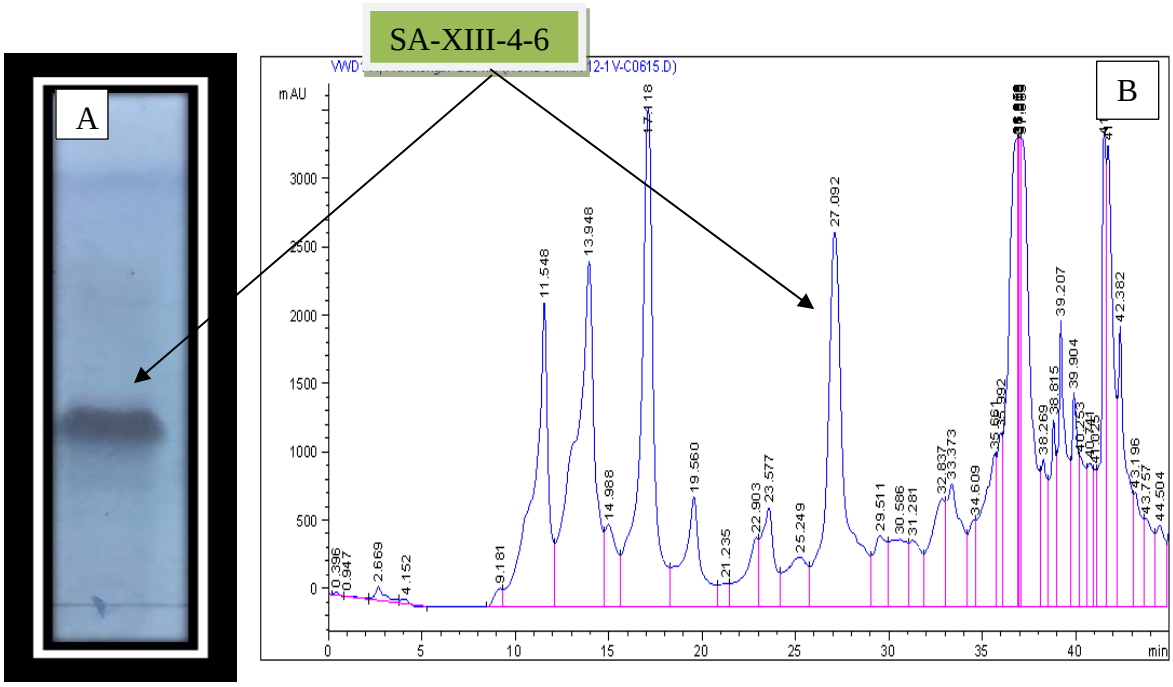

Figure 4.5: TLC plate of SA-XIII-4-6 (Fig. 4.5A) and HPLC chromatogram of sub fraction XIII-4 (Fig. 4.5B).

***Conditions**

Solvent	MeOH:DIW 70:30 to 100% in 45 min
Column	SUPELCO, RP-18 (25 x 1 cm)
Flow rate	1.0 mL/min
Detection	UV at 290 nm

UNIVERSITY of the WESTERN CAPE

4.6.3 Isolation of compound 13 and 15

Main fraction XIV (1077 mg) was subjected to successive silica gel column using Hex/EtOAc gradient (7:3 and 100%), then sephadex (using 95% aqueous methanol). Fractions of 5 mL each were collected and evaporated using rotary evaporator. Fractions obtained were developed on TLC using solvent system C and the fractions that displayed same profiles on the TLC plate were combined as indicated in Table 4.5.

https://etd.uwc.ac.za/

Table 4.5: Fractions grouped from the column

Fraction	Weight (mg)	Assigned code
1-6	33.2	SA-XIV-1
7-21	694.5	SA-XIV-2
22-26	269.2	SA-XIV-3
27-33	155.8	SA-XIV-4
34-39	98.3	SA-XIV-5
40-53	23.7	SA-XIV-6

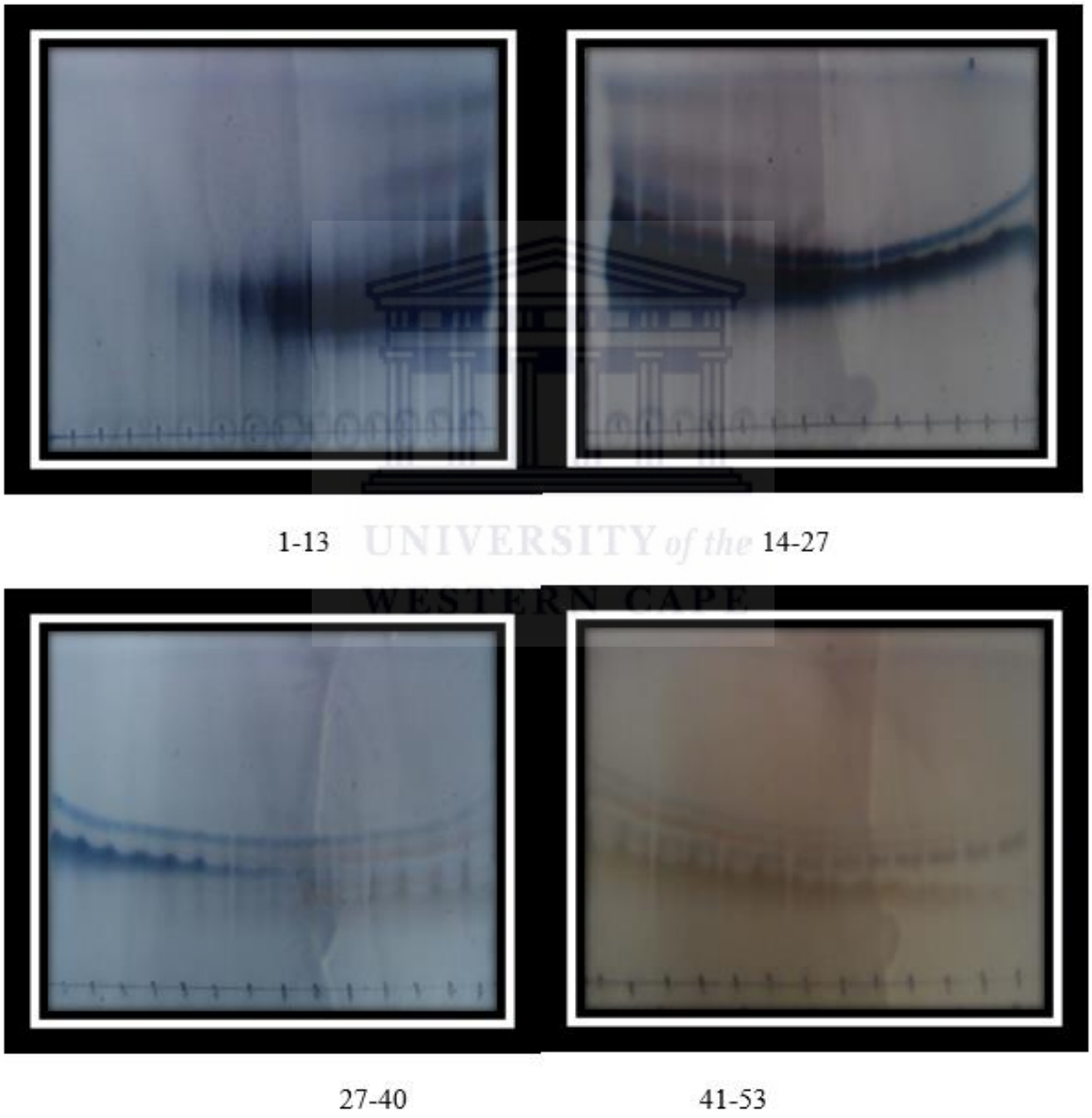

Figure 4.6: TLC plate of combined fractions of SA-XIV

https://etd.uwc.ac.za/

Sub fraction SA-XIV-2 (694.5 mg) was injected to the HPLC and eluted using gradient solvent system of MeOH and de-ionized water (70:30 to 100% MeOH in 45 min), which afforded two prominent peaks as shown in Figure 4.4B, collected and labelled as **SA-XIII-2-4** and **SA-XIV-2-6**. After spotting and developing the fractions on TLC plate using solvent system C, single spots suspected to be a pure compound were observed (Fig 4.7A). The fractions that afforded those single spot were pooled together and labelled as **13** (R_t 19.65 min, 7.1 mg, 0.023%) and **15** (R_t 27.41 min, 7.2 mg, 0.0084%).

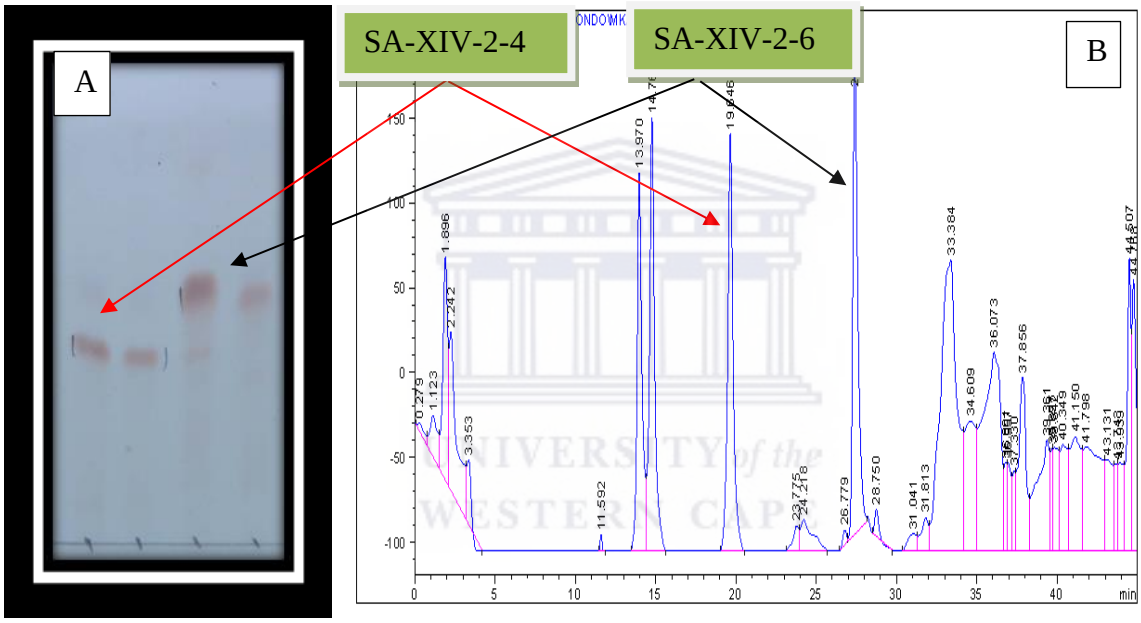

Figure 4.7: TLC silica gel of SA-XIV-2-4 and SA-XIV-2-6 (Fig. 4.7A) and their HPLC chromatogram of XIV-2 (Fig. 4.7B)

***Conditions**

Solvent	MeOH:DIW 70:30 to 100% in 45 min
Column	SUPELCO, RP-18 (25 x 1 cm)
Flow rate	1.0 mL/min
Detection	UV at 290 nm

https://etd.uwc.ac.za/

4.6.5 Isolation of compound 14

Main fraction XI (1504.3 mg) was subjected to successive silica gel column using Hex/EtOAc gradient (7:3 and 100%), then Sephadex (using 95% aqueous ethanol). Fractions of 5 mL each were collected and evaporated using rotary evaporator. Fractions obtained were developed on TLC using solvent system C and the fractions that displayed same profiles on the TLC plate were combined as indicated in Table 4.6.

Table 4.6: Fractions grouped from the column

Fraction	Weight (mg)	Assigned code
1-6	33.2	SA-XI-1
7-10	94.5	SA-XI-2
11-15	169.2	SA-XI-3
16-22	84.5	SA-XI-4

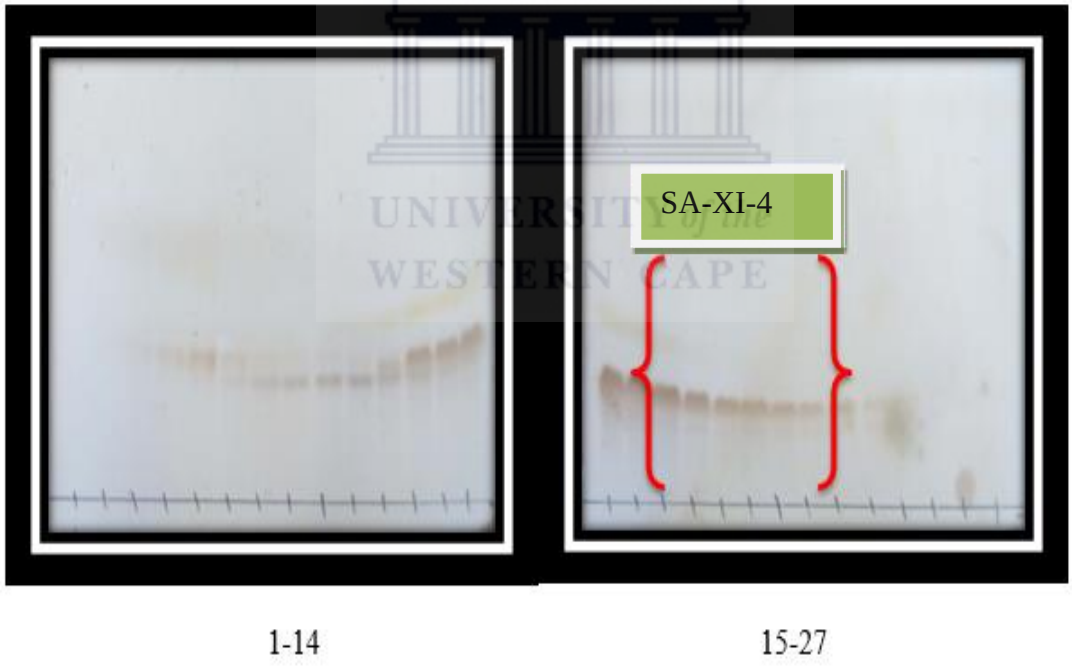

Figure 4.8: TLC plate of combined fractions of SA-XI-4

Fractions 16-22 were suspected pure due to its single spot after development on TLC using solvent system C (Fig. 4.8). These fractions (16-22) were pooled together, evaporated and re-spotted using solvent system C to further confirm the purity of the combined fractions. The

https://etd.uwc.ac.za/

TLC showed only single spot after development, confirmed the purity and labelled the compound as **14** (15.2 mg, 0.017%).

UNIVERSITY of the
WESTERN CAPE

https://etd.uwc.ac.za/

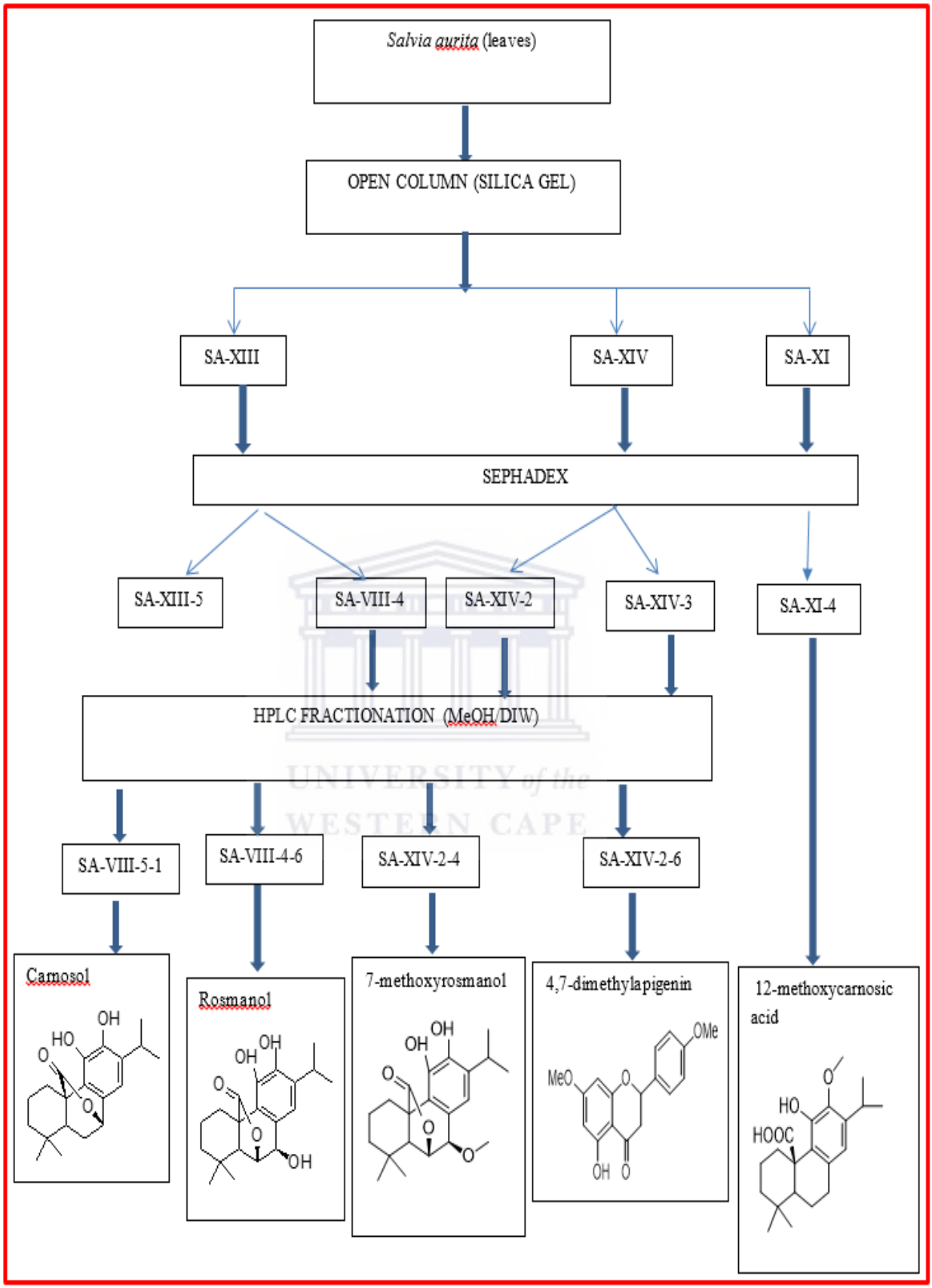

Scheme 4.1: A flow diagram of experimental procedure for the isolation of compounds from *S. aurita*

https://etd.uwc.ac.za/

BIOLOGICAL CHARACTERIZATION OF ISOLATED COMPOUNDS

4.7.1 General experimental procedure for biological assays

4.7.1.1 Reagents

4.7.2 Alpha-glucosidase inhibitory activity

Alpha-glucosidase assay described in section 3.7.2 was carried out.

4.7.3 Alpha-amylase inhibitory activity

Alpha-amylase assay described in section 3.7.3 was carried out.

4.7.4 Total Antioxidant capacities assays

All experimental procedure for the various antioxidant capacity assays (FRAP, ORAC, and TEAC) as described in section 3.7.4 were followed.

4.8 Statistical analysis

Statistical analyses described in section 3.8 was followed

4.9 Results and discussion: Chemical characterization

Chromatographic purification of a methanolic extract of *S. aurita* using different techniques including semi Prep-HPLC yielded four pure terpenoids and one flavonoid (Fig. 4.9). These compounds have been isolated for the first time from *S. aurita.*

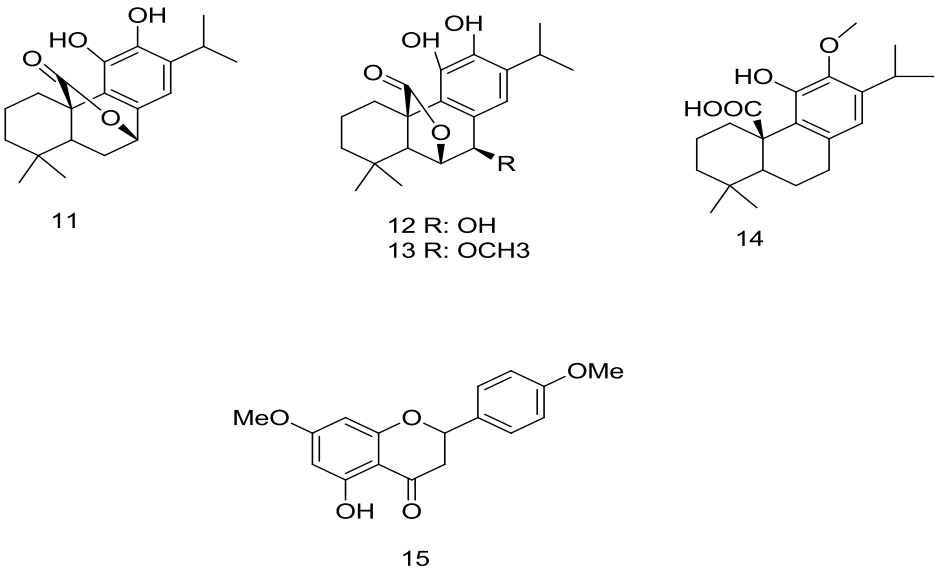

Figure 4.9: Chemical structures of the isolated compounds (**11-15**) from *S. aurita*

https://etd.uwc.ac.za/

4.9.1 Structure elucidation of carnosol (**11**)

Compound **11** (19.9 mg) (Fig. 4.10) was isolated as a white powder as described in Scheme 4.1. Its IR spectrum exhibited bands at 1713 cm^{-1} for the carbonyl lactone group (C=O), 2952 and 2868 for the carbon-hydrogen stretching (C-H) as well as at 3276 cm^{-1} attributed hydroxyl group (OH), which is in agreement the reported data (Fig. 4.14) (Bajpai & Kang, 2015). The Raman spectrum featured characteristic bands at 1661 cm^{-1} related to C=C stretching, 1566 cm^{-1} related to C-C stretching, 1491 and 1441 cm^{-1} related to the deformation vibration of the CH_2/CH_3, 1246 related to C-H deformation in unconjugated cis-double bond (Fig. 4.15) (Belt, et al., 2017; Chain, et al., 2015; Raschi, et al., 2014). It was identified as carnosol based on its NMR data. ^{1}H NMR (Table 4.7) showed two singlets of germinal methyls at 0.86 and 0.90 (Me-18, 19) and two doublets counted for six protons at 1.22 and 1.24 (Me-16, and 17) coupled to a septet at 3.08 (H-15) suggested the presence of an isopropyl group attached to an aromatic ring. The H-5 was coupled with two protons of C-6, a low field shift proton at 5.38 (*dd*, H-7α), a singlet at 6.64 for the aromatic proton H-14. The ^{13}C NMR showed 20 carbons which confirmed the diterpene skeleton. DEPT-135 and HSQC split those carbons into four methyls (22.5/C-16, 22.4/C-17; 31.7/C-18 and 19.7/C-19); four methylenes (29.2/C-1; 18.9/C-2; 41.0/C-3; 29.7/C-6); four methines; one aromatic (112.3/C-14); one hydroxylated (77.9/C-7); in addition, the five signals of 5 aromatic carbons (132.1/C-8; 121.6/C-9; 141.7/C-11; 141.1/C-12; 132.8/C-13) and a carbonyl group (175.8/C-20). The HMBC showed cross peak correlation of H-14 with C-15; C-7; C-9; C11 and/or C-12, H7/C-5; C-6; C-14; C-9; C-8; C-20; C-12, H-15/C-16,17; C-14; C-13; C-11 and C-12. The above data with 2D NMR experiments (HSQC, HMC, and COSY) established the structure of carnosol (**11**) and finally confirmed by comparing the experimental data with literature (Bajpai, et al., 2015; Etsassala, et al., 2019)

https://etd.uwc.ac.za/

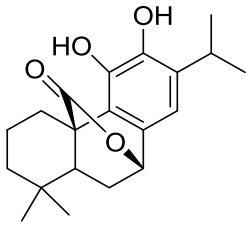

Carnosol

Figure 4.10: Chemical structure of **11**

Table 4.7: ^{1}H and ^{13}C NMR spectroscopic data assignments (400 MHz) for compound **11** (δ in ppm, m, *J* in Hz) in $CDCl_3$

	11		
N^{O}	δ_H (*J* in Hz)	^{13}C	Multiplicity
1	2.91 br d (12.8) 2.40 ddd (4.32, 13.2, 13.2)	29.7	CH_2
2	1.87 dddd (1.4, 10.6, 10.6, 10.6) 1.60 m	18.9	CH_2
3	1.32 d (14.1) 1.30 dd (3.8, 13.6)	41.0	CH_2
4		34.5	C
5	1.6*	45.4	CH
6	1.88 ddd 1.64; 10.8; 10.8 2.03)	29.2	CH_2
7	5.38 dd (1.3; 1.3)	77.9	CH
8		132.1	C
9		121.6	C
10		48.4	C
11		141.1	C
12		141.7	C
13		132.8	C
14	6.64 s	112.3	CH
15	3.08 sept (6.9)	27.3	CH
16	1.22 d (1.6)	22.45	CH_3
17	1.24 d (1.6)	22.52	CH_3
18	0.86 s	31.7	CH_3
19	0.90 s	19.7	CH_3
20		175.8	C

UNIVERSITY of the WESTERN CAPE

https://etd.uwc.ac.za/

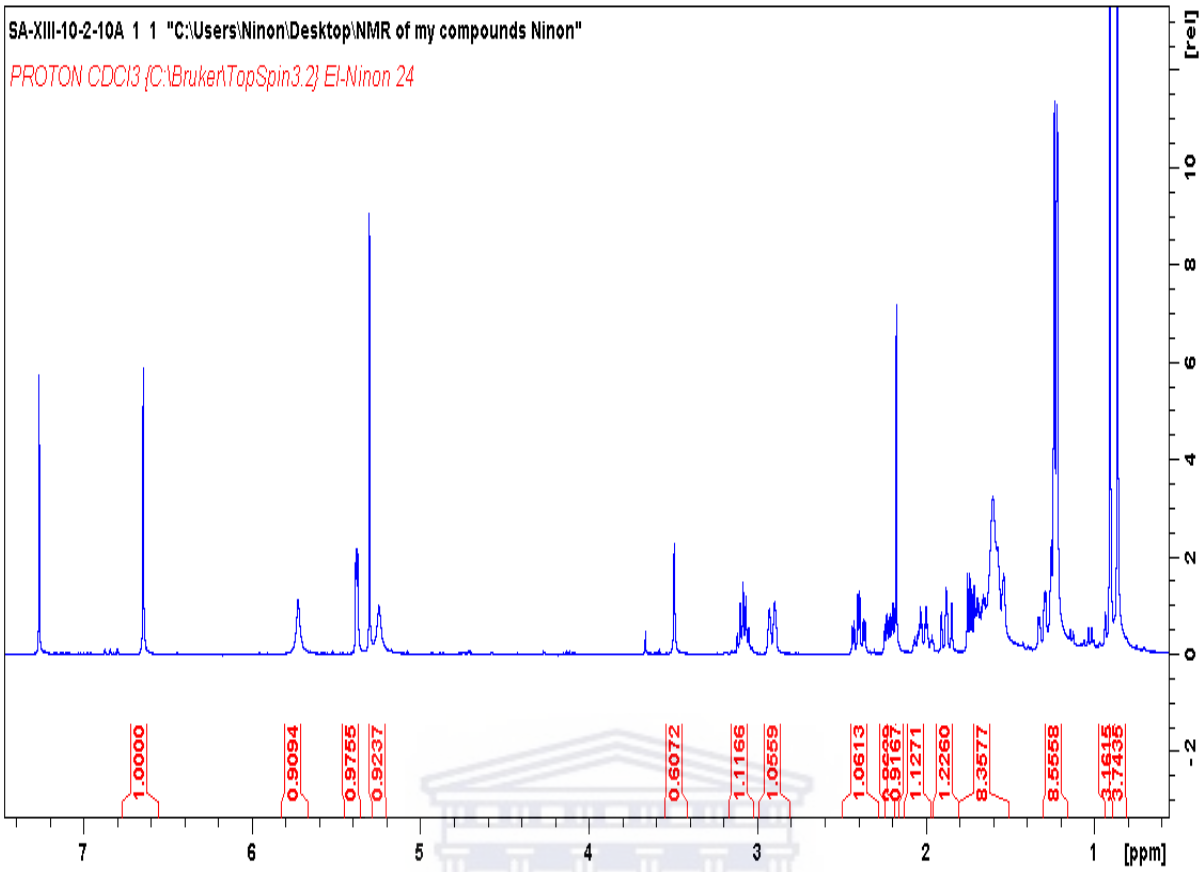

Figure 4.11: ^{1}H NMR (400 MHz, CDCl3) spectrum of **11**

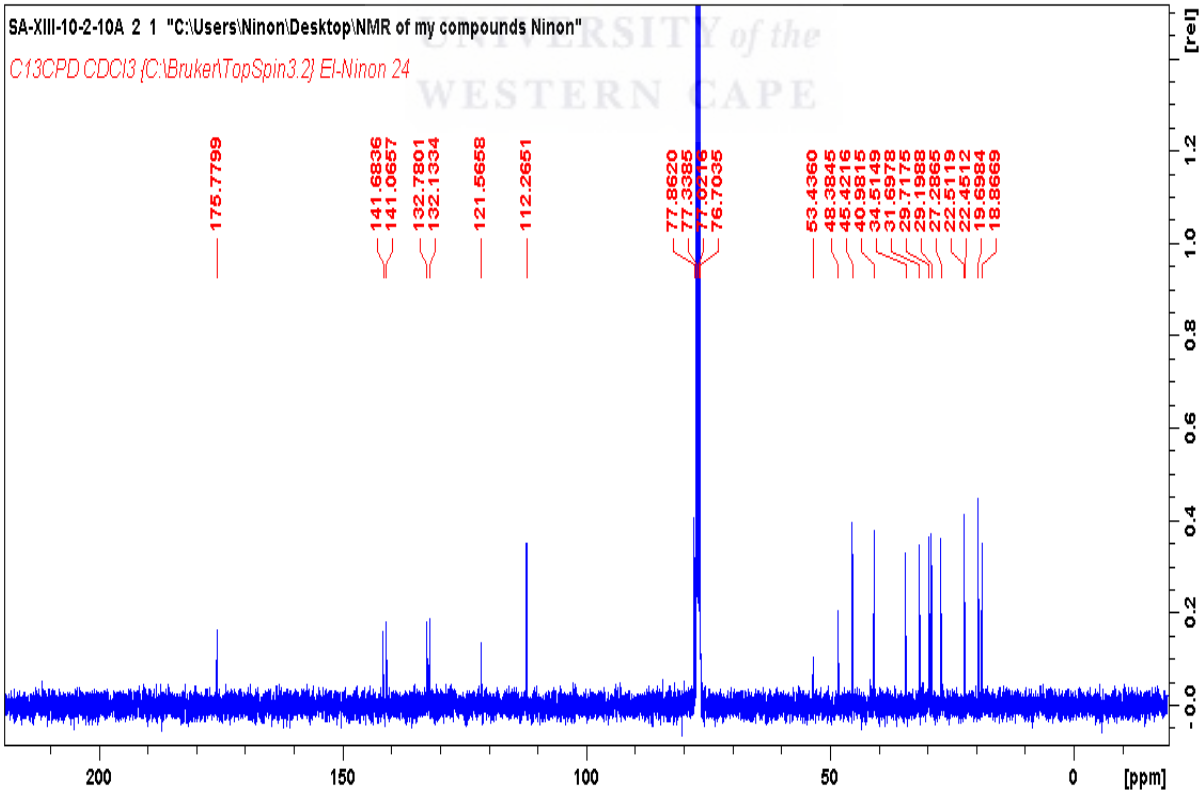

Figure 4.12: ^{13}C NMR (400 MHz, CDCl3) spectrum of **11**

https://etd.uwc.ac.za/

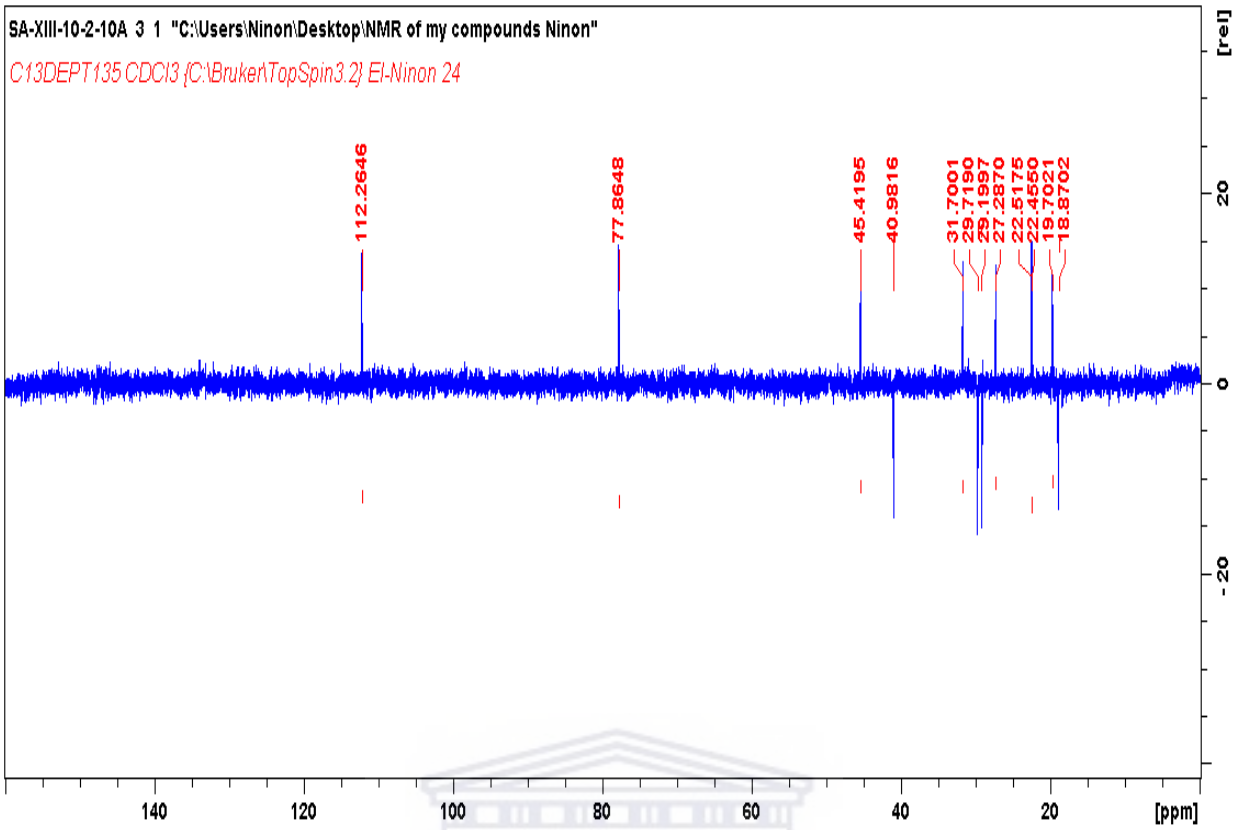

Figure 4.13: DEPT NMR (400 MHz, CDCl3) spectrum of **11**

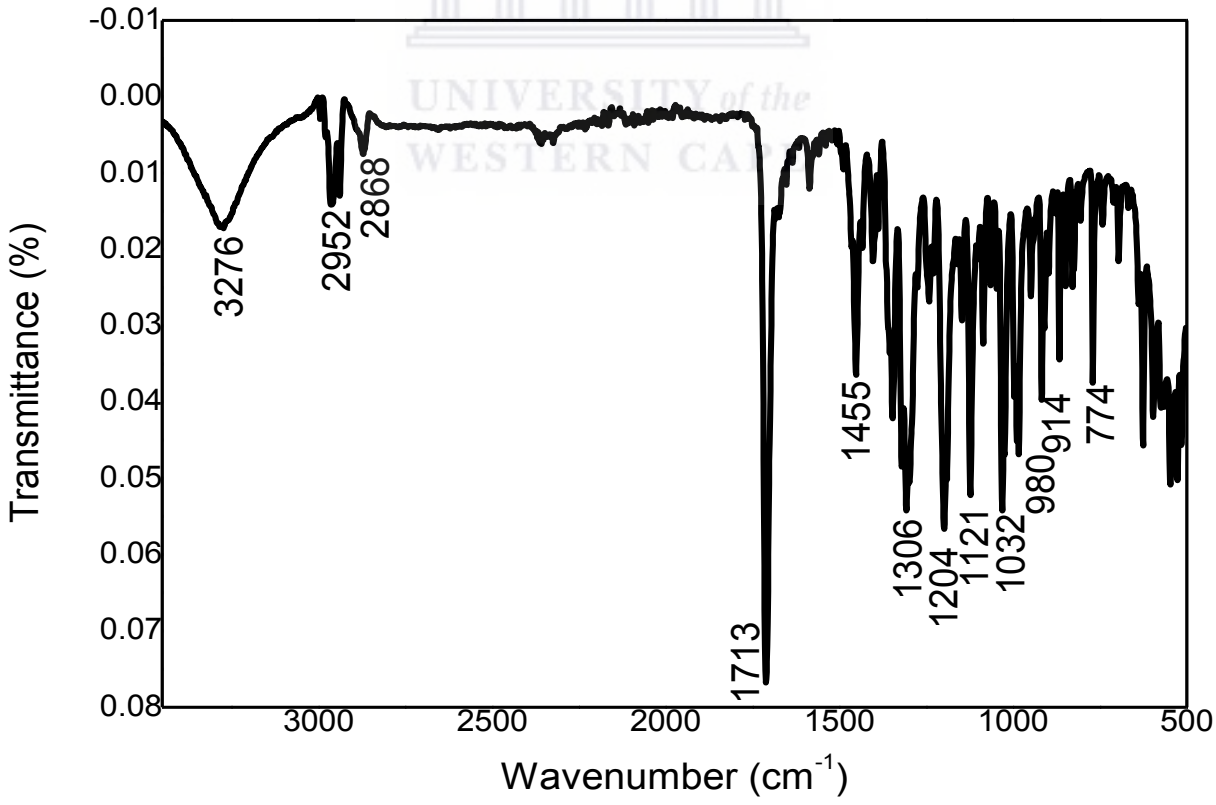

Figure 4.14: FTIR spectrum of **11**

https://etd.uwc.ac.za/

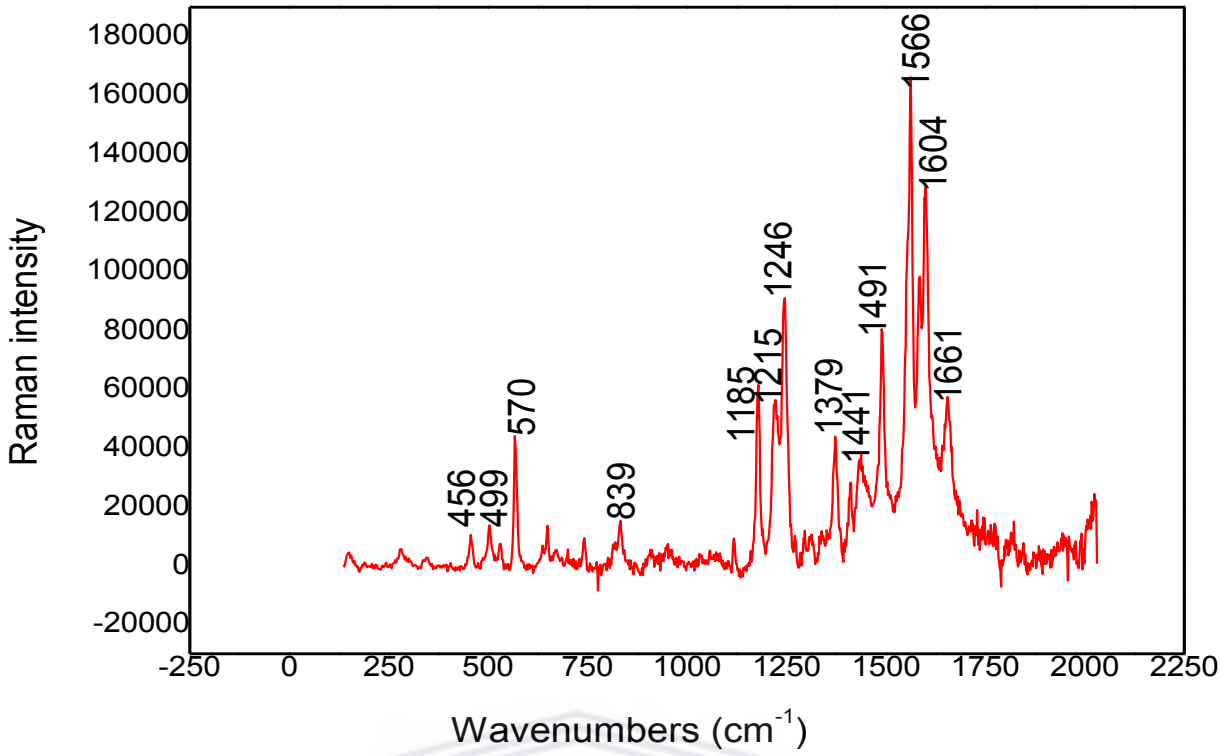

Figure 4.15: Raman spectrum of **11**

RAMAN	Intensity	Assignments
839	w	CH_2 torsion
1215	n	C-H deformation
1246	n	C-H deformation
1379	n	CH_2 wagging
1441	n	CH_2 deformation
1491	n	CH_3 deformation
1566	s	C-C stretching
1604	s	C=C stretching
1661	n	C=C stretching

4.9.2 Structure elucidation of rosmanol (**12**)

Compound **12** (7.1 mg) (Fig. 4.16) was isolated as brown amorphous solid as described in Scheme 4.1. Its IR spectrum exhibited bands at 1752 cm^{-1} for the carbonyl lactone group (C=O), 2945 and 2867 for the carbon-hydrogen stretching (C-H) as well as at 3344 cm^{-1} attributed hydroxyl group (OH), which is in agreement the report data (Fig. 4.20) (Bajpai & Kang, 2015). The Raman spectrum featured characteristic bands at 1924 cm^{-1} related to C-H stretching, 1611 cm^{-1} related to C=C stretching, 1510 cm^{-1} related to C-C stretching, 1453

https://etd.uwc.ac.za/

cm^{-1} related to the deformation vibration of the CH_2, 1354 cm^{-1} related to the CH3 bond vibrations (Fig. 4.21) (Belt, et al., 2017; Chain, et al., 2015; Raschi, et al., 2014). The NMR data of compound **12** showed a typical abietane diterpene skeleton which is similar to compound **11**. The ^{1}H NMR (Table 4.8) showed two doublet signals at 4.49 (*d*, $J_{6.7}$ = 2.7 Hz; H-6); 4.67 (*d*, $J_{6.7}$ = 3.0 Hz; H-7), and a singlet at 6.79 for the aromatic proton H-14; a septet at 3.01 ($J_{15\text{-}16/\text{-}17}$ = 6.9 Hz; H-15); 3.09 (*br d* $J_{1\beta}$ = 13.2 in addition to four methyl signals, two of them appeared as doublets at 1.14 and 1.15 (Me-16; 17; *J* = 6.2 Hz); and the other two as singlets at 0.94 (Me-18) and 0.84 (Me-19). The ^{13}C NMR and DEPT-135 showed 20 carbons, four of them are methyls (22.0; 22.5; 31.5 and 22.2 for Me's 16-19), three methylene signals at 27.3; 19.0 and 38.1 (C1-C3 respectively); five methines, two of them are oxygenated at 78.1/C-6 and 68.4/C-7 and one aromatic at 120.2/C-14, the other two methines attributed to C-5 (50.7) and C-15/27.3. In addition to seven quaternary carbons, five of them belong to the aromatic ring 128.0, 124.4, 142.7, 141.8, 135.0 (C-8, C-9, C-11-C13 respectively) and a carbonyl group at 178.8 (C-20); the other two quaternary carbons belong to C-10 and C-4 (at 47.1 and 31.4). The chemical shift of C-20 appeared at higher field, which indicated the formation of lactone ring, the H-6 only coupled with H-7 but not with H-5, which indicate the 90^o coplanar of H-5 and H-6 and confirm the lactonization at C-6. Finally, the NMR data of rosmanol was identical with those published in literature (Bajpai & Kang, 2015) and established the structure of as rosmanol.

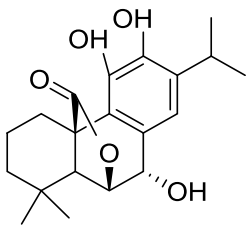

Rosmanol

Figure 4.16: Chemical structure of **12**

https://etd.uwc.ac.za/

Table 4.8: ^{1}H and ^{13}C NMR spectroscopic data assignments (400 MHz) for compound **12** (δ in ppm, m, *J* in Hz) in $CDCl_3$

	12		
N^{O}	δ_H (*J* in Hz)	^{13}C	Multiplicity
1	3.09 br d (14.2) 1.97 ddd (4.4, 13.2, 13.2)	29.3	CH_2
2	1.60 m 1.47 m	19.0	CH_2
3	1.27 ddd 1.41 br d (12.5)	38.1	CH_2
4		31.4	C
5	2.1 s	50.7	CH
6	4.49 d (2.7)	78.1	CH
7	4.67 d (3.0)	68.4	CH
8		128.0	C
9		124.4	C
10		47.1	C
11		142.7	C
12		141.8	C
13		135.0	C
14	6.8 s	120.2	CH
15	3.01 sept (6.3)	27.3	CH
16	1.14 d (6.2)	22.0	CH_3
17	1.15 d (6.2)	22.5	CH_3
18	0.94 s	31.5	CH_3
19	0.84 s	22.2	CH_3
20		178.8	C

UNIVERSITY of the
WESTERN CAPE

https://etd.uwc.ac.za/

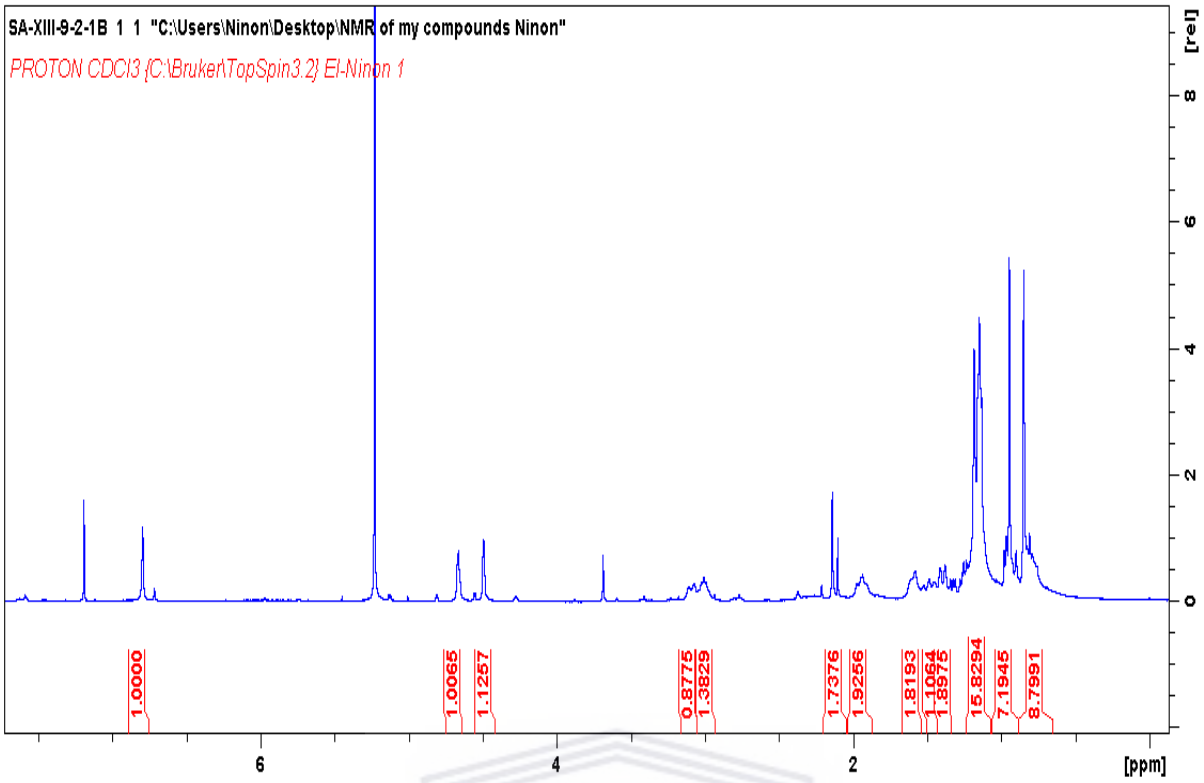

Figure 4.17: ^{1}H NMR (400 MHz, CDCl3) Spectrum of **12**

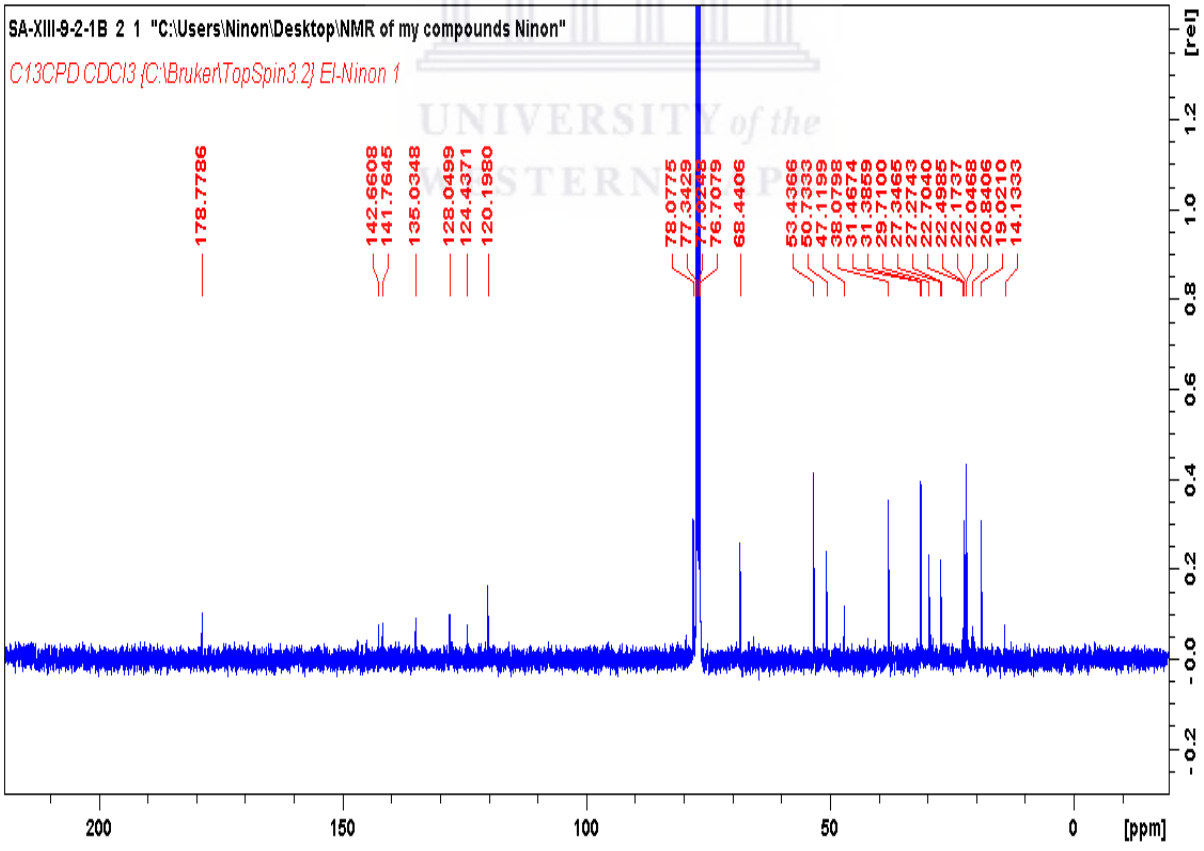

Figure 4.18: ^{13}C NMR (400 MHz, CDCl3) Spectrum of **12**

https://etd.uwc.ac.za/

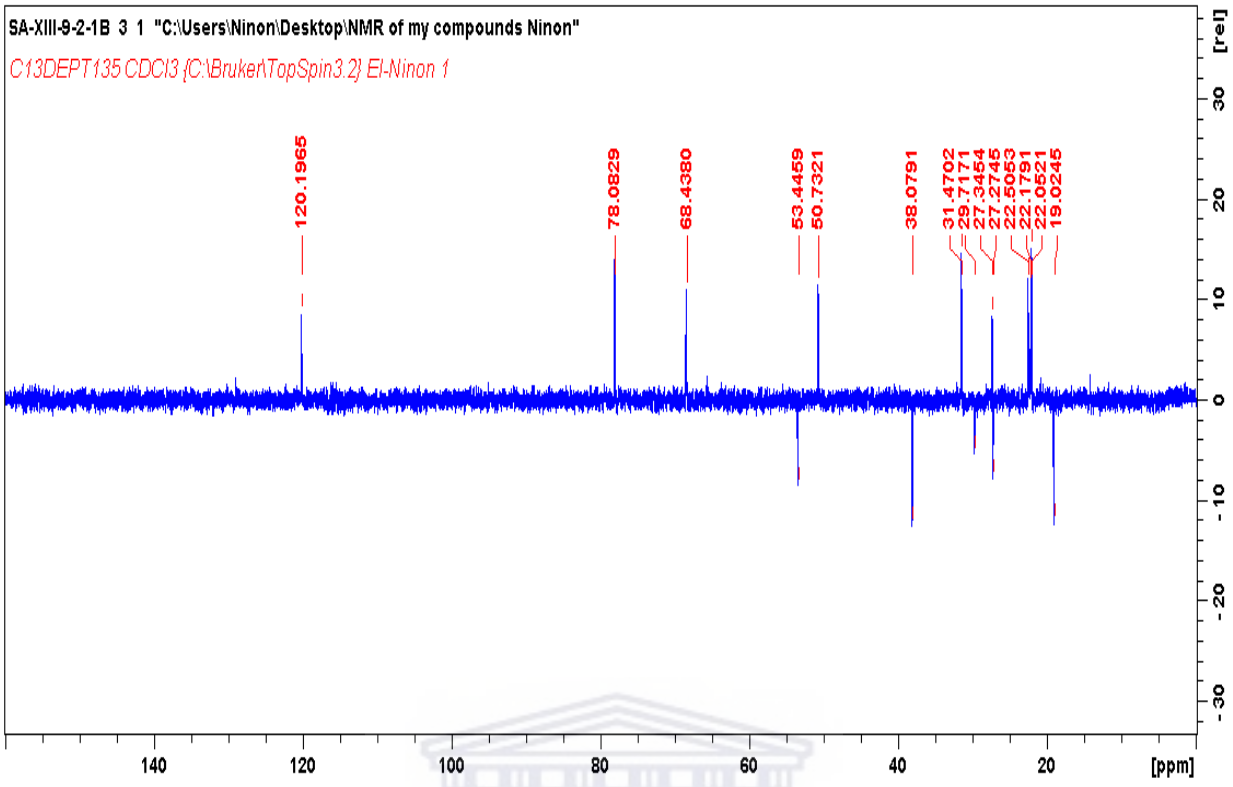

Figure 4.19: DEPT NMR (400 MHz, CDCl3) Spectrum of **12**

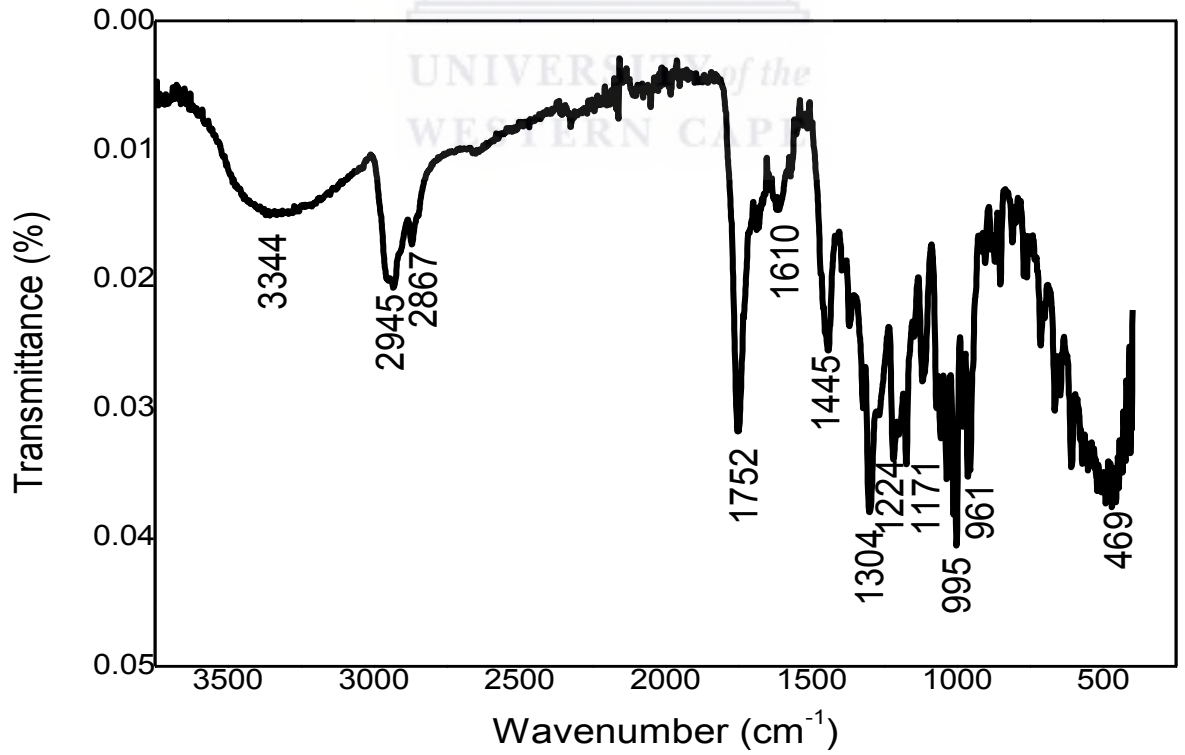

Figure 4.20: FTIR spectrum of **12**

https://etd.uwc.ac.za/

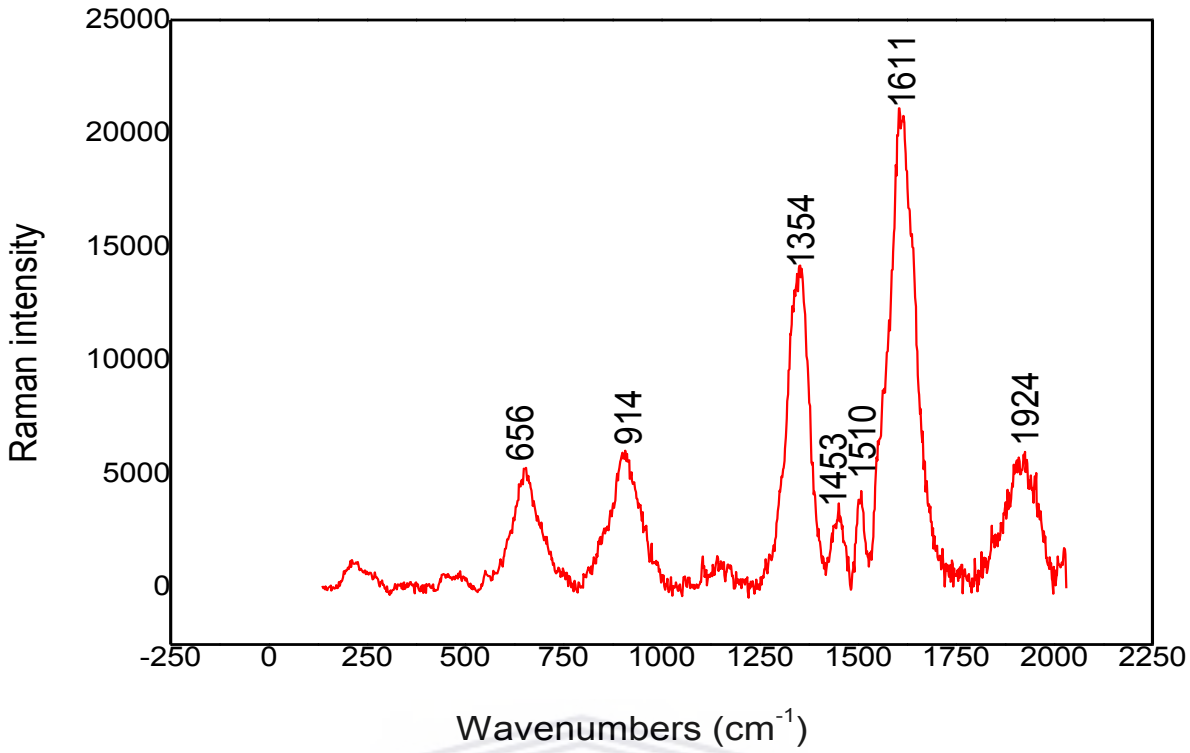

Figure 4.21: Raman spectrum of **12**

RAMAN	Intensity	Assignments
1354	s	CH_3 deformation
1453	w	CH_2 deformation
1510	w	C-C stretching
1611	s	C=C stretching
1924	n	C-H stretching

4.9.3 Structure elucidation of 7-methoxyrosmanol (13)

Compound 13 (13.7 mg) (Fig. 4.22) was isolated as a white powder as described in Scheme 4.1. Its IR spectrum exhibited bands at 1734 cm^{-1} for the carbonyl lactone group (C=O), 2932 and 2864 for the carbon-hydrogen stretching (C-H) as well as at 3233 cm^{-1} attributed hydroxyl group (OH) (Fig. 4.26), which is in agreement the report data. The Raman spectrum featured characteristic bands at 1598 cm^{-1} related to C-C stretching, and 1355 cm^{-1} attributed to the CH_3 bond vibrations (Fig. 4.27) (Belt, et al., 2017; Chain, et al., 2015; Raschi, et al., 2014). The NMR spectra of **13** showed similar signals to compound **12** except the

https://etd.uwc.ac.za/

appearance of the methoxyl group at 3.66 as shown in Table 4.9, which was allocated at position 7 according to the HMBC correlation. Finally, the NMR data of 7-methoxyrosmanol was identical with those published in literature (Richheimer, et al., 1996) and established the structure of as 7-methoxyrosmanol.

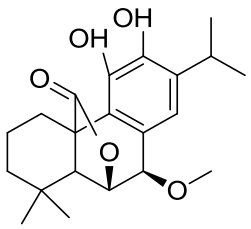

7-methoxyrosmanol

Figure 4.22: Chemical structure of **13**

Table 4.9: ^{1}H and ^{13}C NMR spectroscopic data assignments (400 MHz) for compound **13** (δ in ppm, m, J in Hz) in $CDCl_3$

	13		
N^{O}	δ_H (*J* in Hz)	^{13}C	Multiplicity
1	3.15 br. d (14.3) 2.0 ddd (5.3, 5.3, 13.6)	27.2	CH_2
2	1.67 m 1.56 m	19.0	CH_2
3	1.45 br d (12.5) 1.23 d (1.6)	38.0	CH_2
4		31.3	C
5	3.48 s	50.8	CH
6	4.26 d (3.0)	77.4	CH_2
7	4.71 d (3.0)	74.7	CH_2
8		126.4	C
9		124.5	C
10		47.1	C
11		142.6	C
12		141.5	C
13		134.6	C
14	6.8 s	120.8	CH
15	3.07 sept (6.8)	27.2	CH
16	1.24 d (1.6)	22.2	CH_3
17	1.22 d (1.6)	23.5	CH_3
18	1.01 s	31.6	CH_3
19	0.93 s	22.0	CH_3
20		179.0	C
OCH_3	3.66 s	58.3	CH_3

UNIVERSITY of the WESTERN CAPE

https://etd.uwc.ac.za/

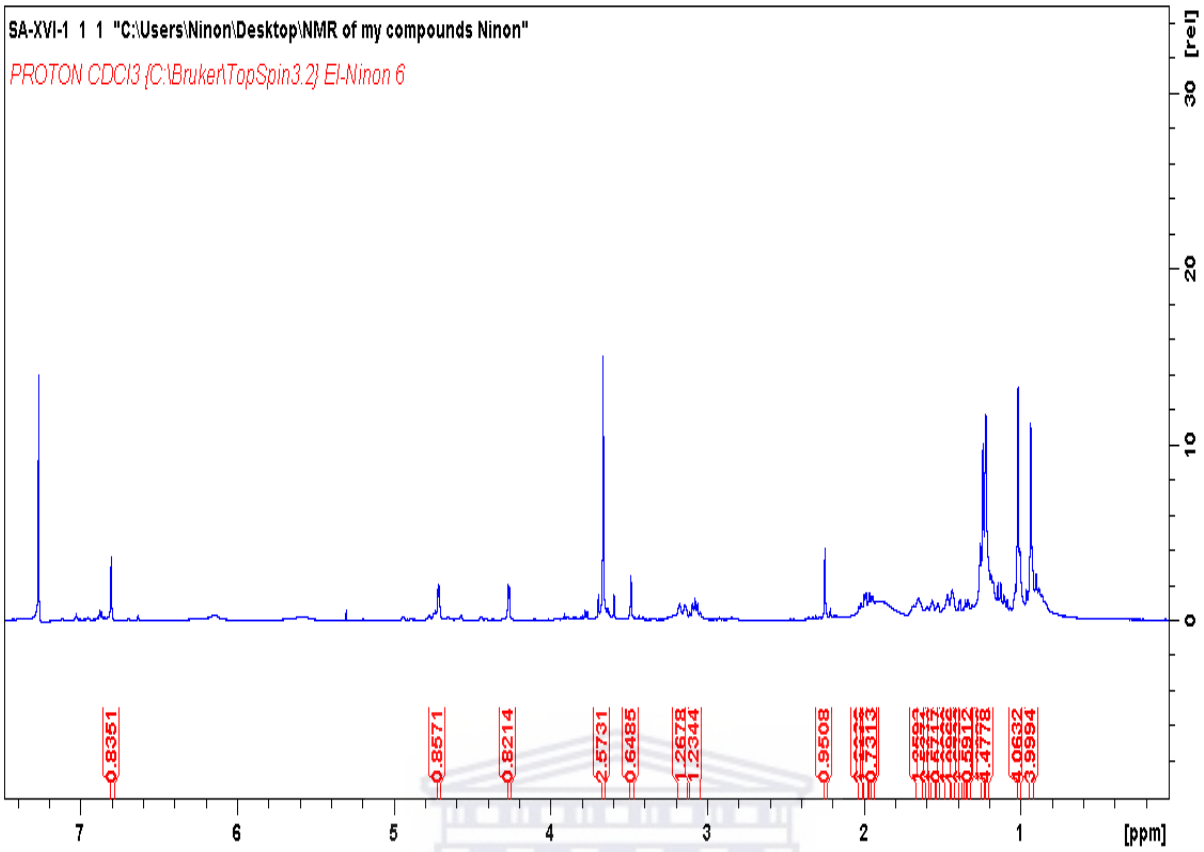

Figure 4.23: ^{1}H NMR (400 MHz, CDCl3) spectrum of **13**

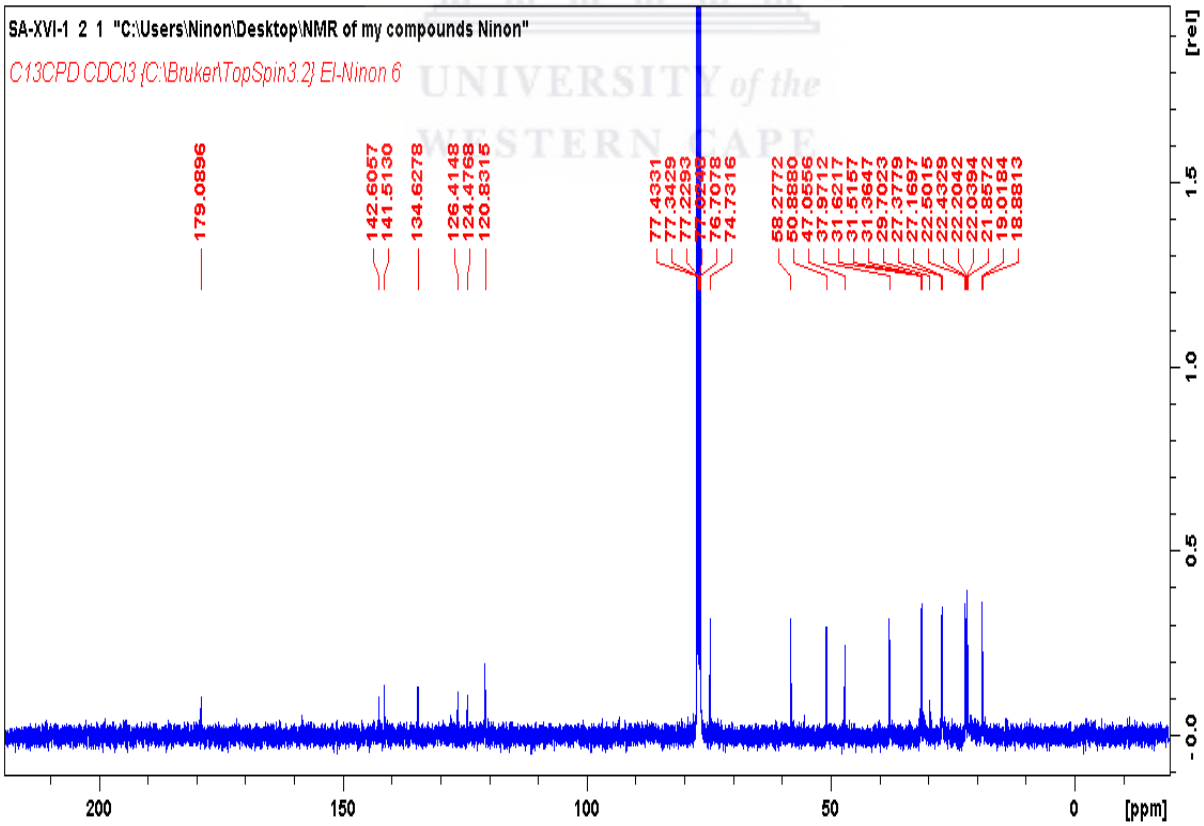

Figure 4.24: ^{13}C NMR (400 MHz, CDCl3) spectrum of **13**

https://etd.uwc.ac.za/

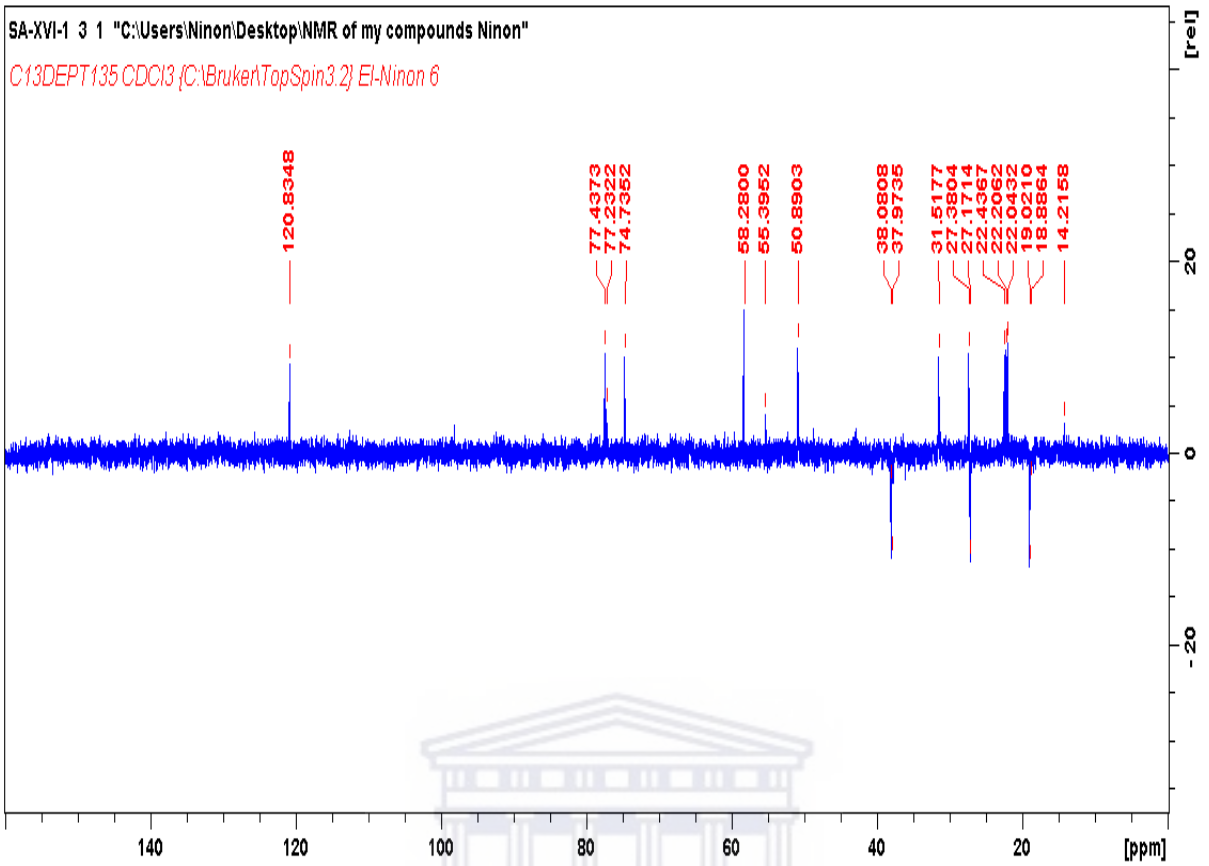

Figure 4.25: DEPT NMR (400 MHz, CDCl3) spectrum of **13**

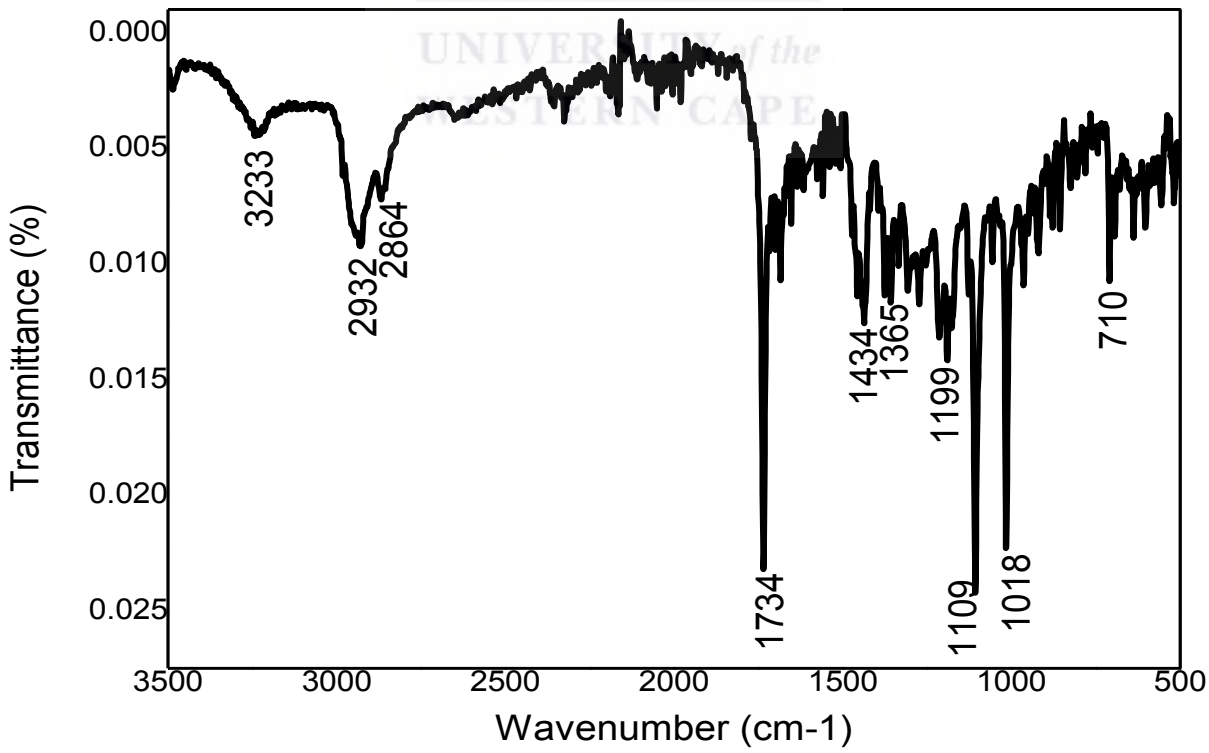

Figure 4.26: FTIR spectrum of **13**

https://etd.uwc.ac.za/

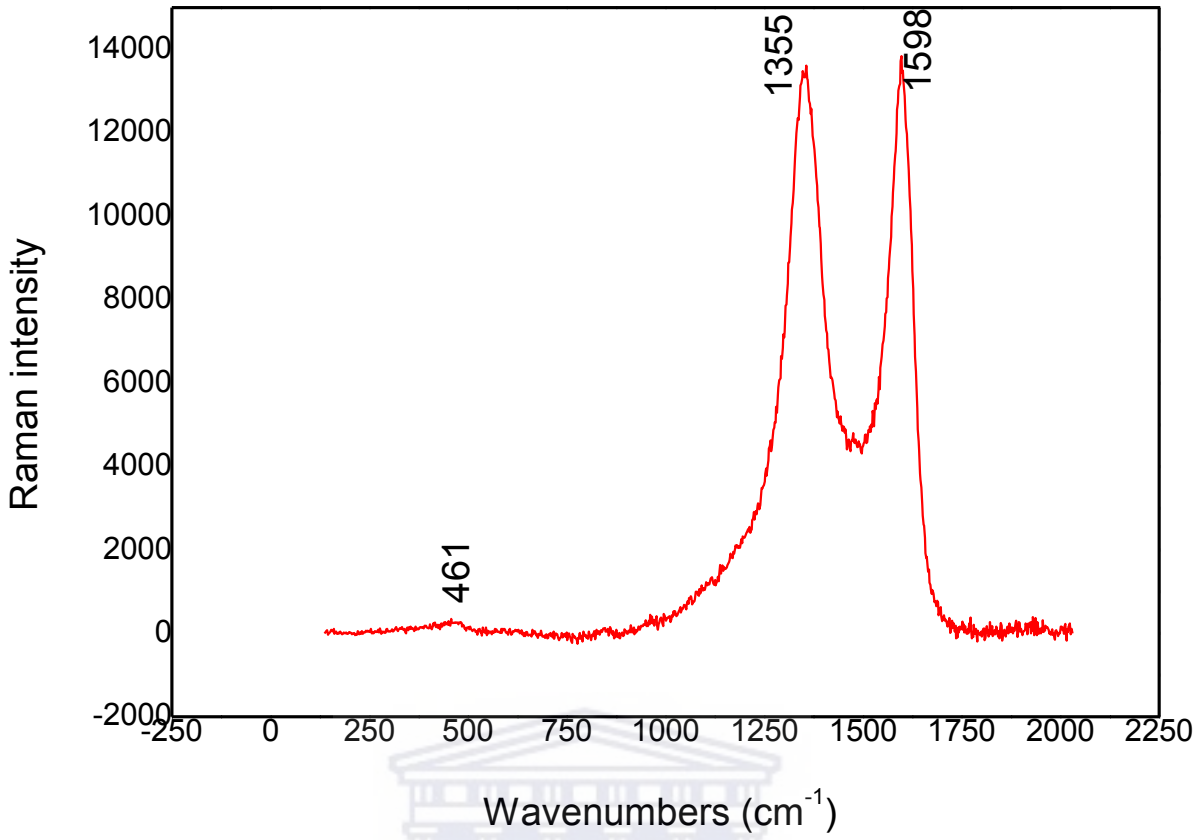

Figure 4.27: Raman spectrum of **13**

RAMAN	Intensity	Assignments
1355	s	CH_3 deformation
1598	s	C-C stretching

UNIVERSITY of the
WESTERN CAPE

4.9.4 Structure elucidation of 12-methoxycarnosic acid (**14**)

Compound **14** (84.5 mg) (Fig. 4.28) was isolated as an amorphous powder as described in Scheme 4.1. Its IR spectrum exhibited bands at 1730 cm^{-1} for the carbonyl lactone group (C=O), 2889 for the carbon-hydrogen stretching (C-H) as well as at 3341 cm^{-1} attributed hydroxyl group (OH) (Fig. 4.32). It was identified as 12-methoxycarnosic acid from its NMR data, which was similar to that of compound **11** except the absence of the signal at 5.38 and the appearance of a methoxyl group at 3.66. The ^{13}C NMR and DEPT-135 (Table 4.10) showed five methylene (extra one than **1**) and three methines (less one than **1**). The ^{13}C signal of the carbonyl carbon was shifted to a lower field (181.0) which indicate the presence of free

https://etd.uwc.ac.za/

carboxyl group. Additionally, other 2D NMR data (HMBC) confirmed the position of the methoxyl group at position C-12. The above data with comparison of the obtained data with literature confirmed the structure of compound **14** as 12-methoxycarnosic acid (Fischedick, et al., 2013; Richheimer, et al., 1996).

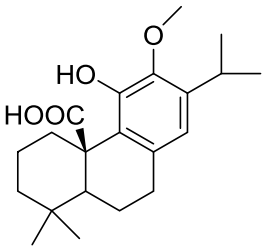

12-methoxycarnosic acid

Figure 4.28: Chemical structure of **14**

Table 4.10: ^{1}H and ^{13}C NMR spectroscopic data assignments (400 MHz) for compound **14** (δ in ppm, m, J in Hz) in $CDCl_3$

	14		
N^{O}	δ_H (*J* in Hz)	^{13}C	Multiplicity
1	3.45 br. d (13.2) 1.17 d (5.8)	34.1	CH_2
2	1.75 br. d (12.8) 1.48 d (14.2)	19.9	CH_2
3	1.43 d (2.9) 1.24 d (4.5	41.5	CH_2
4		34.1	C
5	2.25 ddd (6.9, 12.5, 12.5)	41.5	CH
6	1.77*	18.4	CH_2
7	2.76 m	31.9	CH_2
8		134.5	C
9		125.3	C
10		47.7	C
11		147.8	C
12		142.3	C
13		139.5	C
14	6.44 s	118.1	CH
15	3.09 sept (6.8)	26.5	CH
16	1.12 d (7.2)	23.5	CH_3
17	1.14 d (7.2)	23.8	CH_3
18	0.89 s	32.7	CH_3
19	0.79 s	20.0	CH_3
20		181.0	C
OCH_3	3.66	61.7	CH_3

https://etd.uwc.ac.za/

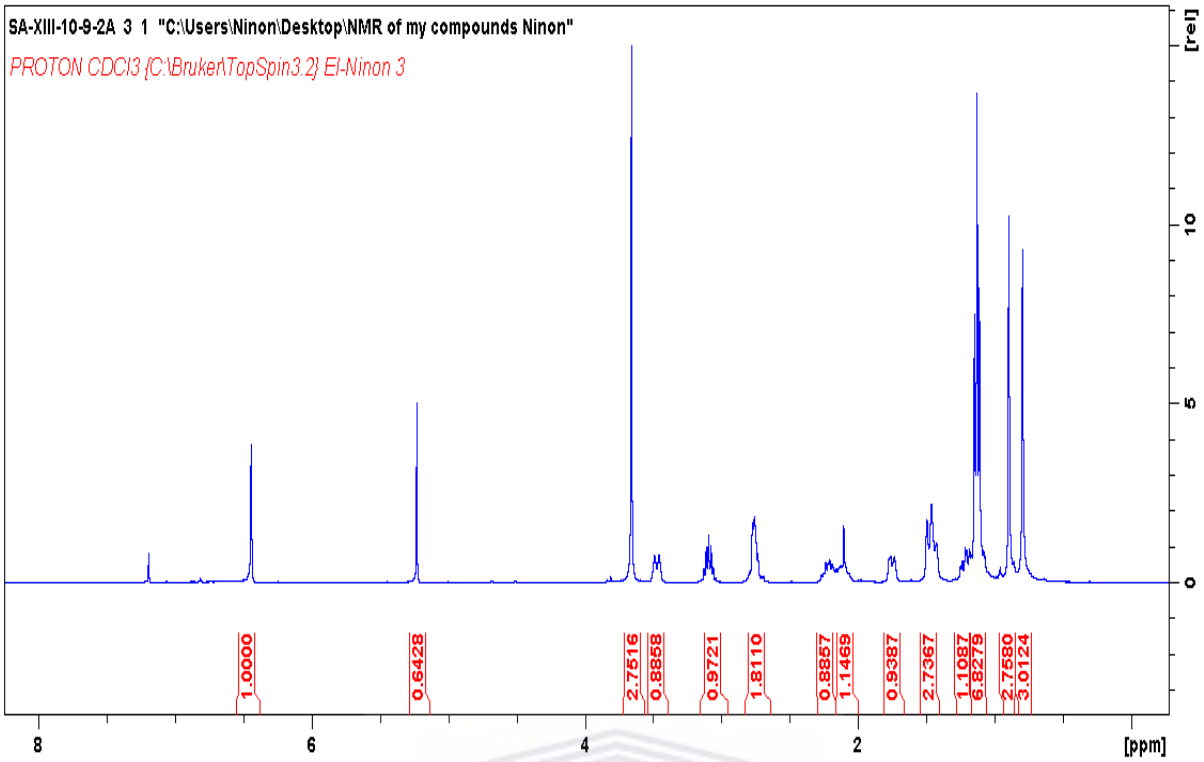

Figure 4.29: ^{1}H NMR (400 MHz, CDCl3) spectrum of **14**

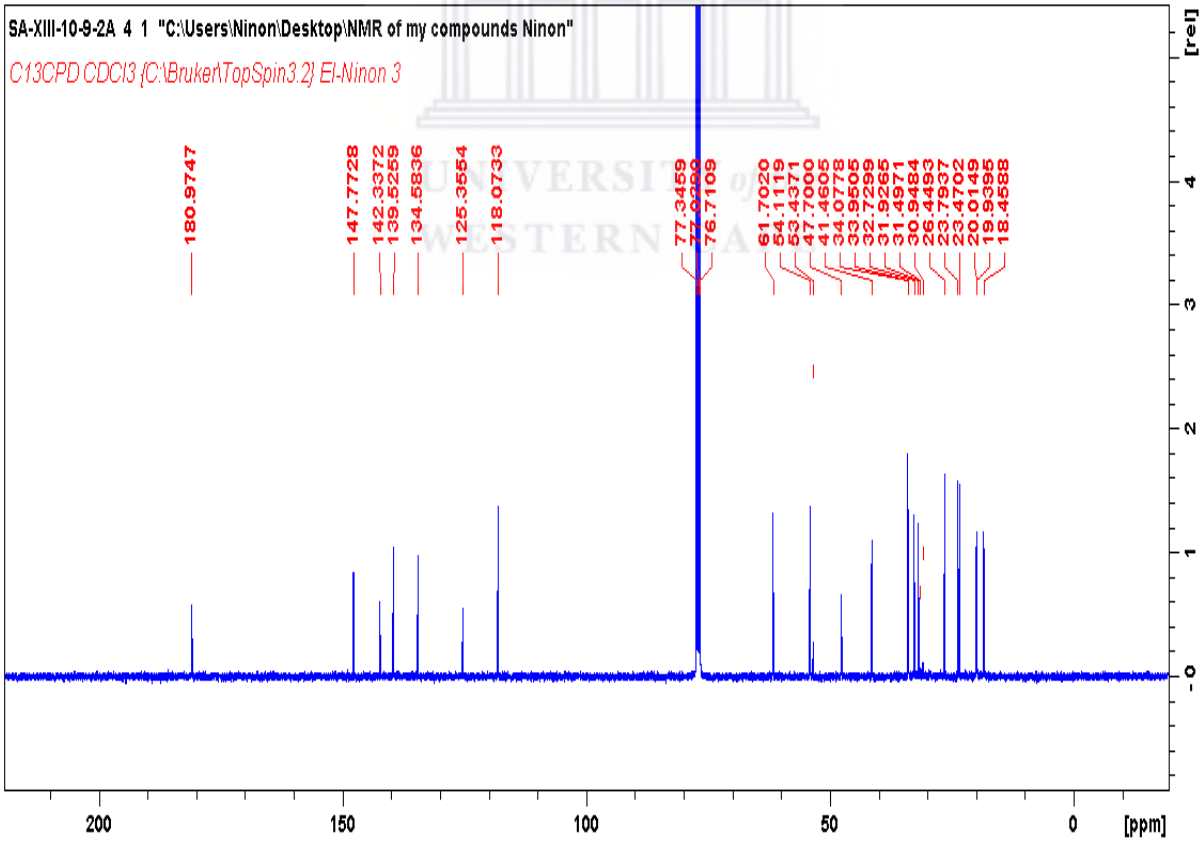

Figure 4.30: ^{13}C NMR (400 MHz, CDCl3) spectrum of **14**

https://etd.uwc.ac.za/

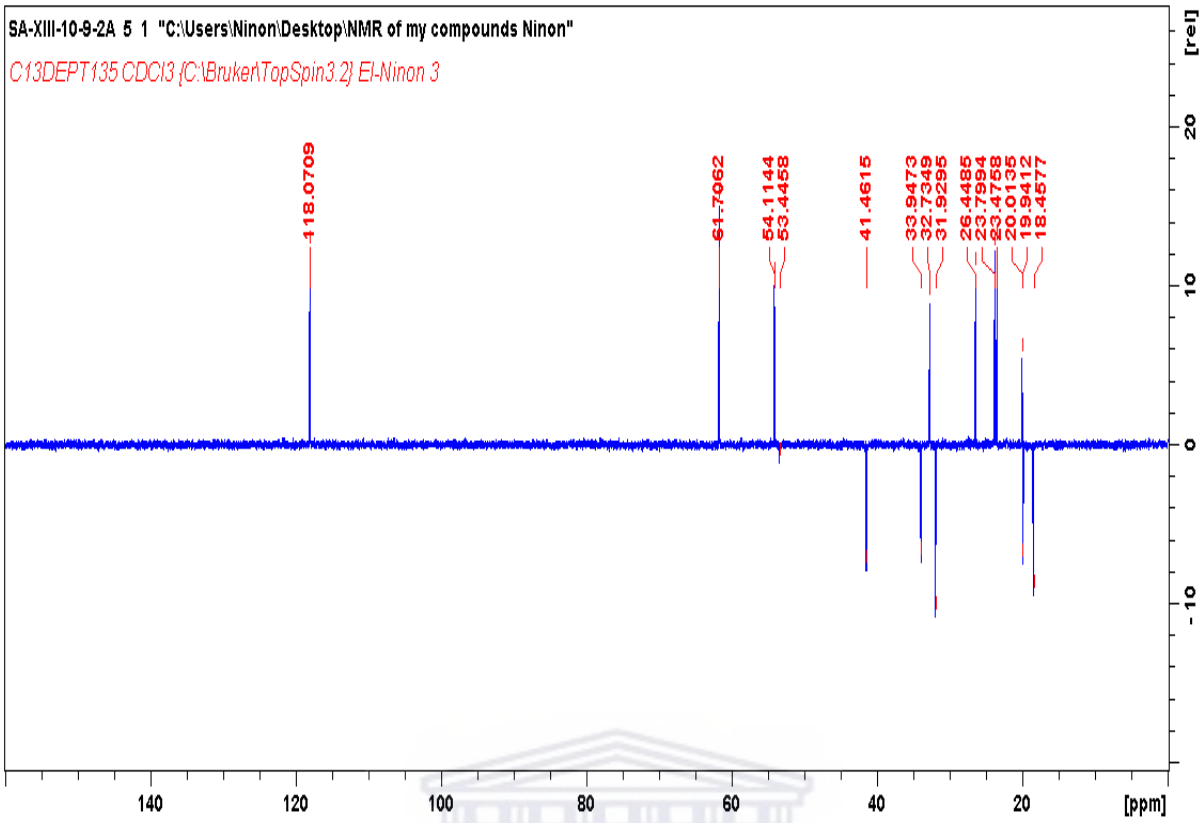

Figure 4.31: DEPT NMR (400 MHz, CDCl3) spectrum of **14**

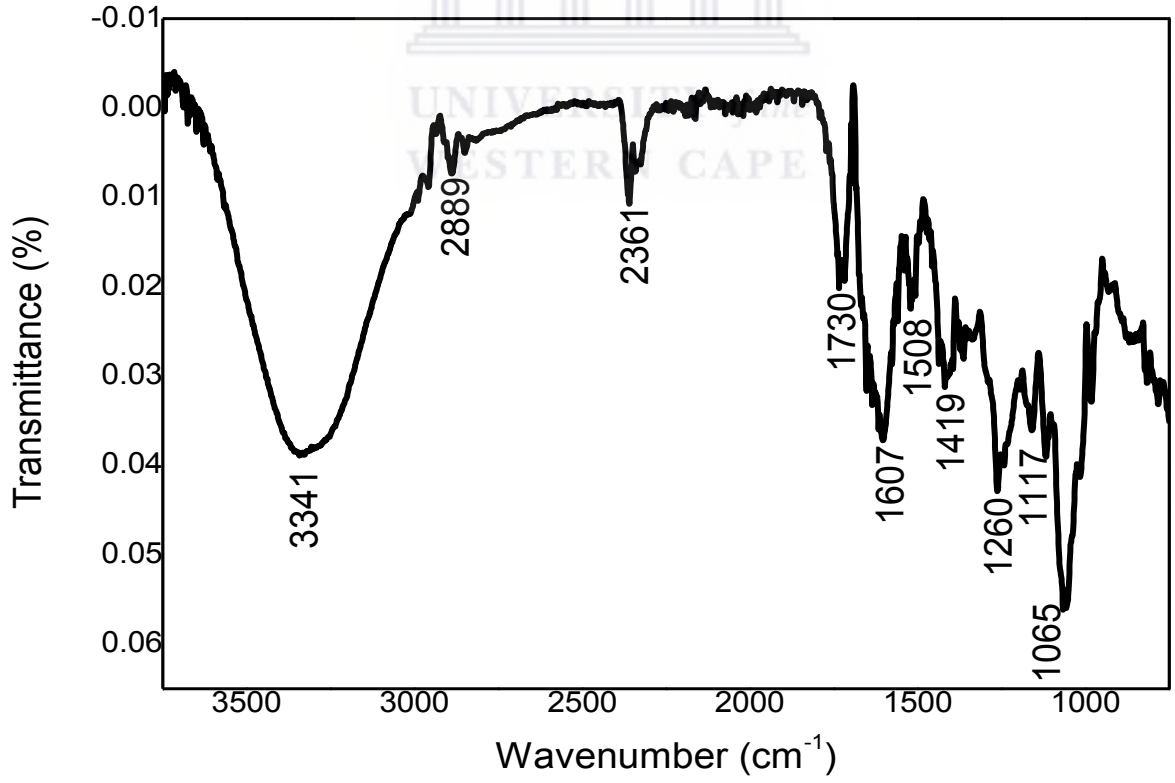

Figure 4.32: FTIR spectrum of **14**

https://etd.uwc.ac.za/

4.9.5 Structure elucidation of 4,7-dimethylapigenin ether (**15**)

Compound **15** (84.8 mg) (Fig. 4.33) was isolated as grey powder as described in Scheme 4.1. Its IR spectrum exhibited bands at 1728 cm^{-1} for the carbonyl lactone group (C=O), 2960 and 2923 for the carbon-hydrogen stretching (C-H) as well as at 3354 cm^{-1} attributed hydroxyl group (OH) (Fig. 4.37). It was identified as 4,7-dimethylapigenin ether from its NMR data, which was similar to the published data (Ruaxgruxgsi, et al., 1981).

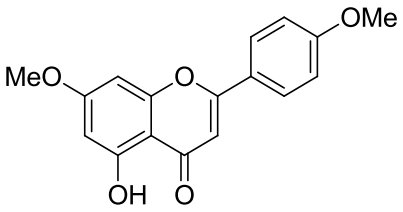

Figure 4.33: Chemical structure of the compound **15**

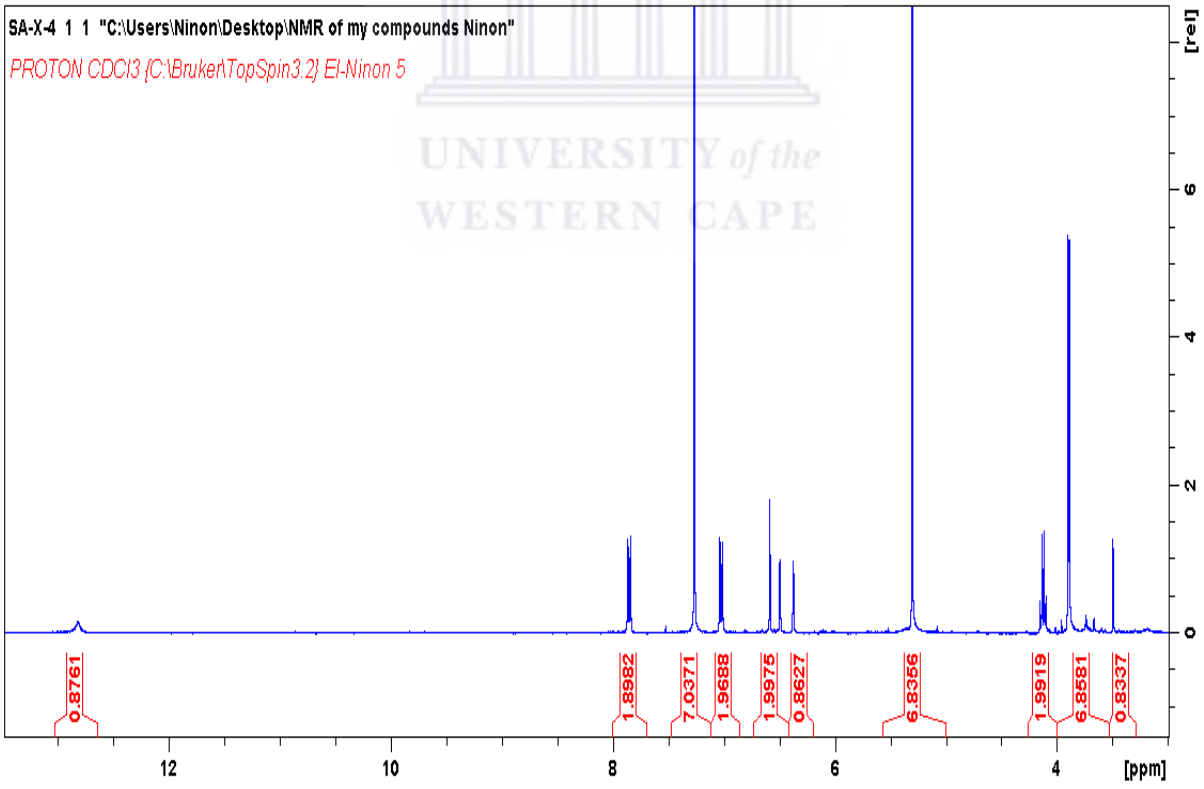

Figure 4.34: ^{1}H NMR (400 MHz, CDCl3) spectrum of **15**

https://etd.uwc.ac.za/

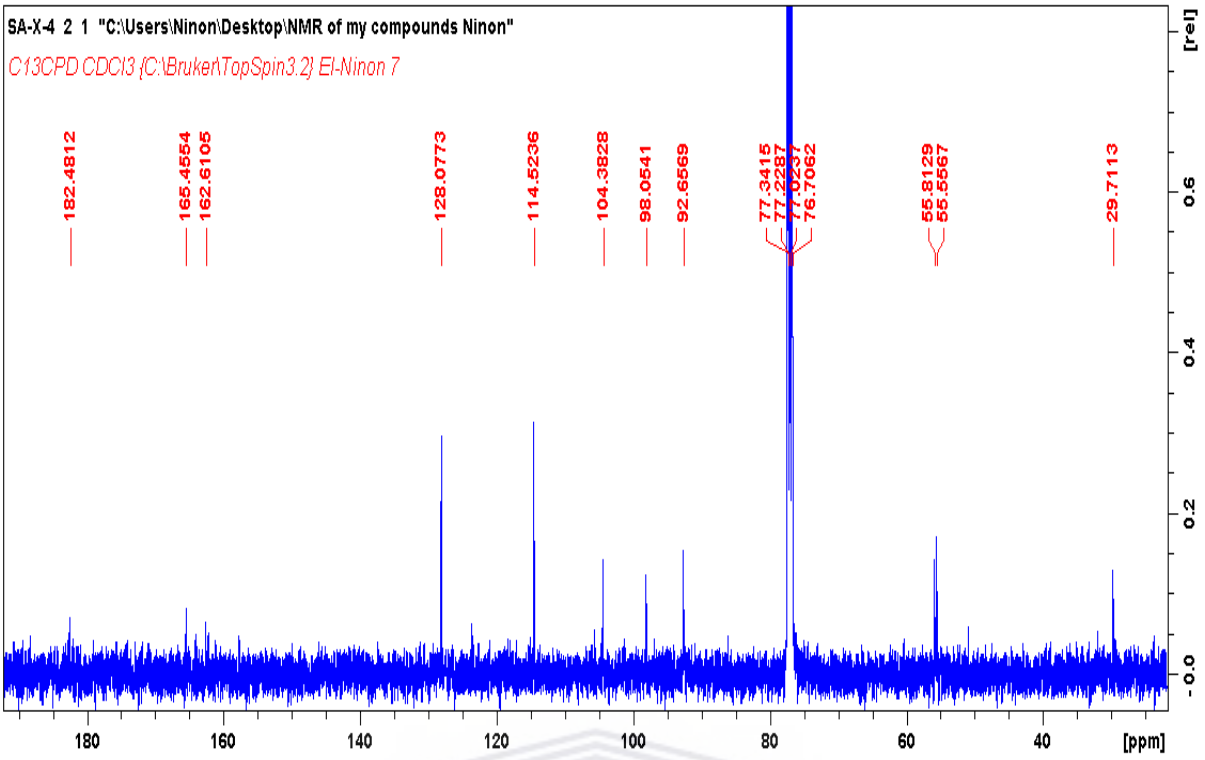

Figure 4.35: ^{13}C NMR (400 MHz, CDCl3) spectrum of **15**

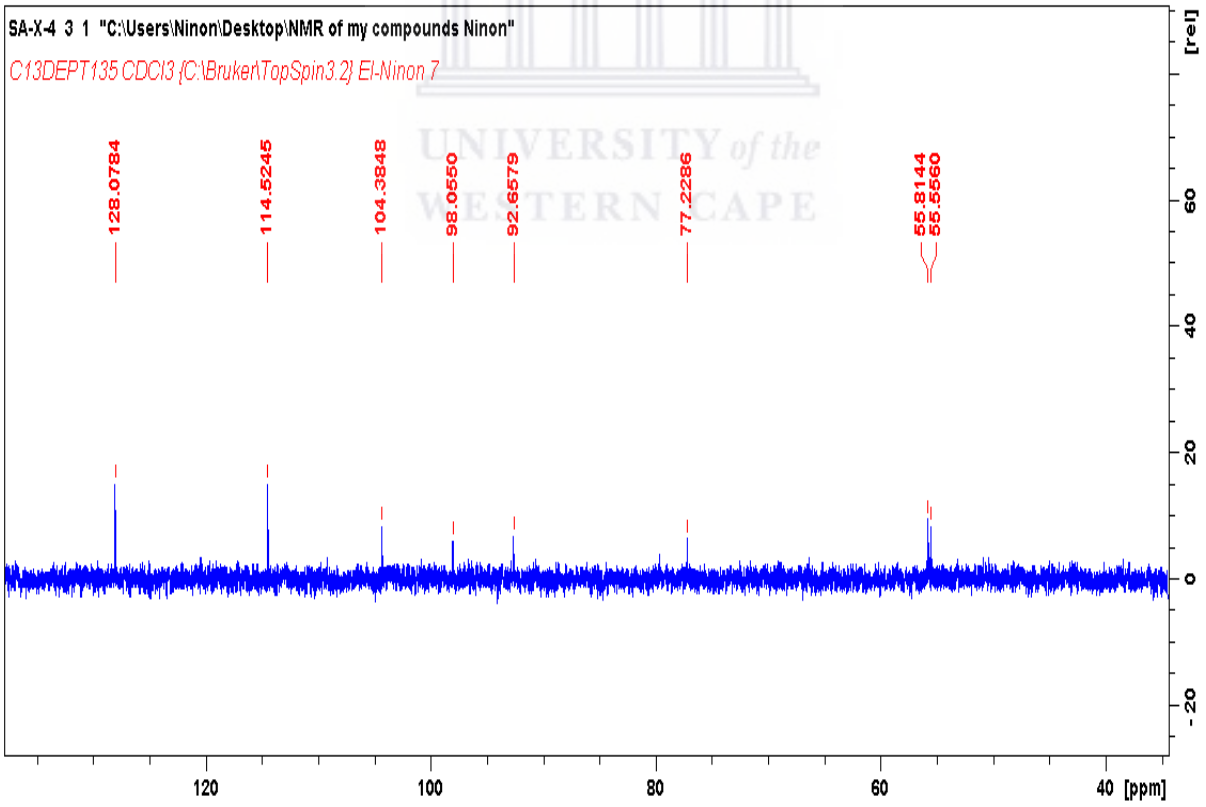

Figure 4.36: DEPT NMR (400 MHz, CDCl3) spectrum of **15**

https://etd.uwc.ac.za/

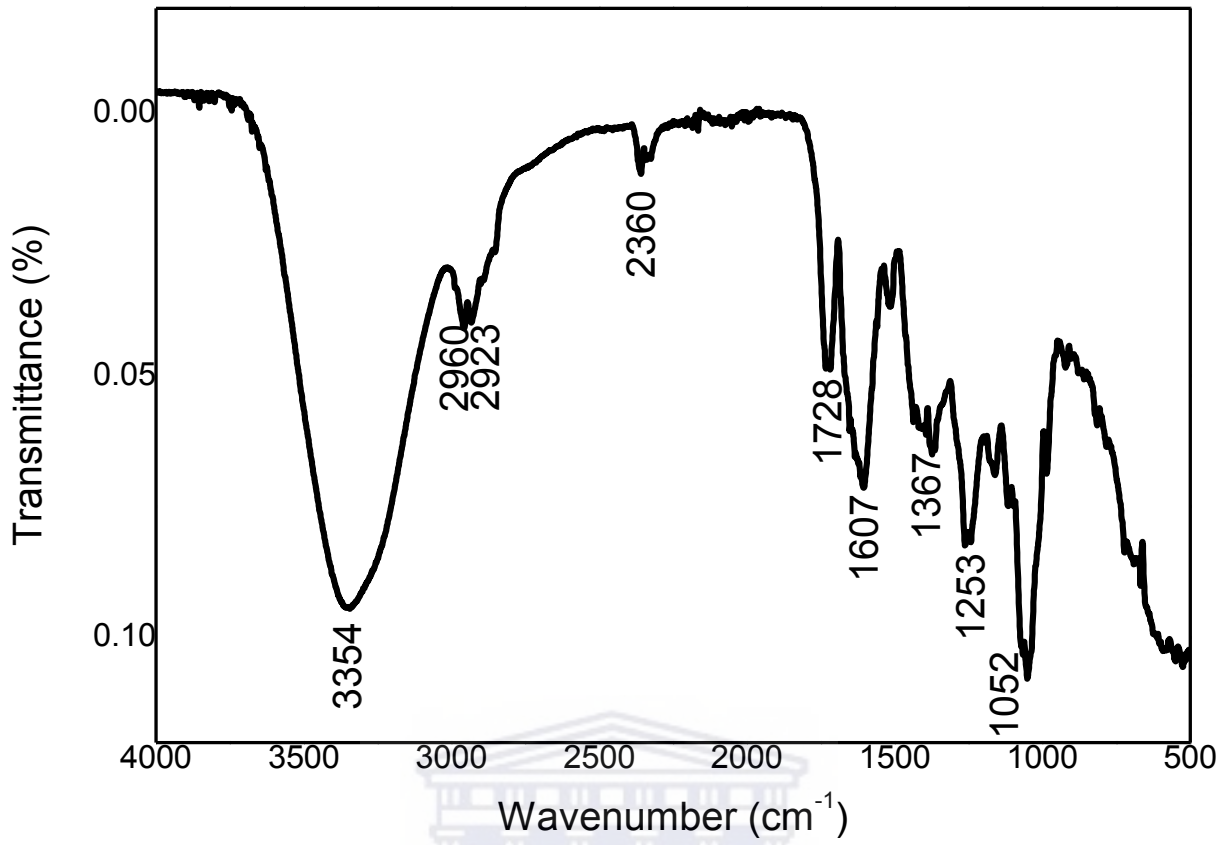

Figure 4.37: FTIR spectrum of **15**

4.10 Biological evaluation: Results and discussion

4.10.1 Alpha-glucosidase and alpha-amylase activities

Alpha-glucosidase and alpha-amylase are the main enzymes involved in the digestion of carbohydrates and lipids (Sindhu, et al., 2013). Their mechanism of action involved the breakdown of carbohydrates by alpha amylase while alpha glucosidase breaks down starch and disaccharides to glucose (Mohamed, 2012; Sindhu, et al., 2013). One of the therapeutic approaches is to decrease the postprandial hyperglycemia by delaying the absorption of glucose through the inhibition of carbohydrate-hydrolyzing enzymes such as alpha-amylase and alpha-glucosidase in the digestive tract (Eom, et al., 2012). Alpha-glucosidase is an enzyme that catalyses the absorption of digested glucose from dietary polysaccharides in the small intestine (Thilagam, et al., 2013). Therefore, inhibitors of these enzymes delay carbohydrate digestion, which cause a reduction in the rate of glucose absorption and

https://etd.uwc.ac.za/

consequently reduce the post-prandial increase of plasma glucose (Obho, 2006). Hence, many efforts have been made to search for more effective and safe inhibitors of alpha-glucosidase and alpha-amylase from natural sources for the development of physiological functional drugs for the prevention and management of diabetes (Wang, et al., 2010). The *in vitro* bio-evaluation of *S. aurita* against alpha-glucosidase and alpha-amylase was investigated and the results showed that **13** demonstrated the highest alpha-glucosidase inhibitory activity with IC_{50} value of 4.2 ± 0.7 µg/mL, followed by **12** and **15** with IC_{50} value of 16.4 ± 1.4 and 28.7 ± 0.9 µg/mL respectively, while **14** demonstrated the highest alpha amylase inhibitory activity with IC_{50} value of 16.2 ± 0.3 µg/mL followed by **11** and **12** with IC_{50} value of 19.8 ± 1.4 and 40.9 ± 1.2 µg/mL respectively as showed in Table 4.11.

Table 4.11: Inhibitory activities of *S. aurita* constituents on alpha-glucosidase and alpha-amylase

Items	**Alpha-glucosidase** IC_{50} (µg/mL)	**Alpha-amylase** IC_{50} (µg/mL)
11	51.8 ± 1.9	19.8 ± 1.4
12	16.4 ± 1.4	40.9 ± 1.2
13	4.2 ± 0.7	NA
14	36.9 ± 2.1	16.2 ± 0.3
15	28.7 ± 0.9	NA
Crude extract	241.9 ± 2.7	NA
Acarbose	610.4 ± 1.0	10.2 ± 0.6

NA not active at the test concentrations. The results are expressed as mean ±SEM for n = 3

Carnosol has been reported to demonstrate significant antidiabetic activities in different models with different mechanism of action. It increases skeletal muscle cell glucose uptake via AMPK-dependent GLUT4 Glucose transporter translocation, which is targeted for glucose homeostasis indicating that it could be a potential antidiabetic compound. Furthermore, structural features of the abietane diterpenes reported to possess antidiabetic activity contain COOH groups, lactone rings and steroid type structures (Vlavcheski, et al., 2018). Carnosol also possesses hypoglycemic, antihyperlipidemic and it has a useful

UNIVERSITY of the WESTERN CAPE
https://etd.uwc.ac.za/

protective effects on the liver and renal functions in diabetic rats (Khan, et al., 2012) as well as it improves diabetes and its complications by the modulation of oxidative stress and inflammatory responses (Samarghandian, et al., 2017). Additionally, carnosol was found to inhibit intracellular de novo triglyceride synthesis by 67.5-90.6% without affecting cell viability (Naimi, et al., 2017), as well as to possess potent inhibitory activity (IC_{50} = 62.5 µM) against rat liver diacylglycerol acyltransferase 1 (DGAT1), which is an enzyme that plays a fundamental role in triglyceride synthesis (Naimi, et al., 2017). 7-O-methylrosmanol (**13**) has been reported to suppress forskolin (FSK)-induced luciferase expression when monitored by cAMP/response element (CRE), Promoters for cytosolic phosphoenolpyruvate carboxykinase (PEPCK-C) and glucose-6-phosphate (G6Pase) gene promoters (Yun, et al., 2013).

Promoters for cytosolic phosphoenolpyruvate carboxykinase (PEPCK-C) and glucose-6-phosphate (G6Pase) play a vital role in the homeostatic regulation of blood glucose levels. Hence, the suppression of cAMP/protein kinase response of the PEPCK-C or G6Pase gene may contribute to the antihyperglycemic activity, which is one of the key in the management of diabetes (Yun, et al., 2013). The alpha glucosidase activity demonstrated by **13** and **11** are in agreement with some published data reporting on different mechanism of action exhibited by these compounds (Samarghandian, et al., 2017; Yun, et al., 2013).

UNIVERSITY of the
WESTERN CAPE

4.10.2 Antioxidant activity

Diabetes mellitus involves oxidative stress in both etiology and pathogenesis partway. However, oxidative stress occurs when the production of free radicals such as reactive oxygen species (ROS) including superoxide radical, hydrogen peroxide, and hydroxyl radical overwhelms the detoxification capacity of the cellular antioxidant system, resulting in biological damages, especially the reduced release of insulin (Liguori, et al., 2018). Hence, oxidative stress plays a vital role in the development of diabetes complications such as

https://etd.uwc.ac.za/

microvascular and cardiovascular (Wright, et al., 2006). The metabolic abnormalities of diabetes cause mitochondrial superoxide overproduction, which is the main mediator of diabetes tissue damage, insulin resistance, β-cell dysfunction, and impaired glucose tolerance (Yatoo, et al., 2016). The usage of medicinal herbs in the management of diabetes mellitus and oxidative stress is widely reported, and these herbs contain bioactive constituents such as polyphenols, flavonoids, terpenoids, alkaloids, carotenoids, vitamins, and several other constituents, which can act as antidiabetics and/or antioxidants/radical scavengers (Kooti, et al., 2016).

Abietane type diterpenes are well known to exhibit strong antioxidant activity due to the presence of o-dihydroxyl groups in the aromatic ring that serve as hydrogen and/or electron donating agents and metal ion-chelators (Habtemariam, 2016). Additionally, the presence of the ortho-dihydroxyl group at the aromatic ring in the abietane diterpenes contribute significantly to the biological activities exhibited by these groups of phytochemicals (Masuda, et al., 2005). Phenolic compounds are a class of compounds that can create beneficial effects in vivo owing to their antioxidant properties (through radical scavenging) and at the same time show hazardous effects due to their pro-oxidant properties. It is expected that the transfer of electrons or donation of protons to reactive radicals may cause resonance stability of the phenoxyl radical produced (Manderville, 2009).

The *in vitro* antioxidant activity of the isolated compounds of the methanolic extract of *S. aurita* was investigated by evaluating their FRAP, TEAC and ORAC activities. The results demonstrated excellent antioxidant activity for **12**, **11** and **13** respectively as ORAC (25789.90 ± 10.53; 23961.76 ± 14.07; 23939.33 ± 2.42) µM TE/g; **11** and **S2** as FRAP (3917.78 ± 2.15; 1522.31 ± 0.95) µM AAE/g; **15** and **12** as TEAC (3190.4 ± 2.85; 2055 ± 2.65) µM TE/g. Our findings showed activity for ORAC as **12>11>13>14>15**, **FRAP** as **15>S2>15>14>11>13** and **TEAC** as **11>12>13>15>14** respectively. The crude extract of *S.*

https://etd.uwc.ac.za/

aurita exhibited moderate antioxidant activity when tested on ORAC (4453.2 ± 1.3 µmole TE/g), TEAC (723.9 ± 6.4 µM TE/g) and FRAP (393.7 ± 2.3 µM AAE/g). Therefore, the activity of **12** and **11** is related to the presence of the ortho dihydroxyl groups located on the aromatic ring, which serve as hydrogen donating agent to peroxyl radicals thereby stabilizing them and giving rise to a relatively stable radical (Özgen, et al., 2011). Additionally, carnosol and rosmanol share common chemical structure framework, which may possibly enhance their bioactivity and mechanism of reactions. Our findings also noticed that the greater the number of hydroxyl groups in these phenolic compounds, the higher is the antioxidant activity. The highest bio-activity demonstrated by rosmanol can then be justify by the fact that it contains 3 free hydroxyl groups compared to carnosol that has only 2 hydroxyl groups. Rosmanol and 7-methoxyl rosmanol share the same chemical structure framework, but the difference in the activity exhibited should be explain by the fact that the substitution of the hydroxyl group in 7-methoxyl rosmanol might be responsible of the decrease of the activity observed. In the structure-activity relationship (SAR), the occupation of C-7 position is directly related to the activity. Although, the antioxidant activity of carnosol is high, the highly-stress lactone ring may open during the course of chemical reaction leading to extension of conjugation and formation of *p*-quininoidal structure. In 7-methoxyrosmanol, antioxidant activity is lower compared to carnosol, and rosmanol, possibly due to substitution of C-7 position with methoxyl group which promotes the hydrophobicity in the compounds.

Table 4.12: Total antioxidant capacity of *S. aurita* constituents

Items	ORAC (µmole TE/g)	TEAC (µmole TE/g)	FRAP (µM AAE/g)
11	23961.8 ± 14.1	331.2 ± 0.6	3917.8 ± 2.1
12	25789.9 ± 10.5	2055 ± 2.6	1522.3 ± 0.9
13	23939.3 ± 2.4	222.3 ±1.6	1322.1 ± 0.9
14	20247.1 ± 9.3	336.7 ± 2.9	508.2 ± 2.6
15	6474.9 ± 4.0	3190.4 ± 2.8	609.8 ± 5.6
Crude extract	4453.2 ± 1.3	723.9 ± 6.4	393.7 ± 2.3
EGCG	3976.8 ± 3.8	4146.4 ± 19.8	7525.0 ± 4.9

https://etd.uwc.ac.za/

Carnosol, carnosic acid and rosmanol are the most abundant phytochemical constituents of Salvia species and Rosemary, and they contribute about 90% of the antioxidant activity of Lamiaceae family (Etsassala, et al., 2019). Carnosol and rosmanol have been reported to exhibit remarkable antioxidant activity, which was in a competitive manner with tocopherol (Mishra, et al., 2011; Pérez-Fons, et al., 2010). These reported data corroborate with our findings.

4.11 Conclusion

The phytochemical and biological investigation of the methanolic extract of *S. aurita* revealed that this plant is a rich source of abietane diterpenes with significant alpha glucosidase and alpha amylase inhibitory activities as well as significant antioxidant activities. The present work is the first scientific report on the phytochemical isolation and in vitro bio-evaluation of alpha glucosidase and alpha amylase inhibitory activities of *Salvia aurita* and the results suggest that the methanolic extract of this plant and/or its individual constituents might become prominent natural therapeutic agents for the inhibition of alpha glucosidase and alpha amylase enzymes and oxidative stress. Therefore, compounds that demonstrated remarkable alpha glucosidase and alpha amylase inhibitory activities as well as potent antioxidant activities might be very good candidate for controlling oxidative stress in diabetic patients as well as management of diabetes complications.

UNIVERSITY of the
WESTERN CAPE

References

Belt, T., Keplinger, T., Hänninen, T and Rautkari, L. (2017). Cellular level distributions of Scots pine heartwood and knot heartwood extractives revealed by raman spectroscopy imaging. *Industrial Crops and Products*, 108, 327-335.

Bajpai, V.K., Park, Y.H., Na, M and Kang, S.C. (2015). Alpha-glucosidase and tyrosinase inhibitory effects of an abietane type diterpenoid taxoquinone from *Metasequoia glyptostroboides*. *BMC Complementary and Alternative Medicine*, 38(5), 399-402.

https://etd.uwc.ac.za/

Chain, F.E., Leyton, P., Paipa, C., Fortuna, M and Brandán, S.A. (2015). FT-IR, FT-Raman, UV-visible, and NMR spectroscopy and vibrational properties of the labdane-type diterpene 13-epi-sclareol. *Spectrochimica Acta part A Molecular and Biomolecular Spectroscopy*, 138, 303-13.

Eom, S.H., Lee, S.H., Yoon, N.Y., Jung, W.K., Jeon, Y.J., Kim, S.K., Lee, M.S and Kim, Y.M. (2012). Alpha-glucosidase and alpha-amylase inhibitory activities of phlorotannins from *Eisenia bicyclis*. *Journal of the Science of Food and Agriculture*, 92, 2084-2090.

Etsassala, N.G.E.R., Adeloye, A.O., El-Halawany, A., Hussein, A.A and Iwuoha, E.I. (2019). Investigation of in-vitro antioxidant and electrochemical activities of isolated compounds from *Salvia chamelaeagnea* P.J.Bergius extract. *Antioxidants*, 8(4), 98.

Fischedick, J.T., Standiford, M., Johnson, D.A and Johnson, J.A. (2013). Structure activity relationship of phenolic diterpenes from *Salvia officinalis* as activators of the nuclear factor E2-related factor 2 pathway. *Bioorganic and Medicinal Chemistry*, 21(9), 2618-2622.

Habtemariam, S. (2016). The Therapeutic potential of Rosemary (*Rosmarinus officinalis*) diterpenes for Alzheimer's disease. *Evidence Based Complementary and Alternative Medicine*, 2680409.

Hedge, I. (1974). Revision of Salvia in Africa including Madagascar and Canary Islands. Notes from the Royal Botanic Garden Edinburgh. 33(1).

Inatani, R., Nakatani, N., Fuwa, H and Seto, H. (1982). Structure of a new antioxidative phenolic diterpene isolated from Rosemary (*Rosmarinus officinalis* L.). *Agriculture and BioIogical Chemistry, 46*(6), 1661-1666.

UNIVERSITY of the WESTERN CAPE

https://etd.uwc.ac.za/

Kalita, D., Holm, D.G., LaBarbera, D.V., Petrash, J.M and Jayanty, S.S. (2018). Inhibition of alpha-glucosidase, alpha-amylase and aldose reductase by potato polyphenolic compounds. *PLoS ONE*, 13(1).

Kamatou, G.P.P., Makunga, N.P., Ramogola, W.P.N., Viljoen, A. (2008). South African *Salvia* species: A review of biological activities and phytochemistry. *Journal of Ethnopharmacology* , 119(3), 664-72.

Khan, I., Ahmad, W., Karim, N., Ahmad, M., Khan, M., Tariq, S.A and Sultana, N. (2017). Antidiabetic activity and histopathological analysis of carnosol isolated from Artemisia indica linn in streptozotocin-induced diabetic rats. *Medicinal Chemistry Research*, 26(2), 335-343.

Kooti, W., Farokhipour, M., Asadzadeh, Z., Ashtary-Larky, D and Asadi-Samani, M. (2016). The role of medicinal plants in the treatment of diabetes: a systematic review. *Electrononic Physician Journal*, 8(1), 1832-1842.

Liguori, I., Russo, G., Curcio, F., Bulli, G., Aran, L., Della-Morte, D., Gargiulo, G., Testa, G., Cacciatore, F., Bonaduce, D and Abete, P. (2018). Oxidative stress, aging, and diseases. *Clinical Interventions in Aging*, 13, 757-772.

Manderville, R. (2009). Ambient reactivity of phenoxyl radicals in DNA adduction. *Journal of Chemistry*, 83,1261–1267.

Masuda, T., Kirikihira, T and Takeda, Y. (2005). Recovery of antioxidant activity from carnosol quinone: Antioxidants obtained from a water-promoted conversion of carnosol quinone. *Journal of Agricultural and Food Chemistry*, 53, 6831-6834.

UNIVERSITY of the WESTERN CAPE

https://etd.uwc.ac.za/

Mishra, S.B., Verma, A., Mukerjee, A and Vijayakumar, M. (2011). Anti-hyperglycemic activity of leaves extract of *Hyptis suaveolens* L. Poit in streptozotocin induced diabetic rats. *Asian Pacific Journal of Tropical Medicine*, 4(9), 689-693.

Mohamed, E.A.H., Siddiqui, M.J.A., Ang, L.F., Sadikun, A., Chan, S.H., Tan, S.C., Asmawi, M.Z and Yam, M.F. (2012). Potent alpha-glucosidase and alpha-amylase inhibitory activities of standardized 50 % ethanolic extracts and sinensetin from *Orthosiphon stamineus* Benth as anti-diabetic mechanism. *BMC Complementary and Alternative Medicine*, 12, 176.

Naimi, M., Vlavcheski, F., Shamshoum, H and Tsiani, V. (2017). *Rosemary* extract as a potential anti-hyperglycemic agent: Current evidence and future perspectives. *Nutrients*, 9(9), 968.

Oboh, G., Isaac, A.T., Akinyemi, A.J and Ajani, R.A. (2014). Inhibition of key enzymes linked to type 2 diabetes and sodium nitroprusside induced lipid peroxidation in rats pancreas by phenolic extracts of avocado pear leaves and fruit. *International Journal of Biomedicinal Sciences*, 10(3), 208–216.

Özgen, U., Mavi, A., Terzi, Z., Kazaz, C., Aşçı, A., Kaya, Y and Seçen, H. (2011). Relationship between chemical structure and antioxidant activity of luteolin and its glycosides isolated from *Thymus sipyleus* subsp. sipyleus var. sipyleus. *Records of Natural Products, 5*(1), 12-21.

Perez-Fons, L., Garzón, M.T and Micol, V. (2009). Relationship between the antioxidant capacity and effect of *Rosemary* (*Rosmarinus officinalis* L.) polyphenols on membrane phospholipid order. *Journal of Agricultural and Food Chemistry*, 58(1), 161-71.

UNIVERSITY of the
WESTERN CAPE

https://etd.uwc.ac.za/

Raschi, A., Romano, E., Castillo, M., Leyton, P., Paipa, C., Maldonado, L and Brandán, S. (2014). Vibrational study of caffeic acid phenethyl ester, a potential anticancer agent, by infrared, Raman and NMR spectroscopy. *Vibrational Spectroscopy*, 70, 100-109.

Richheimer, S., Bernart, M and King, G. (1996). Antioxidant activity of lipid-soluble phenolic diterpenes from Rosemary . *Journal of the Anericam Oil Chemists Society*, 73(4), 507-514.

Ruaxgruxgsi, N., Tappayuthpijarn, P and Taxtiyataxa, P. (1981). Traditional medicinal plants of thailand. Isolation and structure elucidation of two new flavonoids, (2r,3r)-dihydroquercetin-4'-methyletherand(2r,3r)-dihydroquercetin-4',7-dimethylether from blumea balsamifera. *Journal of Natural Products*, 44(5), 541-545

Salah, M.B., Hafedh, A and Manef, A. (2017). Anti-diabetic activity and oxidative stress improvement of Tunisian *Gerboui* olive leaves extract on alloxan induced diabetic rats. *Journal of Materials and Environmental Sciences*, 8,4, 1359-1364.

Samarghandian, S., Borji, A and Farkhondeh. T. (2017). Evaluation of antidiabetic activity of carnosol (Phenolic diterpene in *Rosemary*) in Streptozotocin-induced diabetic rats. *Cardiovascular & Hematological Disorders-Drug Targets*, 17, 1.

Sindhu, S.N., Vaibhavi, K and Anshu, M. (2013). In vitro studies on alpha amylase and alpha glucosidase inhibitory activities of selected plant extracts. *European Journal of Experimental Biology*, 3(1), 128-132.

Thilagam, E., Parimaladevi, B., Kumarappan, C and Mandal, S.C. (2013). Alpha-glucosidase and alpha-amylase inhibitory activity of *Senna surattensis*. *Journal of Acupuncture and Meridian Studies*, 6(1), 24-30.

UNIVERSITY of the WESTERN CAPE

https://etd.uwc.ac.za/

Vlavcheski, F., Baron, D., Vlachogiannis, L.A., MacPherson, R.E.K and Tsiani, E. (2018). Carnosol increases skeletal muscle cell glucose uptake via AMPK-Dependent GLUT4 glucose transporter translocation. *International Journal of Molecular Sciences.*, 19(5), 1321.

Wang, H., Du, Y.J and Song, H.C. (2010). Alpha-glucosidase and alpha-amylase inhibitory activities of guava leaves. *Food Chemistry*, 123, 1, 6-13.

Wright, E.J., Scism-Bacon, J.L and Glass, L.C (2006). Oxidative stress in type 2 diabetes: The role of fasting and postprandial glycaemia. *International Journal of Clinical Practice*, 60(3), 308–314.

Yatoo, M.I., Dimri, U., Gopalakrishan, A., Saminathan, M., Dhama, K., Mathesh, K., Saxena, A., Gopinath, D and Husain, S. (2016). Antidiabetic and oxidative stress ameliorative potential of ethanolic extract of *Pedicularis longiflora* Rudolph. *International Journal of Pharmacology*, 12 (3), 177-187.

Yun, Y.S., Noda, S., Shigemori, G., Kuriyama, R., Takahashi, S., Umemura, M., Takahashi, Y and Inoue, H. (2013). Phenolic diterpenes from Rosemary suppress cAMP responsiveness of gluconeogenic gene gromoters. *Phytotherapy Research*, 27(6), 906-10.

UNIVERSITY of the
WESTERN CAPE

https://etd.uwc.ac.za/

CHAPTER FIVE

PHYTOCHEMICAL ISOLATION AND BIOLOGICAL INVESTIGATION OF *PLECTRANTHUS ECKLONII*

5.1 Abstract

The phytochemical investigation of a methanolic extract of *Plectranthus eckolonii* afforded three pure compounds namely parvifloron D (**16**), parvifloron F (**17**) and parvifloron G (**18**). The chemical structural elucidation of the isolated compounds was determined on the basis of 1D and 2D NMR, FTIR, Raman spectroscopy and in comparison with literature data. Parvifloron G was isolated for the first time from *P. ecklonii*. The *in vitro* bio-evaluation against alpha-glucosidase moderate inhibitory activities for **18** with IC_{50} values of 41.3 ± 1.2. The *in vitro* bio-evaluation of the antioxidant activity of the isolated compounds of the methanolic extract of *P. ecklonii* were investigated by measuring their FRAP, TEAC and ORAC activities, and the obtained results demonstrated that **18** and **16** exhibited strong antioxidant activity on ORAC (25726.1 ± 8.1; 3942.9.6.6 ± 0.1) µM TE/g respectively, which is in a competitive manner with the positive control (EGCG). Compounds **18** showed good activity on TEAC (3526.1 ± 0.6) µM TE/g, followed by **17** (1069.3 ± 2.4) µM TE/g, as well as on FRAP (1455.4 ± 2.0) µM AAE/g when compared to the reference antioxidant epigallocatechingallate (EGCG). The methanolic extract of *P. ecklonii is* a rich source of abietane diterpenes with strong antioxidant activities. This is the first scientific report on the biological investigation and the in vitro bio-evaluation of *P. ecklonii* constituents against alpha glucosidase and amylase.

5.2 Background information

Plectranthus ecklonii is a shrub, which grows up to 3 m and it is widely distributed in South Africa, Australia, New Zealand, Mexico and the United States. In South Africa, *P.*

https://etd.uwc.ac.za/

ecklonii has a wide distribution ranging from Somerset east in the Eastern Cape to Barberton in Mpumalanga. The leaves of this plant are spread out in opposite pairs on the square stems, the hindmost with tufts of purplish hairs along the nodes. *P. ecklonii* is traditionally used in South Africa to treat different kind of diseases such as stomach-aches, nausea, vomiting and meningitis (Burmistrova, et al., 2015). The aerial part (leave) of the plants is also utilised for respiratory anormalities, chest problems and coughs (TB- related problems) (Hussein, 2018). Aerial parts of the plant are used by Zimbabwean for skin diseases and skin hyper-pigmentation problems (Nyila, et al., 2009). *P. ecklonii* grows predominately in semi-shade areas, under-storey at forest margins or on wooded stream banks during rainfall season especially summer.

Retrived from: http://pza.sanbi.org/plectranthus-ecklonii

Figure 5.1: *P. ecklonii* description

This chapter describes:

- Isolation of the different chemical constituents presents in the methanolic extract of *Plectranthus ecklonii* using different chromatographic methods.
- Structural elucidation of each compound using different spectroscopic techniques.
- In-vitro bio-evaluation of alpha-glucosidase and alpha-amylase inhibitory activities of

https://etd.uwc.ac.za/

the isolated compounds.

- Evaluation of the antioxidant capacities of the isolated compounds.

CHEMICAL CHARACTERIZATION OF *P. ECKLONII* CONSTITUENTS

5.3 General experiment procedure

5.3.1 Reagents and solvents

All organic solvents described in section 3.3.1 were used

5.3.2 Chromatography

5.3.2.1 Thin layer chromatography (TLC)

Unless otherwise stated, the solvent systems generally used for the TLC development of *P. ecklonii* fractions are indicated in Table 5.1.

Table 5.1: TLC solvent systems

Solvent system	Ratio	Assigned code
Hex - EtOAc	9:1	A
Hex - EtOAc	7:3	B
DCM - MeOH	9.5:0.5	C
DCM - MeOH	9:1	D
DCM - MeOH	7:3	E

Hex: hexane; EtOAc: ethylacetate; DCM: dichloromethane; MeOH: methanol

All other chromatographic of TLC, column, and HPLC techniques and procedures described in section 3.3.2 were followed.

5.3.3 Spectroscopy

All analytical procedure of spectroscopic techniques described in section 3.3.3 were followed.

UNIVERSITY of the WESTERN CAPE
https://etd.uwc.ac.za/

5.4 Plant material

The aerial part of the plant material used in this study was collected from the botanical garden of Cape Peninsula University of Technology, Cape Town, South Africa. A voucher specimen was identified at the Compton Herbarium, Kirstenbosch by Prof. Christopher Cupido.

5.5 Extraction and purification of different chemical constituents from *P. ecklonii*

The aerial part of the fresh plant material (932.3 g) were blended and extracted with Methanol (2.5 L) at room temperature (± 25 ^{o}C) for 24 hours. The methanol extract was filtered and evaporated to dryness under reduced pressure at 40 ^{o} C to yield 61.2 g (6.56%). The total extract (60 g) was subjected to silica gel column chromatography and eluted using gradient of Hex and EtOAc in order of increasing polarity as indicated in table 5.2. Fifty-one (51) fractions (250 mL each) were collected during the process and numbered according to (1-51).

UNIVERSITY of the
WESTERN CAPE

https://etd.uwc.ac.za/

Table 5.2: Fractionation of the extract of *P. ecklonii*

Solvent system	Solvent volume	Fraction collected
Hex	05L	1-2
Hex - EtOAc (95:5)	0.5L	3-4
Hex - EtOAc (90:10)	1L	5-8
Hex - EtOAc (85:15)	0.5L	9-10
Hex - EtOAc (80:20)	0.5L	12-11
Hex - EtOAc (75:25)	0.5L	13-14
Hex - EtOAc (70:30)	1L	15-18
Hex - EtOAc (65:45)	1L	19-22
Hex - EtOAc (60:40)	1L	23-26
Hex - EtOAc (55:45)	1L	27-30
Hex - EtOAc (50:50)	1L	31-34
Hex - EtOAc (40:60)	1L	35-38
Hex - EtOAc (30:70)	0.5L	39-40
Hex - EtOAc (20:80)	1L	41-44
Hex - EtOAc (10:80)	1L	45-48
EtOAc	2L	49-51

UNIVERSITY of the
WESTERN CAPE

The collected fractions (1-51) were concentrated and combined according to their TLC profiles (Fig 4) using solvent system Hex/EtOAc (7:3) and Hex/EtOAc (8:2) to yield eight (8) main fractions (Fig 5.2). The obtained fractions were coded by roman numbers (I-VIII) and the results are summarized in table 5.3.

https://etd.uwc.ac.za/

Table 5.3: Fractions obtained upon fractionation of total extract of *P. ecklonii*

Combined fraction	Designated number	Code	Weight of fractions (mg)
1-7	I	PE-I	5462.2
8-16	II	PE-II	2444.5
17-29	III	PE-III	3616.5
30-34	IV	PE-IV	1181.4
35-38	V	PE-V	2742.5
39-43	VI	PE-VI	3183.8
44-46	VII	PE-VII	1910.4
47-51	VIII	PE-VIII	1615.5

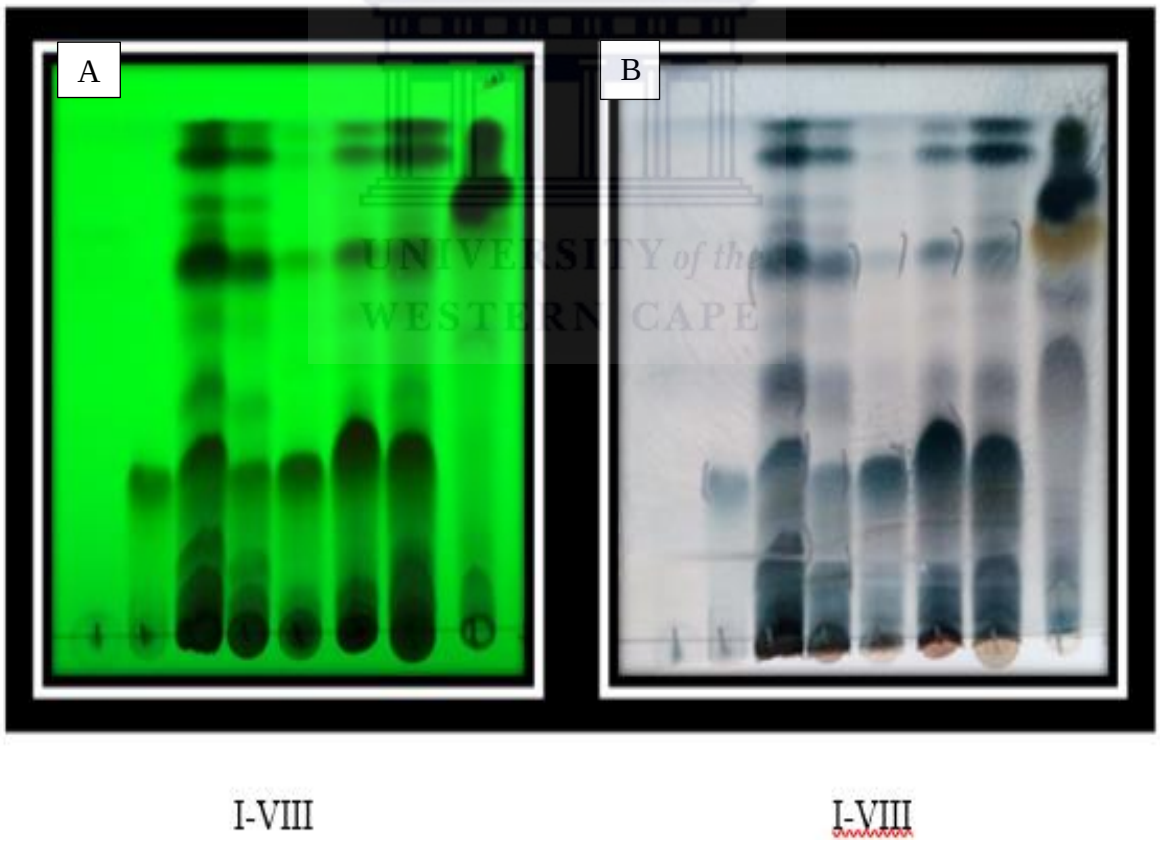

Figure 5.2: TLC plate (silica gel) of combined fractions under UV (254 nm; A), and after spraying with H_2SO_4/vanillin and then heated (B). TLC was developed using solvent system B

https://etd.uwc.ac.za/

5.6 Isolation of pure compounds

5.6.1 Isolation of compound 16 and 17

Main fraction III (3615 mg) was subjected to successive silica gel column using Hex:EtOAc gradient (9:1; 7:3; and 100%). Fractions of 50 mL each were collected and evaporated using rotary evaporator. Fractions obtained were developed on TLC using solvent system B and the fractions that displayed the same profiles on the TLC plate were combined as indicated in Table 5.4.

Table 5.4: Fractions grouped from the column

Fraction	Weight (mg)	Assigned code
0-31	12.1	PE-III-0
32-33	373.2	PE-III-1
34-40	1454.5	PE-III-2
41-43	969.2	PE-III-3
44-47	415.8	PE-III-4
48-51	322.7	PE-III-5

UNIVERSITY of the
WESTERN CAPE

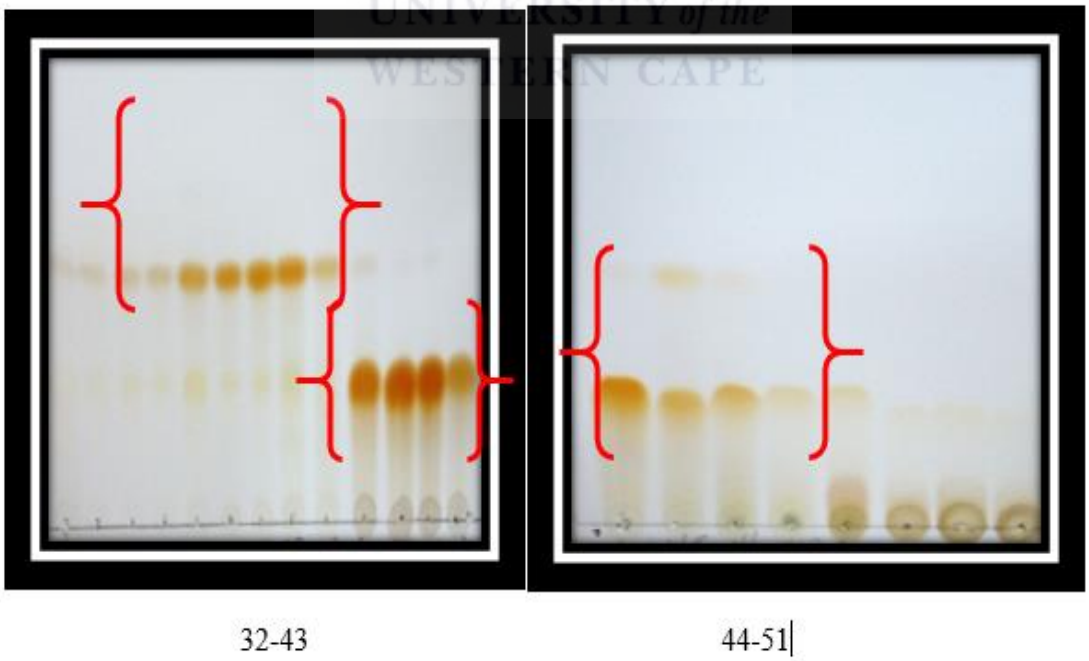

Figure 5.3: TLC silica gel of collected fractions

https://etd.uwc.ac.za/

Fractions 41-43 and 44-47 were suspected pure due to its single spot after development on TLC using solvent system B (Fig. 5.4). These fractions were pooled together, evaporated and re-spotted using solvent system B to further confirm the purity of the combined fractions. The TLC showed only single spot after development, confirmed the purity (Fig. 5.4), and labelled the compound as (**16**, 415.8 mg, 0.045%) and (**17**, 322.7 mg, 0.035%).

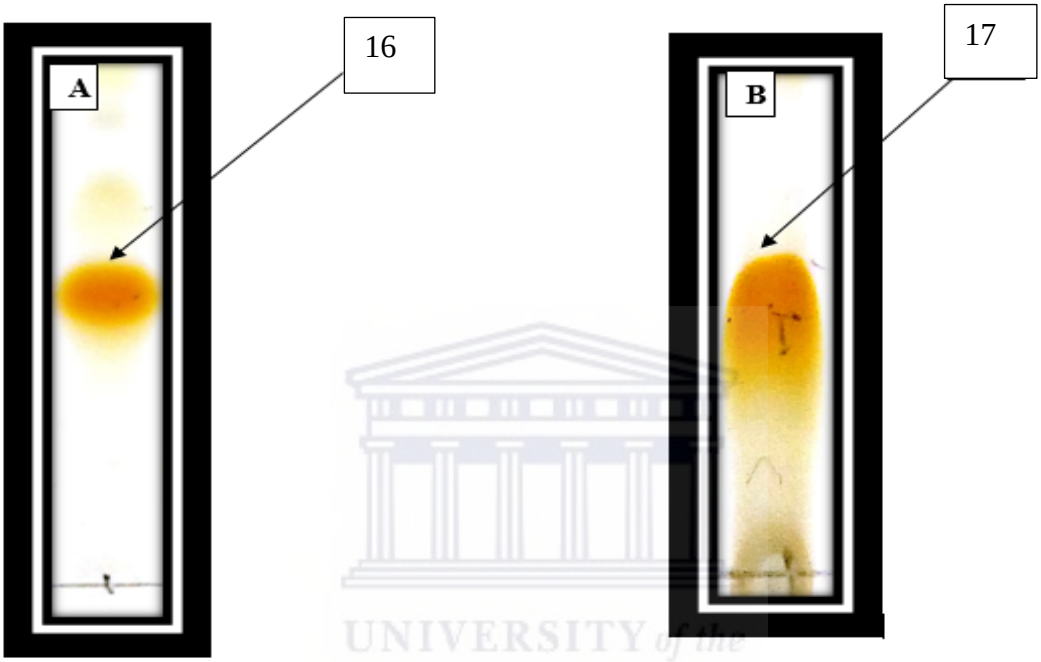

UNIVERSITY of the
WESTERN CAPE

Figure 5.4: TLC plate of **16** (A) and **17** (B)

5.6.2 Isolation of compound 18

Sub fraction PE-III-2 (54.5 mg) was injected to the HPLC and eluted using gradient solvent system of MeOH and de-ionized water (50:50 to 100% MeOH in 60 min), which afforded a prominent peak as shown in Figure 5.5B, collected and labelled as **PE-III-2-1**. After spotting and developing the fractions on TLC plate using solvent system C, a single spot suspected to be a pure compound was observed (Fig 5.5A). The fractions that afforded this single spot were pooled together and labelled as **18** (R_t 42.1 min, 29.9 mg, 0.032%).

https://etd.uwc.ac.za/

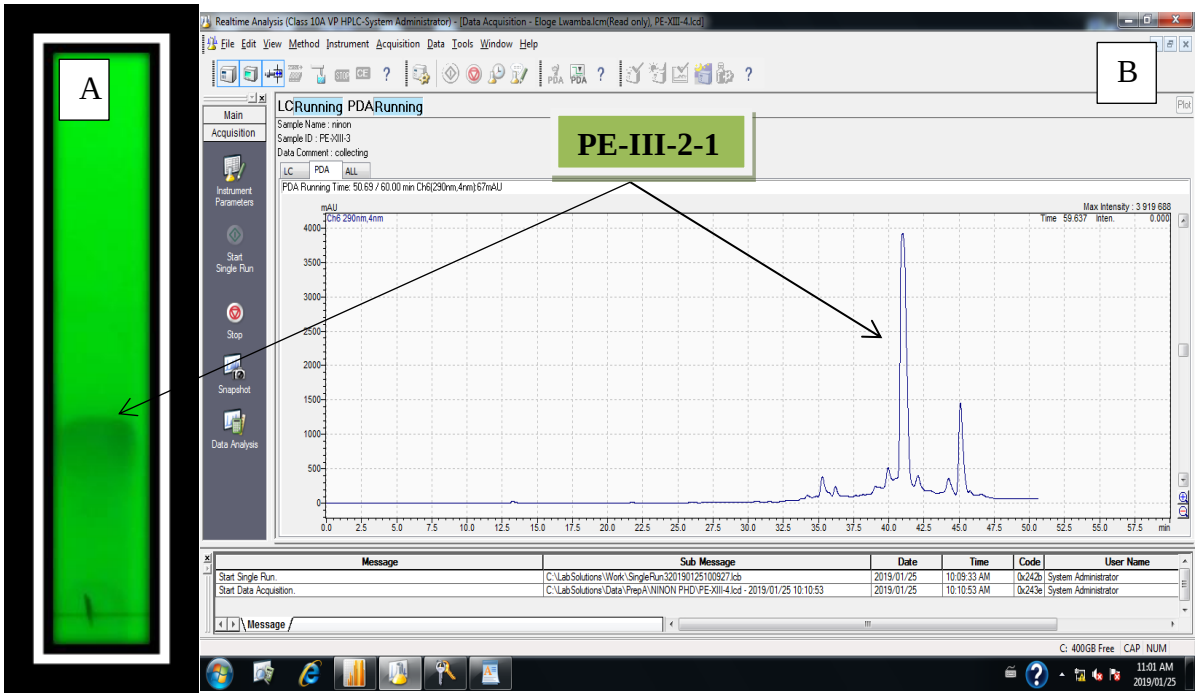

Figure 5.5: TLC silica gel of PE- III-2-1 (Fig. 5.5A) and HPLC chromatogram of sub fraction PE-III-2 (Fig. 5.5B).

***Conditions**

Solvent	MeOH:DIW 70:30 to 100% in 60 min
Column	SUPELCO, RP-18 (25 x 1 cm)
Flow rate	1.0 mL/min
Detection	UV at 290 nm

UNIVERSITY of the
WESTERN CAPE

https://etd.uwc.ac.za/

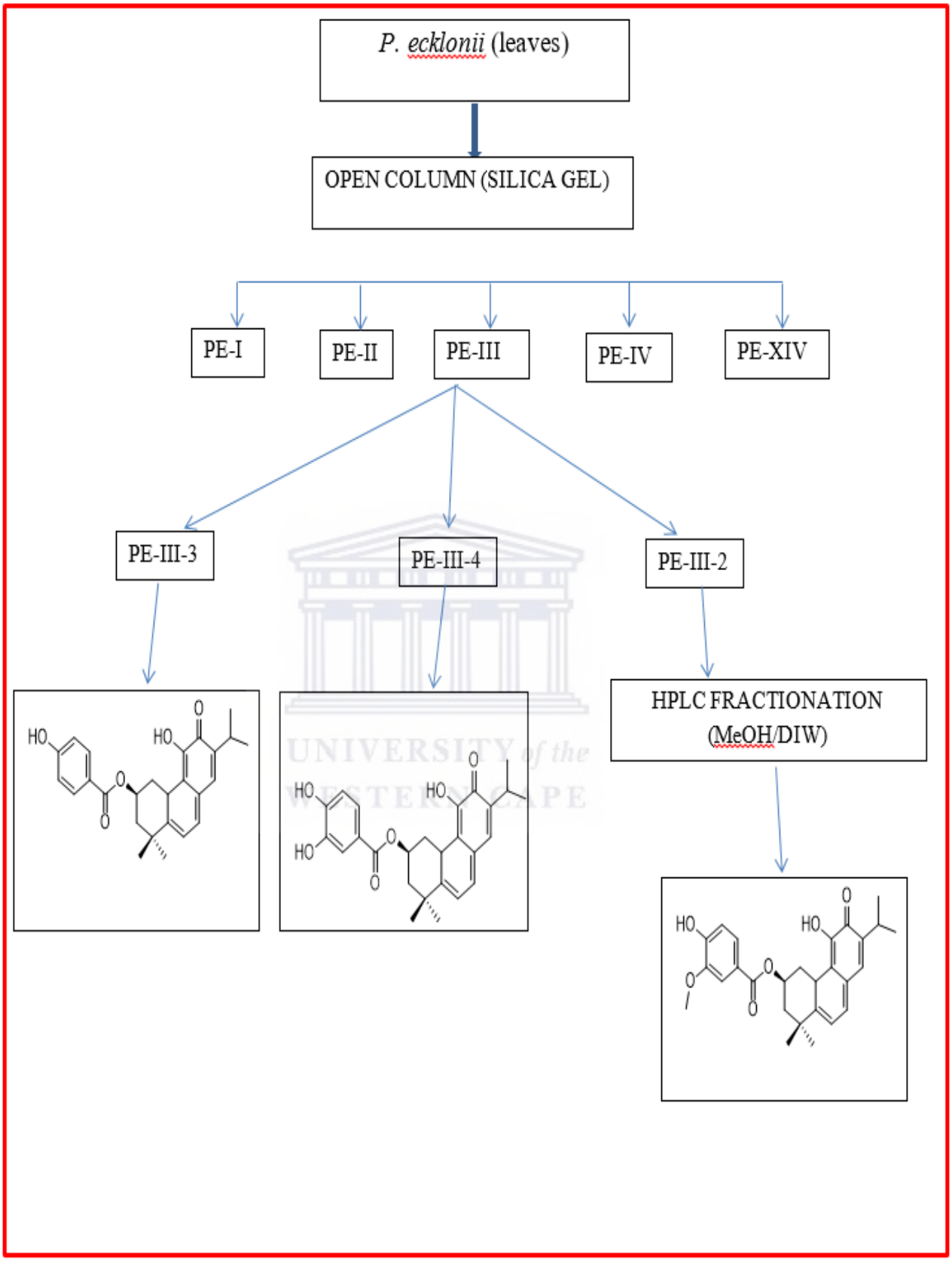

Scheme 5.1: A flow diagram of experimental procedure for the isolation of compounds from *P.ecklonii*

https://etd.uwc.ac.za/

BIOLOGICAL CHARACTERIZATION OF ISOLATED COMPOUNDS

5.7 General experimental procedure for biological assays

5.7.1 Reagents

5.7.2 Alpha-glucosidase inhibitory activity

Alpha-glucosidase assay described in section 3.7.2 was carried out.

5.7.3 Alpha-amylase inhibitory activity

Alpha-amylase assay described in section 3.7.3 was carried out.

5.7.4 Total Antioxidant capacities assays

All experimental procedure for the various antioxidant capacity assays (FRAP, ORAC, and TEAC) as described in section 3.7.4 were followed.

5.8 Statistical analysis

Statistical analyses described in section 3.8 was followed

5.9 Chemical characterization: Results and discussion

Chromatographic purification of a methanolic extract of *P. ecklonii* using different techniques including semi Prep-HPLC yielded three pure terpenoids (Fig. 5.6). One of the compounds has been isolated for the first time from *P. ecklonii*.

https://etd.uwc.ac.za/

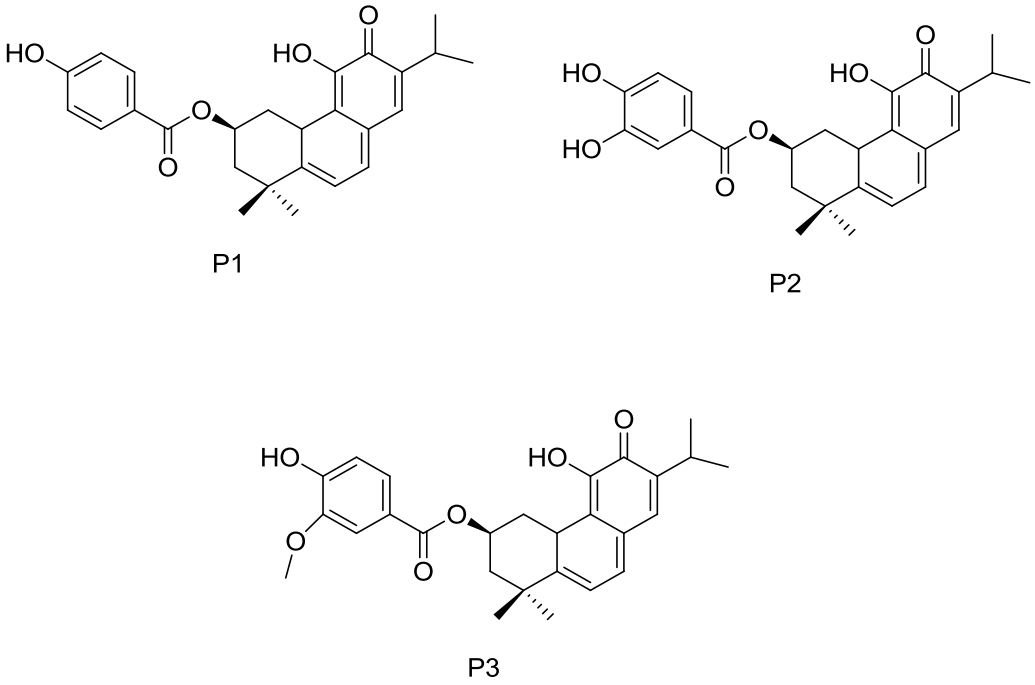

Figure 5.6: Chemical structures of the isolated compounds

5.9.1 Structure elucidation of parvifloron D (**16**)

Compound **16** was isolated as orange powder from as described in Scheme 5.1. Its IR spectrum exhibited bands at 1679 cm^{-1} for the carbonyl lactone group (C=O), 2957 and 2916 cm^{-1} for the carbon-hydrogen stretching (C-H) as well as at 3286 cm^{-1} attributed to hydroxyl group (OH) (Fig. 5.11). The Raman spectrum featured characteristic bands at 1630 cm^{-1} related to C=C stretching, 1523 cm^{-1} related to C-C stretching, 1450 cm^{-1} related to the deformation vibration of the CH_2, 1160 cm^{-1} attributed to C-C-O stretching (Fig. 5.12). (Belt, et al., 2017; Thilagam, et al., 2013; Raschi, et al., 2014). It was identified as parviflorone D based on its NMR data, which showed typical abietane diterpene signals (Figure 5.6). The ^{13}C NMR and DEPT spectra (Fig. 5.9, 10) confirmed the presence of twenty septs (27) carbons consisted of 20 carbons belonging to the diterpene skeleton and 6 of which belong to the signals of p-benzoic acid derivatives. The signal of 2β was shifted to low field due to the esterification of the p-benzoic acid with the OH at the same position. The ^{1}H NMR signals showed five methyl groups signals at 1.16, 1.18 (*d*/each, *J* = 2.8, Me-16,17) 1.30 (*s*, Me-18),

UNIVERSITY of the WESTERN CAPE
https://etd.uwc.ac.za/

1.43 (*s*, Me-19), 1.66 (*s*, Me–20), in addition to signals at 6.42 (*d*, *J* = 6.8; H-6); 6.79 (*d*, *J* = 6.8, H-7); 6.89 (*d*, *J* = 8.6, H-14); 6.97 (*s*, H-2β). The identity of the compound was confirmed by comparing the experimental data with literature (Santos-Rebelo, et al., 2018). This compound was previously isolated from *P. strigosus* Benth (Nyila, et al., 2009).

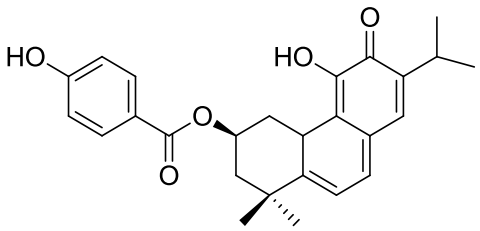

Parvifloron D.

Figure 5.7: Chemical structure of **16**

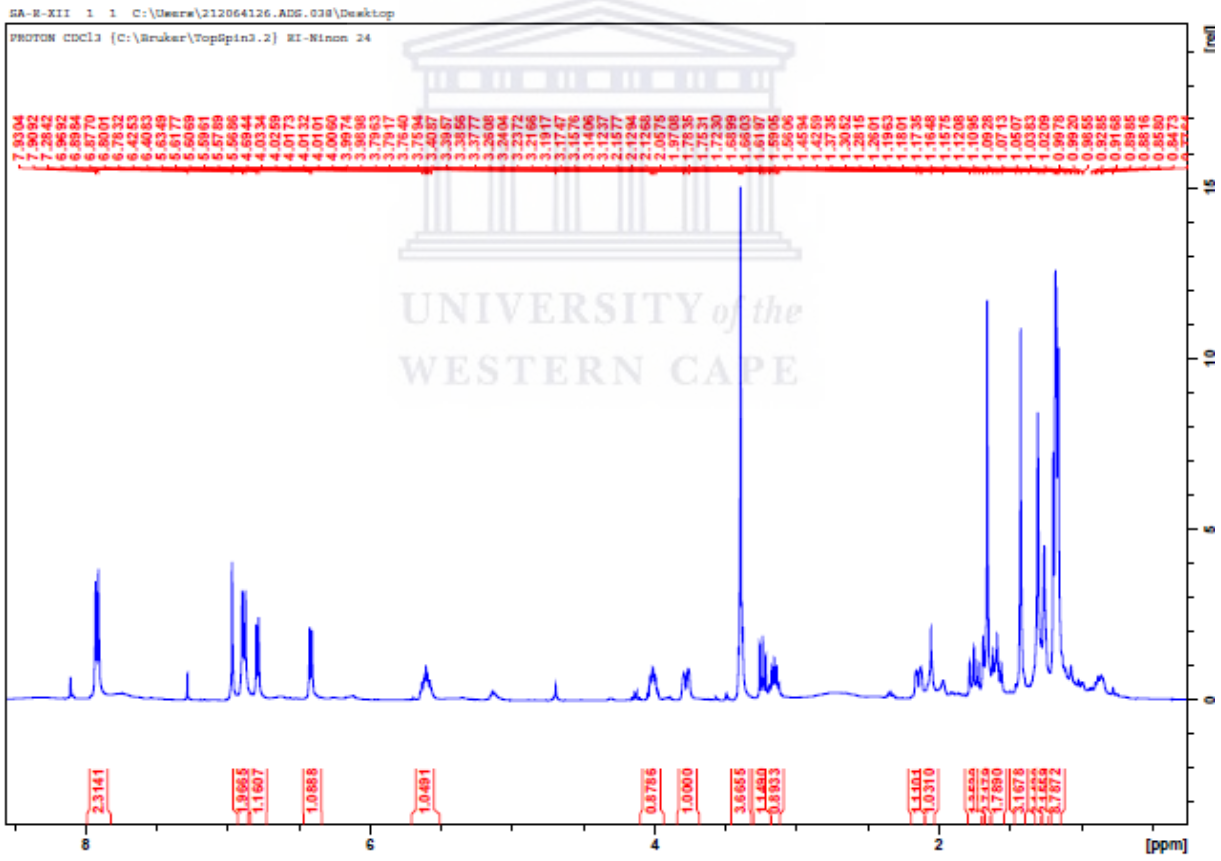

Figure 5.8: ^{1}H NMR (400 MHz, CDCl3) spectrum of **16**

UNIVERSITY of the WESTERN CAPE

https://etd.uwc.ac.za/

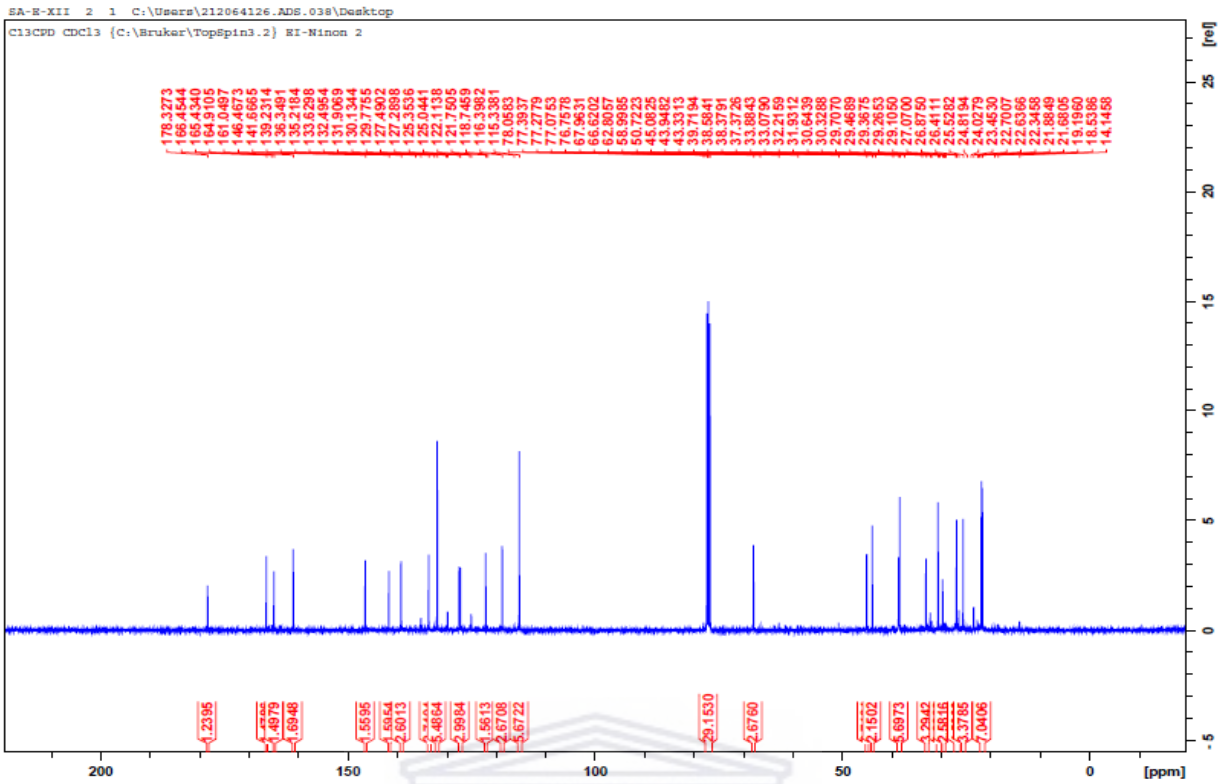

Figure 5.9: ^{13}C NMR (400 MHz, CDCl3) spectrum of **16**

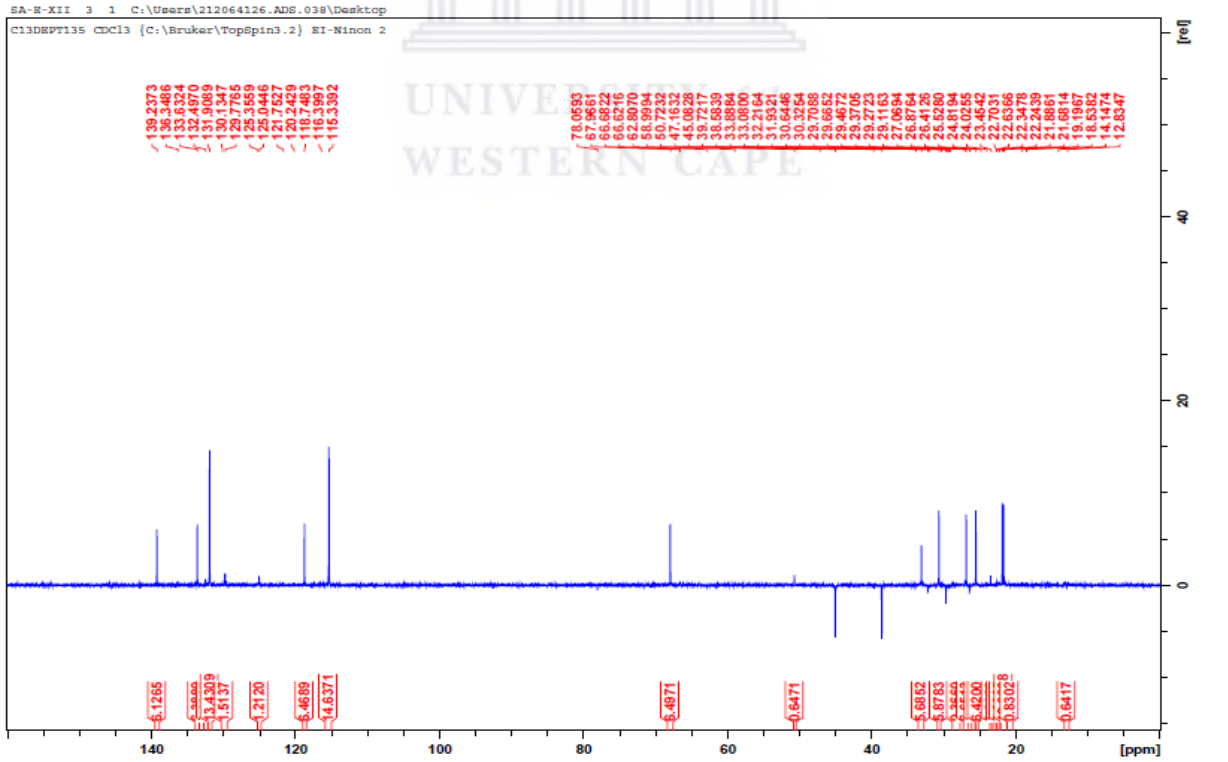

Figure 5.10: DEPT NMR (400 MHz, CDCl3) spectrum of **16**

https://etd.uwc.ac.za/

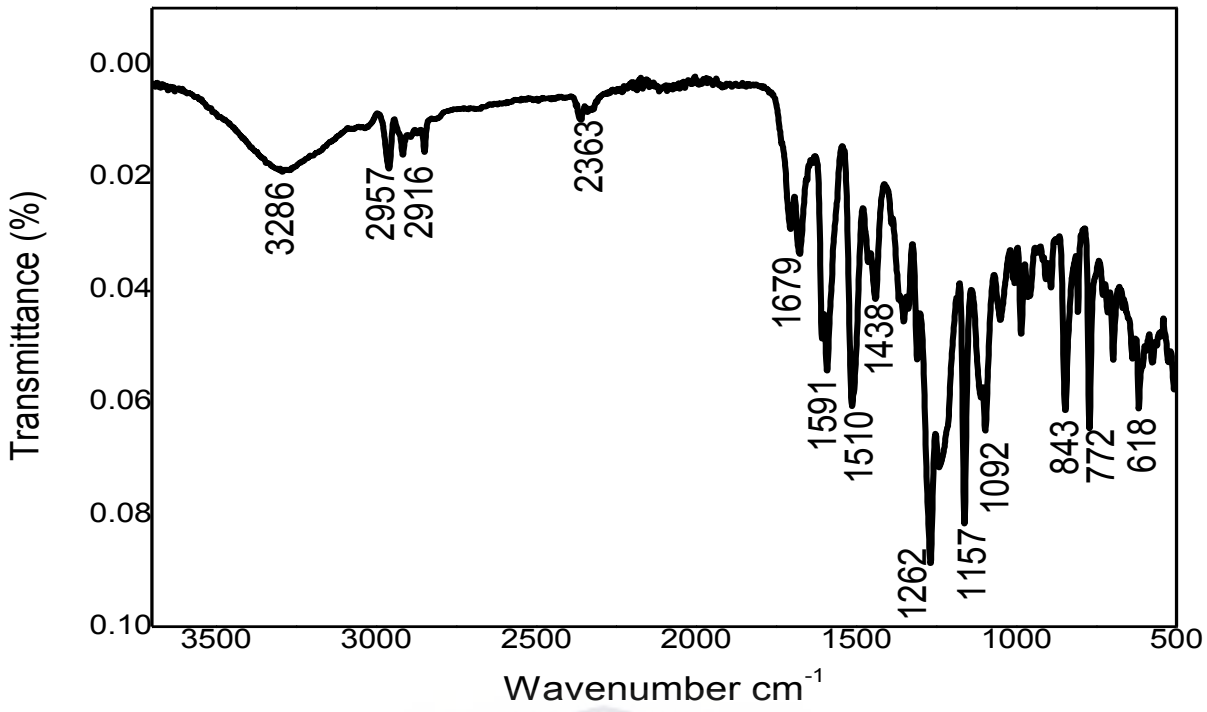

Figure 5.11: FTIR spectrum of **16**

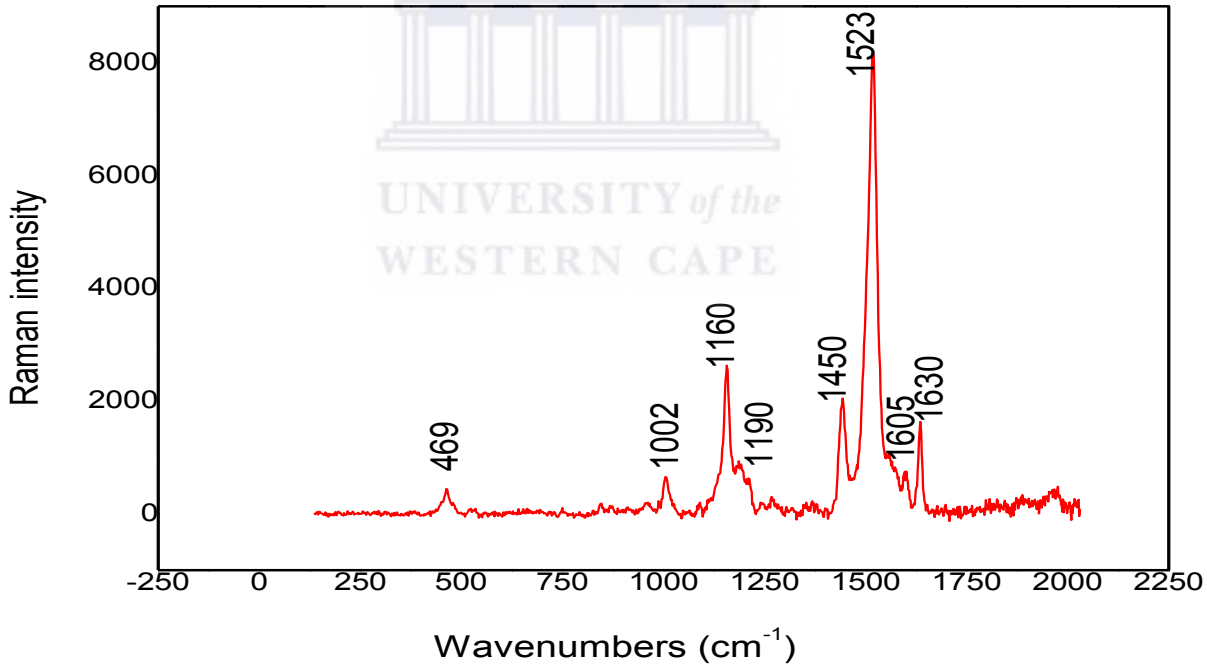

Figure 5.12: Raman spectrum of **16**

RAMAN	Intensity	Assignments
1002	w	C-O-C stretching
1160	n	C-C-O stretching
1450	n	CH_2 deformation
1523	s	C-C deformation
1605	w	C=C stretching
1630	n	C=C stretching

https://etd.uwc.ac.za/

5.9.2 Structure elucidation of parviflorone F (**17**)

Compound **17** was isolated as yellow powder from the polar part of the extract of P. ecklonii. Its IR spectrum exhibited bands at 1703 cm^{-1} for the carbonyl lactone group (C=O), 2957 for the carbon-hydrogen stretching (C-H) as well as at 3302 cm^{-1} attributed hydroxyl group (OH) (Fig.5.17), which is in agreement the report data. The Raman spectrum featured characteristic bands at 1969 cm^{-1} related to C-H stretching, 1636 cm^{-1} related to C=C stretching, 1516 cm^{-1} related to C-C stretching , 1447 cm^{-1} attributed to the deformation vibration of the CH_2 (Fif. 5.18) (Belt, et al., 2017; Thilagam, et al., 2013; Raschi, et al., 2014). It was identified as parvifloron F based on its NMR data, which showed close similarity with **16** except for the side chain, which exhibited signals of 1,3,4- trisubstituted benzoic acid patterns instead of 1,4-disubstituted benzoic acid. The identity of the compound was confirmed by comparing the experimental data with literature (Narukawa, et al., 2001). This compound was previously isolated from *P. nummularius* Briq (Nyila, et al., 2009).

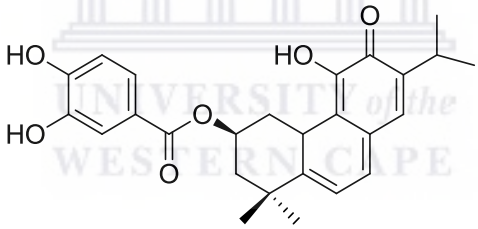

Parvifloron F

Figure 5.13: Chemical structure of **17**

https://etd.uwc.ac.za/

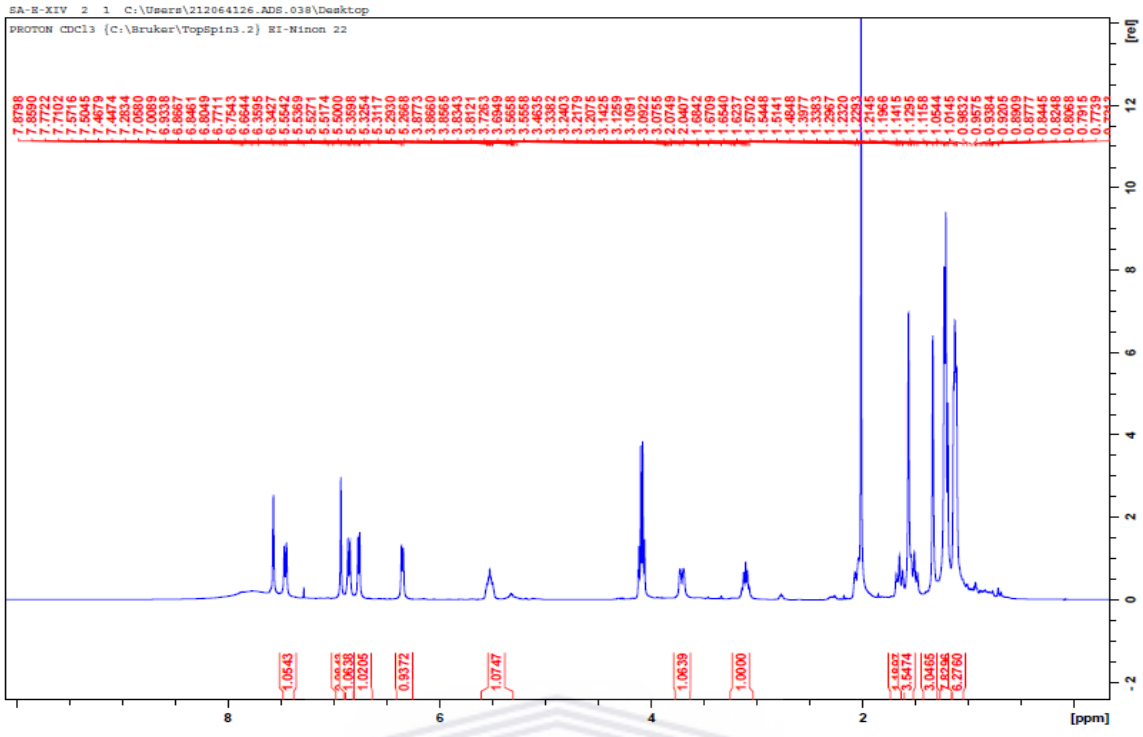

Figure 5.14: ^{1}H NMR (400 MHz, CDCl3) spectrum of **17**

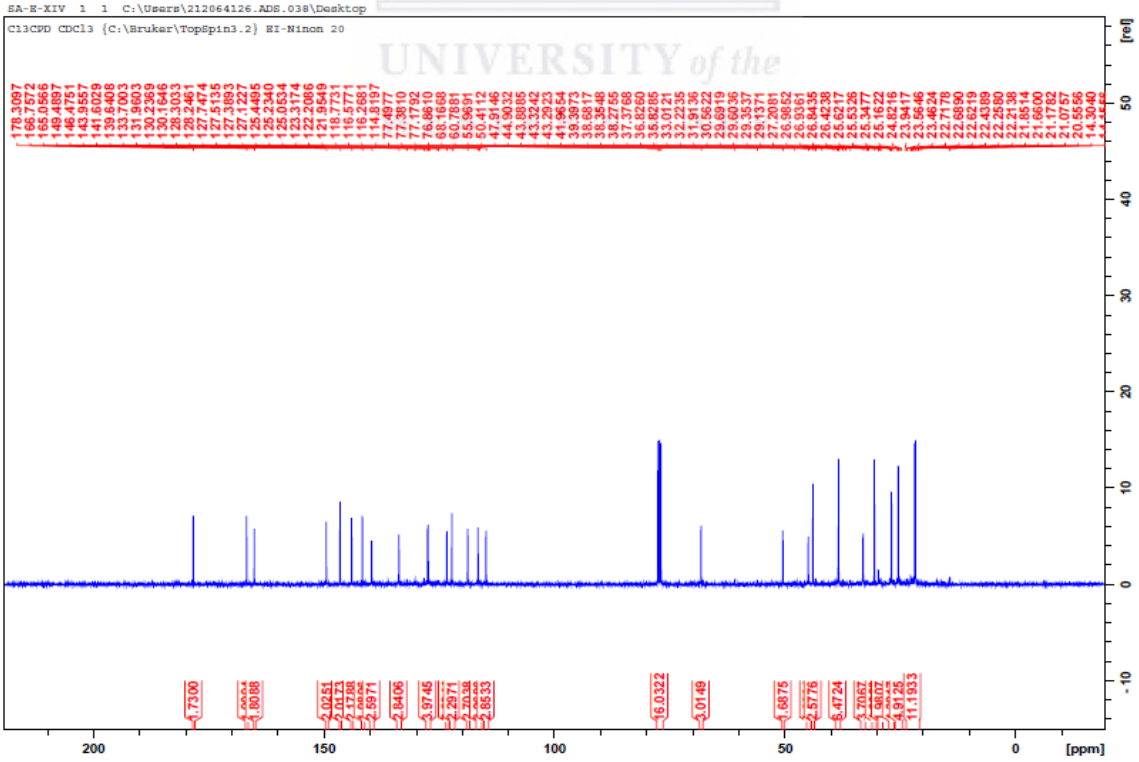

Figure 5.15: ^{13}C NMR (400 MHz, CDCl3) spectrum of **17**

https://etd.uwc.ac.za/

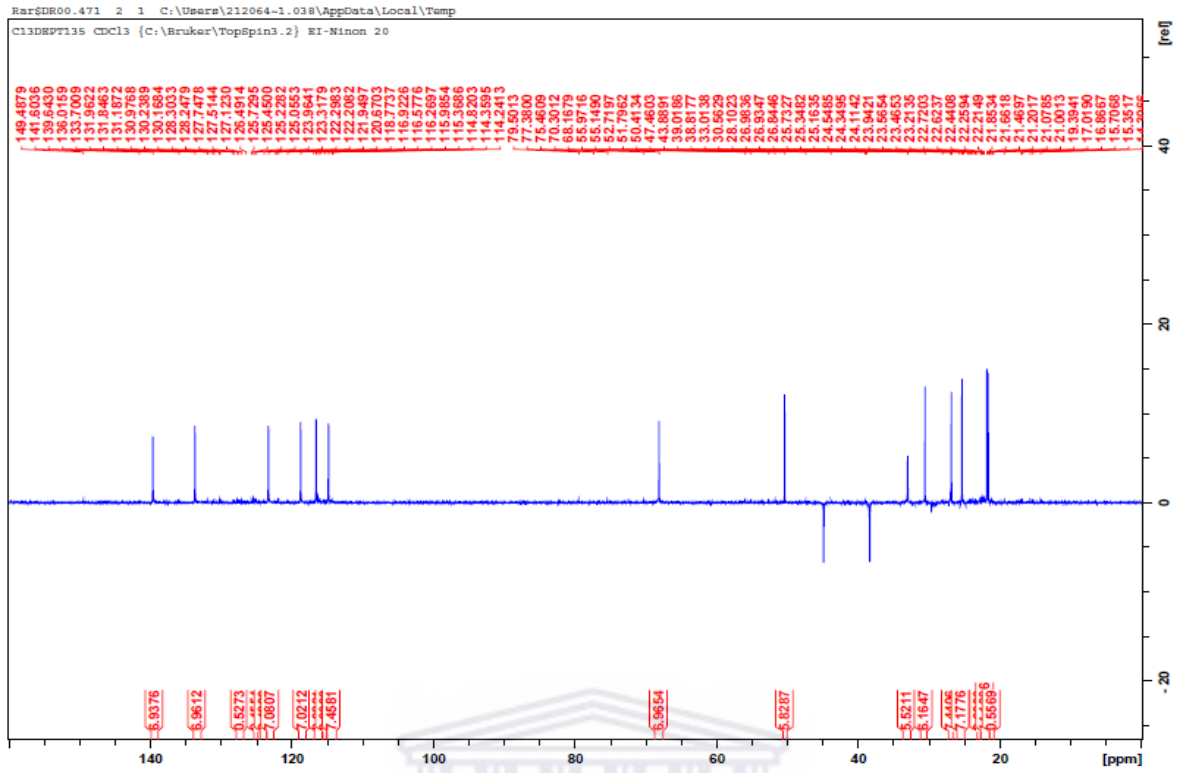

Figure 5.16: DEPT NMR (400 MHz, CDCl3) spectrum of **17**

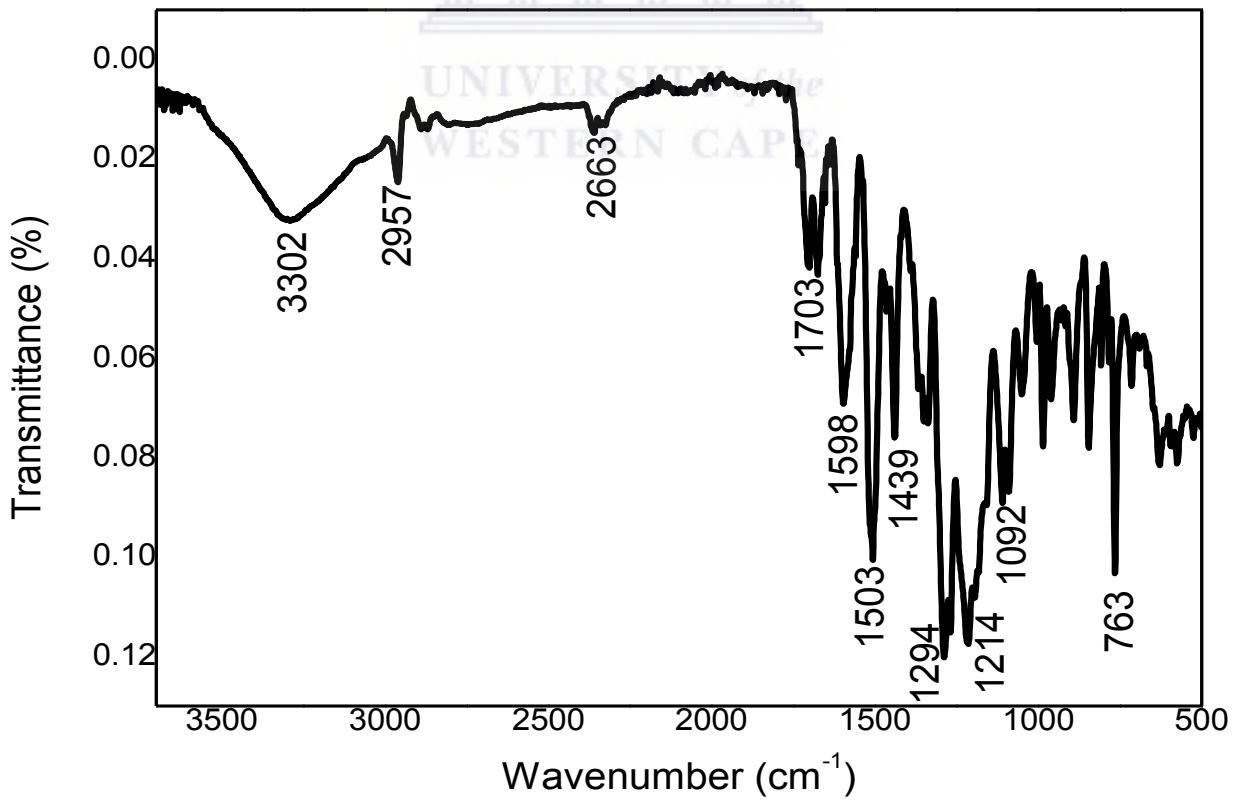

Figure 5.17: FTIR spectrum of **17**

https://etd.uwc.ac.za/

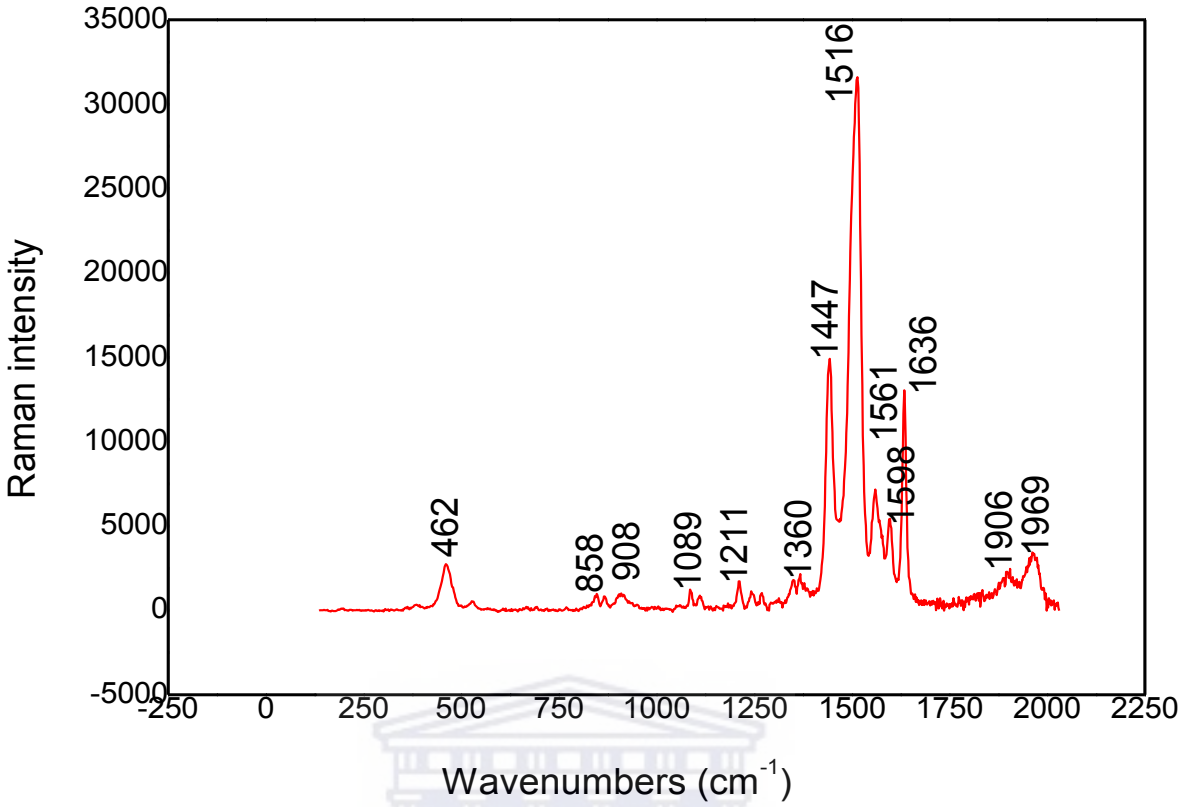

Figure 5.18: Raman spectrum of **17**

RAMAN	Intensity	Assignments
858	w	CH_2 torsion
1089	w	C-C-O stretching
1211	w	O-H deformation
1360	w	CH_2 wagging
1447	n	CH_2 deformation
1516	s	C-C deformation
1561	n	C-C stretching
1598	n	C-C stretching
1636	n	C=C stretching
1906	w	C-H stretching
1969	w	C-H stretching

5.9.3 Structure elucidation of parviflorone G (18)

Compound **18** was isolated as yellow brownish powder from the polar part of the extract of *P. ecklonii*. Its IR spectrum exhibited bands at 1677 cm^{-1} for the carbonyl lactone group (C=O), 2956 and 2876 for the carbon-hydrogen stretching (C-H) as well as at 3292 cm^{-1} attributed hydroxyl group (OH) (Fig. 5.26). It was identified as parvifloron G based on its

https://etd.uwc.ac.za/

NMR data, which showed close similarity with **16** and **17** except the presence of the methoxyl group on the benzoic acid. The identity of the compound was confirmed by comparing the experimental data with literature (Abdel-Mogib, et al., 2002). This is the first report on the isolation of compound **18** from *P. ecklonii*. This compound was previously isolated from *P. strigosus* (Alder, et al., 1984).

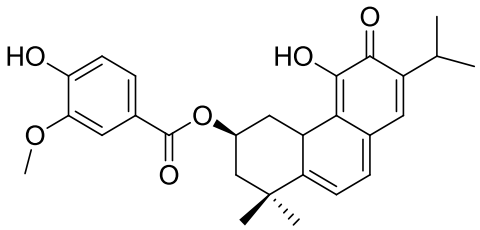

Parviflorone G

Figure 5.19: Chemical structure of **18**

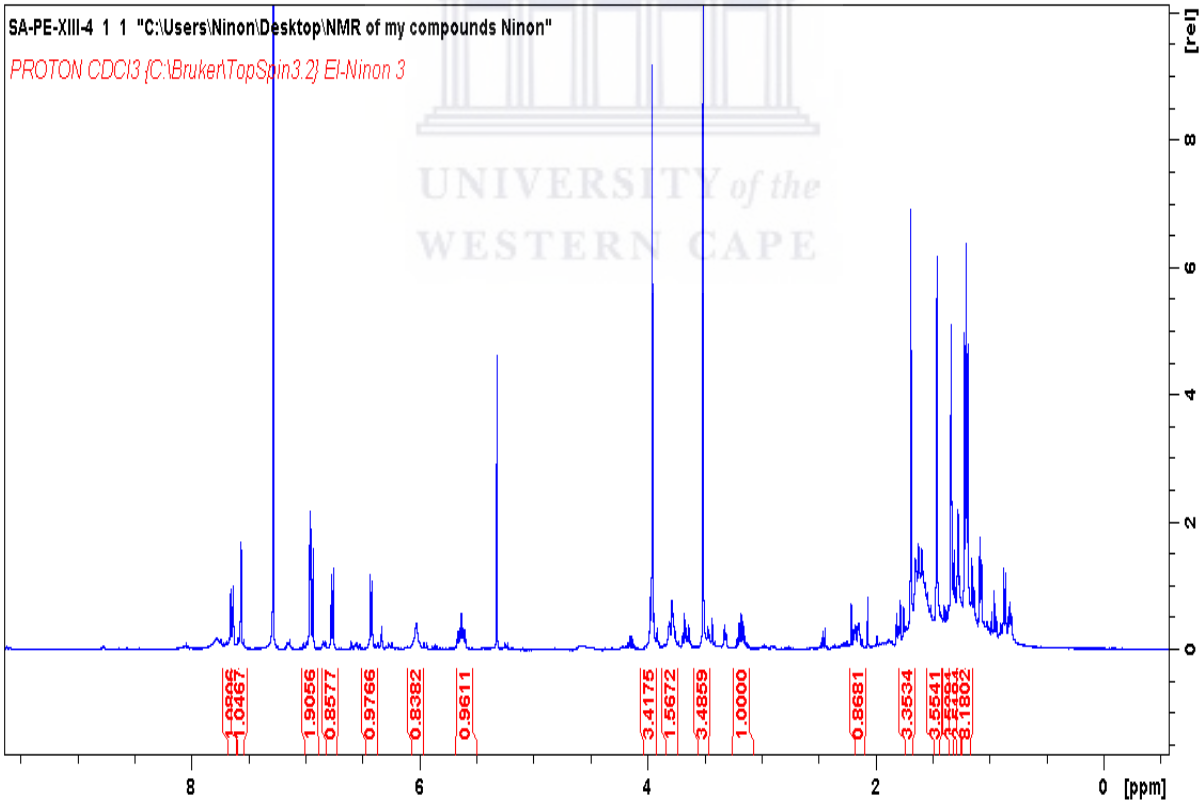

Figure 5.20: ^{1}H NMR (400 MHz, CDCl3) spectrum of **18**

https://etd.uwc.ac.za/

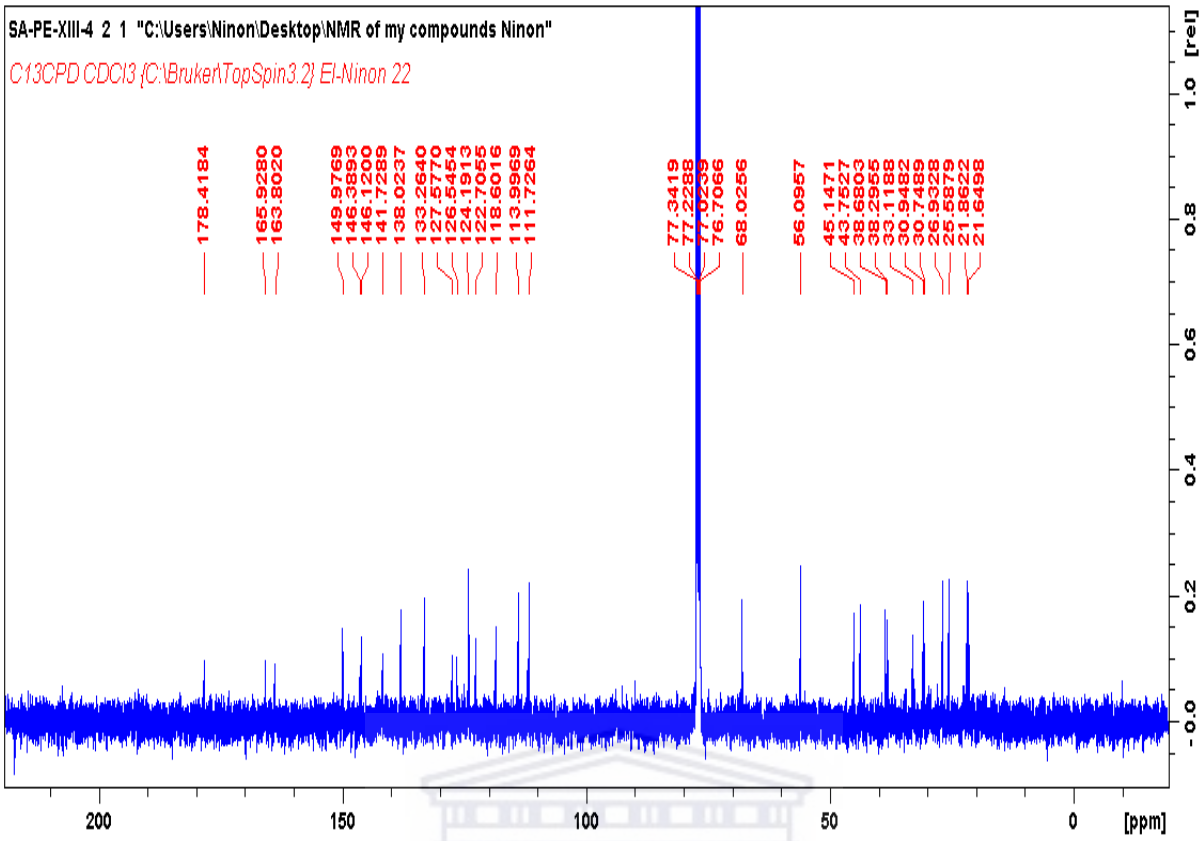

Figure 5.21: ^{13}C-NMR (400 MHz, CDCl3) spectrum of **18**

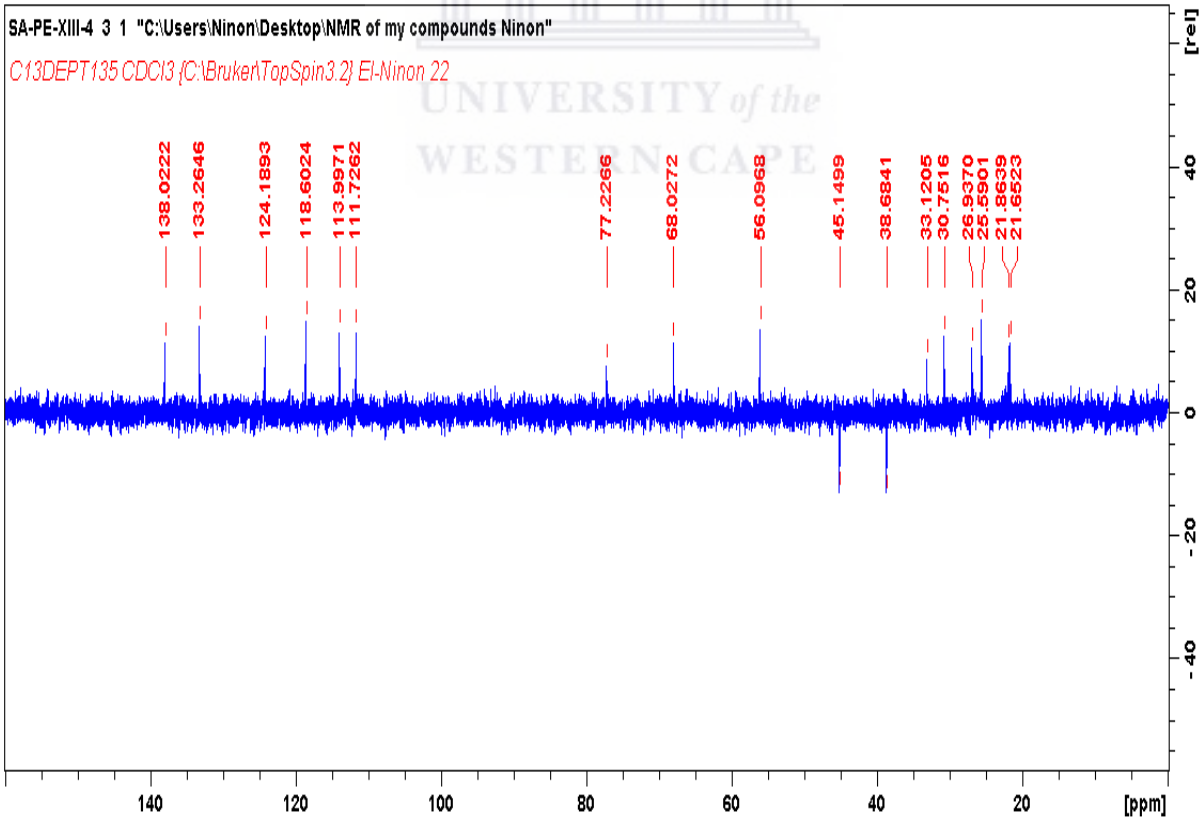

Figure 5.22: DEPT NMR (400 MHz, CDCl3) spectrum of **18**

https://etd.uwc.ac.za/

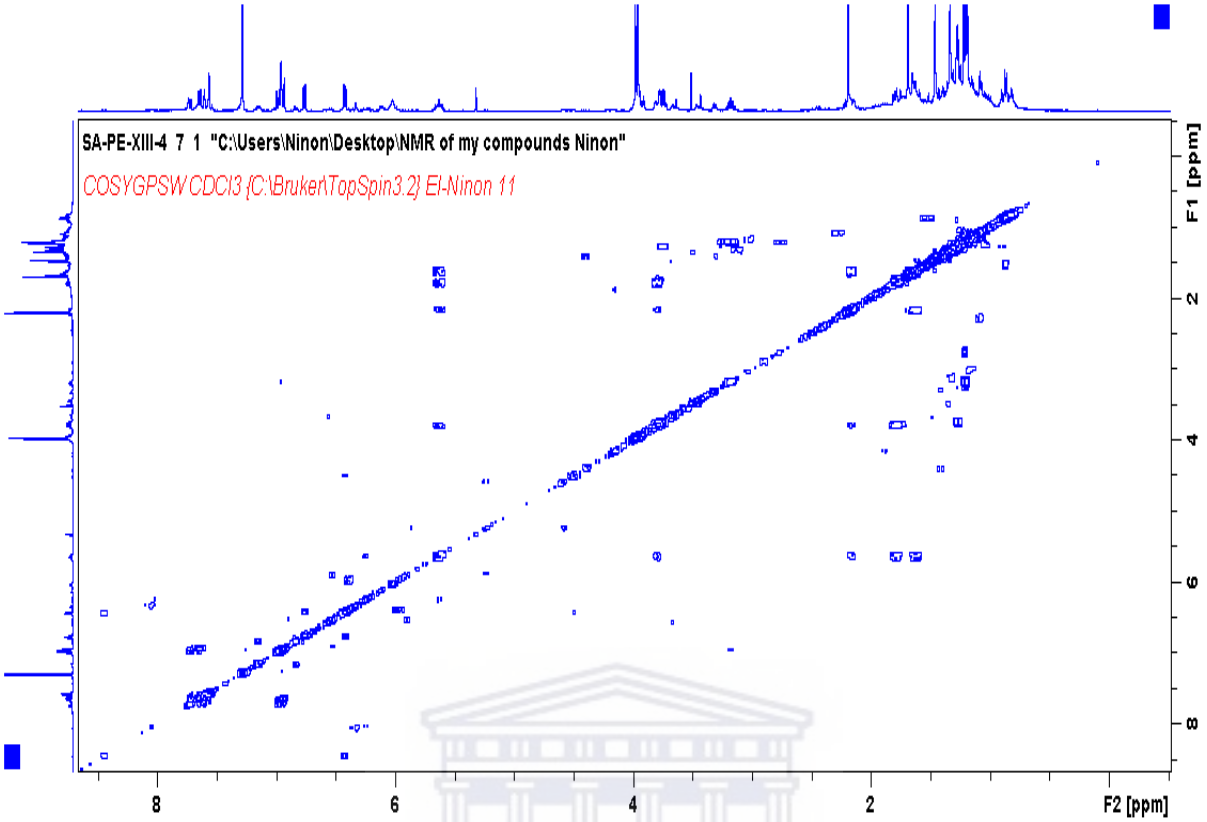

Figure 5.23: COSY (400 MHz, CDCl3) spectrum of **18**

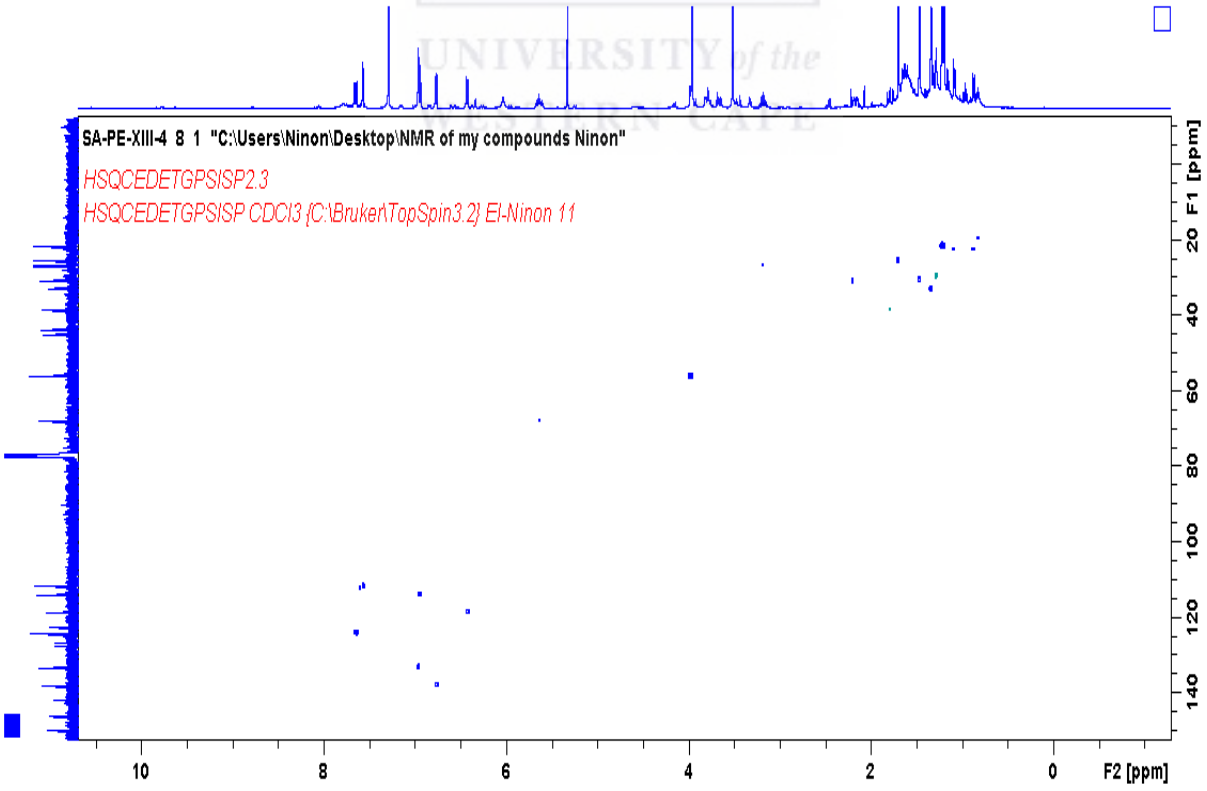

Figure 5.24: HSQC (400 MHz, CDCl3) spectrum of **18**

https://etd.uwc.ac.za/

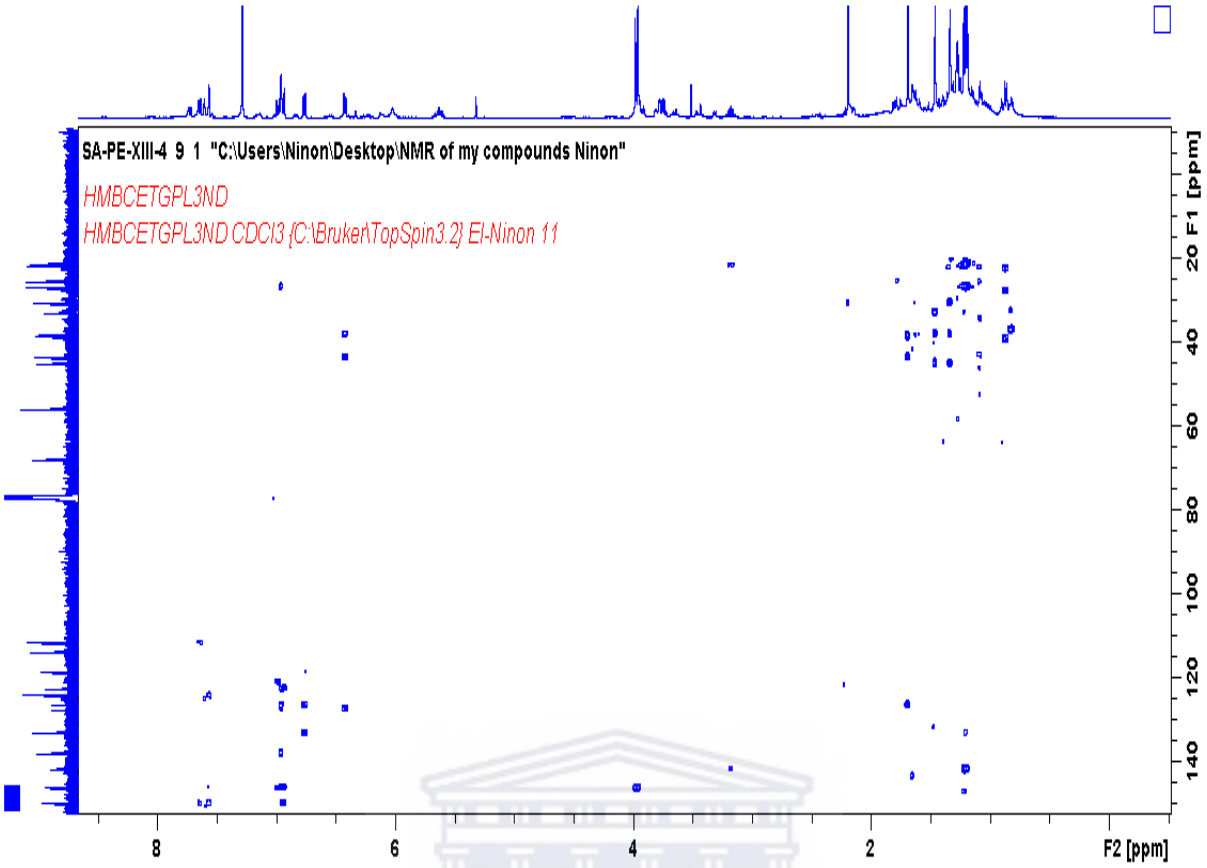

Figure 5.25: HMBC (400 MHz, CDCl3) spectrum of **18**

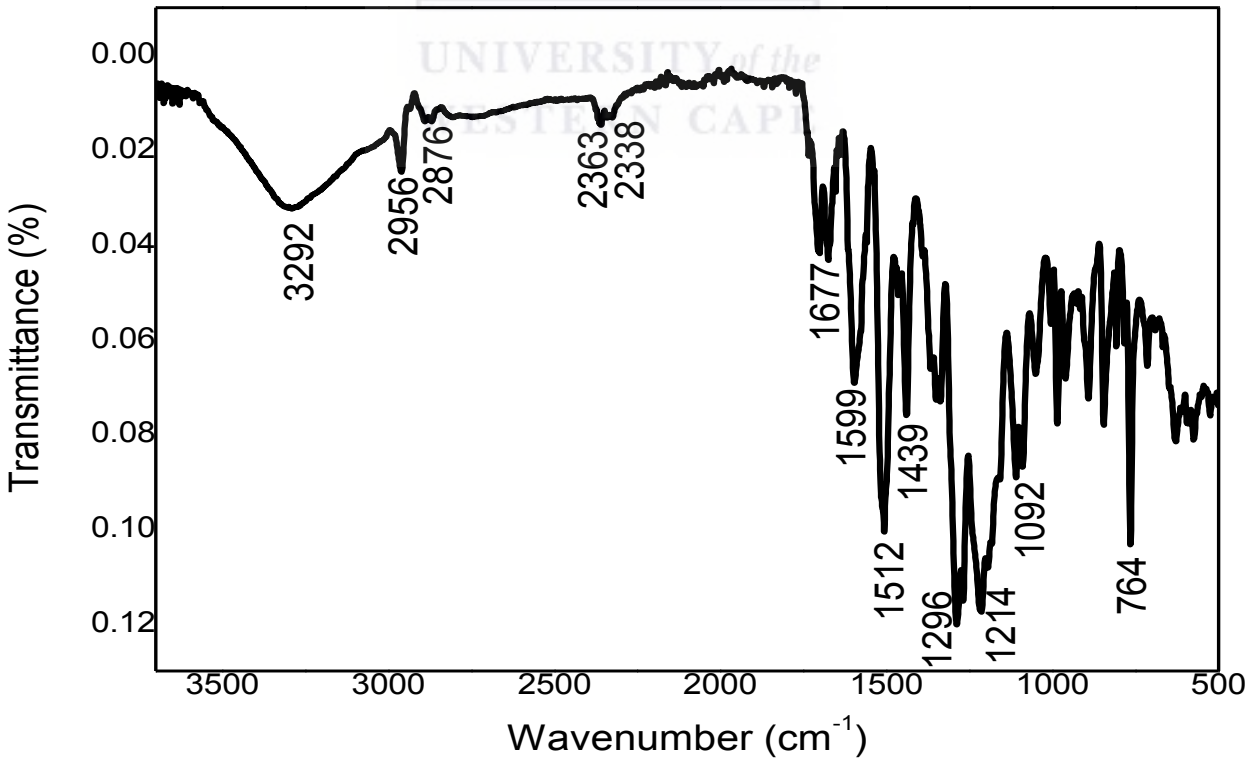

Figure 5.26: FTIR spectrum of **18**

https://etd.uwc.ac.za/

5.10 Biological evaluation: Results and discussion

5.10.1 Alpha-glucosidase and alpha-amylase activities

The search of antidiabetic compounds from natural source has been intensified and a great deal of research is being conducted to identify plants/compounds with prominent anti-diabetic activity with emphasis on the inhibition of the two enzymes, alpha-glucosidase and alpha-amylase. In this study, the inhibitory activity of isolated compounds from *P. ecklonii* was investigated and the results showed that **18** is the only compound that exhibited moderate alpha-glucosidase inhibitory activity with IC_{50} value of 41.3 ± 1.2 µg/mL. The crude extract shown some activity against alpha-glucosidase enzyme with IC_{50} value of 145.4 ± 3.1 µg/mL as shown in Table 5.5. Compounds **16**, **17** and **18** shared the same chemical backbone except the presence of the methoxyl group on the benzoic acid in **18**, which might be responsible for the moderate bio-activty demonstrated.

Table 5.5: Alpha glucosidase and alpha amylase inhibitory activities of the isolated compounds.

Items	**Alpha-glucosidase** IC_{50} (µg/mL)	**Alpha-amylase** IC_{50} (µg/mL)
16	NA	NA
17	NA	NA
18	41.3 ± 1.2	NA
PE	145.4 ± 3.1	NA
Acarbose	610.4 ± 1.0	10.2 ± 0.6

NA not active at the test concentrations. The results are expressed as mean ±SEM for n = 3

5.10.2 Antioxidant activity

Oxidative stress is mainly caused by an over-accumulation of free radicals, which are produce by our body by various endogenous systems such as exposure to various physiochemical conditions or pathological states. Hence, free radicals can alter lipids, proteins, and DNA and set off a number of human diseases including diabetes (Rosa, et al., 2015). One of the therapeutic approaches to combat these diseases is to search for potential antioxidant candidates that can assist in managing oxidative stress and other related diseases

https://etd.uwc.ac.za/

(Lobo, et al., 2010). The *in vitro* bio-evaluation of the antioxidant activity of the isolated compounds of the methanolic extract of *P. ecklonii* were investigated by measuring their FRAP, TEAC and ORAC activities. The results demonstrated that **18** and **16** exhibited strong antioxidant activity on ORAC (25726.1 ± 8.1; 3942.9.6.6 ± 0.1) µM TE/g respectively, which is in a competitive manner with the positive control (EGCG). Compounds **18** showed the strongest activity on TEAC (3526.1 ± 0.6) µM TE/g, followed by **17** (1069.3 ± 2.4) µM TE/g, as well as on FRAP (1455.4 ± 2.0) µM AAE/g when compared to the reference antioxidant epigallocatechingallate (EGCG) as shown in Table 5.6. Additionally, the crude extract of *P. ecklonii* exhibited excellent free radicals scavenging effect with IC50 value of 54. 8 ± 07 µg/mL, which justify the bioactivity demonstrated by its chemical constituents.

Table 5.6: Antioxidant activities of the isolated compounds

Items	ORAC (µmole TE/g)	TEAC (µmole TE/g)	FRAP (µM AAE/g)
16	3942.9 ± 6.6	470.3 ± 2.2	1043.9 ± 2.6
17	1726.1 ± 2.6	1069.3 ± 2.4	1155.5 ± 2.3
18	28726.1 ± 8.1	3526.1 ± 0.6	1455.4 ± 2.0
EGCG	3976.82 ± 3.82	4146.4 ± 19.77	7524.98 ± 4.94

UNIVERSITY of the
WESTERN CAPE

Parvifloron D **(16)** has been reported to have strong antioxidant activity when evaluated for its ability to scavenge the DPPH radical (IC_{50} = 1.27 ± 0.07) mM and its structure-activity relationship might be ascribed by the fact that **16** can generate a molecule with greater resonance stabilization which can easily scavenge the DPPH radical (Rosa, et al., 2015). It has been reported tthat **17** scavenges the DPPH radical more than tocopherol (positive control) with EC_{50} value of 0.131 mM (Narukawa, et al., 2001).

5.11 Conclusion

The phytochemical and biological investigation of the methanolic extract of *P. ecklonii* revealed that this plant is a rich source of abietane diterpenes with moderate alpha glucosidase inhibitory activity as well as significant antioxidant activities. The present work

https://etd.uwc.ac.za/

is the first scientific report on the biological investigation of *P. ecklonii* constituents against alpha glucosidase and amylase enzymes and the results suggest that the methanolic extract of this plant and/or its individual constituents might become potent natural therapeutic agents for oxidative stress. Therefore, compounds that demonstrated potent antioxidant activities may be very good candidate for controlling oxidative stress in diabetic patients.

References

Abdel-Mogib, M., Albar, H.A and Batterjee, S.M. (2002). Chemistry of the Genus *Plectranthus. Molecules*, 7, 271301.

Adler, A.C., Redi, P and Eugster, C.H. (1984). *Helv. Chim. Acta*, 67, 1531.

Belt, T., Keplinger, T., Hänninen, T and Rautkari, L. (2017). Cellular level distributions of Scots pine heartwood and knot heartwood extractives revealed by Raman spectroscopy imaging. *Industrial Crops and Products*, 108, 327-335.

Burmistrova, O., Perdomo, J., Simões, M.F., Rijo, P and Quintana, J. (2015). The abietane diterpenoid parvifloron D from *Plectranthus ecklonii* potent apoptotic inducer in human leukemia cells. *Phytomedicine*, 22(11).

Chain, F.E., Leyton, P., Paipa, C., Fortuna, M and Brandán, S.A. (2015). FT-IR, FT-Raman, UV-visible and NMR spectroscopy and vibrational properties of the labdane-type diterpene 13-epi-sclareol. *Spectrochimica Acta part A Molecular and Biomolecular Spectroscopy*, 138, 303-13.

Hussein, A. (2018). Chemistry of South African Lamiaceae: Structures and biological activity of terpenoids. *Intechopen*, 13-38.

Lobo, V., Patil, A., Phatak, A and Chandra, N. (2010). Free radicals, antioxidants and functional foods: Impact on human health. *Pharmacognosy Reviews* 4(8), 118–126.

UNIVERSITY of the WESTERN CAPE
https://etd.uwc.ac.za/

Narukawa, Y., Shimizu, N., Shimotohno, K and Takeda, T. (2001). Two new diterpenoids from *Plectranthus nummularius* Briq. *Chemical and Pharmaceutical Bulletin*, 49, 1182-1184.

Nyila, M.A., Leonard, C.M., Hussein, A.A and Lall, N. (2009). Bioactivities of *Plectranthus ecklonii* constituents. *Natural Product Communications*, 4,9, 1177-1180.

Raschi, A., Romano, E., Castillo, M., Leyton, P., Paipa, C., Maldonado, L and Brandán, S. (2014). Vibrational study of caffeic acid phenethyl ester, a potential anticancer agent, by infrared, Raman, and NMR spectroscopy. *Vibrational Spectroscopy*, 70, 100-109.

Rosa, S., Correia, V., Ribeiro, I., Rijo, P., Simões, F., Saraiva, N and Fernandes, A. (2015). In vitro antioxidant properties of the diterpenes Parvifloron D and 7α-acetoxy-6β-hydroxyroyleanone. *Biomedical andBiopharmaceutical Research*, 12(1), 59-67.

Santos-Rebelo, A., Garcia, C., Eleutério, C., Bastos, A., Coelho, S.C., Coelho, M.A.N., Molpeceres, J., Viana, A.S., Ascensão, L., Pinto, J.F., Gaspar, M.M., Rijo, P and Reis, C.P. (2018). Development of Parvifloron D loaded smart nanoparticles to target pancreatic cancer. *Pharmaceutics*, 10(4), 216.

Thilagam, E., Parimaladevi, B., Kumarappan, C and Mandal, S.C.J. (2013). Alpha-glucosidase and alpha-amylase inhibitory activity of *Senna surattensis*. *Acupuncture Meridian Studies*, 6(1), 24-30.

UNIVERSITY of the
WESTERN CAPE

https://etd.uwc.ac.za/

CHAPTER SIX

ELECTROCHEMICAL CHARACTERIZATION OF ISOLATED COMPOUNDS

6.1 Abstract

Cyclic voltammetry (CV) is used to study the electrochemical behaviour of phenolic compounds isolated from three different plant species as reported in the previous chapters and establish the correlation between the antioxidant capacity obtained by CV based on the oxidation potentials with those obtained from ORAC, FRAP and TEAC. CV shows that all the abietane diterpenes are electro-active with well-defined oxidation-reduction peaks. Compound **12**, when compared to other compounds, exhibits the lowest oxidation potential value (E_{pa} = 120 mV), indicating that it has the highest antioxidant power, which is in good agreement with ORAC and TEAC. Additionally, compounds with catechol moiety (11,12-dihydroxyl group) in the C ring demonstrated the lowest oxidation potential compared to others. Their mechanism of reaction involve two electrons two protons reversible reaction and form an o-quinone. In conclusion cyclic voltammetry is a reliable analytical method for the characterization of electrochemical behavior of isolated compounds as well as the oxidizing and/or reducing ability of natural phenolic compounds.

UNIVERSITY of the
WESTERN CAPE

6.2 Aim of this chapter

Electrochemical techniques are very reliable tool for the determination/identification of phenolic compounds in plant, wine, food as well as the evaluation of their antioxidant capacities (Dobes, et al., 2013). Cyclic voltammetry (CV) is one of the most widely used electrochemical techniques for the analysis of phenolic compounds, especially for understanding their redox properties due the fact that it is fast, sensitive, reproducible, simple, reliable and affordable (Mourhat, et al., 2017).

https://etd.uwc.ac.za/

This chapter describes:

- The electrochemical characterization of the chemical constituents of *S. africana lutea, S. aurita* and *P. ecklonii* using cyclic voltammetry.
- The relationship between the antioxidant capacities obtained by cyclic voltammetry with those obtained using spectrophotometric techniques such as FRAP, TEAC and ORAC.

ELECTROCHEMICAL ANALYSIS

6.3 General experiment procedure

6.3.1 Reagents and solvents

Organic solvents, methanol, ethanol (HPLC grade) and dimethylsulfoxide were supplied by Merck (Cape Town, South Africa). Phosphate buffer solutions were prepared by mixing appropriate volumes of 50 mM sodium dihydrogen phosphate (NaH_2PO_4) and 50 mM of disodium hydrogen phosphate (Na_2HPO_4) to set the desire pH (6.8). All the compounds were made to a stock solution of 1 mg/mL with either methanol or DMSO. The water was collected from a Millipore Milli-Q system.

UNIVERSITY of the
WESTERN CAPE

6.3.2 Procedure for voltammetry analysis

Cyclic voltammetry was used for monitoring the oxidation-reduction potentials of the isolated compounds. It was performed using the BAS100B electrochemical analyzer (Bioanalytical systems, West Lafayette, IN, USA), a glassy carbon electrode (GCE) as working electrode, Ag/AgCl as a reference electrode, and platinum (Pt) as a counter electrode. The electrodes surface (GCE) was polished with 0.05, 0.3 and 1 µM alumina on a microcloth pad, followed by sonication in ethanol and then Millipore water. The platinum wire, auxiliary electrode was cleaned by fire polishing after rinsing with water. The CV was recorded at 50 mV/s within the potential window ranging from −1200 mV to 1200 mV, with a fixed concentration of samples in 50 mM PBS at pH 6.8 phosphate buffer. A certain volume

https://etd.uwc.ac.za/

of compound was added to a cell containing 10 mL of PBS, and then the experiment was recorded in triplicate at room temperature.

6.3.3 Electrochemical characterization: Results and discussion

6.3.3.1 Cyclic voltammetry of 19β-acetoxy-12-methoxy carnosic acid (1)

The cyclic voltammogram of 19β-acetoxy-12-methoxy carnosic acid is illustrated in Figure 6.1. CV shows two oxidation peaks (1, 2) at the potential of +175 and +470 mV associated with the oxidation of hydroxyl groups as well as a reduction peak (1') appears at the potential of -950 mV, which is due to the reduction of the oxidation products in peak 1. This compound is characterized by the presence of free hydroxyl group in ring C, which can easily be oxidized at a relative low positive potential (+175 mV) and is related with peak 1 in the cyclic voltammogram (Fig. 6.1).

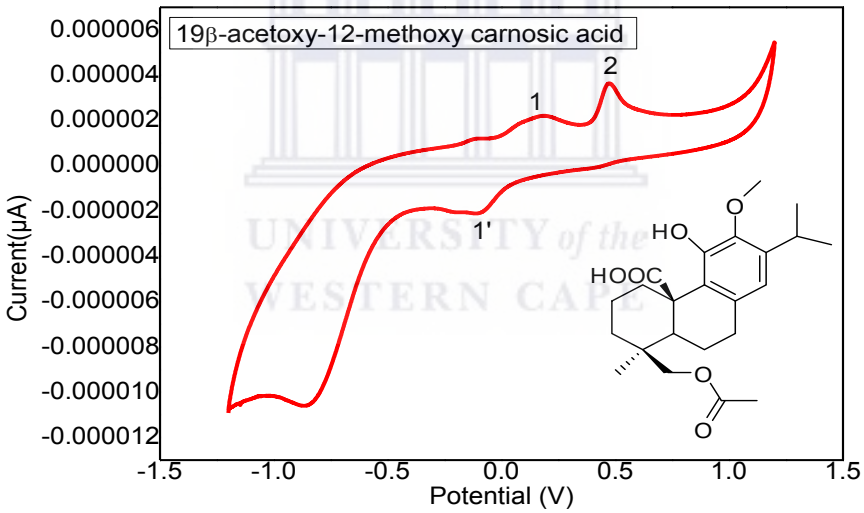

Figure 6.1: Cyclic voltammogram of 19β-acetoxy-12-methoxy carnosic

6.3.3.2 Cyclic voltammetry of 3β-acetoxy-7-methoxy rosmanol (2)

The cyclic voltammogram of 3β-acetoxy-7-methoxy rosmanol is shown in Figure 6.2. CV shows one oxidation peak (1) at the potential of +169 mV associated with the oxidation of hydroxyl groups as well as a reduction peak (1') appears at the potential of -430 mV, which is due to the reduction of the oxidation products in peak 1. This compound is characterized by

https://etd.uwc.ac.za/

the presence of the catechol moiety pharmacophore (11, 12 dihydroxyl group) in ring C, which can easily be oxidized at a relative low positive potential (+169 mV) and is related with peak 1 in the cyclic voltammogram (Fig. 6.2). Hence, the oxidation process involves two electrons and two protons as shown in scheme 6.1 (Markovic, et al., 1996).

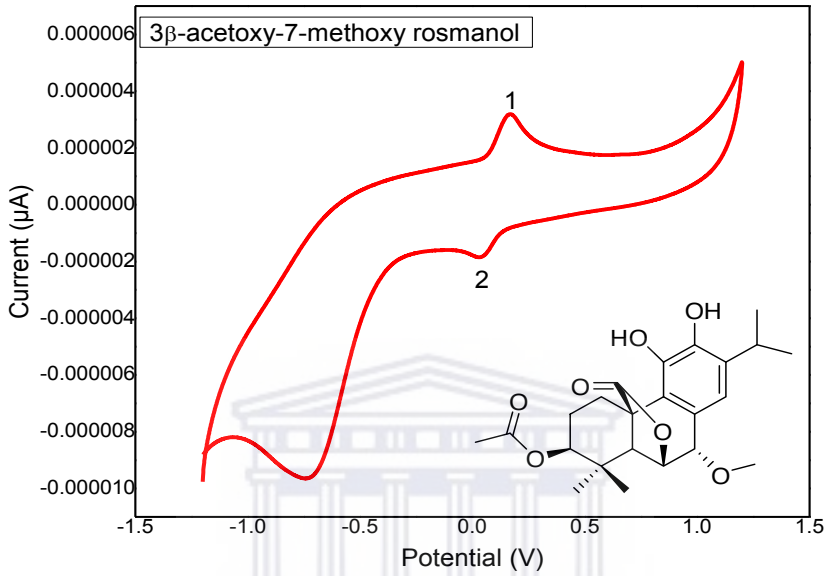

Figure 6.2: Cyclic voltammogram of 3β-acetoxy-7-methoxy rosmanol

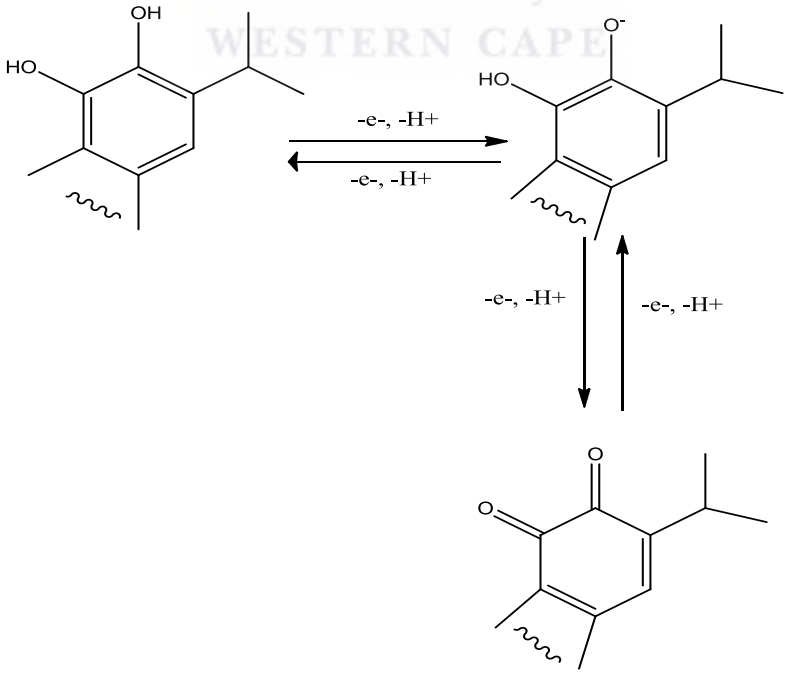

Scheme 6.1: Oxidation of catechol moiety of 3β-acetoxy-7-methoxy rosmanol to o-quinone

https://etd.uwc.ac.za/

6.3.3.3 Cyclic voltammetry of 19-acetoxy-12-methoxy carnosol (3)

The cyclic voltammogram of 19-acetoxy-12-methoxy carnosol is shown in Figure 6.3. CV shows one oxidation peak (1) at the potential of +503 mV associated with the oxidation of hydroxyl groups as well as a reduction peak (1') appears at the potential of -75 mV, which is due to the reduction of the oxidation products in peak 1. This compound is characterized by the presence of free hydroxyl group in ring C, which can easily be oxidized at a positive potential (+503 mV) and is related with peak 1 in the cyclic voltammogram (Fig. 6.3).

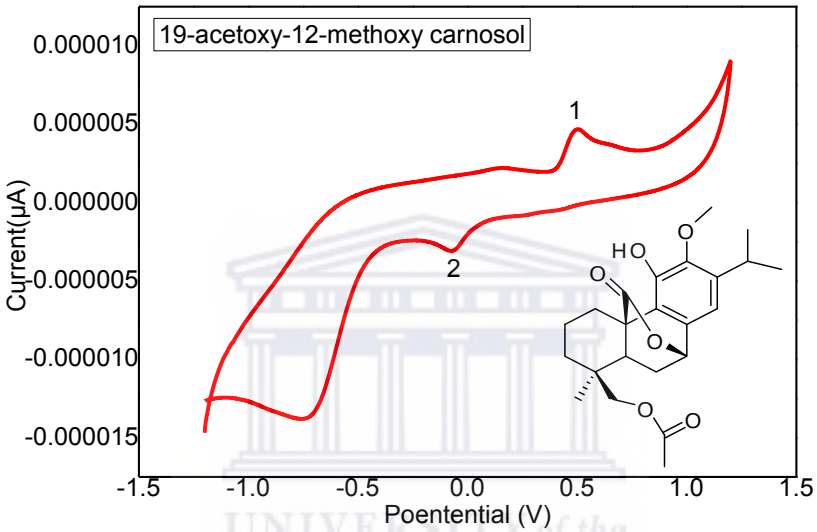

Figure 6.3: Cyclic voltammogram of 19-acetoxy-12-methoxy carnosol

6.3.3.4 Cyclic voltammetry of clinopodiolide A (5)

The cyclic voltammogram of clinopodiolide A is shown in Figure 6.4. CV shows one oxidation peak (1) at the potential of +175 mV associated with the oxidation of hydroxyl groups as well as a reduction peak (1') appears at the potential of -205 mV, which is due to the reduction of the oxidation products in peak 1. Clinopodiolide A is characterized by the presence a free hydroxyl group implicated in the lactone ring, in addition to the catechol moiety pharmacophore in ring C, which can easily be oxidized at a relative low positive potential (+175 mV) and is related with peak 1 in the cyclic voltammogram (Fig. 6.4). Hence,

https://etd.uwc.ac.za/

oxidation process involves two electrons and two protons as shown in scheme 6.1 (Markovic, et al., 1996).

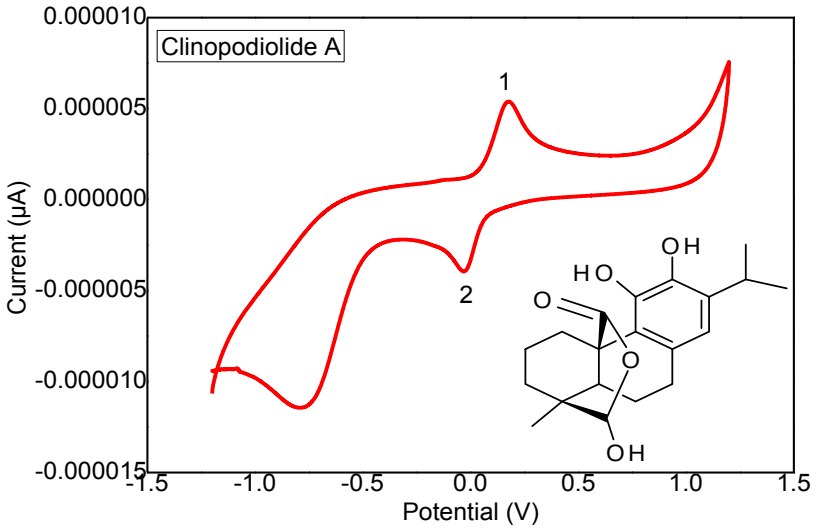

Figure 6.4: Cyclic voltammogram of clinopodiolide A

6.3.3.5 Cyclic voltammetry of clinopodiolide B (6)

The cyclic voltammogram of clinopodiolide B is shown in Figure 6.5. CV shows three oxidation peaks (1-3) at the potential of +422, 636 and 898 mV associated with the oxidation of hydroxyl groups as well as a reduction peak (1') appears at the potential of peak at -164 mV, which is due to the reduction of the oxidation products in peak 1. Clinopodiolide B is characterized by the presence of the free hydroxyl groups, one in aromatic ring C and another implicated in the lactone ring. The oxidation of the hydroxyl group present in the aromatic ring C occurs at low oxidation potential (+422 mV) and is associated with peak 1 in the cyclic voltammogram (Fig 6.5).

https://etd.uwc.ac.za/

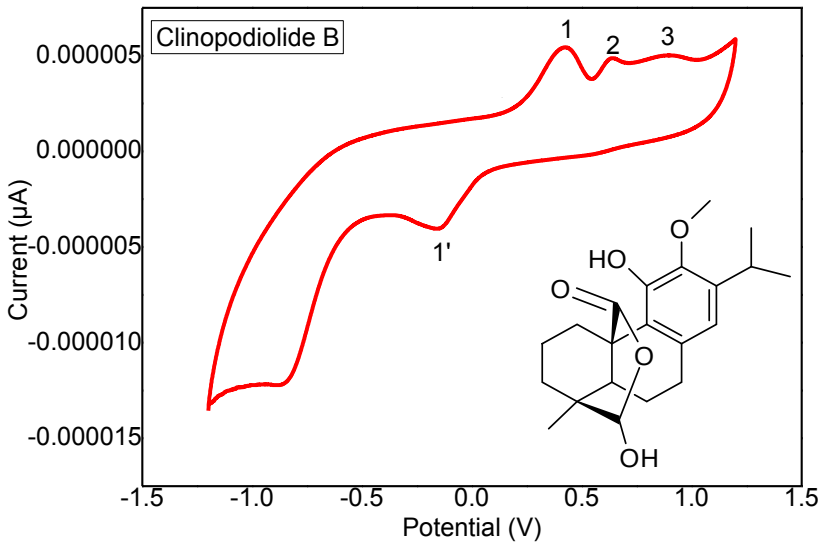

Figure 6.5: Cyclic voltammogram of clinopodiolide B

6.3.3.6 Cyclic voltammetry of carnosol (11)

The cyclic voltammogram of carnosol is shown in Figure 6.6. CV shows two oxidation peak (1,2) at the potential of +165 and 590 mV associated with the oxidation of hydroxyl groups as well as a reduction peak (1') appears at the potential of -473 mV, which is due to the reduction of the oxidation products in peak 1. Carnosol is characterized by the presence of the catechol moiety pharmacophore in ring C, which can easily be oxidized at a relative low positive potential (+165 mV) and is related with peak 1 in the cyclic voltammogram (Fig. 6.6). Hence, oxidation process involves two electrons and two protons as shown in scheme 6.1 (Markovic, et al., 1996).

https://etd.uwc.ac.za/

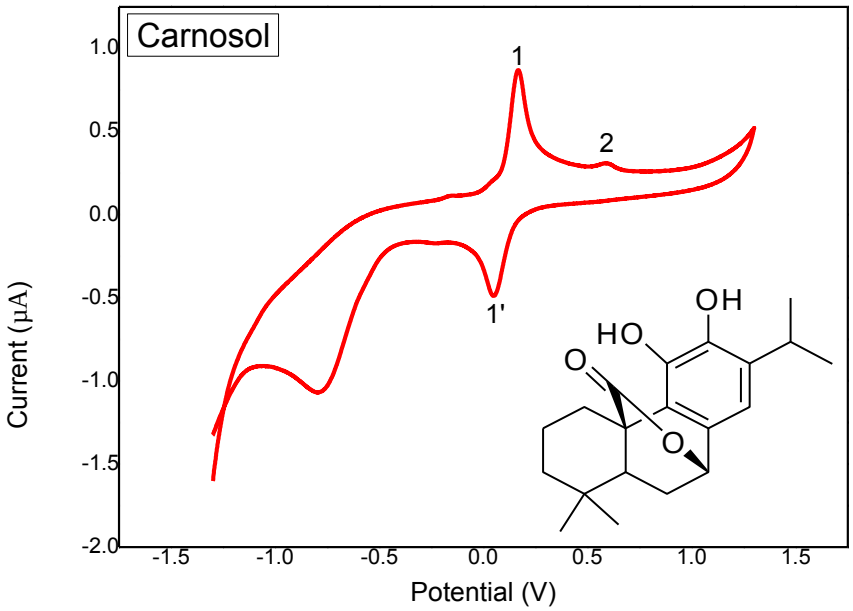

Figure 6.6: Cyclic voltammogram of carnosol

6.3.3.7 Cyclic voltammetry of rosmanol (12)

The cyclic voltammogram of rosmanol is shown in Figure 6.7. CV shows one oxidation peak (1) at the potential of +120 mV associated with the oxidation of hydroxyl groups as well as a reduction peak (1') appears at the potential of -299 mV, which is due to the reduction of the oxidation products in peak 1. Rosmanol is characterized by the presence a free hydroxyl group present at position 7 of ring B and the catechol moiety pharmacophore in ring C, which can easily be oxidized at a relative low positive potential (+120 mV) and is related with peak 1 in the cyclic voltammogram (Fig. 6.7). Hence, oxidation process involves two electrons and two protons as shown in scheme 6.1 (Markovic, et al., 1996).

https://etd.uwc.ac.za/

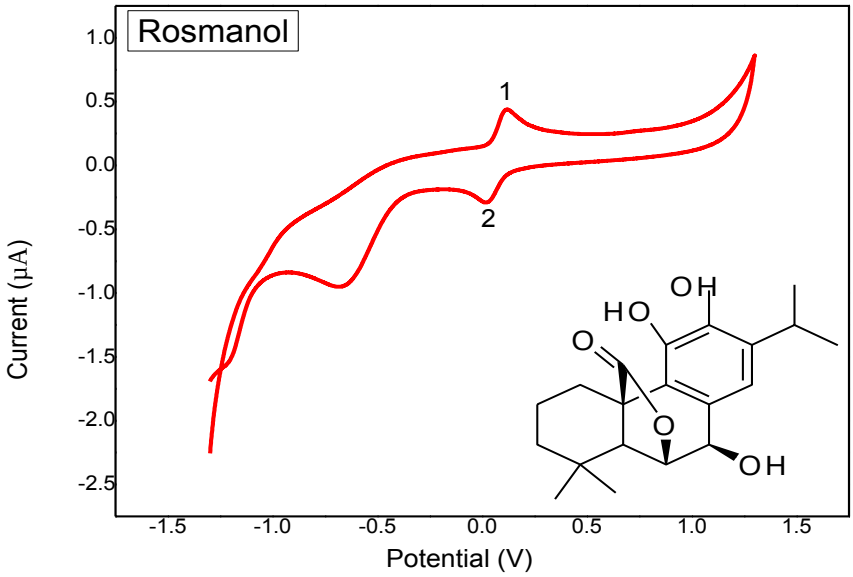

Figure 6.7: Cyclic voltammogram of rosmanol

6.3.3.8 Cyclic voltammetry of 12-methoxycarnosic acid (14)

The cyclic voltammogram of 12-methoxycarnosic acid is shown in Figure 6.8. CV shows two oxidation peaks (1) at the potential of +456 mV associated with the oxidation of hydroxyl groups as well as a reduction peak (1') appears at the potential of -142 mV, which is due to the reduction of the oxidation products in peak 1. This compound is characterized by the presence of a free hydroxyl group in ring C, which can easily be oxidized at a positive potential (+456 mV) and is related with peak 1 in the cyclic voltammogram (Fig. 6.8).

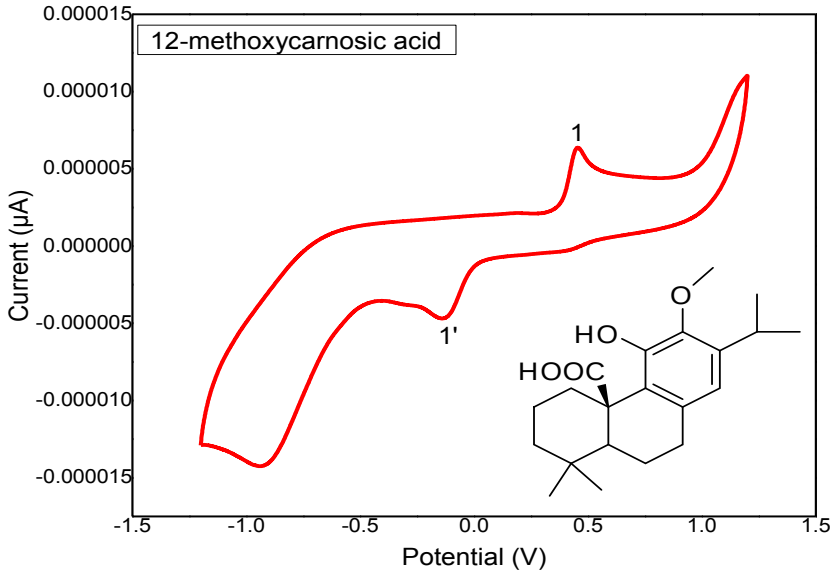

Figure 6.8: Cyclic voltammogram of 12-methoxycarnosic acid

https://etd.uwc.ac.za/

6.3.3.9 Cyclic voltammetry of parvifloron D (16)

The cyclic voltammogram of parvifloron D is shown in Figure 6.9. CV shows two oxidation peak (1, 2) at the potential of +145 mV and 899 mV associated with the oxidation of hydroxyl groups as well as a reduction peak (1') appears at the potential of -667 mV, which is due to the reduction of the oxidation products in peak 1. Parvifloron D is characterized by the presence of free hydroxyl groups; one locates in ring C and another in ring A'. The free hydroxyl group locates at the aromatic ring can easily be oxidized at a relative low positive potential (+145 mV) and is related with peak 1 and the second free hydroxyl group might be related to peak 2 in the cyclic voltammogram (Fig. 6.9).

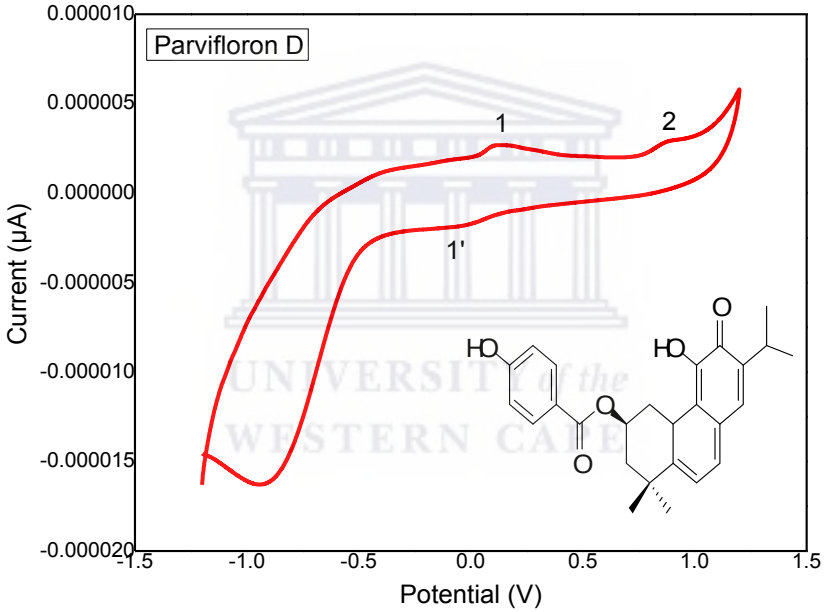

Figure 6.9: Cyclic voltammogram of parvifloron D

6.3.3.10 Cyclic voltammetry of parvifloron F (17)

The cyclic voltammogram of parvifloron F is shown in Figure 6.10. CV shows two oxidation peak (1-2) at the potential of +136 mV and 883 mV associated with oxidation of hydroxyl groups as well as a reduction peak (1') appears at the potential of -329 mV, which is due to the reduction of the oxidation products in peak 1. Parvifloron F is characterized by the presence of a catechol moiety group in ring A, which can easily be oxidized at a relative low

https://etd.uwc.ac.za/

positive potential (+136 mV) and is related with peak 1, and one free hydroxyl group locates at the aromatic ring C, which might be related to peak 2 in the cyclic voltammogram (Fig. 6.10). Hence, the oxidation process involves two electrons and two protons as shown in scheme 6.2.

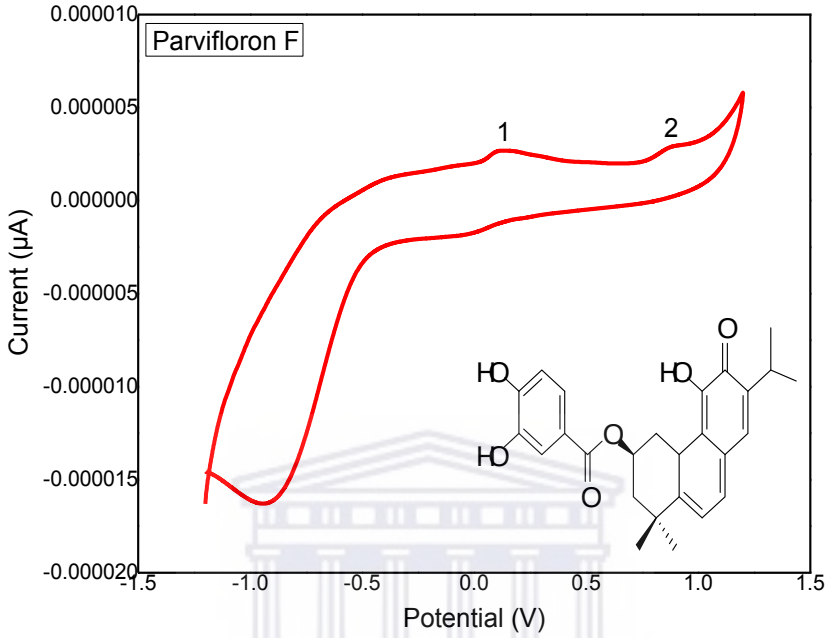

Figure 6.10: Cyclic voltammogram of parvifloron F

UNIVERSITY of the
WESTERN CAPE

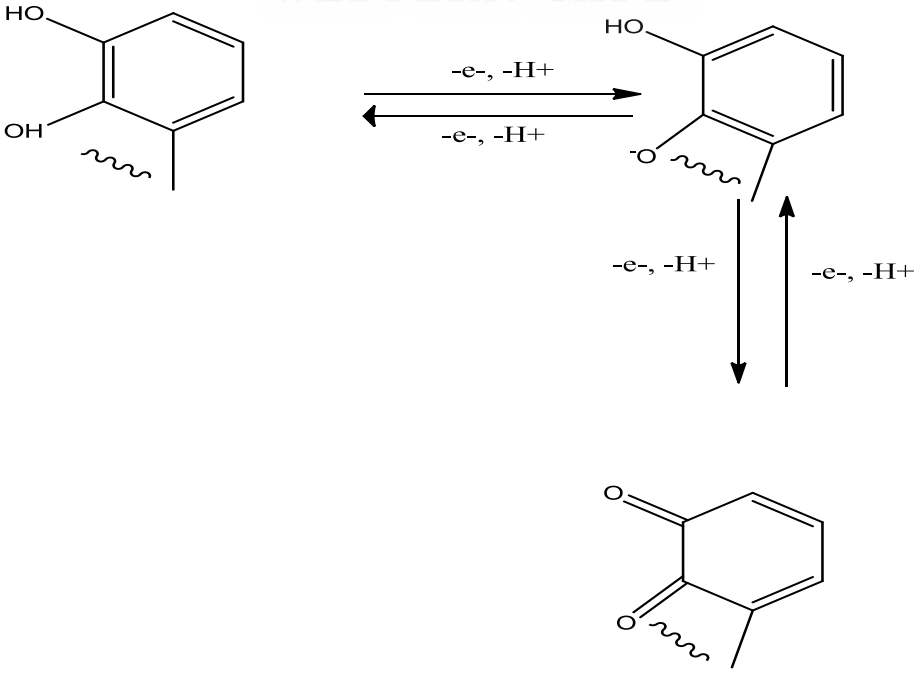

Scheme 6.2: Oxidation of catechol moiety of parvifloron F to o-quinone

https://etd.uwc.ac.za/

Table 6.1: Electrochemical characterization of some isolated compounds

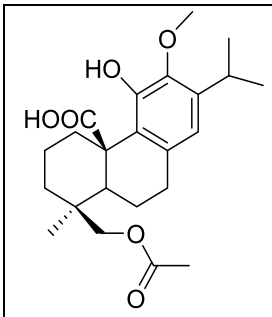	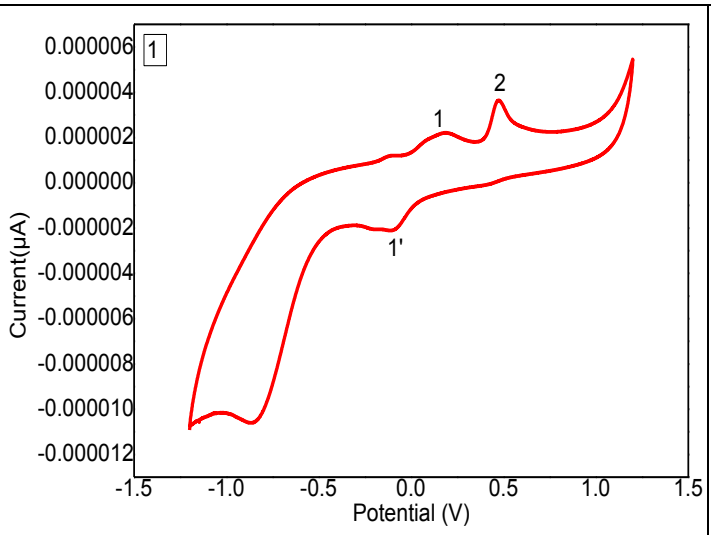	Epa1 = 175 mV Epa2 = 470 mV Epc = -950 mV
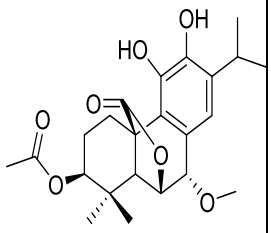	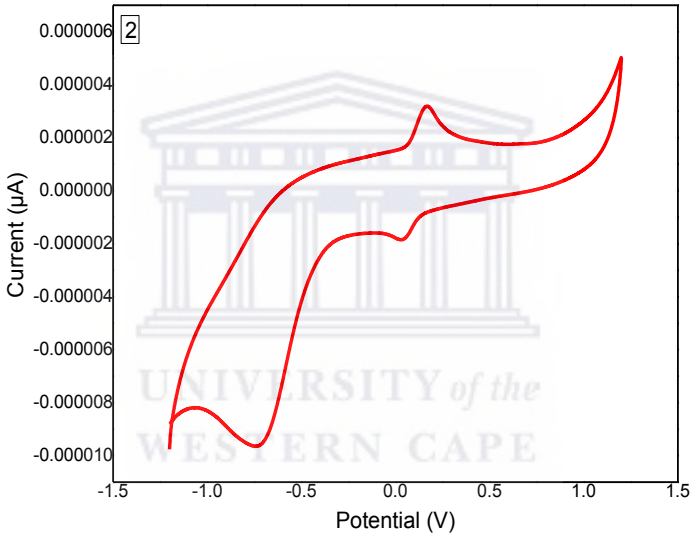	Epa1 = 169 mV Epc = 43 mV
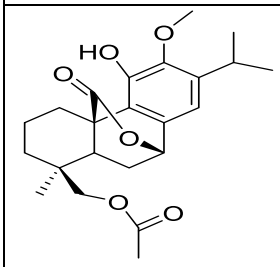	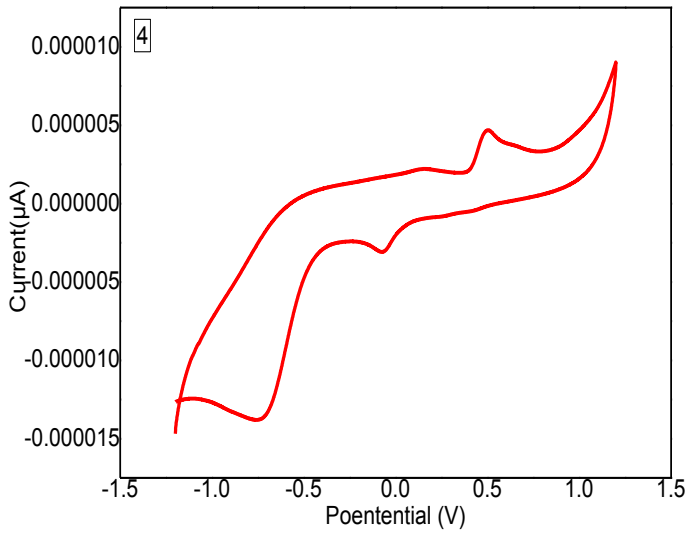	Epa1 = 503 mV Epc = -75 mV

https://etd.uwc.ac.za/

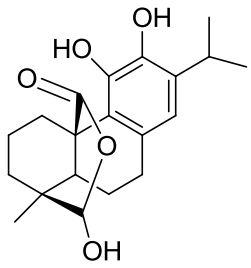	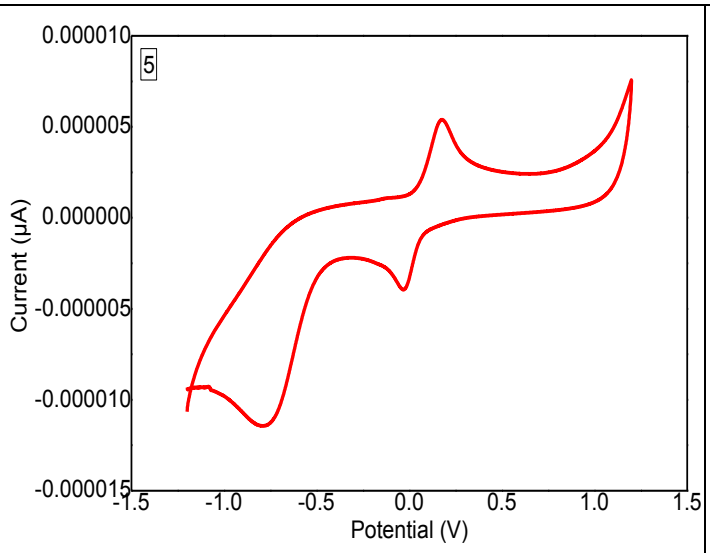	Epa1 = 175 mV Epc = -205 mV
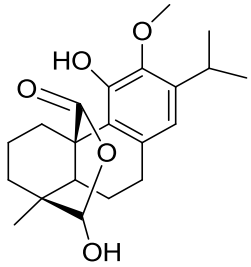	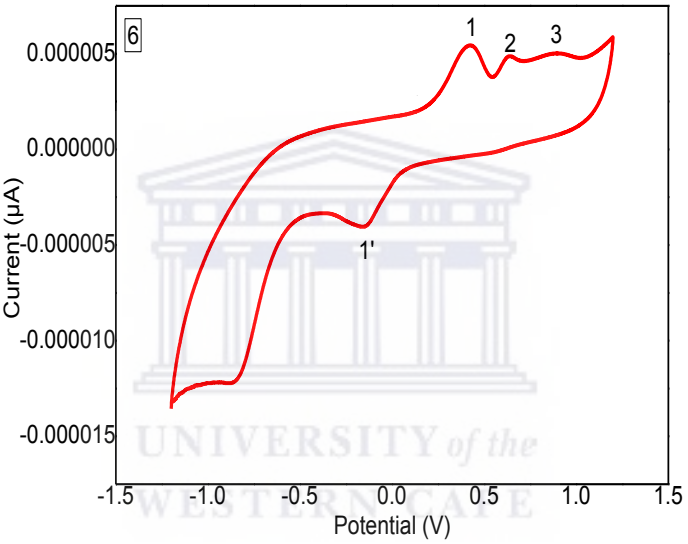	Epa1 = 422 mV Epa2 = 636 mV Epa3 = -898 mV Epc = -164 mV
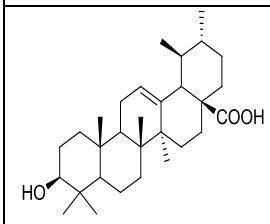	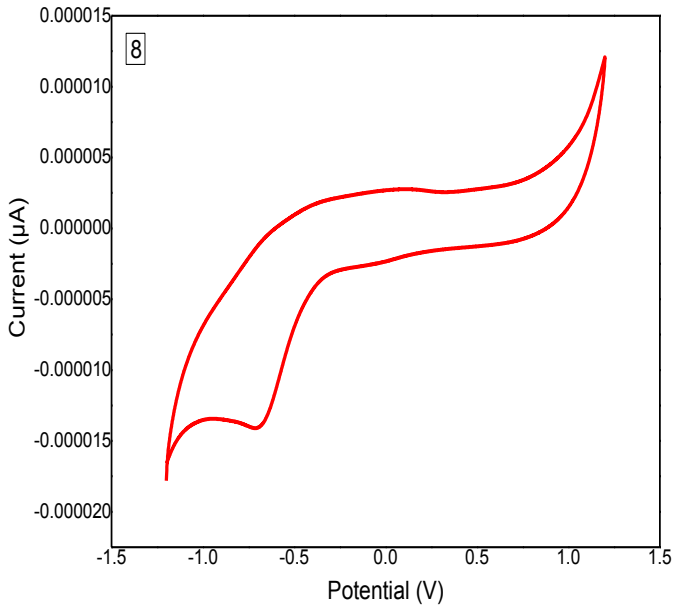	No peaks

https://etd.uwc.ac.za/

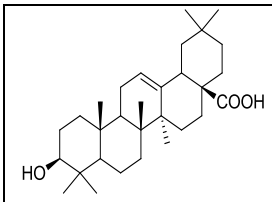	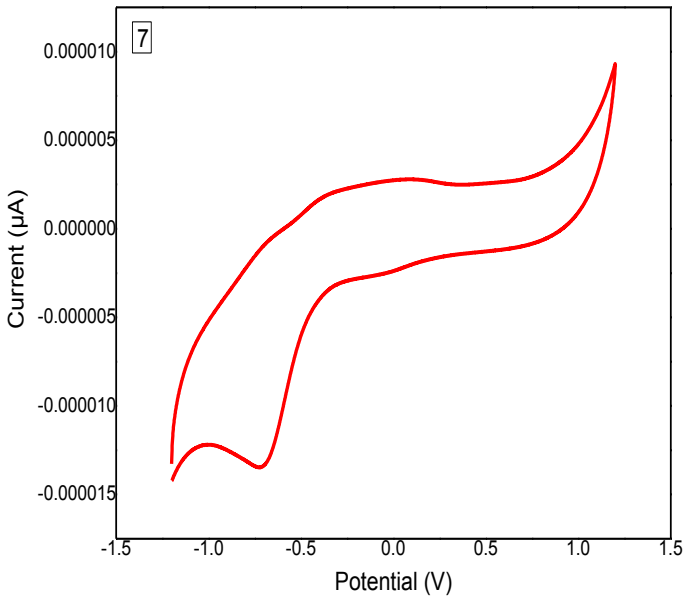	No peaks
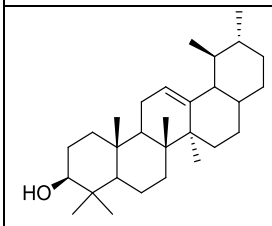	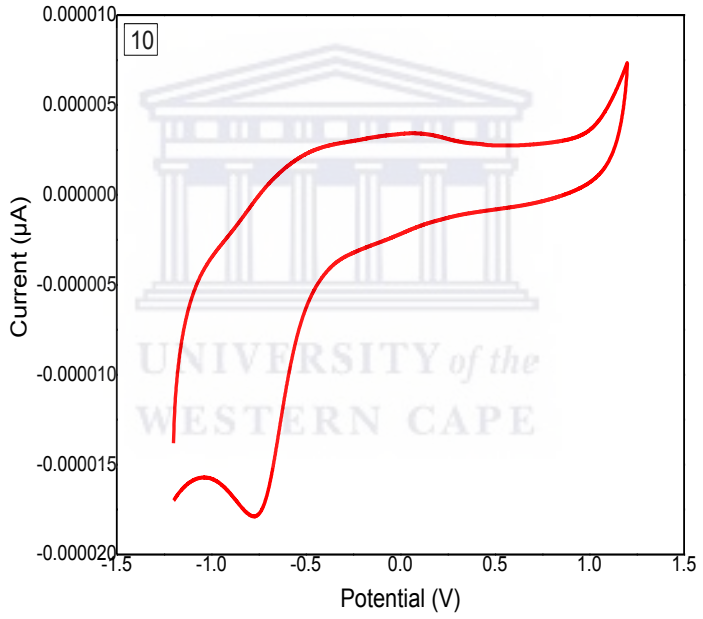	No peaks

UNIVERSITY of the WESTERN CAPE

https://etd.uwc.ac.za/

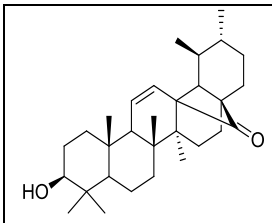	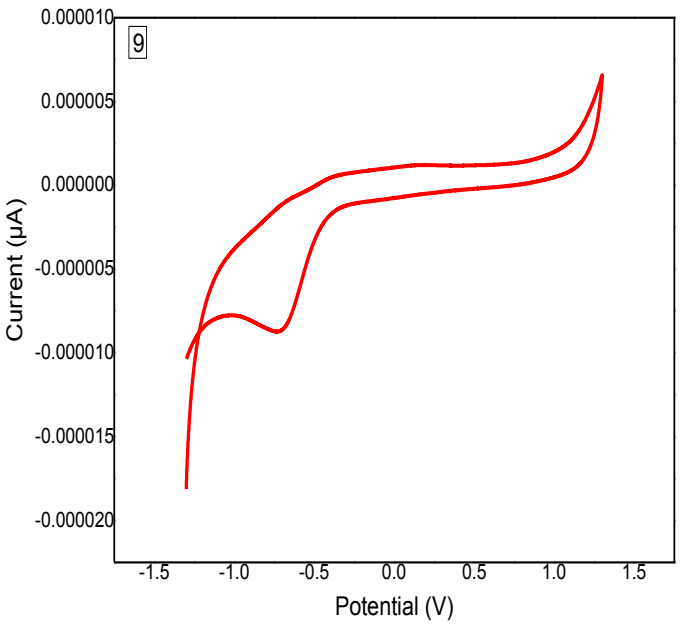	No peaks
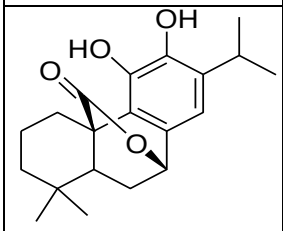	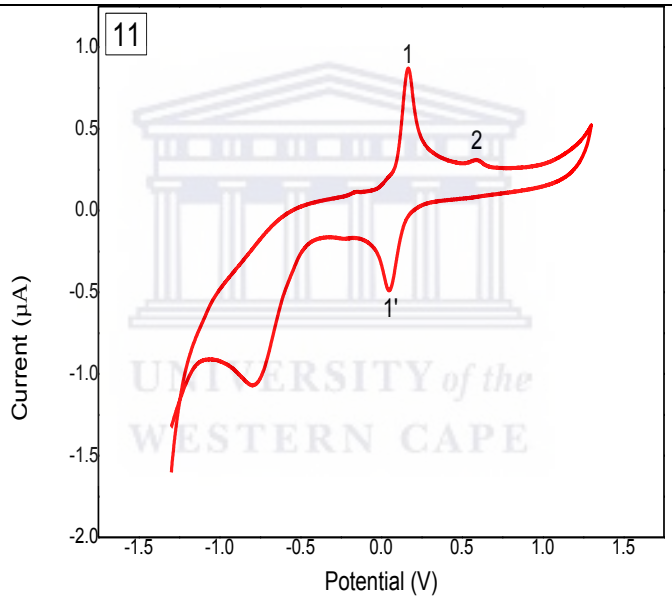	Epa1 = 165 mV Epa2 = 590 mV Epc = -54 mV

UNIVERSITY of the WESTERN CAPE

https://etd.uwc.ac.za/

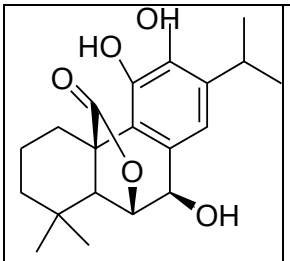	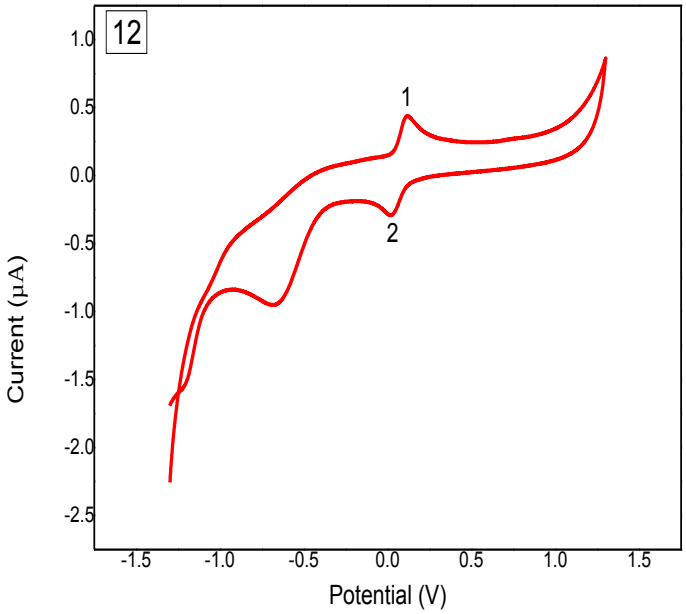	Epa1 = 120 mV Epc = -299 mV
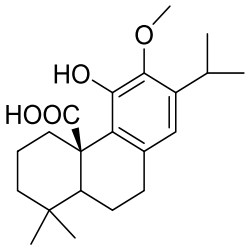	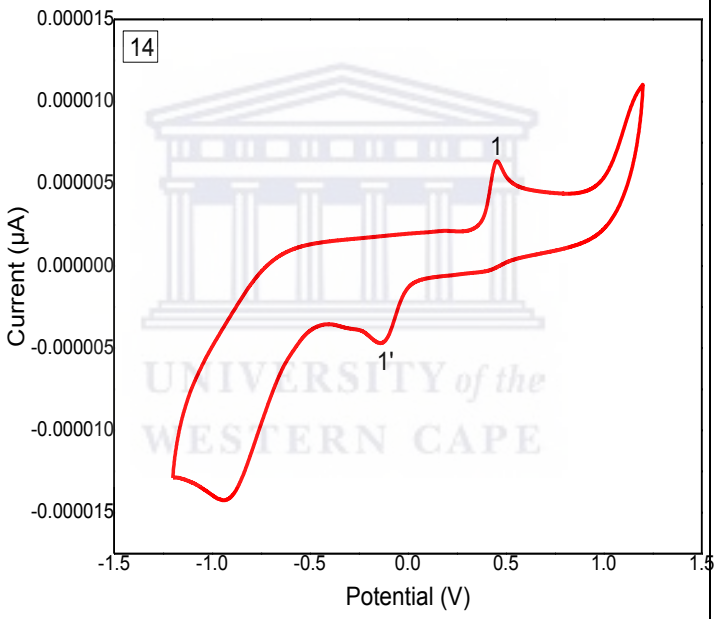	Epa1 = 456 mV Epc = -142 mV

UNIVERSITY of the WESTERN CAPE

https://etd.uwc.ac.za/

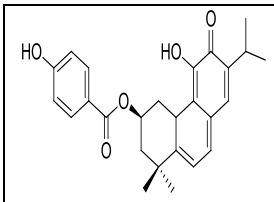	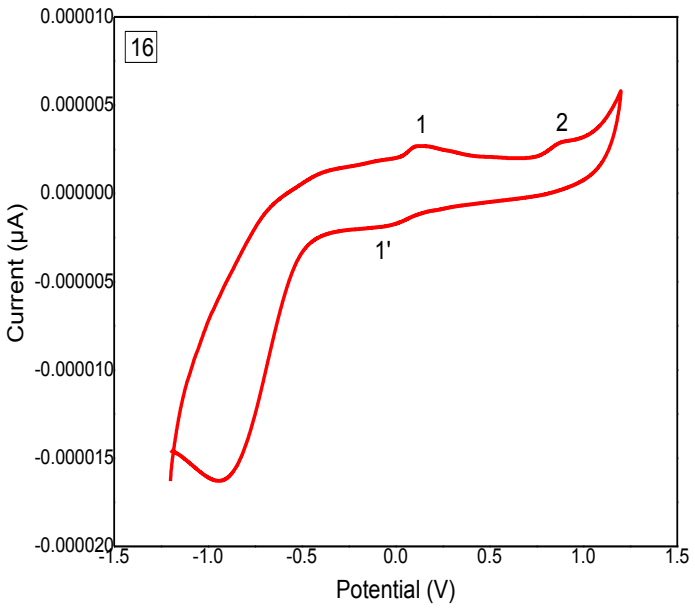	Epa1 = 145 mV Epa2 = 899 mV Epc = -667 mV
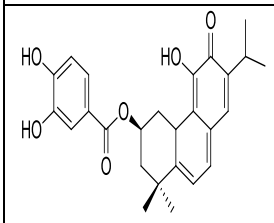	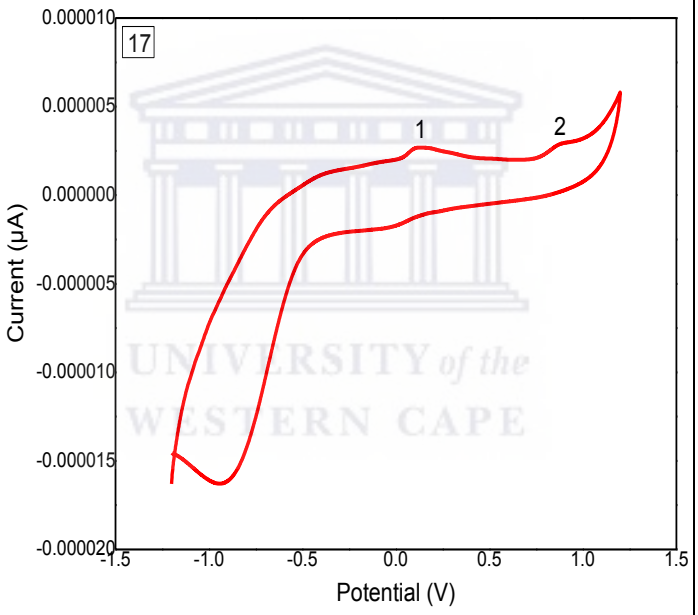	Epa1 = 136 mV Epa2 = 883 mV Epc = -329 mV

6.4 Correlation between cyclic voltammetry and antioxidant capacity

CV is a very suitable technique, commonly used in electrochemistry for characterization of oxidizing and/or reducing the ability of natural polyphenols, of which good relationships have been recorded between oxidation potentials and antioxidant properties (Sochor, et al., 2013). Therefore, a deeper knowledge of the oxidation–reduction is a key for a better understanding of the antioxidation process. Hence, compounds with strong scavenging

https://etd.uwc.ac.za/

capacities have demonstrated to be oxidized at very low potentials (Etsassala, et al., 2019; Galato, et al., 2013). However, the most powerful reducing agents are polyphenols with low potential as they can by autoxidation exert pro-oxidant activity (Simić, et al., 2007). The values of the anodic peak potential (Epa), corresponding to the oxidation potentials of the compounds are listed in Table 6.1. As can be seen in table 6.2, **12** exhibits the lowest oxidation potential value (Epa = 120 mV), indicating that it has the highest antioxidant capacity, which is in agreement with the results obtained in ORAC (25789.9 ± 10.5 µmole TE/g) and TEAC (2055 ± 2.6 µmole TE/g). Others compounds such as **17**, demonstrated the second lowest oxidation potential (136 mV), which also corroborates in the same manner with the TEAC (1069.3 ± 2.4 µmole TE/g). The highest degree of positive correlations/relationships were observed between the oxidation potential observed in CV and antioxidant capacities exhibited in ORAC and TEAC, which may be attributed to electron(s)/hydrogen(s) transfers based mechanism governing these methods. Hence, the results can be presented as **12** (120 mV)>**17** (136 mV)>**16** (145 mV)>**11** (165 mV)>**2** (169 mV)>**5** (175 mV)>**1** (175 mV)>**6** (422 mV)>**14** (456 mV)>**4** (503 mV). Among all the isolated class of compounds, abietane diterpenes are electro-active with well-defined oxidation-reduction peaks. The electro-activity demonstrated may be attributed to the electron transfer and/or hydrogen transfer reactions involving the oxidized product, which is associated with the presence of ortho-dihydroxyl group on the aromatic ring C as well as the high degree of oxygenation, causing steric effects that can lead to a shift in potential observed. It has been reported that the greater the number of hydroxyls linked to the aromatic ring, the greater the antioxidant activity (Mathew, et al., 2015). Furthermore, other aspects such as electron deficiency based on electron-withdrawing effect of a COOH group group may also account for the formation of phenoxoniumion as intermediates if positive charge is on a carbonatom. The methoxylation of the ortho-hydroxyl groups of some abietane

https://etd.uwc.ac.za/

diterpenes is responsible for the shift of the oxidation potential to more positive value as well as for the decrease of the antioxidant activity, by blocking the scavenging reaction (Galato, et al., 2013). None of the triterpene is electro-active, which may be due to the absence of the catechol moiety group in their chemical structure as well as the lesser number of hydroxyl group present within this class of compound. The difference in the oxidation peak potentials of **12**, **17**, **16**, **11**, **2**, **5** and **1** were found to be related to either the presence of catechol moiety pharmacophore or the difference in number of hydroxyl group, which is as higher for **12** than **11** and others except **17**.

Table 6.2: Anodic peak properties of tested samples

Items	Epa_1 (mV)	Epa_2 (mV)	Epa_3 (mV)	Epc (mV)
1	175	470	/	-950
2	169	/	/	430
4	503	/	/	-75
5	175	/	/	-205
6	422	636	898	-164
11	165	/	/	473
12	120	/	/	-299
16	145	/	/	-667
17	136	833	/	-329
14	456	/	/	-142

12>17>16>11> 2>5>1>6>14>4

Hence, the structure-activity relationship demonstrated by rosmanol and parvifloron F is related to the highest number of hydroxyl groups (3 OH) within their chemical skeleton, which can be responsible of the lowest oxidation potential observed as well as the highest antioxidant activities demonstrated.

6.5 Conclusion

The use of cyclic voltammetry as a reliable analytical method for the characterization of electrochemical behavior of isolated compounds as well as the oxidizing and/or reducing ability of natural polyphenols. Additionally, the correlation/relationship between the oxidation potential and the antioxidant capacity were established and compared with

UNIVERSITY of the WESTERN CAPE
https://etd.uwc.ac.za/

spectrophotometric methods. We observed that the measured oxidation potential was closely related to the structures of the investigated compounds. The antioxidant activity of these compounds relates well to the number of OH group in structure, and compounds with two or more electron donating groups have lower anodic peak potentials and higher antioxidant abilities than those with free hydroxyl or mono-substituted phenols/catechol groups as expressed in 19β-acetoxy-12-methoxy carnosic acid, 19-acetoxy-12-methoxy carnosol and clinopodiolide B with OCH_3 at position 12 in aromatic ring C. Therefore, establishing a correlation between the electrochemical and spectrophotometric with the structural features could be a good tool for screening antioxidant substances in order to choose the best substances to use in *in vivo* studies.

References

Dobes, J., Zitka, O., Sochor, J., B, R.N., Babula, P., Beklova, M., Kizek, R. (2013). Electrochemical tools for the determination of phenolic compounds in plants. A review. *International Journal of Electrochemical Science*, 4520-4542.

Etsassala, N.G.E.R., Adeloye, A.O., El--Halawany, A., Hussein, A.A and Iwuoha, E.I. (2019). Investigation of in-vitro antioxidant and electrochemical activities of isolated compounds from *Salvia chamelaeagnea* P.J.Bergius Extract. *Antioxidants,* 8(4), 98.

Etsassala, N.G.E.R., Waryo, T., Popoola, O.K., Adeloye, A.O., Iwuoha, E.I and Hussein, A.A. (2019). Electrochemical screening and evaluation of Lamiaceae plant species from South Africa with potential tyrosinase activity. *Sensors*, 19(5), 1035.

Galato, D., Ckless, K., Susin, M.F., Giacomelli, C., Ribeiro-do-Valle, R.M and Spinelli, A. (2013). Antioxidant capacity of phenolic and related compounds: Correlation among electrochemical, visible spectroscopy methods and structure–antioxidant activity. *Redox Report*, 6:4, 243-250.

UNIVERSITY of the WESTERN CAPE
https://etd.uwc.ac.za/

Markovic, D.A., Djarmati, Z and Jankov, R.M. (1996). Electrochemical behaviour of rosmanol 9-Ethyl Ether, a diterpene lactone antioxidant isolated from Sage. *Mikrochimica Acta*, 124, 219 226.

Mathew, S., Abraham, T.E and Zakaria, Z.A. (2015). Reactivity of phenolic compounds towards free radicals under in vitro conditions. *Journal of Food Sciences and Technol*ogy, 52(9): 5790–5798.

Mourhat, Z., Touzara, S., Maallah, R., Mbarki, M and Chtaini, A.. (2017). Electrochemical evaluation of the antioxidant capacity of phenolic compounds in virgin olive oil. *Journal of Biosensor and Bioelectronics*, 8(1), 2-4.

Simić, A., Manojlović, D., Šegan, D and Todorović, M. (2007). Electrochemical behavior and antioxidant and prooxidant activity of natural phenolics. *Molecules*, 12(10), 2327–2340.

Sochor, J., Dobes, J., Krystofova, O., Ruttkay-Nedecky, B., Babula, P., Pohanka, M., Jurikova, T., Zitka, O., Adam, V and Klejdus, B. (2013). Electrochemistry as a tool for studying antioxidant properties. *International Journal of Electrochemical Sciences*, 8, 8464 - 8489.

UNIVERSITY of the WESTERN CAPE

https://etd.uwc.ac.za/

CHAPTER SEVEN

CONCLUSION AND RECOMMENDATIONS

Despite the fact that an extensive amount of phytochemical research has been conducted on the Lamiaceae family, only a few have been investigated for their biological and pharmaceutical significance, with a huge number of species still untapped. Among such are the three plant species named *S. aficana lutea* (SAL), *S. aurita* (SA) and P. *eckolnii* (PE). Their selections were based on the non-availability of both scientific and traditional information to support their respective traditional uses. This research work therefore is the first scientific report on the phytochemical constituents and their possible biological application as antidiabetics as well as antioxidant candidates for the management of diabetes and oxidative stress related diabetes.

The preliminary phytochemical investigation using thin layer chromatography (TLC) displayed that extracts of SAL, SA and PE (results not shown) exhibited red/yellow/brown/purple spots of chemical constituents after sprayed with vanillin/H_2SO_4. The TLC results indicated that those extracts may contain interesting chemical profile.

The aerial part of three plant material (SAL, SA, PE) were collected in April 2017, from the Cape Flats Nature Reserve, University of the Western Cape, June 2017 from Hogobach pass Eastern Cape, and February 2019 from the Cape Peninsula University of Technology, South Africa, respectively. A voucher specimen of each plant was identified by Prof. Christopher and deposited at the Compton Herbarium, SANBI, Kirstenbosh, South Africa, for documentation.

The aerial part of the fresh plant materials was blended and extracted with methanol at room temperature (25 ^{o}C) for 24 h. The methanol extract was filtered and evaporated to dryness

UNIVERSITY of the WESTERN CAPE
https://etd.uwc.ac.za/

under reduced pressure at 40 ^{o}C, followed by chromatographic fractionations and further purification using Preparative HPLC. The protocols as described in the experimental sections and illustrated in schemes 3.1, 4.1 and 5.1 afforded isolation of eighteen pure compounds.

The structure elucidation of the isolated compounds was carried out using spectroscopic techniques such as 1D and 2D NMR, HRMS, IR, UV, Raman data. Optical rotations of the new compounds with streogenic centres were also done to support the proposed structures.

Table 7.1: Summarized the extensive phytochemical analyses of the isolated compounds

Code	Name	Source	Remark
1	19-acetoxy-12-methoxy carnosic acid	*S. africana-lutea*	new
2	3β-acetoxy-7α-methoxyrosmanol	*S. africana-lutea*	new
3	19-acetoxy-7α-methoxyrosmanol	*S. africana-lutea*	new
4	19-acetoxy-12-methoxy carnosol	*S. africana-lutea*	new
5	clinopodiolides A	*S. africana-lutea*	Known*
6	clinopodiolides B	*S. africana-lutea*	Known*
7	Oleanolic acid	*S. africana-lutea*	Known*
8	Ursolic acid	*S. africana-lutea*	Known*
9	11,12-dehydroursolic acid lactone	*S. africana-lutea*	Known*
10	β-amyrin	*S. africana-lutea*	Known*
11	Carnosol	*S. aurita*	Known*
12	rosmanol	*S. aurita*	Known*
13	7-methoxyrosmanol	*S. aurita*	Known*
14	12-methoxycarnosic acid	*S. aurita*	Known*
15	4,7-dimethylapigenin	*S. aurita*	Known*
16	Parvifloron D	*P. ecklonii*	Known
17	Parvifloron F	*P. ecklonii*	Known

UNIVERSITY of the WESTERN CAPE
https://etd.uwc.ac.za/

18	Parvifloron G	*P. ecklonii*	Known*

*Compounds isolated for the first time from those plant species

The in vitro antidiabetic evaluation was determined using alpha glucosidase and alpha amylase and the in vitro antioxidant capacity was performed using ORAC, TEAC and FRAP.

The phytochemical investigation of *S. africana lutea* (Chapter 3) afforded ten terpenoids, from which (**1**-**4**) were reported for the first time from a natural source, while **5**-**10** were isolated for the first time from *S. africana lutea*. Compounds **8**, **10** and **7** exhibited strong inhibitory activities against alpha-glucosidase with IC_{50} values of 11.3 ± 1.0, 17.1 ± 1.0 and 22.9 ± 2.0 µg/mL respectively while **7** demonstrated the strongest in vitro alpha-amylase inhibitory activity among the tested compounds with IC_{50} of 12.5 ± 0.7 µg/mL. The results of the in vitro antioxidant demonstrated that **1** and **5** exhibited strong activity on ORAC (2588.18 ± 10.10; 2357.18 ± 0.1) µM TE/g respectively. Compounds **5** and **6** showed strong activities on TEAC (862.2 ± 1.36; 705.5 ± 1.99) µM TE/g, whereas **5** and **2** demonstrated significant inhibitory activity on FRAP (2262.89 ± 11.01; 2200.95 ± 14.22) µM AAE/g when compared to the reference antioxidant epigallocatechingallate (EGCG). The significant biological activities demonstrated by **7**, **8** and **10** in addition to others assays such as glucose uptake (drafted article) nominated them and *S. africana lutea* as good candidates for the management of diabetes and might be submitted for in vivo studies as well as clinical trials. These findings on alpha glucosidase and alpha amylase inhibitory activities of *S. africana lutea* and its constituents were already published in an international Journal.

The phytochemical investigation of *S. aurita* (Chapter 4) afforded five known compounds, which were isolated for the first time from this plant species. The *in vitro* bio-evaluation against alpha-glucosidase showed strong inhibitory activities for **13** and **12** with IC_{50} values of 4.2 ± 0.7 and 16.4 ± 1.1 µg/mL respectively while **14** and **11** demonstrated the strongest *in vitro* alpha-amylase inhibitory activity among the tested compounds with IC_{50} of 16.2 ± 0.3

UNIVERSITY of the WESTERN CAPE
https://etd.uwc.ac.za/

and 19.8 ± 1.4 µg/mL. Additionally, excellent total antioxidant capacities were demonstrated by **12**, **11** and **13** respectively as ORAC (25789.9 ± 10.5; 23961.8 ± 14.1; 23939.3 ± 2.4) µM TE/g; **11**, and **S2** as FRAP (3917.8 ± 2.1; 1522.3 ± 0.9) µM AAE/g; **15** and **12** as TEAC (3190.4 ± 2.8; 2055.0 ± 2.6) µM TE/g. The methanolic extract of *S. aurita is* a rich source of terpenoids and flavonoids with strong antioxidant and anti-diabetic activities. This is the first scientific report on the chemical and biological profile of *Salvia aurita*. Documenting of the antidiabetic and antioxidant compounds isolated from the methanolic extract of *S. aurita* is currently on writing process and awaiting publication.

The phytochemical investigation of a methanolic extract of *Plectranthus eckolonii* afforded three pure compounds (**16-18**), of which **18** was isolated for the first time from this plant species. The *in vitro* bio-evaluation against alpha-glucosidase moderate inhibitory activities for **18** with IC_{50} values of 41.3 ± 1.2. The *in vitro* bio-evaluation of the antioxidant activity of the isolated compounds of the methanolic extract of *P. ecklonii* were investigated by measuring their FRAP, TEAC and ORAC activities, and the obtained results demonstrated that **18** and **16** exhibited strong antioxidant activity on ORAC (25726.1 ± 8.1; 3942.9.6.6 ± 0.1) µM TE/g respectively, which is in a competitive manner with the positive control (EGCG). Compounds **18** showed the strongest activity on TEAC (3526.1 ± 0.6) µM TE/g, followed by **17** (1069.3 ± 2.4) µM TE/g, as well as on FRAP (1455.4 ± 2.0) µM AAE/g when compared to the reference antioxidant epigallocatechingallate (EGCG). The methanolic extract of *P. ecklonii is* a rich source of abietane diterpenes with strong antioxidant activities. This is the first scientific report on the biological investigation on the in vitro bio-evaluation of *P. ecklonii* constituents against alpha glucosidase and amylase. These notable findings displayed by *P. ecklonii* are currently written and awaiting publications.

Cyclic voltammetry was used for characterization of the electrochemical properties of the isolated compounds as well as for establishing the correlation between the oxidation potential

UNIVERSITY of the WESTERN CAPE
https://etd.uwc.ac.za/

and the antioxidant capacities, in comparison with spectrophometric methods. CV shows that all the abietane diterpenes are electro-active with well-defined oxidation-reduction peaks. Rosmanol, when compared to other compounds, exhibits the lowest oxidation potential value (E_{pa} = 120 mV), indicating that rosmanol has the highest antioxidant power, which is in good agreement with ORAC and TEAC. Compounds with catechol moiety (11,12-dihydroxyl group) in the C ring such as **2**, **5**, **11**, **12**, **18** demonstrated the lowest oxidation potential compared to others, and their mechanism of reaction involve two electrons two protons reversible reaction and form an o-quinone. Cyclic voltammetry is a reliable analytical method for the characterization of electrochemical behavior of isolated compounds as well as the oxidizing and/or reducing ability of natural phenolic compounds. These notable observations will be drafted for publication.

From the above, it is recommended that

1. Extensive biological studies of the new compounds against other biological target (especially cancer, alzheimer, HIV), to explore their potential as bioactive constituents.
2. Further biological investigations in animal models and clinical trials need to be done for compound **13**, **7** and **8** as well as toxicity.
3. The compounds that exhibited lowest oxidation potentials with well-defined redox properties need to be fully investigated in different pH solution, scan range for the establishment of their mechanism of reaction.

UNIVERSITY of the
WESTERN CAPE

https://etd.uwc.ac.za/

ANNEXURE

Compound **9**

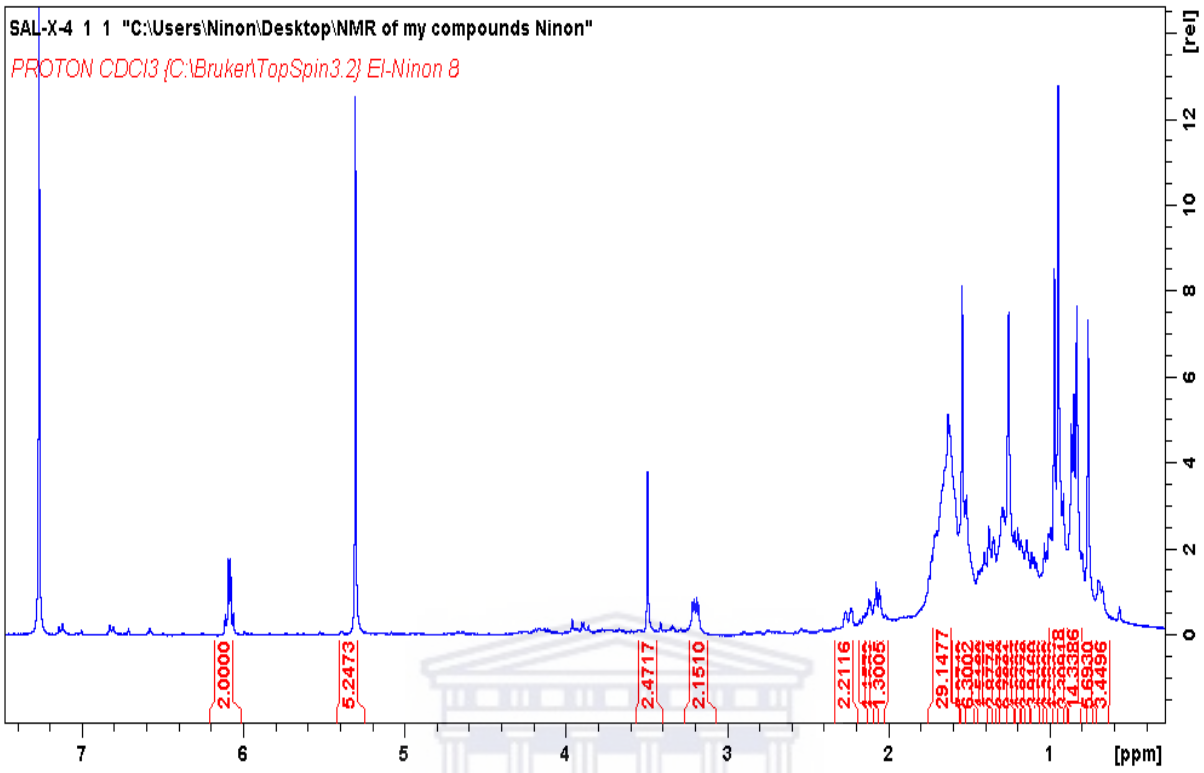

^{1}H NMR (400 MHz, CDCl3) spectrum of compound **9**

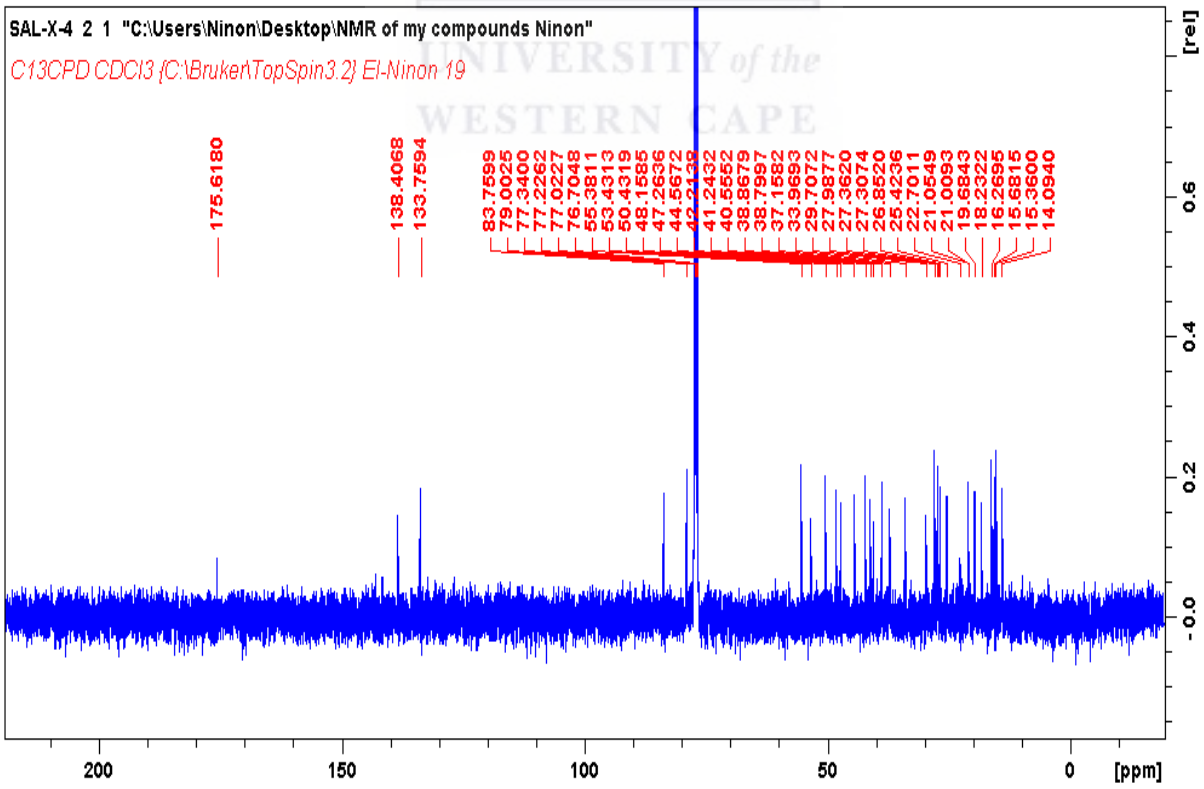

^{13}C NMR (400 MHz, CDCl3) spectrum of compound **9**

https://etd.uwc.ac.za/

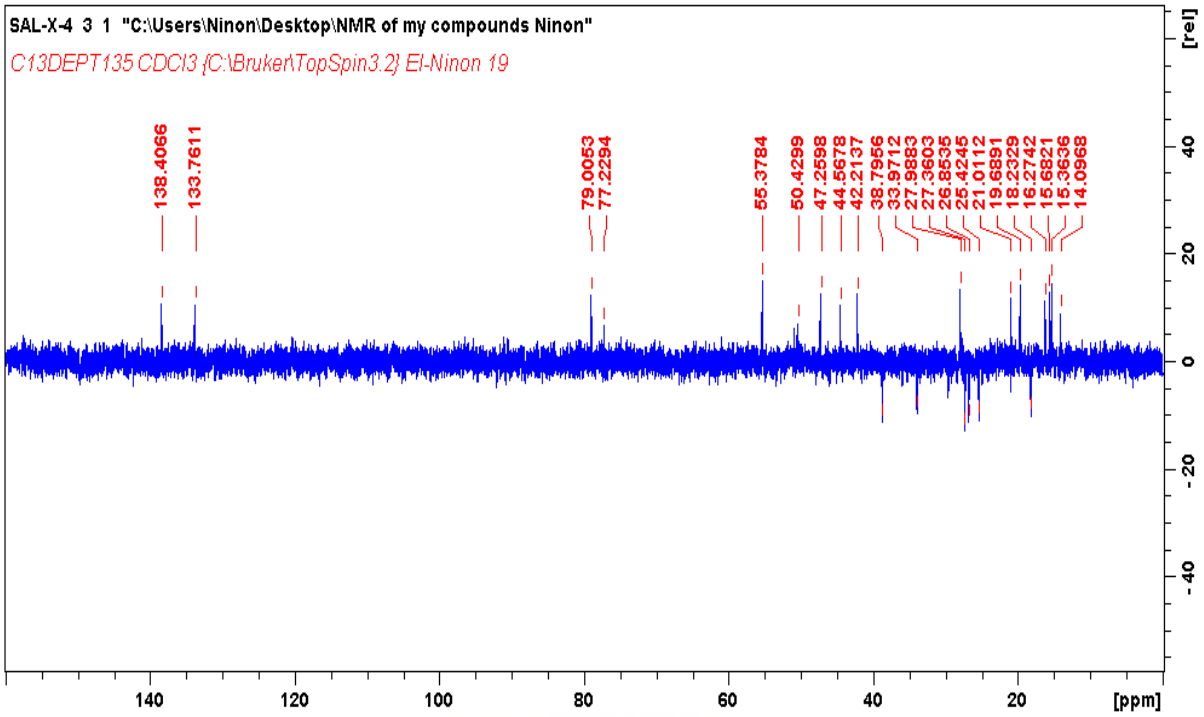

DEPT NMR (400 MHz, CDCl3) spectrum of compound **9**

Compound **10**

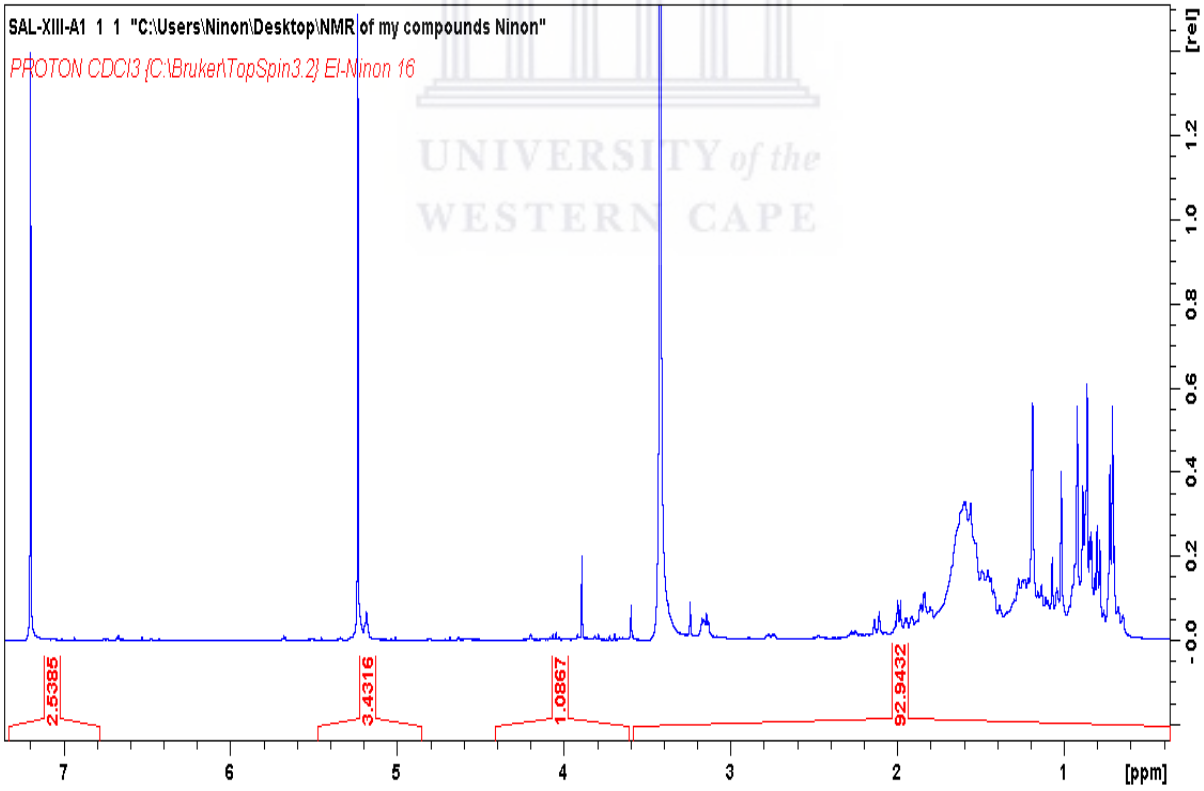

^{1}H NMR (400 MHz, CDCl3) spectrum of compound **10**

https://etd.uwc.ac.za/

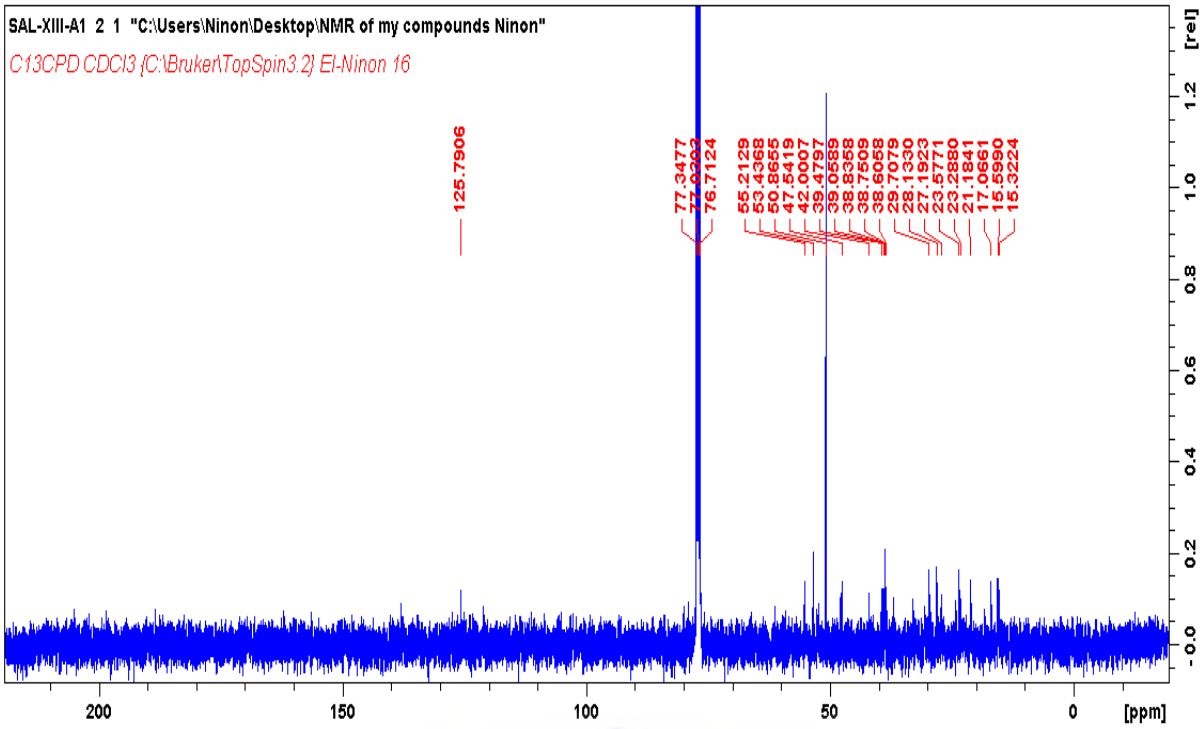

^{13}C NMR (400 MHz, CDCl3) spectrum of compound **10**

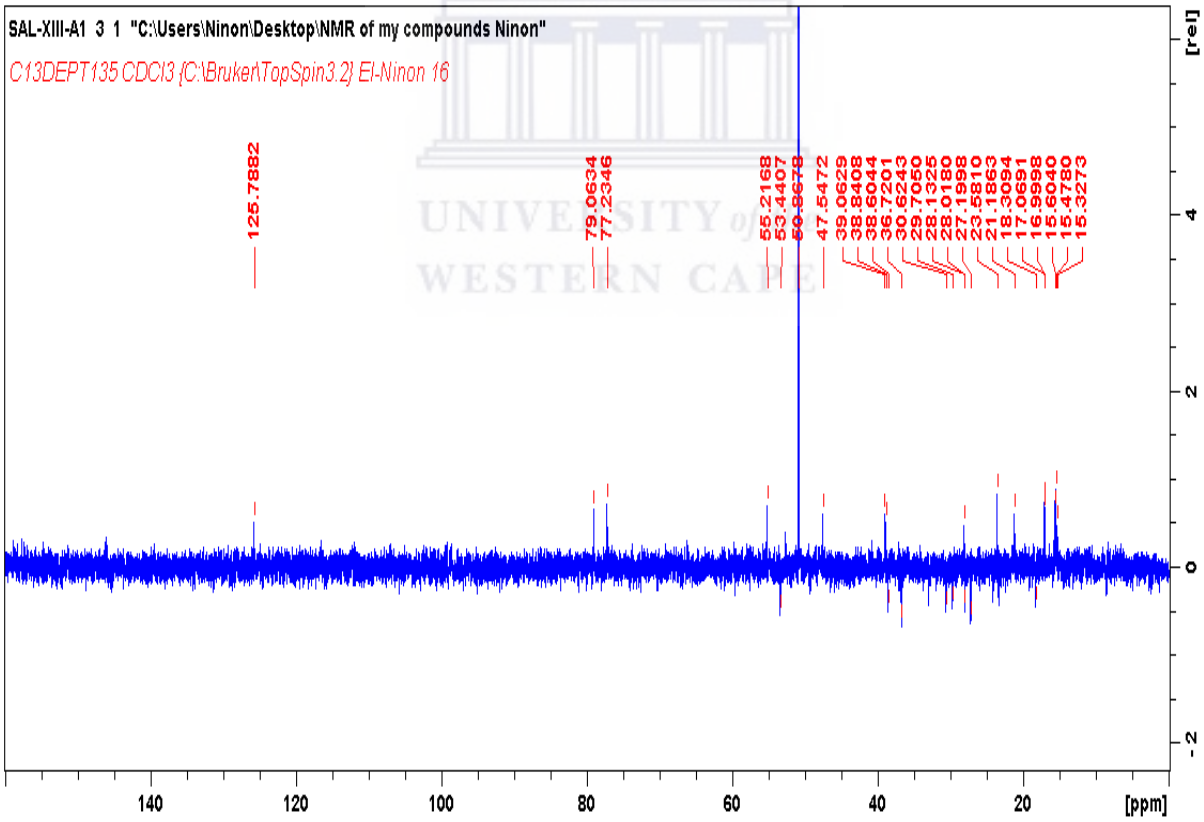

DEPT NMR (400 MHz, CDCl3) spectrum of compound **10**

https://etd.uwc.ac.za/

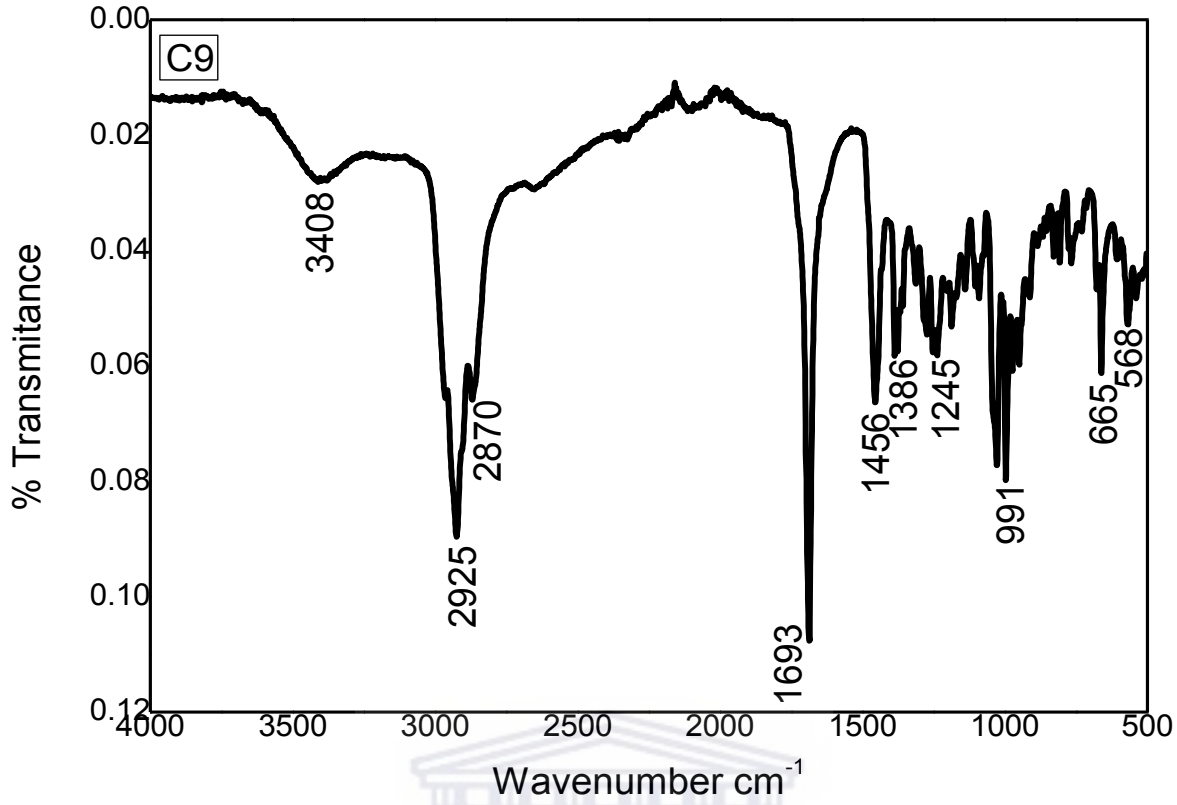

FTIR spectrum of compound **10**

UNIVERSITY of the
WESTERN CAPE

https://etd.uwc.ac.za/